MIXED-SANDWICH COMPLEXES OF LOW-VALENT URANIUM FOR THE REDUCTIVE ACTIVATION OF SMALL MOLECULES

by

Joy Hannah Farnaby

Submitted for the degree of Doctor of Philosophy

March, 2011

The work described in this thesis was carried out at the University of Sussex from October 2006 to April 2010, under the supervision of Professor F. G. N. Cloke. All the work is my own, unless stated to the contrary and has not been previously submitted for any degree at this or any other university.

Joy Hannah Farnaby

March, 2011

UNIVERSITY OF SUSSEX

JOY HANNAH FARNABY FOR THE DEGREE OF DOCTOR OF PHILOSOPHY

MIXED-SANDWICH COMPLEXES OF LOW-VALENT URANIUM FOR THE REDUCTIVE ACTIVATION OF SMALL MOLECULES

SUMMARY

Recent work in our laboratory has shown that cyclopentadienyl mixed-sandwich complexes of uranium(III) display novel reactivity towards small molecules; a particular result is the reductive coupling of CO, which depending on steric constraints can react selectively to form several members of the oxocarbon series. This reaction takes a poisonous and readily available C_1 source and transforms it into a biologically useful compound. This thesis is in three parts. The first seeks to expand on the reactivity already observed by extending it to other small molecules and although well-defined coupling reactions were not achieved, several novel complexes were isolated. The chemical removal of the coupled CO product was also investigated. The second and third parts are linked as they examine the effects on stability and reactivity of the uranium(III) complex, of substituting two very different monoanionic ligand classes in the place of the cyclopentadienyl ligand. Two novel complexes were synthesised using the trispyrazolylborate and the cyclooctatetraenyl or pentalenyl ligands. The complexes display very different reactivity to each other and to the cyclopentadienyl ligands. Density functional calculations support the experimental findings. The final class of ligand, the indenyl ligand is much closer in type to the original system. The two novel indenyl complexes synthesised display reactivity towards CO and CO_2, including the isolation of a reductively coupled CO complex. This demonstrates that the novel reactivity exhibited by the cyclopentadienyl mixed-sandwich complexes of uranium(III) can be replicated using a different ligand system. However, the reactivity observed is not only comparable, but also complementary. The structural and reactivity data presented in this thesis are instructive to our understanding of low-valent uranium chemistry and provide an insight into how the use of different ligand classes can effect the overall reactivity of the low-valent system.

ACKNOWLEDGEMENTS

My thanks to Geoff, foremost for the opportunity to work on the project and consequently to work with such a brilliant mind.

The members of Lab 14 past and present.

Dr O. T. Summerscales

Dr M. P. Coles

Dr A. S. P. Frey

Dr L. T. Evans

Dr P. B. Hitchcock

Dr A. Abdul-Sada

Dr I. J. Day

Dr I. R. Crossley

Dr J. F. C. Turner

Prof. J. C. Green

Dr G. Aitken

Prof. D. M. O'Hare

Dr A. Ashley

Dr. A. Sella

Dr K. Merz

Heartfelt thanks to my family and friends,

without their support I would have gone under long ago.

ABSTRACT

MIXED-SANDWICH COMPLEXES OF LOW-VALENT URANIUM FOR THE REDUCTIVE ACTIVATION OF SMALL MOLECULES

Joy Hannah Farnaby

DPhil Thesis

An introduction to the binding and activation of small molecules by low-valent uranium complexes is covered in Chapter 1, with reference to f-block and Group 4 complexes where appropriate. Chapter 2 describes further small molecule chemistry of the two known complexes [U(η-Cp^{Me4H})(C_8H_6{Si^{i}Pr$_3$-1,4}$_2$)(THF)] and [U(η-Cp^{Me5})(C_8H_4{Si^{i}Pr$_3$-1,4}$_2$)(THF)]. This includes the attempted synthesis of [U(η-Cp^{Me4H})(C_8H_4{Si^{i}Pr$_3$-1,4}$_2$)(THF)] and the structure and themolysis of [U(η-Cp^{Me4H})(C_8H_6{Si^{i}Pr$_3$-1,4}$_2$)(κ^1-NCMe)]. In order to chemically remove the labelled carbocyclic species resulting from the reaction of [U(η-Cp^{Me4H})(C_8H_6{Si^{i}Pr$_3$-1,4}$_2$)(THF)] with ^{13}CO, the complex [U(η-Cp^{Me4H})(C_8H_6{Si^{i}Pr$_3$-1,4}$_2$)]$_2$($^{13}C_4O_4$) was synthesised and quenched with a variety of reagents. The effect on stability and reactivity of substituting the Tp^{Me2} ligand for the Cp^R ligand is investigated in Chapter 3. The synthesis and full characterisation of the novel half-sandwich complexes [U(κ^3-Tp^{Me2})(C_8H_6{Si^{i}Pr$_3$-1,4}$_2$)] and [U(κ^3-Tp^{Me2})(C_8H_4{Si^{i}Pr$_3$-1,4}$_2$)] is reported. The complex [U(κ^3-Tp^{Me2})(C_8H_6{Si^{i}Pr$_3$-1,4}$_2$)] was found to be unreactive towards CO, CO_2 and MeNC under mild conditions. This finding agrees with DFT calculations carried out on the model complex [U(κ^3-Tp^{Me2})(C_8H_6{SiH_3-1,4}$_2$)].

However, when heated with an excess of MeNC, the oxidation product [U(C_8H_6{Si^{i}Pr$_3$-1,4}$_2$)(κ^2-dmpz)$_2$(η^1-CNMe)] was formed. Chapter 4 details the synthesis and reactivity of mixed-sandwich complexes using methylated indenyl ligands. The complexes [U(η^5-Ind^{Me6})(C_8H_6{Si^{i}Pr$_3$-1,4}$_2$)] and [U(η^5-Ind^{Me7})(C_8H_6{Si^{i}Pr$_3$-1,4}$_2$)] react with small molecules under the mild conditions observed for the [U(η-Cp^R)(C_8H_6{Si^{i}Pr$_3$-1,4}$_2$)(THF)] complexes and their reactivity was studied by multi-nuclear NMR and solution FTIR. The structure of [U(η^5-Ind^{Me6})(C_8H_6{Si^{i}Pr$_3$-1,4}$_2$)]$_2$(C_4O_4) is described. A conclusion is provided in Chapter 5 and experimental method and characterising data are contained in the appendices.

LIST OF NEW COMPOUNDS

$[U(\eta\text{-}Cp^{Me4H})(\eta\text{-}C_8H_6\{Si^iPr_3\text{-}1,4\}_2)(\eta^1\text{-}NCMe)]$ (**2.3**)

$[U(\eta\text{-}Cp^{Me5})(\eta\text{-}C_8H_6\{Si^iPr_3\text{-}1,4\}_2)(\eta^1\text{-}CNMe)]$ (**2.4**)

$^{13}C_4O_4(SiPh_3)_2$ (**2.6**)

$[U(\kappa^3\text{-}Tp^{Me2})(\eta\text{-}C_8H_6\{Si^iPr_3\text{-}1,4\}_2)]$ (**3.1**)

$[U(\kappa^3\text{-}Tp^{Me2})(\eta\text{-}C_8H_4\{Si^iPr_3\text{-}1,4\}_2)]$ (**3.2**)

$[U(\eta\text{-}C_8H_6\{Si^iPr_3\text{-}1,4\}_2)(\kappa^2\text{-}dmpz)_2(\eta^1\text{-}CNMe)]$ (**3.3**)

$[U(\eta^5\text{-}Ind^{Me6})(\eta\text{-}C_8H_6\{Si^iPr_3\text{-}1,4\}_2)]$ (**4.1**)

$[U(\eta^5\text{-}Ind^{Me7})(\eta\text{-}C_8H_4\{Si^iPr_3\text{-}1,4\}_2)]$ (**4.2**)

$[(U(\eta^5\text{-}Ind^{Me6})(\eta\text{-}C_8H_6\{Si^iPr_3\text{-}1,4\}_2))_2(\mu\text{-}\eta^2\text{:}\eta^2\text{-}C_4O_4)]$ (**4.3**)

$[U(\eta^5\text{-}Ind^{Me7})(\eta^8\text{-}C_8H_6\{Si^iPr_3\text{-}1,4\}_2)(^{13}CO)]$ (**4.4**)

LIST OF ABBREVIATIONS USED IN THE TEXT

An	Actinide
br	Broad
Cp	Cyclopentadienyl
Cp^{Me4}	Tetramethylcyclopentadienyl
Cp^{Me5}	Pentamethylcyclopentadienyl
CV	Cyclic Voltammetry/ Cyclic Voltammogram
d	Doublet
DFT	Density Functional Theory
DME	1,2-Dimethoxyethane
dmpz	dimethylpyrazolyl
EI	Electron Impact
FTIR	Fourier Transform Infra Red
GC-MS	Gas Chromatography – Mass Spectrometry
$\{^1H\}$	Proton Decoupled
HOMO	Highest Occupied Molecular Orbital
Ind	Indenyl
Ind^{Me6}	Hexamethylindenyl
Ind^{Me7}	Permethylindenyl
^iPr	*iso*-Propyl
IR	Infrared

Ln	Lanthanide
LUMO	Lowest Unoccupied Molecular Orbital
m	Multiplet
M	Metal
Me	Methyl
MO	Molecular Orbital
NMR	Nuclear Magnetic Resonance
^{n}Pr	*n*-Propyl
OTf	Triflate
Ph	Phenyl
ppm	Parts Per Million
s	Singlet
SCF	Self-Consistent Field
SOMO	Singly-Occupied Molecular Orbital
t	Triplet
tacn	Triazacyclononane
TIPS	Triisopropylsilyl
THF	Tetrahydrofuran
TMS	Trimethylsilyl
Tp	Trispyrazolylborate
Tp^{Me2}	3,5-diimethyltrispyrazolylborate

TABLE OF CONTENTS

“All our knowledge brings us nearer to our ignorance”

T. S. Eliot

Choruses from *The Rock*

CHAPTER ONE: SMALL MOLECULE ACTIVATION

1.1 Introduction to low-valent uranium chemistry

1.1.1 Properties of U(III):

Of the naturally occurring actinides, only thorium and uranium are present in the earth's crust in a useful amount and at 8.1 ppm and 2.3 ppm respectively, they are far from rare;[1] uranium is over 40 times more abundant than silver. Their abundance and their chemical properties make them an attractive alternative to the more expensive transition metals for catalytic transformations. Although organoactinide research is synthetically and spectroscopically challenging, the advances to chemical understanding and practical application that have been made in this field are uniquely significant. Although all the actinides are radioactive, depleted uranium may be handled in the laboratory without using any special precautions, as it is only dangerous if inhaled or ingested.

The chemical properties of an element determine its chemical behaviour. In the lanthanide and actinide series the f orbitals are being filled and moving from the 4f of the lanthanides to the 5f of the actinides there is a radial node. The 5f orbitals of the actinide series are less shielded by the 6s and 6p electrons than the 4f orbitals of the lanthanide series are by the 5s and 5p, which allows them to participate more readily in bonding. In the less contracted early actinides this incomplete shielding means that there is sufficient radial expansion for significant overlap with ligand orbitals, leading to greater chemical versatility.

The 6d and 5f are similar enough in energy for mixed ground-states to be common and for the early actinides the ground-state is determined principally by the interelectronic repulsion. In contrast to the transition metals where ligand-field splitting is larger than spin-orbit coupling and the lanthanides where spin-orbit coupling is larger than ligand-field splitting, the spin-orbit coupling and the ligand-field splitting are of a similar magnitude in the early actinides. This may lead to magnetic data and electronic spectra that are non-trivial. [2,3] Computational modelling of the f-block remains difficult[4] but advances in technology and new methodologies have meant that f-block chemistry benefits from a multi-discipliniary approach.[5]

Uranium shares many of the properties common to f-block elements, a largely ionic or electrostatic mode of bonding and highly nodal core-like orbitals, however the radial node of the 5f and the extent of the radial expansion mean that uranium has a wide range of oxidation states available to it (+3 to +6), which because of its large size are able to be stabilised by high coordination numbers.[2,3] Uranium(III) is a powerful reductant as U(IV) state is stable under inert atmosphere with respect to U(III). The U(IV)/U(III) reduction potential has been estimated to lie between -1.5 and -2.2 V *versus* ferrocene.[6] The reduction potential of a given U(III) complex will depend on the electronic properties of the ligand environment.[7] The one electron reduction is the most common,[8] often resulting in the reaction of two U(III) centres with a substrate to yield a dimeric structure bridged by the reduced substrate dianion, U(IV)-(μ-substrate)$^{2-}$-U(IV).

1.1.2 Important discoveries in the field:

The first well characterised organometallic complex of an actinide[9] was synthesised by Wilkinson from the slow addition of 1.8 equivalents of NaCp to [UCl_4]; subsequent reflux and sublimation led to the isolation of red-black crystals of [$U(Cp)_3Cl$] in up to 85 % yield. The complex was found to be thermally stable up to 300 °C and extremely air sensitive, it displayed no reactivity with malic anhydride and was stable to ligand redistribution to form ferrocene on mixing with [$FeCl_2$]. This lack of reactivity suggested the bonding was different from that observed in the previously synthesised [$Ln(Cp)_3$] complexes.[10] MO treatment by Moffit, in which the C_5H_5 were treated as neutral π species, suggested extensive 5f participation.

A further theoretical examination of the bonding in sandwich complexes, incorporating the planar, aromatic cyclooctatetrene dianion,[11] suggested that a $U(C_8H_8)$ complex might be stable,[12] a prediction that paved the way for the discovery of [$U(\eta^8\text{-}C_8H_8)$], known as uranocene, in 1968.[13] Cyclooctatetrene was reacted with potassium in dry THF at - 30 °C and the resultant yellow solution added to [UCl_4] in THF at 0 °C under nitrogen. Extraction with toluene or benzene and sublimation yielded green crystals of [$U(\eta^8\text{-}C_8H_8)$] in an 80 % yield. Uranocene was found to be pyrophoric in air, which complicated spectroscopic analysis but the structural assignment of the complex as a sandwich complex was confirmed by X-ray diffraction.[14] This result was important in organoactinide chemistry as it represented the first example of a π-bonded sandwich complex of uranium and a new class of "metallocenes" .[15]

The advent of the use of substituted cyclopentadienyl ligands, in particular the Cp^{Me5} anion, to achieve steric saturation and impart greater solubility and crystallinity to complexes formed led to the synthesis of $[U(\eta^5\text{-}Cp^{Me5})_2Cl_2]$.[16] This complex was stable, unlike the unsubstitued complex $[U(\eta^5\text{-}Cp)_2Cl_2]$, which disproportionates to $[U(\eta^5\text{-}Cp)Cl_3]$ and $[U(\eta^5\text{-}Cp)_3Cl]$ and led to a rich derivative chemistry,[17] pioneered by the Marks' group and workers at Los Alamos.[18] However, the development of the chemistry of trivalent uranium was impeded by the lack of straightforward synthetic routes to trivalent starting materials.

1.1.3 Synthesis of UI_3:

Anhydrous uranium trihalides exist as polymeric solids.[19] They are insoluble in common solvents and quite unreactive, for example the reaction of [UCl_3] with KCp yields [U(η^5-Cp_3)] but in a 10.4 % yield after reflux of the reagents in benzene for 7 days and a lengthy extraction process.[20] Commercially available [UCl_4] can be reduced in THF[21] using a variety of reducing agents to yield a solid formulated as [UCl_3(THF)*x*] or reacted *in situ* in the presence of the reducing agent and the alkali metal salt of the ligand of choice. There were problems associated with this route, not least of which was that the [UCl_3(THF)*x*] precursor was not well understood as a material:[22] the reductions did not go to completion and the yields were inconsistent or the products contaminated by U(IV) side products.

[UI_4] was found to be unstable and decompose to [UI_3] and iodine, either on exposure to vacuum or in solution,[23] and investigation into synthetic routes to triiodo uranium complexes led in 1989 to the synthesis of [$UI_3(THF)_4$].[24] The byproduct of the reaction was found to be an oily green material presumed to be a product of ring-opening THF; reactivity with THF is observed for a number of U(III) complexes,[25] and can be avoided in this synthesis by maintaining the temperature of the reaction below 10 °C.[26]

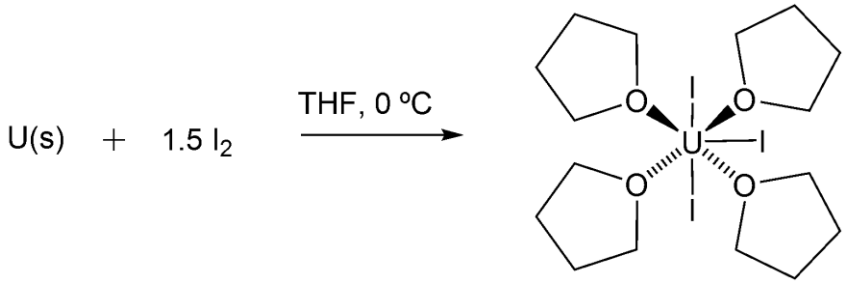

Figure 1: Synthetic route to $[UI_3(THF)_4]$

To avoid reactivity with THF and for the synthesis of base-free complexes, unsolvated starting material is a prerequisite. Cloke[27] reported an efficient preparation of $[UI_3]$ from uranium turnings and mercuric iodide in a similar manner to the synthesis of $[LnI_3]$ reported by Corbett.[28]

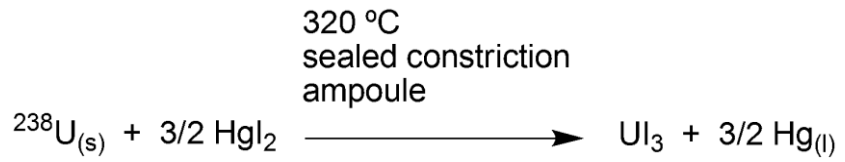

Figure 2: Synthetic route to base-free $[UI_3]$

The above synthesis utilises toxic mercuric iodide and requires a high-vacuum set-up; alternative methodologies have been proposed. Evans has reported a mercury-free synthesis[29] based on the Bochkarev synthesis of divalent lanthanides,[30] which is fast, efficient and uses an inexpensive set-up. Most recently Arnold[31] has reported the synthesis of both solvated and unsolvated uranium triiodides from uranium turnings and iodine at room temperature; though the elemental analysis for the $[UI_3]$ synthesised in this manner show that small amounts of carbon and hydrogen are present.

1.1.4 Outlook:

The abundance of uranium, the viability of bonding between the uranium centre and π-ligands and the availability of the neighbouring +3 and the significantly more stable +4 oxidation states make it a strong candidate for research investment. Improvements in experimental techniques and reliable syntheses of low-valent starting materials have led to the rapid development of the chemistry of uranium(III).[32] Complexes of U(III) have been shown to possess reactivity, some of which is unique, towards small molecules.[33] As evidenced by recent reviews the field is moving towards uranium-based catalytic processes.[34] Section 1.2 reviews the reactions of complexes of trivalent uranium and where appropriate the divalent lanthanides, with CO, N_2 and CO_2.

1.2 Binding and activation of small molecules by low-valent f-block complexes

1.2.1 Binding and activation of CO:

The binding of CO to a transition metal centre[35] can be described as anionic, neutral or cationic and the resultant bond order is dependant on whether C-M σ-donation or M-C π-back-donation dominates. The M-C π-bond populates an orbital which is anti-bonding with respect to the C=O, therefore lengthening and weakening it; in a manner similar to the Dewar-Chatt-Duncanson model[36] developed for the binding of ethylene to platinum complexes. The C-O stretching vibrational frequencies can be regarded as being independent of other vibrations within the molecule and the lowering of the ν_{CO} on binding, relative to that of free CO (2143 cm^{-1})[37] is a useful indication of the level of back-bonding from the metal to the CO. It is notable that all isolable neutral carbonyl complexes of the d-block require the metal to participate in M-CO back-bonding.[38]

Given the traditional electrostatic model for bonding in the f-block, it was not thought that the core-like f-orbitals would be able to participate in back-bonding. Uranium carbonyl complexes were targeted without success as a means of isotope separation based on the volatility of transition-metal analogues in the Manhatten Project.[3,15] More recently uranium carbonyl complexes have been isolated by matrix isolation techniques at low temperature and are stable below 30 °K.[39] IR bands at 1961 cm^{-1} and 1938 cm^{-1} were assigned to $[U(CO)_6]$ and $[U(CO)_5]$ respectively, these frequencies correlate to those observed for $[Ta(CO)_6]$ and $[Ta(CO)_5]$ under the same conditions. The ν_{CO}

observed is significantly lowered from that of free CO and suggested that the uranium metal centre could act as a π-donor.

The first molecular carbon monoxide complex of uranium $[U(\eta^5\text{-}Cp^{SiMe3})_3(CO)]$[40] was prepared by Anderson *et al.* in 1985 from exposure of solutions of the base-free $[U(\eta^5\text{-}Cp^{SiMe3})_3]$ to 1 atm of CO at 20 °C. The reaction is accompanied by a colour change from deep green to burgundy and shown to be reversible by loss of CO on exposure to vacuum or purging with Ar; though the burgundy solution was able to be stored at low temperature for an extended period of time. The IR spectra of $[U(\eta^5\text{-}Cp^{SiMe3})_3(CO)]$ showed the ν_{CO} at 1976 cm^{-1} using ^{12}CO, the assignment of which as the carbonyl was confirmed by isotopic labelling and that $[U(\eta^5\text{-}Cp^{SiMe3})_3]$ also reversibly absorbs CO in the solid state. They were unable to isolate and structurally characterise the $[U(\eta^5\text{-}Cp^{SiMe3})_3(CO)]$ but they assumed the CO to be carbon-bound and linear by analogy to the structure of the closely related $[U(\eta^5\text{-}Cp^{SiMe3})_3(\eta^1\text{-}CNEt)]$.[40] The synthesis and structural characterisation of actinide phosphine complexes[41] provided further evidence that the complexes $[U(\eta^5\text{-}Cp^{R})_3L]$ (L = $N(CH_2CH_2)_3CH$, $P(OCH_2)_3CEt$) were not too thermodynamically unstable to exist and there was shown to be a strong correlation between the length and the strength of the M-L bond in the solid state, which was attributed to U-L π-back-bonding.[42]

Carmona and Parry succeeded in isolating and structurally characterising the first example of an actinide carbonyl complex $[U(\eta^5\text{-}Cp^{Me4})_3(CO)]$ in 1994.[43] The IR spectrum shows the ν_{CO} at 1880 cm^{-1} (^{12}CO) and 1840 cm^{-1} (^{13}CO) in the solid state and

1900 cm^{-1} (^{12}CO) in solution. This substantial lowering of the ν_{CO} from that observed for [U(η^5-Cp^{SiMe3})$_3$(CO)] was unexpected in spite of the more electron donating ligand set. The [U(η^5-Cp^{Me4})$_3$(CO)] was also observed to lose CO less readily than [U(η^5-Cp^{SiMe3})$_3$(CO)], requiring prolonged exposure to vacuum in solution. Solid samples could be stored at room temperature under inert atmosphere for several months and showed no signs of decomposition when exposed to dynamic vacuum for 5 hours.

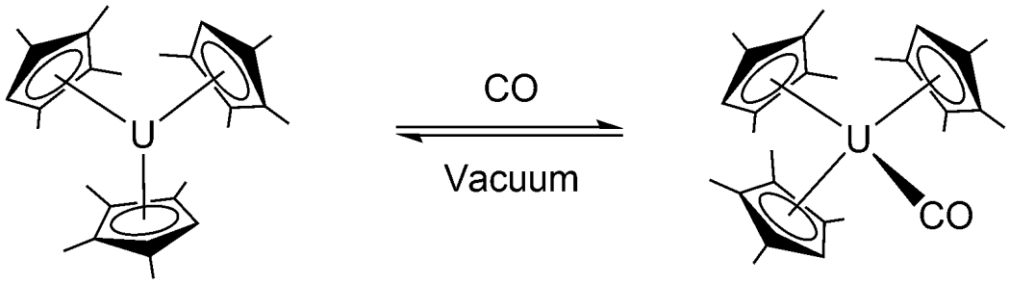

Figure 3: Reaction of [U(η^5-Cp^{Me4})$_3$] with CO

The carbonyl is carbon-bound and the U-Cp^{Me4} distances are comparable to those of the [U(η^5-Cp^{Me4})$_3$Cl] precursor[44]. The U-C-O angle is almost linear at 175.2(6)° and the

U-C(CO) separation of 2.383(6) Å is shorter than the 2.57(3) Å found in [U(η^5-Cp^{SiMe3})$_3$(η^1-CNEt)].[40] The C-O distance of 1.142(7) Å is similar to that observed in [Ti(η^5-Cp^{Me5})$_2$(CO)$_2$] (1.149 Å).[45] The reaction was observed to be quantitative by ^{1}H NMR and the complex is fluxional in solution at room temperature. Variable temperature NMR studies[46] reveal that between 0 °C and -70 °C the complex exhibits Curie-Weiss behaviour but that above 50 °C the averaged chemical shifts of the Cp-CH_3 are non-linear with T^{-1}. This observation suggests that the reaction at high temperatures

is best viewed as an equilibrium between [U(η^5-Cp^{Me4})$_3$(CO)] and [U(η^5-Cp^{Me4})$_3$] by dissociative loss of the CO.

Carmona *et al.* exposed a number of tris-cyclopentadienyl uranium(III) complexes to CO,[46] the IR values are tabulated below. A significant lowering of the CO stretching frequency of between 155-260 cm^{-1} is observed for each of the complexes on coordination to CO and shows that the ν_{CO} decreases as the substituents on the Cp ring become more electron donating, $Cp^{1,3(SiMe3)2}$> Cp^{SiMe3}> Cp^{tBu}> Cp^{Me4}. The coordination is reversible in all cases and no adducts except the aforementioned [U(η^5-Cp^{Me4})$_3$(CO)] were able to be isolated.

Table 1: IR data for $[U(\eta^5\text{-}Cp^R)_3(CO)]$ complexes

Complex	ν_{CO} in cm^{-1}	State
$[U(\eta^5\text{-}Cp^{SiMe3})_3(CO)]$	1976	hexane
$[U(\eta^5\text{-}Cp^{SiMe3})_3(^{13}CO)]$	1935	hexane
$[U(\eta^5\text{-}Cp^{SiMe3})_3(CO)]$	1969	KBr
$[U(\eta^5\text{-}Cp^{SiMe3})_3(^{13}CO)]$	1922	KBr
$[U(\eta^5\text{-}Cp^{tBu})_3(CO)]$	1960	hexane
$[U(\eta^5\text{-}Cp^{1,3(SiMe3)2})_3(CO)]$	1988	methylcyclohexane
$[U(\eta^5\text{-}Cp^{Me4})_3(CO)]$	1880	Nujol
$[U(\eta^5\text{-}Cp^{Me4})_3(^{13}CO)]$	1840	Nujol
$[U(\eta^5\text{-}Cp^{Me4})_3(C^{18}O)]$	1793	Nujol

The bulky $[U(\eta^5\text{-}Cp^{Me5})_3]$ was also shown to react with CO in benzene at room temperature by Evans *et al.* to give $[U(\eta^5\text{-}Cp^{Me5})_3(CO)]$.[47] The reaction was monitored by ^1H NMR and found to be quantitative after 6 hrs. This complex was also structurally characterised, though the linearly bound CO is crystallographically disordered. There is no change in the molecular geometry observed for $[U(\eta^5\text{-}Cp^{Me5})_3]$ on CO binding, unlike $[U(\eta^5\text{-}Cp^{Me4})_3]$; this is presumed to be a result of the steric constraints acting on the bulkier complex. The structural refinement was poorer when it was modelled as an

isocarbonyl,[48] the carbon-bound structure has also been calculated to be the more stable.[49]

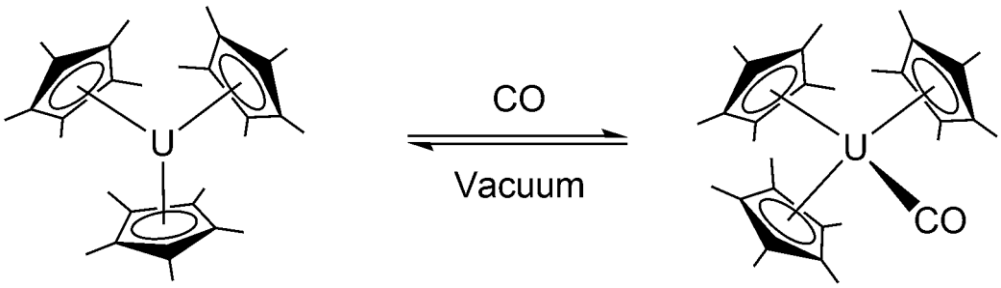

Figure 4: Reaction of $[U(\eta^5\text{-}Cp^{Me5})_3]$ with CO

The U-Cp^{Me5} average distance of 2.587 Å is identical to that found in $[U(\eta^5\text{-}Cp^{Me5})_3Cl]$.[50] The U-C(CO) distance of 2.485(9) Å is considerably longer than the 2.383(6) Å in $[U(\eta^5\text{-}Cp^{Me4})_3(CO)]$ and the C-O separation 1.13(1) Å is identical within the error limits to both that of the $[U(\eta^5\text{-}Cp^{Me4})_3(CO)]$ (1.142(7) Å) and free CO (1.128 Å).[51] The ν_{CO} of 1917 cm^{-1} is lower than those observed for $[U(\eta^5\text{-}Cp^{R})_3(CO)]$ (where R= $SiMe_3$, 1,3$(SiMe_3)_2$ and ^{t}Bu) and confirmed by isotopic labelling. It is however, 37 cm^{-1} higher than that observed for $[U(\eta^5\text{-}Cp^{Me4})_3(CO)]$, this may be a consequence of the longer U-C(CO) distance. The binding of CO is reversible and the half-life of the complex is *ca*. 12 hrs. No further reactivity was observed at higher pressures of CO or on irradiation.

Early calculations[49] confirmed $[U(\eta^5\text{-}Cp^R)_3]$ could behave as a π-donor and concluded that the three electrons in the $5f_\pi$ orbitals were involved in back-bonding and that the uranium contribution had predominantly f-character. In the uranium(III) metallocenes, the substituent on the Cp has a marked effect on the ν_{CO} of the resultant adduct (see Table 1). This is not the case for $[Zr(\eta^5\text{-}Cp^R)_2(CO)_2]$ complexes:[52] the difference between the ν_{CO} of $[Zr(\eta^5\text{-}Cp)_2(CO)_2]$ and $[Zr(\eta\text{-}Cp^{Me5})_2(CO)_2]$ is only 33 cm^{-1} and the difference between $[Zr(\eta^5\text{-}Cp^{Me4})_2(CO)_2]$ and $[Zr(\eta^5\text{-}Cp^{Me5})_2(CO)_2]$ is 5 cm^{-1}. The smaller substituent effect observed in the zirconocenes[53] was thought to result from the bent-sandwich structure, in which the d-orbitals available for CO binding are non-bonding relative to the Cp^R ligands. Anderson and co-workers[54] have suggested that the large substituent effect observed in the uranium(III) complexes, indicates the importance of the U-Cp^R orbitals in bonding to CO. The results of their calculations on $[U(\eta^5\text{-}Cp^R)_3]$ (R = H, $SiMe_3$, Me_4, Me_5) are tabulated below.

Table 2: Calculated and experimental bond distances and the difference in ν_{CO} between free and coordinated CO in solution

ligand		U-Cp_{ave} (Å)	U-C(CO) (Å)	$\Delta\nu_{CO}$* cm^{-1}
C_5H_5	calc.	2.49	2.38	-180
	expt.			
$C_5H_4SiMe_3$	calc.	2.50	2.41	-195
	expt.			-167
C_5HMe_4	calc.	2.55	2.34	-241
	expt.	2.53	2.383(6)	-243
C_5Me_5	calc.	2.60	2.34	-221
	expt.	2.59	2.485(9)	-218

* free ν_{CO} 2143 cm^{-1}, 2175 cm^{-1} (calculated)

The calculated values for $[U(\eta^5\text{-}Cp^{Me4})_3(CO)]$ and $[U(\eta^5\text{-}Cp^{Me5})_3(CO)]$ are in excellent agreement with the experimental evidence. The calculated valve of $\Delta\nu_{CO}$ for $[U(\eta^5\text{-}Cp^{SiMe3})_3(CO)]$ is higher than that observed experimentally but the trend of decreasing ν_{CO} $[U(\eta^5\text{-}Cp^{SiMe3})_3(CO)]>[U(\eta^5\text{-}Cp^{Me5})_3(CO)]>[U(\eta^5\text{-}Cp^{Me4})_3(CO)]$ observed experimentally is also predicted theoretically. The calculated complex $[U(Cp)_3(CO)]$ also shows the smallest decrease in the ν_{CO} relative to free CO.

The authors conclude that the only orbitals that are available for back-bonding are the ligand-based orbitals with π-symmetry, which are used for bonding in the [U(η^5-Cp^R)$_3$] fragment. The differences in ν_{CO} observed experimentally are thus rationalised by the direct involvement of the specific ligands. This bonding model is very different to that proposed by Bursten[49] and may also rationalise why the 4f metallocenes [Ce(η^5-Cp^{SiMe3})$_3$] and [Nd(η^5-Cp^{SiMe3})$_3$] do not react with CO.[55] The smaller radial extension of the 4f[56] may result in less interaction with the π-system of the Cp and the $4f_\pi/5d_\pi$ orbitals of the [Ln(η^5-Cp^R)$_3$] complexes not partaking in the transfer of π-electron density to the π* orbitals on the CO. It was consequently speculated that if the $5f_\pi/6d_\pi$ orbitals on uranium were more stabilised than in the [U(η^5-Cp^R)$_3$], that back-bonding to π-ligands would be weak at best and the lack of coordination chemistry of [U{N($SiMe_3$)$_2$}$_3$][57] is cited as a possible example.

The activation of C1 feedstock, such as CO is of great current importance; the chemical industries rely on the products of the oil refining process but it is unclear how long this will be the most economic option. The ability of [U(η^5-Cp^R)$_3$] uranium complexes to bind CO has been demonstrated but in all cases the reactions are reversible and no further chemistry is observed. The stabilisation of the uranium centre in a low oxidation state does not necessarily engender reactivity, but as the work of the Meyer group has shown, the ligand environment can be designed specifically for the purpose of binding small molecules.[58]

In the complex [U({ArO}$_3$tacn)][59] (Ar = 3,5-di-tert-butylbenzyl, tacn = 1,4,7-triazacyclononane) the macrocyclic polyamide ring anchors and supports the uranium centre from below, the pendant arms bind from above and the bulky tert-butyl substituents create a protected pocket of access to the uranium centre. This complex reacts with CO[60] at room temperature and atmospheric pressure to yield a pale brown residue. This product could only be isolated in a very poor yield (9.8 %) and displays a band in the infra-red spectrum at 2092 cm^{-1}, this value is significantly higher than those observed for the [U(η^5-Cp^R)$_3$] complexes and could not be confirmed as all attempts to synthesise labelled isotopomers failed. This was attributed to the lower purity of the labelled gases as [U({ArO}$_3$tacn)] reacts rapidly with O_2 or CO_2 to form the oxo-bridged dimer [(U({ArO}$_3$tacn))$_2$(μ-η^1:η^1-O)], which was the only product isolated from the labelling studies.

X-ray single crystal diffraction studies of [(U({ArO}$_3$tacn))$_2$(μ-η^1:η^1-CO)] revealed the μ:$\eta^1\eta^1$-CO binding mode, unprecedented in uranium chemistry but as the CO fragment lies on a crystallographic inversion centre, no reliable CO distances could be obtained. The bridging CO was modelled as an asymmetric U-OC-U with a shorter U-C interaction and a longer U-O interaction. As the analogous bridging dinitrogen complex could not be synthesised, even at *ca*. 80 psi N_2, the assignment of the bridging CO atoms is unambiguous. The uranium out-of-plane shift within (ArO)$_3$tacn ligand system can be used as an indication of the U-L$_{ax}$ interactions and oxidation state of the uranium. In this case the uranium is situated 0.38 Å below the trisaryloxide plane, this value is between the 0.32 Å observed in the uranium(IV) complex [(U({ArO}$_3$tacn))$_2$(μ-η^1-N$_3$)]

and the 0.44 Å found in the uranium(III) acetonitrile adduct [U({ArO}$_3$tacn)(η^{1-}NCMe)].[61]

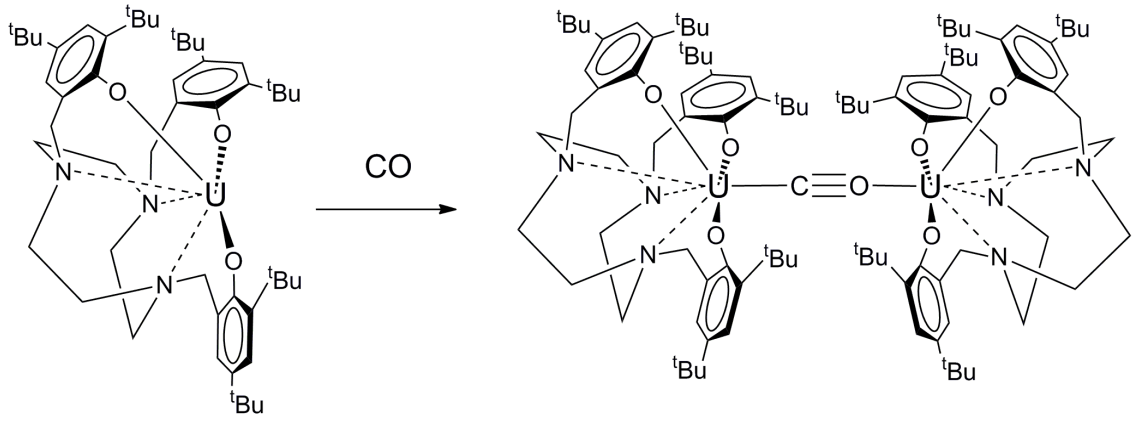

Figure 5: Reaction of [U({ArO}$_3$tacn)] with CO

This monoanionic product of a one election reduction of CO is thought to be formed by nucelophilic attack of a charge-separated U(IV)-$CO^{\cdot-}$ species on the coodinatively unsaturated U(III) species. Charge-separated character had been observed by Anderson in the complex [(η^5-Cp^{Me5})$_2$(THF)Yb(μ-η^1:η^1-OC)Co(CO)$_3$], the product of the reaction of [Yb(η^5-Cp^{Me5})$_2$(OEt$_2$)] with [Co$_2$(CO)$_8$] and the charge disparity thought to increase the likelihood of further reactivity of the bridging CO towards nucleophilic or electrophilic reagents.[62] No further chemistry has been reported for the [(U({ArO}$_3$tacn))$_2$(μ-η^1:η^1-CO)] complex, though the formation of two U(IV) centres might have been thought to be energetically favourable. However, when the uranium(IV) terminal azido complex [(U({ArO}$_3$tacn))$_2$(η^1-N$_3$)] (not synthesised directly from [U({ArO}$_3$tacn)]) was reacted with an equimolar amount of

[U({ArO}$_3$tacn)] the result was the azo-bridged complex [(U({ArO}$_3$tacn))$_2$(μ-η^1:η^3-N_3)], which has an out-of-plane-shift that is essentially identical to that observed for [(U({ArO}$_3$tacn))$_2$(μ-η^1:η^1-CO)].

The closely related [U({^{Ad}ArO}$_3$tacn)][63] (^{Ad}Ar = 3-tert-butyl-5-adamantylbenzyl, tacn = 1,4,7-triazacyclononane) has no reported reactivity with CO, even though both complexes react with CO_2,[60,64] it is unclear why the CO could not coordinate to the metal centre. In the U(V) imido complexes [U({^{R}ArO}$_3$tacn)(NSiMe$_3$)][65] (R= ^{t}Bu, Ad) it is the bulkier complex that reacts with CO to form [U({^{Ad}ArO}$_3$tacn)(NCO)], this is however attributable to bent nature of the imido unit in [U({^{Ad}ArO}$_3$tacn)(NSiMe$_3$)], whereas the [U({ArO}$_3$tacn)(NSiMe$_3$)] contains a linear imido unit and does not react with CO.

1.2.2 Reductive coupling of CO:

Bercaw, following the discovery that the reaction of $[Ti(\eta^5\text{-}Cp^{Me5})_2]$ with CO to form $[Ti(\eta^5\text{-}Cp^{Me5})_2(CO)_2]$ was irreversible,[66] showed that $[Zr(\eta^5\text{-}Cp^{Me5})_2H_2]$ was capable of stoichiometerically reducing CO.[67] Further work[68] showed that the reaction of

$[Zr(\eta^5\text{-}Cp^{Me5})_2H_2]$ with CO at - 80 °C yields an intermediate that on warming to - 50 °C forms the reductively coupled trans $[(Zr(\eta^5\text{-}Cp^{Me5})_2H)_2(\mu\text{-}\eta^2\text{-}OCHCHO)]$ in a 95 % yield. The intermediate was proposed to be a formyl species formed by the migratory insertion of the CO into one of the Zr-H bonds, although this is a thermodynamically unfavourable process for the transition metals.[35] In the case of the early transition metals the proposed η^2 coordination (by analogy to the acyl) of the formyl would result in stabilisation of the metal centre by donation from the oxygen lone-pair, leading to carbene-like character in the intermediate and this combined with the oxophilicity of the metal centre would overcome the unfavourable thermodynamics.

The combination of Lewis acidity, multiple metal centres and conjunctive M-O and M-C bonding has extended the scope of reductive coupling of CO by transition metals but they remain relatively few.[69] Work by Lippard *et al.*[70] has produced reductively coupled CO, CNR and cross-coupled species using high-coordinate group six metals (Mo and W), these reactions are observed to proceed stepwise, though the mechanism of the final carbene-carbyne coupling step was not able to be elucidated. Wayland *et al.* demonstrated the ability of porphyrinogen complexes of rhodium to reduce CO,[71] the CO reaction products of which were dependant on the stability of the metallo-radical $Rh^{II.}$ species and the size of the ligand.

Examples of the insertion of CO into U-X (X = alkyl or hydride) and U-N bonds are known for higher-valent uranium systems, but few examples result in C-C bond formation.[72,73] The reaction of $[U(\eta^5\text{-}Cp)_4]$ with CO in d_6-benzene was reported to result in the insertion of CO into the U-C bond of the Cp ligand to give the dimeric bridging structure $[(U(\eta^5\text{-}Cp)_2)(\mu\text{-}\eta^2\text{:}\eta^1\text{-}CO(C_5H_4))_2]$.[74] This preferential insertion into the M-C bond is more usually observed in 4f complexes, for example $[Nd(\eta^5\text{-}Cp^{Me5})_3]$ which is isoelectronic with $[U(\eta^5\text{-}Cp^{Me5})_3]$ reacts with CO to form a non-classical carbonium ion complex, $[Nd(\eta^5\text{-}Cp^{Me5})_3(O_2C_7Me_5)]$[75] by insertion of the CO into a Nd-C($\eta^1\text{-}Cp^{Me5}$) bond, reactivity also found for $[Sm(\eta^5\text{-}Cp^{Me5})_3]$.[75] This is a rare example of a direct experimental comparison between the reactivity of isomorphous complexes of the $4f^3$ and $5f^3$.

The reductive chemistry of the divalent lanthanides, however, has provided examples of reactivity, which are relevant in this context. In 1981 Evans reported the first soluble divalent lanthanide complex synthesised by the vapourisation of samarium metal into a mixture of pentamethylcyclopentadiene in hexane in a rotary metal vapourisation reactor.[76] The resultant complex $[Sm(\eta^5\text{-}Cp^{Me5})_2(THF)_2]$ reacts with 1 atm CO at room temperature, but due to the complexity of the reaction and the number of species formed, the products remained unidentified. Multiple products are also formed from the reaction of $[Sm(\eta^5\text{-}Cp^{Me5})_2(THF)_2]$ at 90 psi CO but when the reaction was carried out in minimum THF in a Fischer-Porter reaction vessel a crystalline product formed over 3 days in a 20 % yield.[77]

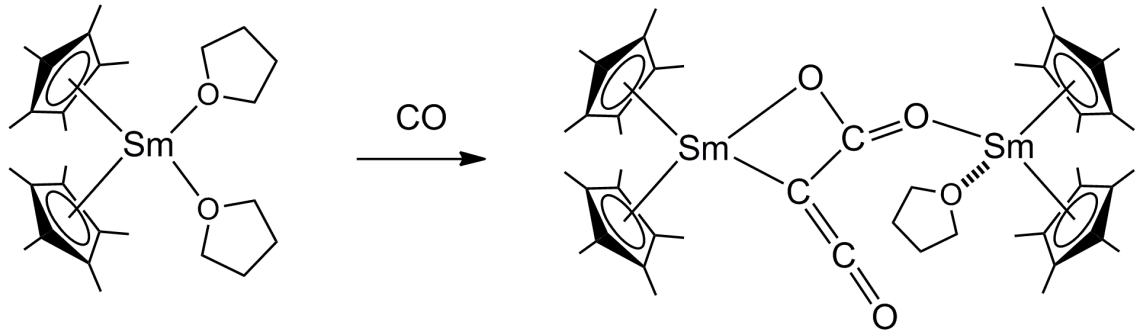

Figure 6: Reaction of $[Sm(\eta^5\text{-}Cp^{Me5})_2(THF)_2]$ with CO

Single crystal X-ray diffraction showed the product to be the dimeric species $[(Sm(\eta^5\text{-}Cp^{Me5})_2)[\mu\text{-}\eta^1\text{:}\eta^2\text{:}\eta^1\text{-}O_2CCCO](Sm(\eta^5\text{-}Cp^{Me5})_2(THF))]$ each monomer bridged by a ketenecarboxylate unit and the dimer held together by O(3)-Sm(1') donor bonds. The C(2)-C(3)-O(3) distances and angles in the $(O_2CCCO)^{2-}$ unit are comparable to those found in other metal ketene or dimetal ketene carboxylic acid complexes, respectively.[78] The Sm(2)-O(2) distance of 2.25(1) Å is consistent with a single bond but the C(1)-O(2), 1.31(2) Å interaction is shorter than a normal C-O single bond. The Sm(1) centre is bound to the O(1) by 2.39(1) Å, this value is within the range found for O-Sm(III) donor bonds. The Sm(1)-C(2) interaction of 2.77(2) Å is longer than previously observed Sm(II)-C distances. The FTIR spectrum shows a strong absorption at 2100 cm^{-1} in the ketene region but the insolubility and paramagnetism of the complex prevented useful NMR data from being obtained.

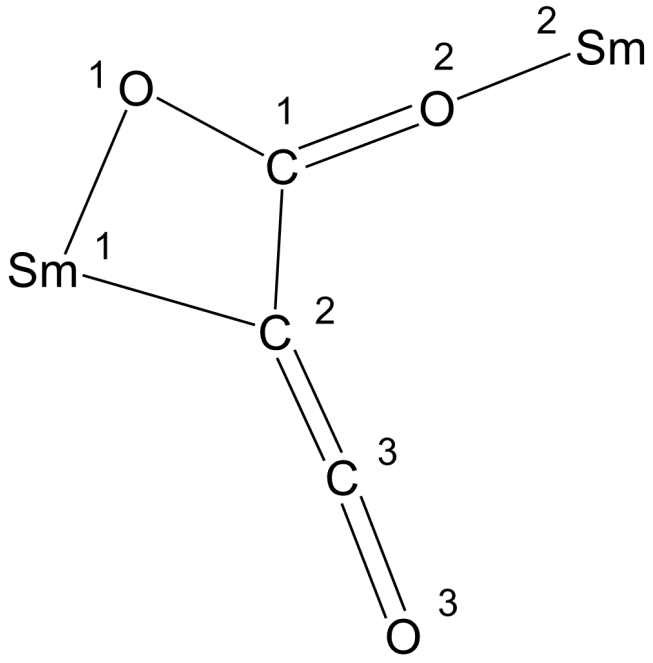

Figure 7: Ketenecarboxylate core including the samarium centres

The ketenecarboxylate skeleton is the product of two Sm(II)-Sm(III) one electron reductions though the mechanism of this transformation is unclear. More recently Evans has reported that when the $[(La(\eta^5\text{-}Cp^{Me5})_2(THF))_2(\mu\text{-}\eta^2\text{:}\eta^2\text{-}N_2)]$ complex is reacted with CO under the same conditions as $[Sm(\eta^5\text{-}Cp^{Me5})_2(THF)_2]$ the analogous lanthanum ketenecarboxylate complex $[(La(\eta^5\text{-}Cp^{Me5})_2)[\mu\text{-}\eta^1\text{:}\eta^2\text{:}\eta^1\text{-}O_2CCCO](La(\eta^5\text{-}Cp^{Me5})_2(THF))]$ is formed in a similar yield.[79] Its molecular structure exhibits the same bridging structure and the parameters reflect a similar divergence from the norm, which provides evidence for significant delocalisation in the ketenecarboxylate unit. The increased solubility of the lanthanum ketenecarboxylate, the diamagnetism of Ln^{3+} and the synthesis of the ^{13}C-labelled complex enabled the observation and assignment of the ketenecarboxylate moiety by $^{13}C\{^1H\}$ NMR.

The $^{13}C\{^{1}H\}$ NMR spectrum displays three doublets of doublets at 23.4, 129.7 and 167.2 ppm in d_8-thf. The resonances centred at 23.4 ppm displayed two different strong couplings, $^{1}J_{CC}$ = 103 and 165 Hz and were assigned to C^2 and confirmed by a 2D $^{13}C/^{13}C$ COSY experiment. The other two sets of resonances centred at 129.7 and 167.2 ppm display similar couplings of $^{1}J_{CC}$ = 165, $^{2}J_{CC}$ =16 Hz and $^{1}J_{CC}$ = 103, $^{2}J_{CC}$ = 16 Hz, respectively. These resonances were assigned as the carboxylate (C^1),167.2 ppm and the carbonyl (C^3), 129.7 ppm on the basis of chemical shift. Atom C^3 might be expected to have a stronger coupling to C^1 as they are formally connected by a double bond.

High-pressure solution IR studies on the reaction of [Sm(η^5-Cp^{Me5})$_2$] with CO in methylcyclohexane, failed to show anything other than a very weak absorption at

2153 cm^{-1}, even when the specific experimental conditions were replicated.[80] In the light of this result and observation that the experimental conditions are very sensitive it was suggested that the [(Sm(η^5-Cp^{Me5})$_2$)[μ-η^1:η^2:η^1-O_2CCCO](Sm(η^5-Cp^{Me5})$_2$(THF))] complex was not the product of the reaction with CO alone. The IR spectrum of [(La(η^5-Cp^{Me5})$_2$)[μ-η^1:η^2:η^1-O_2CCCO](La(η^5-Cp^{Me5})$_2$(THF))] displays an absorption at 2142 cm^{-1} and a lower energy shoulder, close to the value of free CO. Confirmation that the observed absorption does arise from the ketenecarboxylate was provided by the disappearance of the band at 2142 cm^{-1} and an absorption at 2071 cm^{-1} with a shoulder of lower energy, in the IR spectrum of the ^{13}C-labelled complex. The IR and NMR data of the isotopomers provide compelling evidence that the ketenecarboxylate is the product of reductive coupling of CO.

The formation of the ketenecarboxylate requires the cleavage of a C-O bond. The dissociation of CO to metal oxides and carbides is thought to be the initial step in heterogeneous Fischer-Tropsch catalysis, followed by homologation, but there are only a few examples of cleavage of CO by homogeneous systems that yield homologated products.[81] Direct dimerisation of CO is highly thermodynamically unfavourable and all neutral cyclic oligomers of CO, C_nO_n, are calculated to be unstable at standard temperatures and pressures.[82]

The mixed-sandwich uranium(III) complex [U(η^8-C_8H_6{Si^{i}Pr$_3$-1,4}$_2$)(η^5-Cp^{Me5})(THF)] reacts with CO at ambient pressures to yield a dimeric U(IV) complex in a 40 % isolated yield.[83] The molecular structure was determined as [(U(η^8-C_8H_6{Si^{i}Pr$_3$-1,4}$_2$)(η^5-Cp^{Me5}))$_2$(μ-η^1:η^2-C_3O_3)], bridged by the reductively homologated CO trimer known as the deltate dianion. This reaction is the first example of selective, spontaneous, low-temperature reductive homologation of CO and provides the first crystallographic study of a deltate salt.

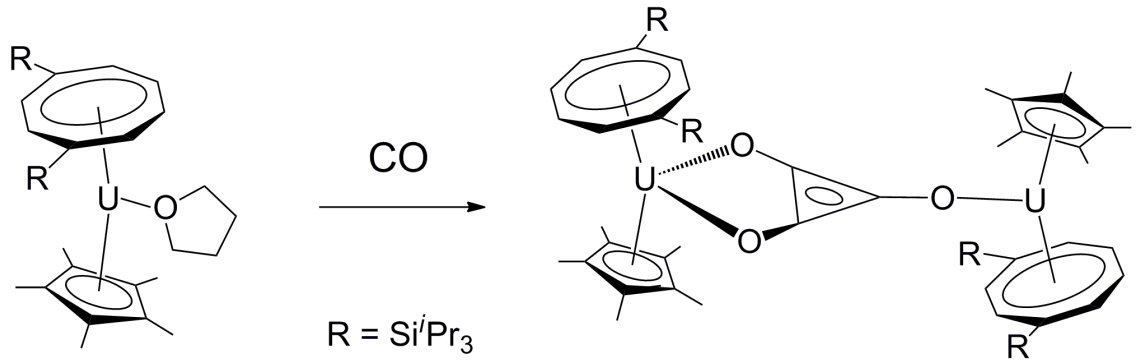

Figure 8: Reaction of [U(η^{8}-C_8H_6{Si^{i}Pr$_3$-1,4}$_2$)(η^{5}-Cp^{Me5})(THF)] with CO

The average metal to ligand bond distances are slightly longer for the η^2-bound uranium centre than the η^1-bound uranium centre. However, the change in oxidation state is not reflected in the overall structural parameters. This was also seen in the reaction of the related U(III) mixed-sandwich complex [U(η^{8}-C_8H_4{Si^{i}Pr$_3$-1,4}$_2$)(η^{5}-Cp^{Me5})] with dinitrogen,[84] in which the dianionic ligand is the substituted pentalenyl ligand rather than the substituted cyclooctatetrenyl ligand. There is no change in structural parameters between the parent U(III) complex and the U(IV) complex

[(U(η^{8}-C_8H_4{Si^{i}Pr$_3$-1,4}$_2$)(η^{5}-Cp^{Me5}))$_2$(μ-η^{2}:η^{2}-N_2)], this was attributed to steric crowding in the U(IV) dimer.

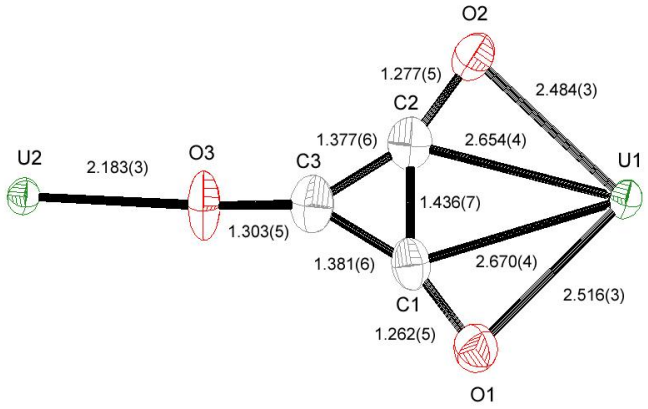

Figure 9: Core stucture of $[(U(\eta^{8}\text{-}C_8H_6\{Si^{i}Pr_3\text{-}1,4\}_2)(\eta^{5}\text{-}Cp^{Me5}))_2(\mu\text{-}\eta^{1}\text{:}\eta^{2}\text{-}C_3O_3)]$ including the uranium centers

The planar $C_3O_3^{2-}$ unit is situated slightly above U1 (0.09 Å) and below U2 (0.17 Å) and although all the U-O distances are long, the U2-O3 2.183(3) Å distance is much shorter than U1-O1 2.516(3) Å and U1-O2 2.484(3) Å. Complementary to which, the C3-O3 distance is longer than C1-O1 and C2-O2 distances, and their distances are between the typical values for a single and a double bond. The C_3 skeleton is distorted, the C3-C2 and C3-C1 distances are significantly shorter than C2-C3, which shows some interaction with U1.

DFT calculations were performed to further investigate the bonding within the structure using the unsubstituted model complex $[U_2(\eta^{8}\text{-}C_8H_6)_2(\eta^{5}\text{-}Cp)_2(\mu\text{-}\eta^{1}\text{:}\eta^{2}\text{-}C_3O_3)]$. There was found to be good agreement between the experimental and the calculated bond distances and angles, and the calculated structure reproduced the distortion in the C_3 skeleton and the C-O and U-O patterns described above. The calculations suggest that each uranium is best described as having a $5f^2$ configuration, consistent with U(IV).

Fragment analysis was also carried out on ($U(C_8H_6)(Cp)$) and (C_3O_3), and shows that on binding to the uranium, the primary interaction is the donation of electron density from the oxygen atoms of the $(C_3O_3)^{2-}$ to the uranium atoms. There is, however, a secondary, more complex interaction that occurs between the lengthened C2-C3 bond and a uranium f-orbital. The molecular orbital of the model complex comprises a bonding interaction between U1 and O1, O2 and also a bonding interaction between U1 and C1, C2. The result is a weakening of the C1-C2 bond and a strengthening of the C1-O1 and C2-O2 bonds. The agostic C-C interaction would appear responsible for the distortion of the C_3 skeleton.

This is the first example of agostic bonding of this type for an f-element, though due to the quantity of highly-nodal, unoccupied f-orbitals uranium complexes may be well-suited to these interactions. The C-C σ-orbitals of three-membered carbocycles are destabilised by the non-optimal s and p overlap in the strained triangular skeleton.[85] The agostic interaction may contribute to the stabilisation of the deltate dianion and rationalise the reaction with CO under such facile conditions. It is less likely that the less diffuse 4f orbitals would be able to support agostic bonding, though Evans has suggested that the ketenecarboxylate may be formed by the ring-opening and reorganisation of a deltate intermediate.[77]

The ^{1}H NMR spectrum of $[(U(\eta^8\text{-}C_8H_6\{Si^iPr_3\text{-}1,4\}_2)(\eta^5\text{-}Cp^{Me5}))_2(\mu\text{-}\eta^1\text{:}\eta^2\text{-}C_3O_3)]$ at room temperature is fully fluxional and so does not reflect the asymmetry of the solid-state structure. The process of equilibration of the deltate was studied by $^{13}C\{^1H\}$ NMR using the labelled complex $[(U(\eta^8\text{-}C_8H_6\{Si^iPr_3\text{-}1,4\}_2)(\eta^5\text{-}Cp^{Me5}))_2(\mu\text{-}\eta^1\text{:}\eta^2\text{-}^{13}C_3O_3)]$,

which displays a singlet, $\nu_{1/2}$ = 12 Hz at 225 ppm at 25 °C. Cooling to – 100 °C, resulted in the expected change in chemical shift for a paramagnet and significant broadening, but no evidence of the stopping of the fluxional process. It is therefore unclear whether the mechanism involves the motion of O1 (or O2) between the uranium centres or a rotation involving all three oxygen atoms.

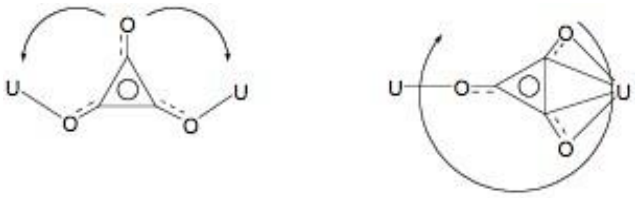

Figure 10: Possible modes of equilibration of the deltate dianion

The oxocarbon series $(CO)_n^{2-}$ were indentified and classified as such by West[86] in the 1960s, and their aromatic structure and potential relevance in molecular transformations of CO have been the subject of investigation.[87] The reductive coupling of CO by the U(III) complex described above is remarkable, as prior to which, trace amounts of labelled lithiated deltate, assigned on the basis of a $^{13}C\{^1H\}$ NMR shift of 140 ppm, in a complex mixture of products, was the only evidence for its synthesis directly from CO.[88] The squarate dianion can be synthesised in *ca.* 35% yield by high-pressure (300-400 bar) electrochemical methods in polar solvents,[89] further work showed that the reaction requires a minimum 10 bar overpressure.[90] In a similar high-pressure system the mechanism is proposed to proceed by concerted reductive cyclisation of surface-bound CO, after adsorption onto the cathode, followed by desorption.[91] Interestingly no

evidence of squarate salts has been reported from the high-pressure reaction of CO with alkali metals.

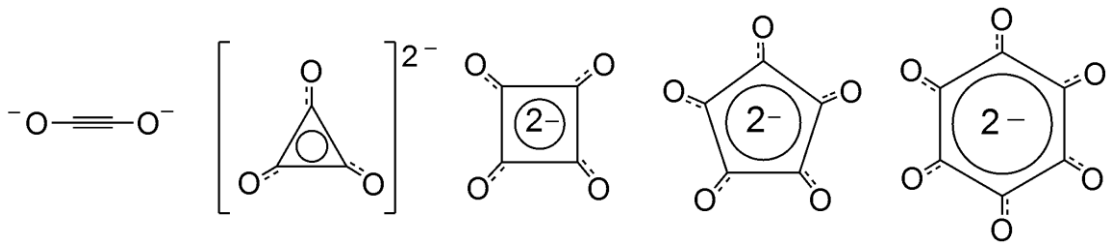

Figure 11: Oxocarbon dianion series: $C_2O_2^{2-}$ ynediolate, $C_3O_3^{2-}$ deltate, $C_4O_4^{2-}$ squarate, $C_5O_5^{2-}$ croconate, $C_6O_6^{2-}$ rhodizonate

As has been intimated, a change in the ligand environment, be it steric or electronic may have a marked effect on the reactivity of the complex. The deltate dianion is the second in the series of cyclic aromatic dianions, the oxocarbons. It was thought that a change of the Cp^{Me5} ligand for the smaller Cp^{Me4H} ligand, might allow access to larger members of the oxocarbon series, while maintaining the desirable mixed-sandwich architecture. Quite apart from the small decrease in the steric bulk, caused by the loss of a methyl group, disparity in the reactivity of complexes containing the Cp^{Me5} or Cp^{Me4H} ligands is known. In low-valent uranium chemistry more diverse reactivity is reported for the bulkier $[U(\eta^5\text{-}Cp^{Me5})_3]$ than $[U(\eta^5\text{-}Cp^{Me4H})_3]$, this includes sterically induced reduction, ring-opening of THF and binding of dinitrogen.[47,92] Both complexes form CO adducts[43,47] and it is the $[U(\eta^5\text{-}Cp^{Me4H})_3(CO)]$ complex that contains the more 'activated' CO (*vide supra*).

The exposure of $[U(\eta^8\text{-}C_8H_6\{Si^iPr_3\text{-}1,4\}_2)(\eta^5\text{-}Cp^{Me4H})(THF)]$ to 1 bar of CO at – 30 °C, yielded the dimeric uranium complex $[(U(\eta^8\text{-}C_8H_6\{Si^iPr_3\text{-}1,4\}_2)(\eta^5\text{-}Cp^{Me4H}))_2(\mu\text{-}\eta^2\text{:}\eta^2\text{-}C_4O_4)]$ as a red crystalline solid (66 %).[93] The structure was determined and is bridged by the squarate dianion, next in the oxocarbon series, the product of reductive tetramerisation of CO. The U-ligand centroid distances are similar to those found in the deltate complex, the $C_4O_4^{2-}$ is likewise planar, though the uranium centres are further displaced above and below the plane by 0.43 Å. The U-O distances are identical to those found in the η^2-bound half of the uranium deltate complex, however, the U-C_{ave} distance is considerably longer at 3.045 Å (shortened by the agostic interaction to 2.662 Å in the deltate complex). The O-C-C angle of 127° in the squarate complex is significantly more acute than the O-C-C_{ave} of 159° in the deltate complex, this may prevent interaction between the C-C and the uranium metal centers. There are no notable distortions to the geometry or bonding of the squarate unit. The $^{13}C\{^1H\}$ NMR spectrum of the ^{13}C-labelled squarate complex in d_8-thf shows a broad resonance at – 111.4 ppm for the $^{13}C_4O_4^{2-}$ unit. The very large difference in chemical shift between the deltate (225 ppm) and the squarate complex is of note. However, the paramagnetism of the complex precludes a rationalisation of the chemical shift.

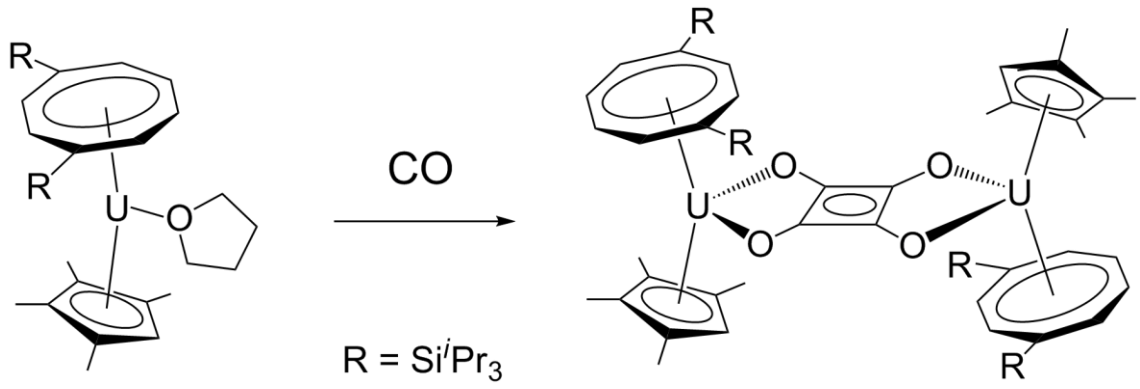

Figure 12: Reaction of [U(η^8-C_8H_6{Si^{i}Pr$_3$-1,4}$_2$)(η^5-Cp^{Me4H})(THF)] with CO

A DFT study and fragment analysis of the model complex [U_2(η^8-C_8H_6)$_2$(η^5-Cp)$_2$(μ-η^2:η^2-C_4O_4)] were undertaken. The experimental and calculated data were in excellent agreement and confirm the U(IV) oxidation state. Gas-phase SCF energies of the model complex η^2:η^2-bound and η^1:η^1-bound show that the η^2:η^2-bound structure is approximately 127 kJ mol^{-1} more stable and that the binding of the fourth CO to [U_2(η^8-C_8H_6)$_2$(η^5-Cp)$_2$(μ-η^1:η^2-C_3O_3)] is favourable by 136 kJ mol^{-1}.[94] The gas-phase SCF energies for the η^2:η^2-bound $C_5O_5^{2-}$ croconate and η^2:η^2-bound $C_6O_6^{2-}$ rhodizinate were also calculated to be lower in energy than any combination of η^1-bound modes[95] and are illustrated below. The calculations suggest that the 5- and 6-membered carbocycles may be accessible. The unsubstitued complex [U(η^8-C_8H_6)(η^5-Cp)(THF)] and [U(η^8-C_8H_6{Si^{i}Pr$_3$-1,4}$_2$)(η^5-Cp^{Me})(THF)], using the smaller Cp^{Me} ligand, were synthesised and reacted with CO but although both underwent a colour change indicative of reaction, in neither case were the products able to be characterised.[96]

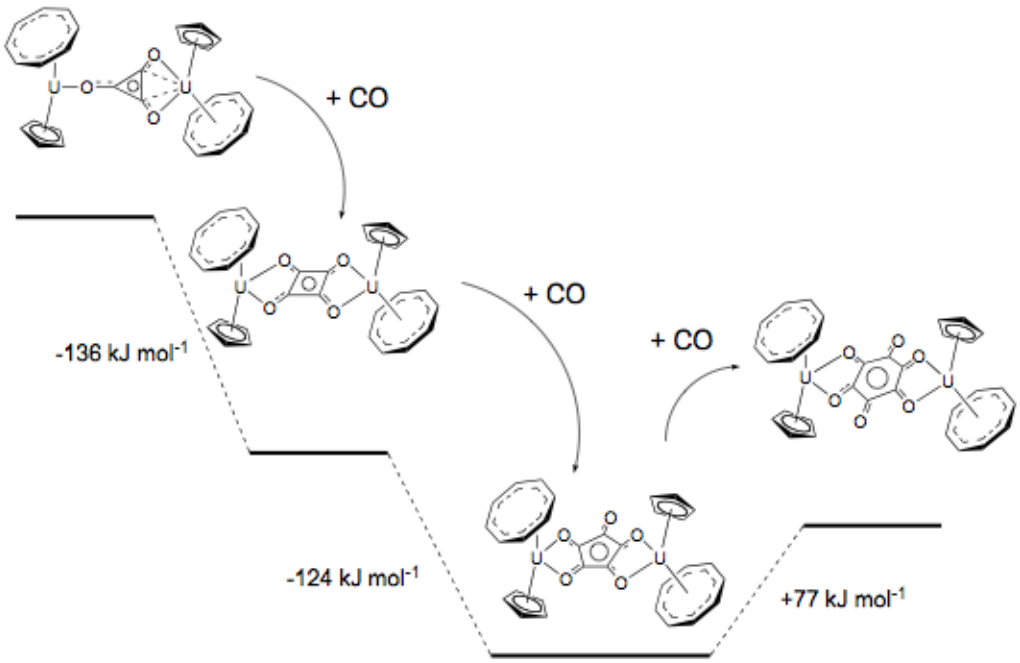

Figure 13: Gas-phase SCF energies of U(IV) oxocarbons

Gmelin isolated salts of croconate and rhodizonate as early as 1825[97] but it was Liebig that demonstrated in 1834 that they could be synthesised directly from CO from the reaction of molten potassium at 180 °C in the presence of CO.[98] The black product observed by Liebig was extremely air and moisture sensitive, and explosive on contact or decomposition. The experimental difficulties and the very reactive nature of the products meant that although further research in this area was undertaken and no definitive formulation of the product or products was possible.[99] In the early 1960s Weiss and Buechner, given a free hand at the newly created Cyanamid European Research Institute in Geneva, devised a relatively gentler set of conditions by bubbling CO through a solution of an alkali metal in liquid ammonia, until discolouration

occurred.[100] The products of the reactions were microcrystalline powders and their formulation remained unclear until powder diffraction methods were finally successful and revealed the molecular structure to be $[M_2(\mu\text{-}\eta^1\text{:}\eta^1\text{-}C_2O_2)]$ (M = Na,[101] K, Rb, Cs), the ynediolate salt.[102] They also repeated the experiment under Liebig's conditions and found that a reaction temperature of 62.3 °C yielded ynediolate and another compound[103] with the same empirical formula but a reaction temperature of 180 °C gives $[K_6O_6C_6]$ as the major product.[104] On heating the $[K_2(C_2O_2)]$ was shown to cylotrimerise and was isolated as $[K_6(C_6O_6)]$, which oxidises on exposure to air to the rhodizonate salt.[105]

There is no definitive mechanism for the formation of oxocarbons from the various reductions of CO. Electrochemical studies[106] suggest that the $(C_2O_2)^{2-}$ may be formed either by the dimerisation of $CO^{\cdot}$ radicals or by the one-electron reduction of $(C_2O_2)^{\cdot-}$, resultant of the coupling of CO^- and CO. Larger oxocarbons could then be formed by the addition of neutral CO to the ynediolate. The experimental evidence suggests the specific product formed is determined by the specific reaction conditions. The isolation of the ynediolate or $[K_6O_6C_6]$ as the main product, as a result of varying the reaction temperature suggests that the reaction may proceed *via.* trimerisation of the ynediolate, followed by oxidation to the rhodizonate. There is also the evidence in the electrochemical synthesis of $(C_4O_4)^{2-}$, in which no intermediates were observed, suggestive of a concerted pathway.[91]

The ynediolate provides a logical entry into the study of the mechanism of the reductive coupling of CO. To this end the aforementioned complex $[U(\eta^8\text{-}C_8H_6\{Si^iPr_3\text{-}1,4\}_2)(\eta^5\text{-}$

Cp^{Me5})(THF)] was desolvated by heating at 90 °C under high-vacuum (10^{-5} mbar). The desolvation of the U(III) complex increases it's solubility and obviates the presumably initial dissociation of the THF. The reaction of the desolvated complex [U(η^8-C_8H_6{Si^{i}Pr$_3$-1,4}$_2$)(η^5-Cp^{Me5})] with a sub-stoichiometric 0.9 equivalents of ^{13}CO in d_8-toluene at -78 °C revealed a new labelled product in the $^{13}C\{^1H\}$ NMR spectrum with a shift of 313 ppm, together with small amounts of the deltate complex.[107] The new complex was able to be separated by fractional crystalisation from diethyl ether and the isotopic distribution of the molecular ion at 1637 amu was correct for [U(η^8-C_8H_6{Si^{i}Pr$_3$-1,4}$_2$)(η^5-Cp^{Me5})]$_2$[(^{13}CO)$_2$].

The existence of a C-C bond in the (^{13}CO)$_2$ unit was tested by repeating the reaction with a 50/50 mixture of ^{12}CO/^{13}CO. This resulted in a $^{13}C\{^1H\}$ NMR spectrum in which the new peak displayed a secondary isotopic shift of 0.18 ppm. These findings were confirmed by single crystal X-ray diffraction studies and the molecular structure shown to be [U(η^8-C_8H_6{Si^{i}Pr$_3$-1,4}$_2$)(η^5-Cp^{Me5})]$_2$(μ-η^1:η^1-C_2O_2)]. The structure contains an essentially linear bridging ynediolate with a very short C-C distance of 1.177(12) Å comparable to the 1.19 ± 0.3 Å found in [$Na_2(C_2O_2)$][101]. This is the first synthesis of the ynediolate from reductive coupling of CO by an organometallic complex.

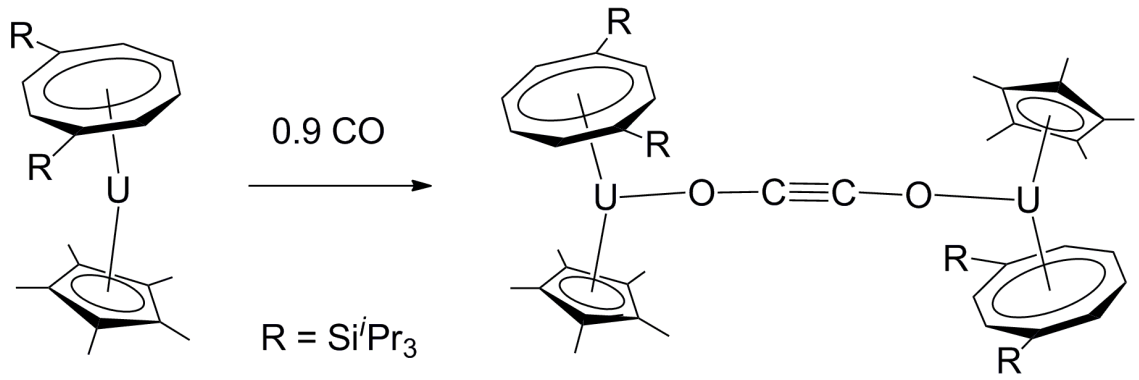

Figure 14: Reaction of [U(η^{8}-C_8H_6{Si^{i}Pr$_3$-1,4}$_2$)(η^{5}-Cp^{Me5})] with 0.9 equivalents of CO

When the labelled complex [U(η^{8}-C_8H_6{Si^{i}Pr$_3$-1,4}$_2$)(η^{5}-Cp^{Me5})]$_2$[(μ-η^{1}:η^{1}-$^{13}C_2O_2$)] was reacted with excess ^{13}CO, no further reaction was observed even after heating at 60 °C for 3 days, as determined by ^{13}C{^{1}H} NMR spectroscopy. This suggests that the sequential addition of CO to the ynediolate to form either the deltate or squarate complexes is not the correct mechanism for this system. Solution IR of the reaction mixture of [U(η^{8}-C_8H_6{Si^{i}Pr$_3$-1,4}$_2$)(η^{5}-Cp^{Me5})] and 1 ^{12}CO in d_8-toluene exhibited an absorption at 1920 cm^{-1} (shifted to 1882 cm^{-1} with ^{13}CO) in the 1880-1988 cm^{-1} range observed for the tris-cyclopentadienyl uranium(III) carbonyls (Table 1). The value observed for the [U(η^{8}-C_8H_6{Si^{i}Pr$_3$-1,4}$_2$)(η^{5}-Cp^{Me5})(CO)] is closer to the 1922 cm^{-1} observed for the [U(η^{5}-Cp^{Me5})$_3$(CO)] than the 1880 cm^{-1} [U(η^{5}-Cp^{Me4H})$_3$(CO)], though both of those values are solid state measurements rather than solution, which has been seen to increase the ν_{CO}[46] by up to 13 cm^{-1}. The decrease in the value of the ν_{CO} would seem not to be an accurate indication of the likelihood of subsequent reactivity.

The CO absorption of the [U(η^8-C_8H_6{Si^{i}Pr$_3$-1,4}$_2$)(η^5-Cp^{Me5})(CO)] was seen to decay rapidly over 15 min at room temperature. This timescale is much shorter than the appearance of [U(η^8-C_8H_6{Si^{i}Pr$_3$-1,4}$_2$)(η^5-Cp^{Me5})]$_2$(μ-η^1:η^1-$^{13}C_2O_2$)] by $^{13}C\{^1H\}$ NMR under the same conditions, which is not observed until several hours have passed. These observations suggest the formation of a relatively long-lived intermediate. A DFT study was carried out into the mechanism of the reaction to form the ynediolate complex. In this study all the ring substituents were replaced by hydrogen atoms and three minima were identified on a possible reaction pathway from [U(η^8-C_8H_6)(η^5-Cp)(CO)] to the ynediolate, the structures of which are shown below.

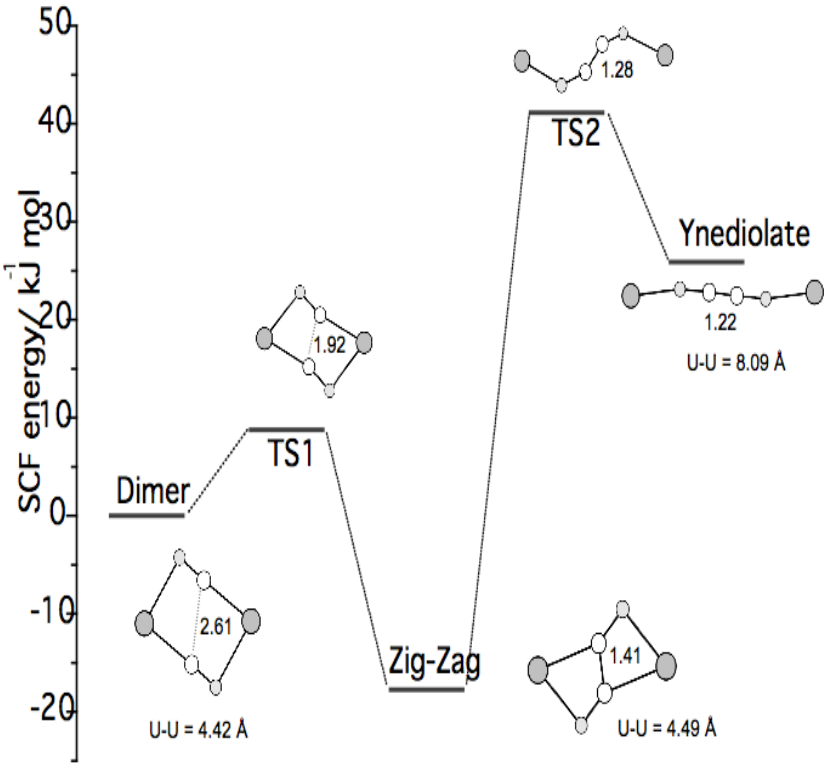

Figure 15: Reaction pathway for the formation of ynediolate

The first step is the dimerisation of the monocarbonyl, the CO oxygen atoms coordinate to opposing uranium atoms and the C-C bond distance is calculated to be 2.61 Å. There is no energetic barrier to the formation of the dimeric species. C-C bond formation then occurs to give the C_2O_2 unit the Zig-Zag, with a C-C distance of 1.41 Å and the retention of U-O bonding. The transition state TS1 between dimer and the Zig-Zag lies just 9 kJ mol^{-1} above the dimer, which suggests the formation of the Zig-Zag would be rapid. The core dimensions of the modelled ynediolate are close to the values observed experimentally. The TS2 between the Zig-Zag and the ynediolate has a larger energetic barrier of 59 kJ mol^{-1}, this is consistent with the slower formation of the ynediolate relative to the disappearance of the monocarbonyl. The calculated frequencies for the minima indicate that it is only the monocarbonyl that would display an identifiable CO band in the region above 1800 cm^{-1}. These findings are in keeping with the experimental data.

In the monocarbonyl, one of the three unpaired electrons is confined in a localised f-orbital and the other two have partial f and $_{CO}$ π^* character. The formation of the dimer, brings the carbon atoms close together and aligns the π^* orbitals for the C-C bond formation in the Zig-Zag. It was proposed that the Zig-Zag is the relatively long-lived intermediate in the reaction of uranium(III) mixed-sandwich complexes of the type $[U(\eta^8\text{-}C_8H_6\{Si^iPr_3\text{-}1,4\}_2)(\eta^5\text{-}Cp^R)]$ (R = Cp^{Me5}, Cp^{Me4H}) with excess CO, which depending on the steric constraints, reacts with a further molecule of CO to form the deltate complex or with a further two molecules of CO to form the squarate complex. In the absence of further CO, the Zig-Zag rearranges to give the ynediolate, by breaking the U-C bonds.

The gas phase energy of the ynediolate (- 5 *E*/kJ mol^{-1}) is calculated to be higher than that of the Zig-Zag (- 47 *E*/kJ mol^{-1}), which would suggest that the Zig-Zag should be the more stable of the two structures. It was suggested that the bulky substituents in the real complex destabilise the Zig-Zag relative to the ynediolate, resulting in its formation. This is not unreasonable given the role the steric environment is seen to play in the reactions of these mixed-sandwich complexes with CO. It was concluded that the uranium centre in this reaction not only coordinates and reduces the bound CO, but also acts as Lewis acid in binding to the oxygen atom of the second uranium-bound carbonyl, thus aligning the two molecules in a favourable orientation for C-C bond formation.

The low-valent uranium mixed-sandwich system has shown itself to be both capable of the reductive coupling of CO to form useful carbocyclic products and provided mechanistic insight into the process. The DFT studies complement the experimental results, rationalising the solid-state core structure of the deltate complex by means of a C-C agostic interaction with the uranium centre and by identifying a possible reaction intermediate.

1.2.3 Binding and Activation of N_2:

Dinitrogen is isoelectronic with CO but whereas CO is a strong π-acid, N_2 is both a weaker σ-donor and π-acceptor. This is because the π* orbital, although lower in energy than the CO π* orbital, is equally distributed over N^1 and N^2, resulting in a smaller M-N π* overlap. The binding of N_2 is less effective than CO and the back-donation is more important for stability of the M-N interactions. Nevertheless, dinitrogen complexes of most of the transition metals have been prepared. The bonding mode of the N_2 depends greatly on the specific metal centre(s), the oxidation state of the metal(s) and the choice of ligand environment. The binding modes known for N_2 are numerous but are generally divided into: end-on mononuclear or dinuclear, side-on dinuclear and rarely, side-on end-on dinuclear. The degree of activation of N_2, the result of electron density donation by the metal centre into the N_2 π*-orbitals, is determined by the lengthening of the N-N bond from the 1.098 Å distance and a decrease in the N-N stretching frequency of 2331 cm^{-1} found in the N_2 neutral diatomic.[108]

The first structurally characterised f-element complex of N_2, $[(Sm(\eta^5\text{-}Cp^{Me5})_2)_2(\mu\text{-}\eta^2\text{:}\eta^2\text{-}N_2)]$[109] and the first example of side-on dinuclear binding was reported by Evans in 1988 as a by-product of the metal vapour synthesis of the base free metallocene $[Sm(\eta^5\text{-}Cp^{Me5})_2]$. The Sm-N and the Sm-Cp distances and the ^{13}C NMR data were consistent with two Sm(III) centres implying a reduction of the N_2 unit but the N-N distance of 1.088(12) Å was found to be unchanged from free N_2. This contradictory result has not been fully rationalised. The reaction was found to be reversible, when

[(Sm(η^5-Cp^{Me5})$_2$)$_2$(μ-η^2:η^2-N_2)] was dissolved in toluene N_2 gas was evolved. It was also found that freshly sublimed [Sm(η^5-Cp^{Me5})$_2$] reacts in the solid state with N_2, albeit less efficiently, and that the exposure of [(Sm(η^5-Cp^{Me5})$_2$)$_2$(μ-η^2:η^2-N_2)] to high vacuum for 4 hrs regenerates [Sm(η^5-Cp^{Me5})$_2$]. VT ^{1}H NMR studies revealed that there is a temperature-dependant equilibrium between the two complexes in solution. At ambient temperature after exposure to N_2, the ratio of [Sm(η^5-Cp^{Me5})$_2$] to [(Sm(η^5-Cp^{Me5})$_2$)$_2$(μ-η^2:η^2-N_2)] is 40:1, the concentration of dinitrogen complex increases as the temperature decreases but complete conversion is not achieved (3.5:1 at - 20°C).

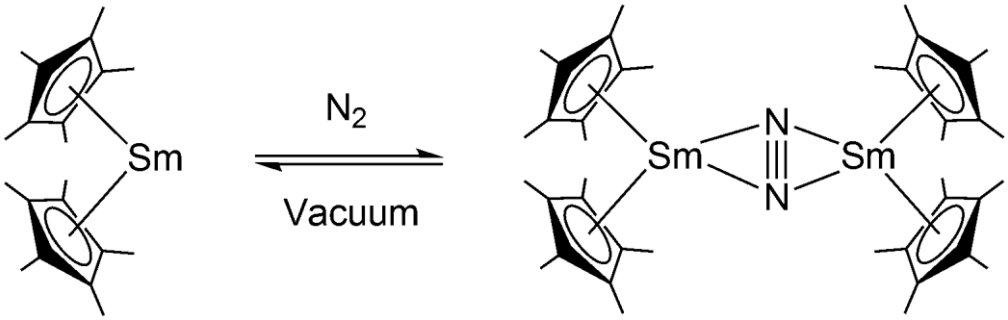

Figure 16: Reaction of [Sm(η^5-Cp^{Me5})$_2$] with N_2

The trivalent lanthanides also form analogous dinitrogen complexes if reduced in the presence of N_2, which led to the development of the LnZ_3/M (Z = $N(SiMe_3)_2$, Cp^{Me5}, M = K, KC_8) system.[110] These lanthanide dinitrogen complexes, which have been structurally characterised and contain the reduced $(N_2)^{2-}$ unit, are reducing agents and have been shown to reductively couple CO[77] (see section 1.2.3) and CO_2[111] (see section 1.2.5). Dinitrogen activation has also been demonstrated by complexes of the lanthanides with macrocyclic and porphyrinogen ligand systems.[112]

Actinide complexes have also been shown to completely cleave and reduce dinitrogen.[113] The reaction of the macrocyclic uranium salt [(Et_8-calix[4]tetrapyrrole)U(dme)][K(dme)] with potassium napthanalide under nitrogen yielded [{K(dme)(Et_8-calix[4]tetrapyrrole)U}$_2$(μ-η^1:η^1-NK)$_2$][K(dme)$_4$], a mixed valence U(IV)/U(V) complex in which the uranium centres are bridged by a two single N-K units, with U-N distances of 2.076(6) and 2.099(5) Å but no N-N interaction.

There is historical precedent for the reactivity of uranium complexes with N_2 that dates from 1909, as Haber's ammonia patent used a uranium catalyst.[114] However, uranium dinitrogen complexes are not numerous. The first example was synthesised by Scott and Roussel[115] in 1998, using the base-free complex [U(NN'$_3$)] (NN'$_3$= N(CH_2CH_2N{Si^{t}BuMe$_2$}$)_3$). Exposure of a purple solution of [U(NN'$_3$)] to N_2 in d_6-benzene led to colour change to red and the appearance of a new species by ^{1}H NMR. This reaction was quantitative when the pressure of N_2 was increased to over 1 atm, but when the sample was freeze-thaw degassed, [U(NN'$_3$)] was regenerated. The molecular structure was determined as [{U(NN'$_3$)}$_2$(μ-η^2:η^2-N_2)] with the N_2 unit in a side-on bridging mode with a bond distance of 1.109(7) Å unchanged from that in free N_2. The molecular pseudo-trigonal monopyramidal geometry is maintained and the only structural deviation from the parent complex is unexpectedly short U-N distances to the apical amido nitrogen atoms.

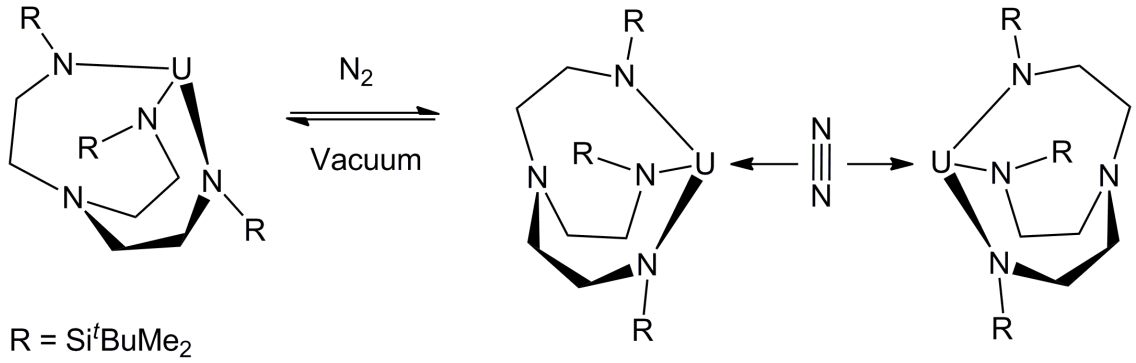

Figure 17: Reaction of [U(NN'$_3$)] with N_2

The spectroscopic data also did not suggest a formal change in oxidation state, although the magentisation data was consistent with both U(III) and U(IV). It was proposed that the N_2 is σ-bonded in a dative fashion to the uranium centres, however, DFT calculations carried out on the model complex [{$(NH_2)_3(NH_3)U$}$_2$(μ-η^2:η^2-N_2)], revealed the only significant U-N_2-U interaction to be 5f to π_g back-bonding.[116] This result was supported by further calculations, which also suggested that the optimised N-N bond distance would be significantly longer than in free dinitrogen accompanied by a significant reduction in the U-N(N_2) distance.[117] The short N-N and long U-N(N_2) distances observed experimentally, were rationalised by the bulky NN'$_3$ groups resulting in a steric barrier to U-N and U-U shortening in the real complex.

The role of the sterics in this complex is twofold: firstly, the lack of perturbation to the molecular geometry on N_2 binding and secondly the bulk of the ligand set in the dimer prevents the closer approach of the metal centres, resulting in less than optimal overlap and no increase in the N-N distance. It is of note that [U(NN'$_3$)][118] displayed reactivity towards 2-butyne, ^{t}BuNC and CO, but not H_2. However, though the oxidation to U(IV)

was evidenced by the UV spectra, the reaction products gave ambiguous spectroscopic data and were not able to be analysed crystallographically.[119]

This result was closely followed by the report by Cummins *et al.* of the isolation of heterodinuclear complexes of dinitrogen from the 1:1 reaction of $[U(N\{R\}Ar)_3(THF)]$ with either $[Mo(N\{^tBu\}Ph)_3]$ or $[Mo(N\{Ad\}Ar)_3]$ (R = $C(CD_3)_2CH_3$, Ar = 3,5-$C_6H_3Me_2$, Ad = 1-adamantyl) in the presence of N_2 in toluene at room temperature.[120] The reaction was determined to be quantitative by ^1H NMR within 20 min and the orange products isolated in 66 % and 64 % yields, respectively. The structures were determined as $[(N\{R\}Ar)_3U(\mu\text{-}N_2)Mo(N\{^tBu\}Ph)_3]$ and $[(N\{R\}Ar)_3U(\mu\text{-}N_2)Mo(N\{Ad\}Ar)_3]$. The more hindered $[(N\{R\}Ar)_3U(\mu\text{-}N_2)Mo(N\{Ad\}Ar)_3]$ complex displays a prominent ν_{NN} at 1568 cm^{-1}, which shifts to 1527 cm^{-1} in the $^{15}N_2$ complex. The ν_{NN} in $[(N\{R\}Ar)_3U(\mu\text{-}N_2)Mo(N\{^tBu\}Ph)_3]$ could not be identified but as the ν_{NN} of 1547 cm^{-1} was observed in 1527 when $^{15}N_2$ was used, the lack of the ν_{NN} in the unlabelled complex was attributed to overlap with aryl ring ν_{CC} absorption.

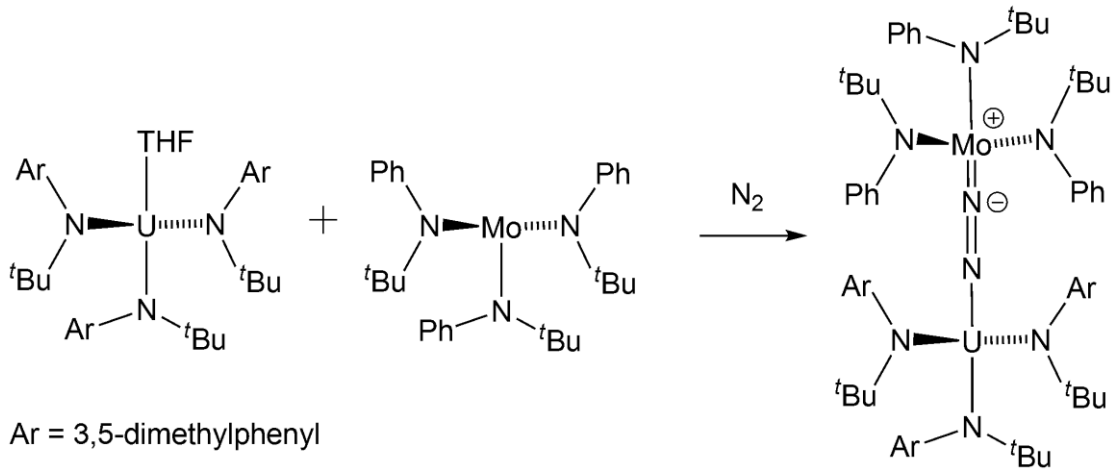

Figure 18: Reaction of $[U(N\{R\}Ar)_3(THF)]$ with $[Mo(N\{^tBu\}Ph)_3]$ under N_2

Both structures are bridged by N_2 in a linear mononuclear end-on fashion, with a N-N bond distance in $[(N\{R\}Ar)_3U(\mu\text{-}N_2)Mo(N\{^tBu\}Ph)_3]$ of 1.232(11) Å, 0.13 Å longer than in N_2. The U-N(N_2) distance of 2.220(9) Å is not significantly shorter than the average U-N_{amido} distance of 2.257 Å in the complex but is shorter than the typical U-amido distance of 2.28 Å. These distances, together with the Mo=N bond distance of 1.773(8) Å, suggest both metals are in the +4 oxidation state and the N_2 unit has been reduced. The uranium complex $[U(N\{R\}Ar)_3(THF)]$ does not display any reactivity towards N_2, whereas the reactivity of $[Mo(N\{^tBu\}Ph)_3]$ and derivatives thereof, is well documented.[121] It was therefore suggested that this reaction occurs via the trapping of the initial intermediate complex[122] $[(N_2)Mo(N\{^tBu\}Ph)_3]$ by $[U(N\{R\}Ar)_3(THF)]$, and that this is more efficient process than the reaction with further $[Mo(N\{^tBu\}Ph)_3]$.

The base-free mixed-sandwich complex [U(η^8-C_8H_4{Si^{i}Pr$_3$-1,4}$_2$)(η^5-Cp^{Me5})] was shown to react reversibly with N_2 at room temperature.[27] This complex utilises the less-studied pentalene ligand in the place of the COT ligand, though both have the same bulky silyl-substituents. Exposure to an atmospheric pressure of N_2 at room temperature generated a set of new resonances in the ^{1}H and ^{29}Si{^{1}H} NMR spectra. These resonances disappeared when the sample was freeze-thaw degassed. Even under 50 psi, the reaction did not proceed beyond 75 %. Crystals suitable for X-ray analysis were grown under 5 psi of N_2 and the structure was revealed as [(U(η^8-C_8H_4{Si^{i}Pr$_3$-1,4}$_2$)(η^5-Cp^{Me5}))$_2$(μ-η^2:η^2-N_2)].

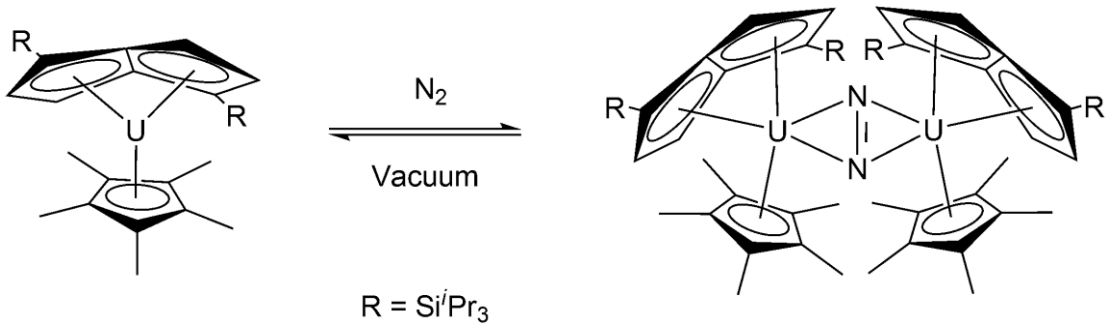

Figure 19: Reaction of [U(η^8-C_8H_4{Si^{i}Pr$_3$-1,4}$_2$)(η^5-Cp^{Me5})] with N_2

The structure is binuclear with the uranium centres bridged by side-on N_2. Curiously, the bulky (C_8H_4{Si^{i}Pr$_3$-1,4}$_2$)$^{2-}$ ligands are cis to each other, rather than the trans arrangement found in products of the related complex [U(η^8-C_8H_6{Si^{i}Pr$_3$-1,4}$_2$)(η^5-Cp^{Me5})] with CO[83]. This may be a result of the ability of the pentalene ligand to fold from the bridgehead around the metal centres. The N-N distance is 1.232 (10) Å,

lengthened from that in N_2 and identical to that found in [(N{R}Ar)$_3$U(μ-N_2)Mo(N{^{t}Bu}Ph)$_3$],[120] consistent with a reduced N_2^{2-} unit. The U-N distances of 2.401(8) – 2.423(8) Å are however comparable to those found in the [{U(NN'$_3$)}$_2$(μ-η^2:η^2-N_2)] (NN'$_3$= N(CH$_2$CH$_2$N{Si^{t}BuMe$_2$})$_3$)[115] (2.39 – 2.44 Å), in which the N_2 is not reduced. The difference in bond-order between these two complexes may be a consequence of the different frontier orbital geometries. Although the N=N stretch was predicted to be IR active, it was not observed either in the unlabelled or $^{15}N_2$ labelled complex.

The reversibility of the reaction was considered to be due to steric relief from the congestion in [(U(η^8-C$_8$H$_4${Si^{i}Pr$_3$-1,4}$_2$)(η^5-Cp^{Me5}))$_2$(μ-η^2:η^2-N_2)]; the formal change in oxidation state is also not reflected in the structural parameters. The complex [(U(η^8-C$_8$H$_4${Si^{i}Pr$_3$-1,4}$_2$)(η^5-Cp^{Me5}))$_2$(μ-η^2:η^2-N_2)] loses N_2 very easily both in solution and in the solid state, whereas [{U(NN'$_3$)}$_2$(μ-η^2:η^2-N_2)] although not thermally stable, was able to be characterised by elemental analysis. This is perhaps a reflection of the aforementioned 'pre-organisation' towards N_2 of the ligand environment in [U(NN'$_3$)].[115] The formal oxidation of U(III) to U(IV) and the reduction of N_2 to N_2^{2-} was supported by DFT calculations on the model complex [U$_2$(η^8-C$_8$H$_6$)$_2$(η^5-Cp)$_2$(μ^2-N_2)].[123] The calculated N-N, U-N distances and the U_2N_2 core structure were in excellent agreement with the values observed experimentally. The calculated U-C distances and the fold-angle of the pentalene ligands were found to deviate from those experimentally observed, indicating an extent of steric control acting on the real complex caused by the substituents on the ligands.

The [U(η^5-Cp^{Me5})$_3$] complex shows no perceptible reactivity with atmospheric pressure of N_2 but when pressurised to 80 psi, the solution was observed to darken and dark purple crystals formed in a 16 % yield.[92b] X-ray analysis revealed the structure to be [U(η^5-Cp^{Me5})$_3$(η^1-N_2)], the first monometallic mononuclear f element complex of dinitrogen, with the N_2 bound in an end-on fashion. The N-N distance of 1.120(14) Å is essentially identical to that of free N_2 and the U-N distance of 2.492(10) Å is longer than the distances observed in the other uranium dinitrogen complexes. As in [U(η^5-Cp^{Me5})$_3$(η^1-CO)][47] there is no molecular rearrangement on complexation of the N_2. The bound N_2 is lost very easily, solutions of [U(η^5-Cp^{Me5})$_3$(η^1-N_2)] in C_6D_6 lose N_2 to regenerate [U(η^5-Cp^{Me5})$_3$] quantitatively when the pressure of N_2 is lowered to 1 atm. The crystals were sufficiently stable to observe a N-N stretch at 2207 cm^{-1}, which shifted to 2134 cm^{-1} when $^{15}N_2$ was used. This reduction in ν_{NN} of 124 cm^{-1} from free N_2 (2331 cm-1) is less than the $\Delta\ \nu_{CO}$ of 221 cm^{-1} in [U(η^5-Cp^{Me5})$_3$(η^1-CO)] and may explain their stability relative to each other.

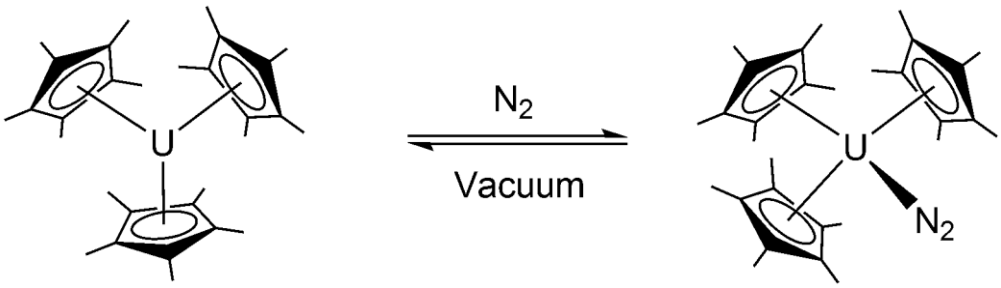

Figure 20: Reaction of [U(η^5-Cp^{Me5})$_3$] with N_2

As the most stable carbonyl complex of uranium forms with the tetramethyl substituted cyclopetadienyl ligand set, [U(η^5-Cp^{Me4H})$_3$] was reacted with N_2 under the same

conditions. However, the only crystalline species formed was the parent metallocene. It is unclear whether this is due to the reduced solubility of $[U(\eta^5\text{-}Cp^{Me4H})_3]$ relative to $[U(\eta^5\text{-}Cp^{Me5})_3]$ causing it to crystallise preferentially over the theoretical N_2 complex or whether it is another example of the different chemical behaviour of the differently substituted cyclopentadienyl ligands on low-valent uranium.[124] Zirconocene chemistry presents a relevant example: using Cp^{Me4H} allows the side-on binding of N_2.[125] not observed in $[(Zr(\eta^5\text{-}Cp^{Me5})_2(\eta^1\text{-}N_2))(\mu\text{-}\eta^1\text{:}\eta^1\text{-}N_2)]$,[126] and effects the hydrogenation of N-N bond to yield NH_3.

Of the uranium dinitrogen complexes only the heterodinuclear complexes $[(N\{R\}Ar)_3U(\mu\text{-}N_2)Mo(N\{^tBu\}Ph)_3]$ and $[(N\{R\}Ar)_3U(\mu\text{-}N_2)Mo(N\{Ad\}Ar)_3]$ are thermally stable and not in equilibrium with their respective starting materials. This stability may be attributable to the molybdenum being a better π-base than uranium.[120] The reversibility of these reactions, especially when the N_2 has been formally reduced, is more usual in lanthanide chemistry.[110] The sterics have been shown to have a significant influence on the stability of the dinitrogen complexes. It is interesting that the there is no reported reactivity with N_2 for either the mixed-sandwich complexes $[U(\eta^8\text{-}C_8H_6\{Si^iPr_3\text{-}1,4\}_2)(\eta^5\text{-}Cp^R)]$ or the $[U(\{^RArO\}_3tacn)]$ complexes, since they display such novel reactivities with CO and CO_2.[58] The dearth and nature of these N_2 complexes, highlights the difficulty of obtaining well-defined and isolable species from the reaction of a low-valent uranium species with N_2.

1.2.4 Binding and activation of CO_2:

The binding and activation of CO_2[127] is easier than either N_2 or CO and can be achieved by chemical, enzymatic, electrochemical or photo-chemical means. Some of these are multi-electron processes but the most common processes are two electron reductions.[128] CO_2 is an attractive C1 source, particularly because it is one of the major contributors to the build-up of greenhouse gases in the atmosphere, but the double bonds must be reduced for it to be a useful building block in the chemical industries. The linear triatomic molecule has a C=O bond length of 1.16 Å that is shorter than a normal double bond and the different electronegativities of the atoms lead to a polarisation of the molecule with a partial positive charge on the carbon atom and a partial negative charge on the oxygen atoms. The two sets of π molecular orbitals, orthogonal to each other, result in a variety of binding modes and bridging modes of the CO_2 at a metal centre. The CO_2 chemistry of the transition metals is well-developed and transition metal mediated transformations of CO_2 are likely to be very important in the future.[129] As with the other small molecules covered in this introduction, the examples of low-valent f-block metal CO_2 complexes are few in number in comparison to the transition metals. The reduction of CO_2 in non-aqueous media is usually described by one of the equations detailed in Figure 21.

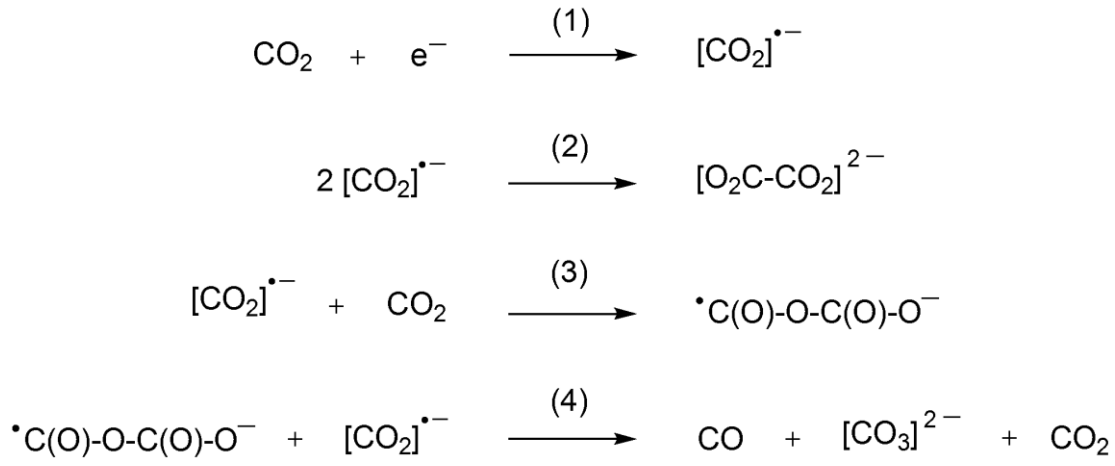

Figure 21: Reactions with CO_2 in non-aqueous media

The reaction of the divalent samarium complex [(Sm(η^5-Cp^{Me5})$_2$(THF)$_2$] with CO_2[130] in toluene or hexanes at room temperature or at – 78 °C yields a mixture of products by ^{1}H NMR. However, the reaction in THF at room temperature with 1 atm CO_2 resulted in an immediate colour change from purple to orange and stirring for a further 5 min gave reductively coupled oxalate complex [(Sm(η^5-Cp^{Me5})$_2$)$_2$(μ-η^2:η^2-O_2CCO_2)] in a 92 % yield. The crystallographic data obtained was only of sufficient quality to confirm the bridging bidentate mode of the oxalate and the overall structure. The NMR data are consistent with oxidation to Sm(III) and the oxalate carbon atoms were identified in the $^{13}C\{^1H\}$ NMR spectrum in d_6-benzene at δ 200 ppm by using $^{13}CO_2$. This reaction is proposed to be the result of the coupling of two, initially formed, [(η^5-Cp^{Me5})$_2$(THF)$_x$Sm]$^+$[CO_2]$^-$ radical species. When the reaction is done in THF, it is fast and selective, in less polar solvents the mixtures of products observed suggests that several pathways may be competing.

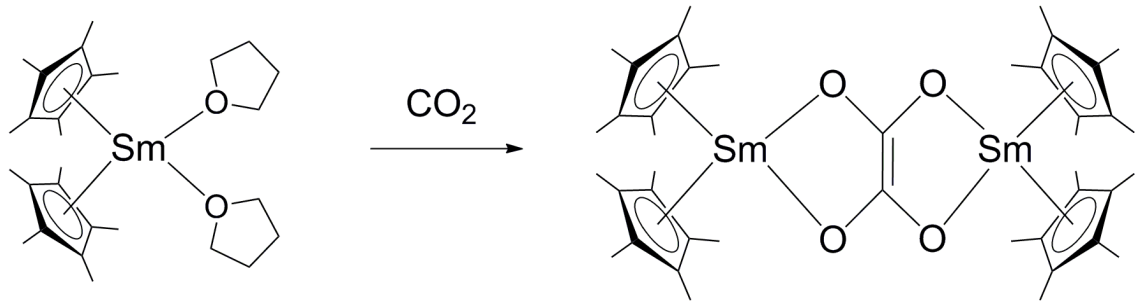

Figure 22: Reaction of [(Sm(η^5-Cp^{Me5})$_2$(THF)$_2$] with CO_2

When [(Sm(η^5-Cp^{Me5})$_2$(THF)$_2$] was reacted under the same conditions with the isoelectronic COS, the disproportionation product [(Sm(η^5-Cp^{Me5})$_2$)(μ-η^2:η^1-S_2CO)(Sm(η-Cp^{Me5})$_2$(THF))] was isolated as the main product of the reaction. The minor product was not identified but using higher concentrations of [(Sm(η^5-Cp^{Me5})$_2$(THF)$_2$] the disproportionation product was able to obtained in an over 90 % yield. There was no evidence for the formation of the [(Sm(η^5-Cp^{Me5})$_2$)$_2$(μ-O)][142] oxo complex, often seen in samarium chemistry, so it is not surprising that the reaction by-product was not identified as the other product of disproportionation of COS to S_2CO^{2-} would be CO and the only crystalline product from the reaction of [(Sm(η^5-Cp^{Me5})$_2$(THF)$_2$] with CO was obtained from a high-pressure reaction.[77]

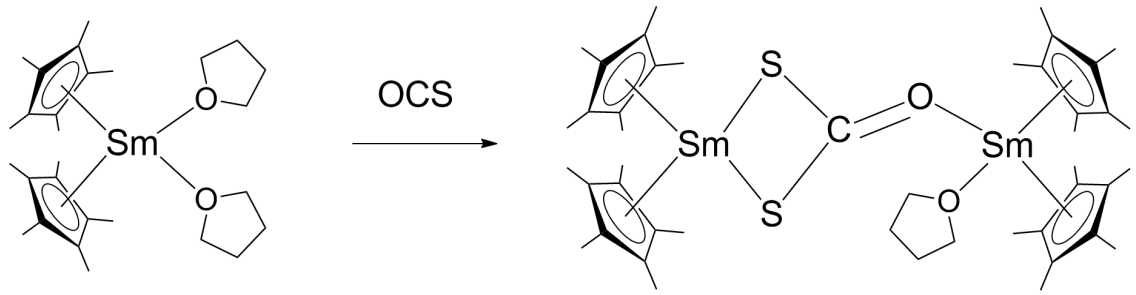

Figure 23: Reaction of $[(Sm(\eta^5\text{-}Cp^{Me5})_2(THF)_2]$ with COS

Evans has recently demonstrated that dinitrogen complexes of both diamagnetic extremes of the lanthanide series can be accessed (for which divalent complexes have proved inaccessible).[131] The lanthanum complex $[(La(\eta^5\text{-}Cp^{Me4H})_2(THF))_2(\mu\text{-}\eta^2\text{:}\eta^2\text{-}N_2)]$ reacts with CO_2 to yield a complex mixture of products, but the lutetium complex $[(Lu(\eta^5\text{-}Cp^{Me4H})_2(THF))_2(\mu\text{-}\eta^2\text{:}\eta^2\text{-}N_2)]$ reacts in an analogous manner to $[(Sm(\eta^5\text{-}Cp^{Me5})_2(THF)_2]$ to yield the oxalate product $[(Lu(\eta^5\text{-}Cp^{Me4H})_2)_2(\mu\text{-}\eta^2\text{:}\eta^2\text{-}O_2CCO_2)]$[111] in a 95 % yield. The reactivity of the lanthanum complex may be complicated by the insertion of CO_2 into La-C(Cp^{Me4H}) bonds.[132] The insertion of CO_2 into U-C,[133] U-H,[72] U-S[134] and U-N[135] is known for U(IV) complexes, as is the incorporation of CO_2 to form a carbamato U(IV) species.[136] The chemistry of $[An(\eta^5\text{-}Cp^{Me5})_2(Me)_2]$ (An = U, Th) is particularly well-developed and this is still an active area of research.[137]

The first report of the reactivity of low-valent uranium with CO_2 analogues was the reaction of $[U(\eta^5\text{-}Cp^{Me})_3(THF)]$ and $[U(\eta^5\text{-}Cp^{SiMe3})_3]$ with CS_2 to form $[(U(\eta^5\text{-}Cp^{R})_3)_2(\mu\text{-}\eta^1\text{:}\eta^2\text{-}CS_2)]$ (R = Me, $SiMe_3$).[138] The data were consistent with the two

electron reduction of CS_2 with concomitant oxidation to U(IV). The μ-η^1:η^2 bridging mode is unusual and the U-C(CS_2) distance of 2.53(2) Å is in the range observed for [U(η^5-Cp^R)$_3$(R)] complexes but the crystallographic centre of symmetry results in identical U-S distances of 2.792(3) Å. The reaction of [U(η^5-Cp^{Me})$_3$(THF)] with COS results in a similar oxidation of the uranium centre and reduction of the substrate but in this case *via* the cleavage of the COS unit with loss of CO, to give [(U(η^5-Cp^{Me})$_3$)$_2$(μ-S)] bridged by a single sulphur atom.[139] The U-S-U angle deviates from linearity at 164.9(4)º and the average U-S distance 2.60(1) Å, is significantly shorter than that seen in [(U(η^5-Cp^R)$_3$)$_2$(μ-η^1:η^2-CS_2)].

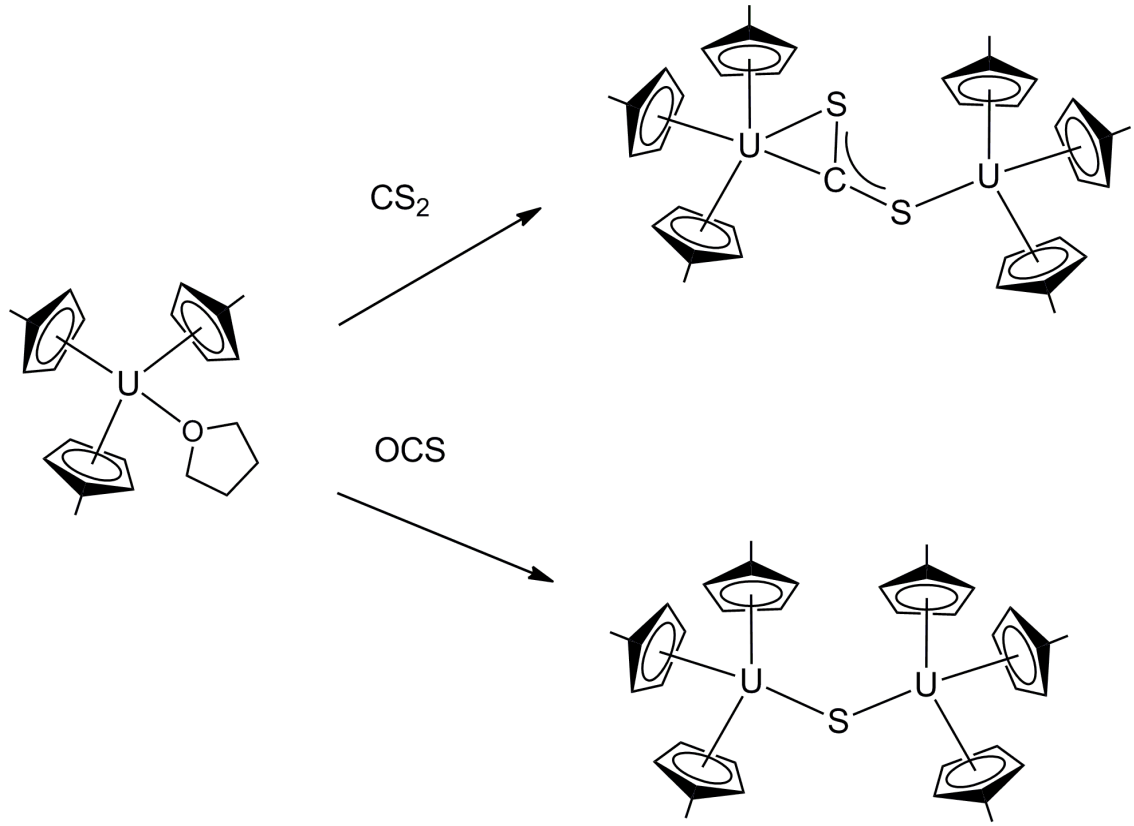

Figure 24: Reaction of [U(η^5-Cp^{Me})$_3$(THF)] with CS_2 and COS

The reaction of $[U(\eta^5\text{-}Cp^{SiMe3})_3]$ with CO_2, in solution results in a colour change from green to red and the red product was isolated in a 54 % yield.[140] The structure was determined as the bridging oxo complex $[(U(\eta^5\text{-}Cp^{SiMe3})_3)_2(\mu\text{-}O)]$ resulting from the deoxygenation of CO_2. The reaction of $[U(\eta^5\text{-}Cp^{SiMe3})_3]$ with N_2O, used as an oxygenating agent in transition metal[141] and f-block[142] chemistry, or with both gases in the solid state also resulted in the bridging oxo species by ^1H NMR. The U-O-U unit is linear and the U-O distance is 2.10503(2) Å, comparable to the U-O distances in $[(U(\eta^5\text{-}Cp)_3)_2(\mu\text{-}O)]$[143] (2.0881(4) Å) and longer than the 2.057(1) Å U-O distance found in the cationic indenyl complex,[144] $[\{(\eta^5\text{-}Ind)UBr(MeCN)_4\}_2(\mu\text{-}O)]^{2+}$.

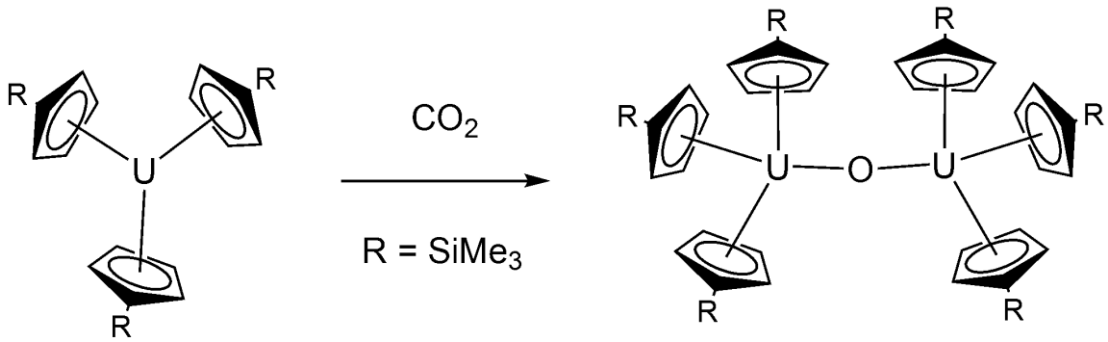

Figure 25: Reaction of $[U(\eta^5\text{-}Cp^{SiMe3})_3]$ with CO_2

Analogous reactivity with N_2O and COS has been demonstrated for the uranium(III) aryloxide complex $[U(OAr)_3]$ (OAr = 2,6-di-tert-butylphenoxide) to form the bridging chalcogenide complexes $[\{(OAr)_3U\}_2(\mu\text{-}O)]$ and $[\{(OAr)_3U\}_2(\mu\text{-}S)]$. However, the reaction of $[U(OAr)_3]$ with molecular oxygen did not result in the isolation of the oxo species but in the known $[U(OAr)_4]$ species, the product of ligand re-distribution.[145] A

bridging oxo complex is also the product of the reaction of $[(\eta^5\text{-Cp})_2\text{TiCl}]_2$ with CO_2, though this requires forcing conditions (90 °C, 10 atm CO_2).[146] The different reactivities observed between $[U(\eta^5\text{-Cp}^{SiMe3})_3]$ with CO_2 and CS_2 to form either the bridging oxo $[\{U(\eta^5\text{-Cp}^{SiMe3})_3\}_2(\mu\text{-O})]$ or the bridging CS_2 structure $[\{U(\eta^5\text{-Cp}^{R})_3\}_2(\mu\text{-}\eta^1\text{:}\eta^2\text{-CS}_2)]$ are presumably the result of the CS_2 being a better σ-donor and π-acceptor than CO_2.[147] It was proposed that the reaction of CO_2 to the bridging oxo might involve an intermediate bridging CO_2 complex with an $\mu\text{-}\eta^1\text{:}\eta^2$ binding mode, followed by loss of CO.

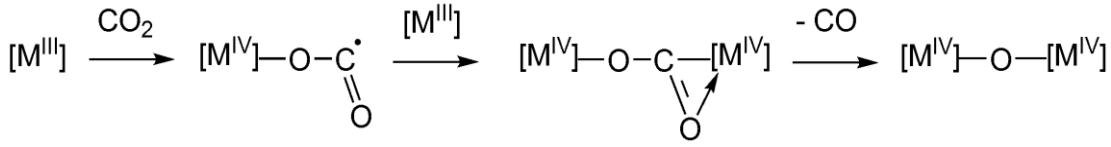

Figure 26: Possible mechanism for the formation of the U(IV)-O-U(IV) complex from CO_2

The $[U(\{ArO\}_3tacn)]$[59] and $[U(\{^{Ad}ArO\}_3tacn)]$[63] (Ar = 3,5-di-tert-butylbenzyl, ^{Ad}Ar = 3-adamantyl-5-tert-butylbenzyl, tacn = 1,4,7-triazacyclononane) uranium(III) complexes previously introduced both show reactivity with CO_2. When benzene or toluene solutions of $[U(\{^{Ad}ArO\}_3tacn)]$, stirring at room temperature, were sparged with CO_2, a colour change from red/brown to pale green was observed within 5 min and the pale blue-green product was isolated in a 49 % yield.[64] This discolouration on reaction with CO_2 was also observed to occur in the solid state. The IR spectrum of the product exhibited a band at 2188 cm^{-1}, significantly lowered from free CO_2 (2349 cm^{-1}), and

was confirmed by a shift to 2128 cm^{-1} in the $^{13}CO_2$ product. The structure was determined to be [U({^{Ad}ArO}$_3$tacn)(η^1-OCO)]. This is the first structurally characterised example of this linear oxygen-bound η^1-OCO coordination mode of CO_2 on any metal.[127,128] It has been proposed from theoretical, kinetic and structural studies that oxygen coordination is vital for the subsequent functionalisation of the carbon atom in photosynthetic CO_2 fixation[148].

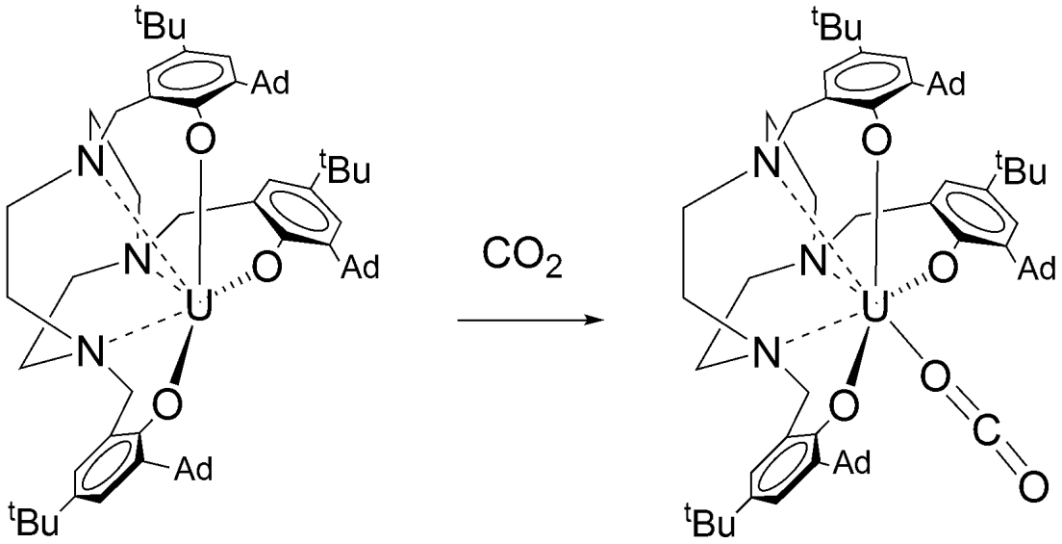

Figure 27: Reaction of [U({^{Ad}ArO}$_3$tacn)] with CO_2

The U-O(OCO) distance of 2.351(3) Å is longer than η^1-O but shorter than the η^2-O distances seen in both the uranium-bound oxocarbon complexes in section 1.2.3 and the uranium carbonate complex [(U(η^8-C_8H_6{Si^{i}Pr$_3$-1,4}$_2$)(η^5-Cp^{Me4H}))$_2$(μ-η^1:η^2-CO_3)][149] formed from the reductive disproportionation of CO_2 (*vide infra*). The C-O distances of 1.122(4) Å and 1.277(4) Å in [U({^{Ad}ArO}$_3$tacn)(η^1-OCO)] are significantly different

from each other and the U-O-C 171.1(2)º and O-C-O 178.0(3)º angles are close to linear. The crystallographic and IR data suggest that the CO_2 is activated as a result of a one electron reduction and that the structure may best be described as a charge-separated species with the $CO_2^{\bullet-}$ radical anion coordinated to a U(IV) centre. This was supported by variable temperature superconducting quantum interference device (SQUID) magnetisation data and electronic absorption spectra. This result is significant as the first structural example of the η^1-OCO coordination mode of CO_2 and because the stabilisation of a charge-separated species on the uranium centre suggests that other reactive intermediates, important for catalysis, may be able to be stabilised by uranium complexes.

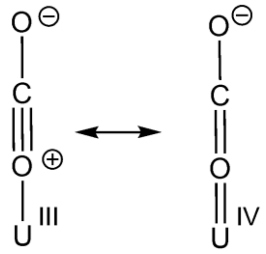

Figure 28: Resonance structures for [U({^{Ad}ArO}$_3$tacn)(η^1-OCO)]

When the less bulky [U({ArO}$_3$tacn)] complex was reacted with CO_2 under the same conditions, the product was able to be isolated in an essentially quantitative yield.[60] The structure was revealed to be the bridging oxo complex [(U({ArO}$_3$tacn))$_2$(μ-O)], previously obtained from the activation of ethers and as a side-product of the reaction with CO and ^{13}CO. This is similar to the reactivity of [U(η^5-Cp^{Me})$_3$(THF)] with COS[139] (*vide supra*). The evolution of CO was detected by IR and when isotopically labelled

$C^{18}O_2$ was used the labelled complex [(U({ArO}$_3$tacn))$_2$(μ-^{18}O)] was formed. It was proposed that the reaction proceeds through a short-lived CO_2 bridged intermediate, which reacts further to [(U({ArO}$_3$tacn))$_2$(μ-O)] with extrusion of CO, the lesser bulk of the [U({ArO}$_3$tacn)] being insufficient to prevent dimerisation and therefore the reduction of CO_2 to CO and O^{2-}. The bridging O^{2-} is contained within the coordination sphere of the tacn ligand and the further addition of CO_2 does not result in any reaction.

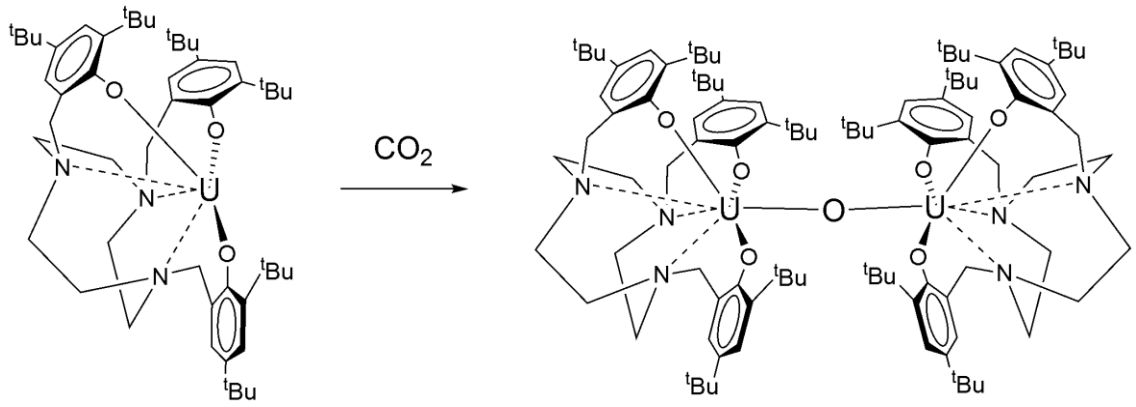

Figure 29: Reaction of [U({ArO}$_3$tacn)] with CO_2

The Meyer group has since synthesised two U(III) complexes using the same pendant aryloxide arms but with a mesitylene anchor [({ArO}$_3$mes)U] (Ar = 3,5-di-tert-butylbenzyl, mes = 1,3,5-trimethylbenzene) and a single nitrogen anchor [({^{Ad}ArO}$_3$N)U(dme)] (^{Ad}Ar = 3-adamantyl-5-methylbenzyl).[150] This latter complex differs from the other U(III) complexes in that the uranium sits above the plane formed by the aryloxide oxygen atoms and the complex contains a coordinated molecule of dme

in the axial position. Both of these complexes react with 1 atm CO_2 at room temperature to form carbonate complexes.[151]

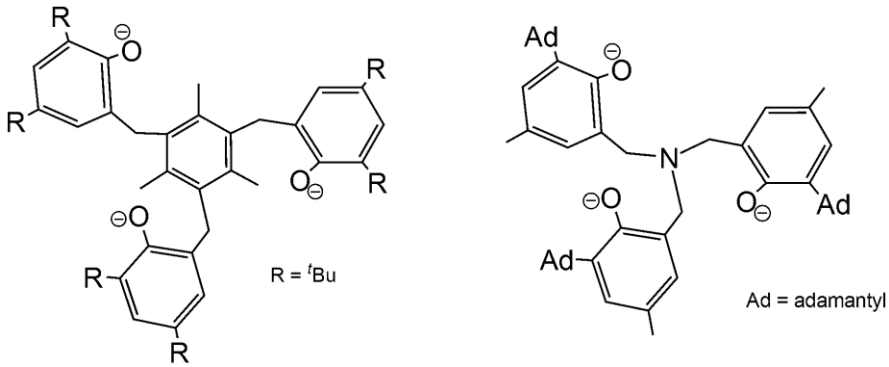

Figure 30: The $(\{ArO\}_3mes)^{3-}$ and $(\{^{Ad}ArO\}_3N)^{3-}$ ligands

The molecular structure of $[((\{ArO\}_3mes)U)_2(\mu\text{-}\eta^2\text{:}\eta^2\text{-}CO_3)]$ features two short U-O(CO_3) bonds 2.333(4) Å and 2.323(3) Å and two long bonds 2.659(4) Å and 2.603(4) Å (Figure 31). The core contains two shorter C-O distances of 1.279(7) Å and 1.285(6) Å and one longer C-O distance of 1.305(6) Å. These distances and the $\mu\text{-}\eta^2\text{:}\eta^2\text{-}CO_3$ bridging mode are comparable to those found in the Sm(III)/Sm(III) macrocyclic carbonate complex synthesised by Gardiner[152] (*vide infra*). The other structure $[((\{^{Ad}ArO\}_3N)U)_2(\mu\text{-}\eta^1\text{:}\eta^2\text{-}CO_3)]$ is comparable to $[(U(\eta^8\text{-}C_8H_6\{Si^iPr_3\text{-}1,4\}_2)(\eta^5\text{-}Cp^{Me4H}))_2(\mu\text{-}\eta^1\text{:}\eta^2\text{-}CO_3)]$.[149] Its core structure consists of two similar C-O distances of 1.263(10) Å and 1.281(10) Å to the η^2-bound oxygen atoms and one slightly longer C-O distance of 1.305(11) Å to the η^1-bound oxygen atom. There is no direct $(\mu\text{-}\eta^1\text{:}\eta^2\text{-}CO_3)$ core comparison as the core in the mixed-sandwich carbonate complex was a 50/50 mixture of $(\mu\text{-}\eta^1\text{:}\eta^2\text{-}CO_3)$ and $(\mu\text{-}\eta^2\text{:}\eta^1\text{-}CO_3)$.

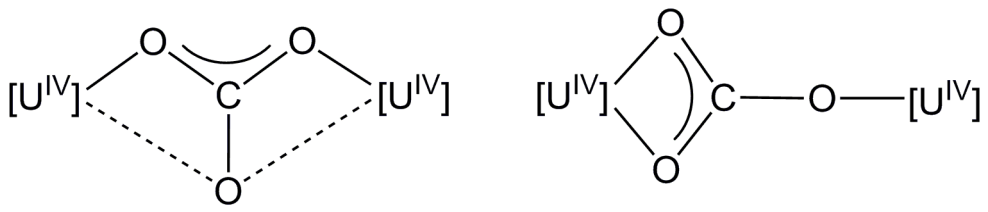

μ–η²:η²–CO_3 μ–η¹:η²–CO_3

Figure 31: Bridging modes of the CO_3^{2-} unit

The mechanism of the [({ArO}$_3$mes)U] and [({^{Ad}ArO}$_3$N)U(dme)] reactivity with CO_2, attributable to the increased flexibility of these ligands in comparison to the tacn complexes, was investigated. Both complexes were reacted with 1 atm of N_2O to form the bridging oxo species, though only the [(({^{Ad}ArO}$_3$N)U(dme))$_2$(μ-O)] complex was structurally characterised. The U-O-U unit is identical to that found in [(U({ArO}$_3$tacn))$_2$(μ-O)]. When the bridging oxo complexes were reacted with CO_2, the aforementioned carbonate complexes were formed. This reaction is proposed to proceed *via* the reductive activation of CO_2 to O^{2-} and CO, followed by nucleophilic attack on CO_2 by the bridging oxo species. CO was detected in the gas phase IR spectrum of the head space of the reaction of [({^{Ad}ArO}$_3$N)U(dme)] with CO_2 to form [(({^{Ad}ArO}$_3$N)U)$_2$(μ-η¹:η²-CO_3)]. However, the evolution of CO would also be detected if reductive disproportionation was the mechanism of the reaction with CO_2 to form carbonate. The reaction has not been done stoichiometrically and further definite proof that the reaction proceeds *via* the oxo intermediate is needed to prove the mechanism. The reactivity of [({ArO}$_3$mes)U] and [({^{Ad}ArO}$_3$N)U(dme)] with CO has not been reported.

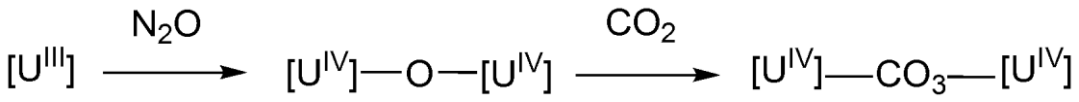

Figure 32: Schematic representation of the reactivity of [({ArO}$_3$mes)U] and [({^{Ad}ArO}$_3$N)U(dme)]

The differing reactivities of the [({ArO}$_3$mes)U] and [({^{Ad}ArO}$_3$N)U(dme)] complexes and the [U({ArO}$_3$tacn)] and [U({^{Ad}ArO}$_3$tacn)] complexes has been rationalised in terms of sterics. In [(U({ArO}$_3$tacn))$_2$(μ-O)][60] the oxo unit is prevented from reacting further with CO_2 by the steric bulk of the tacn ligand, or in the bulkier [U({^{Ad}ArO}$_3$tacn)] prevented from forming at all, resulting in the isolation of [U({^{Ad}ArO}$_3$tacn)(η^1-OCO)].[64] This does not explain the experimental observation of an intermediate in the reaction of [U({ArO}$_3$tacn)] with CO_2 to form [(U({ArO}$_3$tacn))$_2$(μ-O)]. It is not unreasonable, in the context of the reactivity of the other systems, to propose an equilibrium between the thermodynamic drive of oxidation to U(IV) and the steric barrier to dimerisation in the smaller but less flexible [U({ArO}$_3$tacn)] complex.

The first example of the reductive disproportionation of CO_2 to CO_3^{2-} and CO by an f-element was demonstrated by Gardiner from the reaction of the samarium(II) complex [(porphyrinogen)Sm(THF)$_2$][153] (porphyrinogen = *trans-N,N'*-dimethyl-*meso*-octaethylporphyrinogen) with CO_2.[152] The reaction of a purple solution of [(porphyrinogen)Sm(THF)$_2$] in toluene with excess CO_2 at room temperature over 30

min resulted in a colour change to orange and the formation of a yellow precipitate. The product was isolated in a 54 % yield and structurally characterised as [{(porphyrinogen)Sm}$_2$(μ-η^2:η^2-CO_3)].

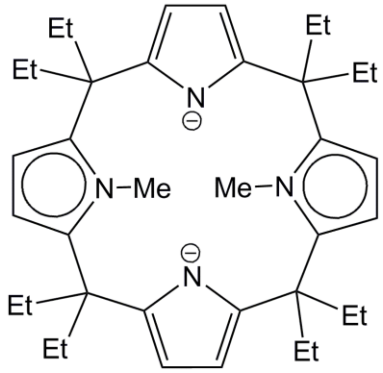

Figure 33: The *trans-N,N'*-dimethyl-*meso*-octaethylporphyrinogen dianionic ligand

The core distances (C-O 1.276(4) Å, 1.317(7) Å) as previously mentioned are comparable to [(({ArO}$_3$mes)U)$_2$(μ-η^2:η^2-CO_3)].[151] The Sm-O distances are disparate at 2.340(3) Å and 2.580(1) Å. The bond to the bridging oxygen is long and the ^{1}H NMR at room temperature indicates that there is a fluxional process resulting in effective C_{2v} symmetry in solution. Although the rotation of the macrocyclic units about the Sm-O-C-O unit could account for the observed ^{1}H NMR spectrum, the authors suggest it is more likely, given the steric constraints and the length of the Sm-O(μ) that this bond is labile in solution, allowing the rotation of the macrocylic unit around the shorter Sm-O bond. The carbonate was observed at 190.9 ppm in the ^{13}C{^{1}H} NMR spectrum. The reaction pathway of the reaction was established by high-resolution GC-MS to be the reductive disproportionation of CO_2 to CO and CO_3^{2-}.

Gardiner suggests that the carbonate may arise either from the deoxygenation of CO_2 followed by CO_2 insertion favoured by Meyer or by the loss of CO from an initially formed $C_2O_4^{2-}$ oxalate complex, like the product synthesised by Evans from the reaction of $[(Sm(\eta^5\text{-}Cp^{Me5})_2(THF)_2]$ with CO_2.[130] If an initial oxalate complex, formed by the reductive coupling of CO_2, were destabilised by not being able to adopt the preferred side-on binding,[154] then loss of CO to form carbonate might result. In the case of [(porphyrinogen)Sm$(THF)_2$], the narrow binding groove of the macrocycle might limit the binding of an oxalate complex to end-on, resulting in carbonate formation. The steric constraints of the two ligands systems on samarium are clearly different as illustrated by the Sm(III) complexes: [(porphyrinogen)Sm(R)] (R = Me, CH_2SiMe_3) complexes are monomeric and base-free,[155] whereas although $[(Sm(\eta^5\text{-}Cp^{Me5})_2(THF)(Me)]$ is monomeric, $[(Sm(\eta^5\text{-}Cp^{Me5})_2(Me)]_x$ crystallises as an asymmetric trimer.[156]

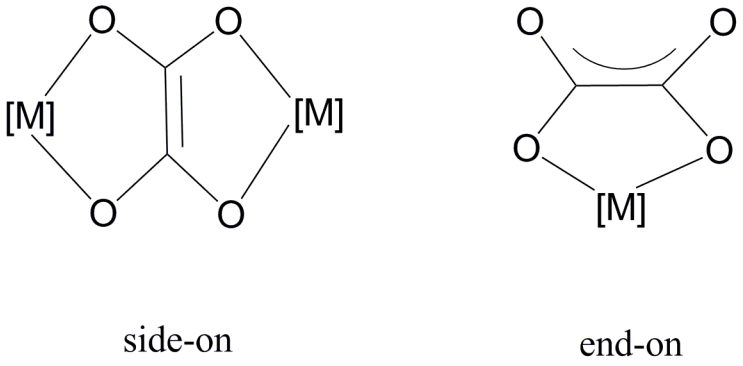

Figure 34: Oxalate binding modes

The role of the THF in the reductive coupling of CO_2 by $[(Sm(\eta^5\text{-}Cp^{Me5})_2(THF)_2]$ to form the oxalate complex $[(Sm(\eta^5\text{-}Cp^{Me5})_2)_2(\mu\text{-}\eta^2\text{:}\eta^2\text{-}O_2CCO_2)]$ has not been rationalised. The formation of the disproportionation product $[(Sm(\eta^5\text{-}Cp^{Me5})_2)(\mu\text{-}\eta^2\text{:}\eta^1\text{-}S_2CO)(Sm(\eta^5\text{-}Cp^{Me5})_2(THF))]$ under the same reaction conditions with the isoelectronic COS[130] is interesting in the light of Gardiner's suggestion, and the differing reactivities observed in the reactions of $[U(\eta^5\text{-}Cp^{SiMe3})_3]$ with CO_2[140] and CS_2.[138] The reductive coupling of CO_2 is proposed to proceed via the coupling of Sm(III)-$CO_2^{\cdot-}$ radical anion species. In the oxalate product the samarium centers are bound $\mu\text{-}\eta^2\text{:}\eta^2$ to the oxlate, the preferred side-on binding. In the disproportionation reaction from COS, both sulphur atoms are bound to one of the samarium centres, forming one side of the $(\mu\text{-}\eta^2\text{:}\eta^1\text{-}S_2CO)$ unit. This suggests that the initial coordination of the triatomic molecule to the metal may be important in determining the subsequent reductive coupling and stability of the dimer formed. With the symmetrical CO_2, the reaction is dependant on the presence of coordinating solvent and the disproportionation product retains a molecule of THF bound to the η^1-O(S_2CO) samarium centre. In the asymmetric COS, the relative stability of the initially bound COS complex, either oxygen or sulphur bound, will also affect the subsequent reactivity.

The low-valent mixed-sandwich complexes $[U(\eta^8\text{-}C_8H_6\{Si^iPr_3\text{-}1,4\}_2)(\eta^5\text{-}Cp^R)(THF)]$

(R = Me_5, Me_4H) react with excess CO_2 at -30 °C to yield the $[(U(\eta^8\text{-}C_8H_6\{Si^iPr_3\text{-}1,4\}_2)(\eta^5\text{-}Cp^R))_2(\mu\text{-}\eta^1\text{:}\eta^2\text{-}CO_3)]$ carbonate complexes in 40 % and 30 % isolated yields, respectively.[149] The single crystal X-ray diffraction data were of insufficient quality in the $[U(\eta^8\text{-}C_8H_6\{Si^iPr_3\text{-}1,4\}_2)(\eta^5\text{-}Cp^{Me5})(THF)]$ complex to do more than confirm the

connectivity. The [(U(η^8-C_8H_6{Si^{i}Pr$_3$-1,4}$_2$)(η^5-Cp^{Me4H}))$_2$(μ-η^1:η^2-CO_3)] structure has U-O distances of 2.422(10) Å , 2.427(10) Å and 2.227(12) Å comparable to those found in [(({^{Ad}ArO}$_3$N)U)$_2$(μ-η^1:η^2-CO_3)][151] and [(U(η^8-C_8H_6{Si^{i}Pr$_3$-1,4}$_2$)(η^5-Cp^{Me5}))$_2$(μ-η^1:η^2-C_3O_3)].[83] ^{13}C{^{1}H} NMR studies of the reaction using $^{13}CO_2$ revealed ^{13}C-labelled carbonate resonances in d_8-toluene at 111.7 ppm for [(U(η^8-C_8H_6{Si^{i}Pr$_3$-1,4}$_2$)(η^5-Cp^{Me5}))$_2$(μ-η^1:η^2-CO_3)] and 137.6 ppm for [(U(η^8-C_8H_6{Si^{i}Pr$_3$-1,4}$_2$)(η^5-Cp^{Me4H}))$_2$(μ-η^1:η^2-CO_3)] and in both cases free ^{13}CO was observed at 185 ppm. The data suggest the reaction proceeds *via* the reductive disproportionation of CO_2.

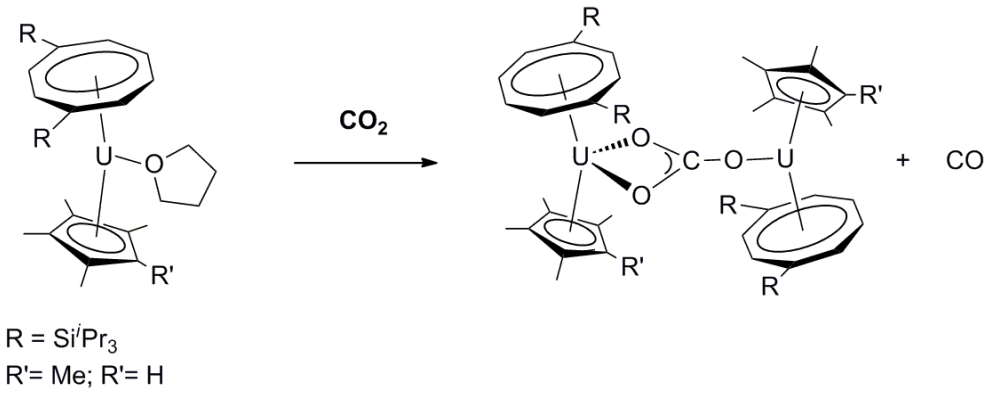

Figure 35: Reactivity of [U(η^8-C_8H_6{Si^{i}Pr$_3$-1,4}$_2$)(η^5-Cp^R)(THF)] (R = Me_5, Me_4H) with CO_2

The ^{13}C{^{1}H} NMR spectrum in d_8-toluene of the reaction of [U(η^8-C_8H_6{Si^{i}Pr$_3$-1,4}$_2$)(η^5-Cp^{Me4H})(THF)] with excess $^{13}CO_2$ also revealed a peak at -112.4 ppm assigned to the labelled squarate complex [(U(η^8-C_8H_6{Si^{i}Pr$_3$-1,4}$_2$)(η^5-Cp^{Me4H}))$_2$(μ-η^2:η^2-$^{13}C_4O_4$)],[93] the product of the reductive coupling of ^{13}CO. The reaction of [U(η^8-

$C_8H_6\{Si^iPr_3\text{-}1,4\}_2)(\eta^5\text{-}Cp^{Me4H})(THF)]$ with the ^{13}CO produced by the disproportionation reaction, in the presence of excess $^{13}CO_2$ suggests the reaction with CO is significantly faster than the reaction with CO_2. Using a ¼ molar excess of the U(III) complex and adding $^{13}CO_2$ accurately *via* Toepler pump, connected to a high vacuum line, resulted in the consumption of the ^{13}CO produced in the reaction and significant peaks for both $[(U(\eta^8\text{-}C_8H_6\{Si^iPr_3\text{-}1,4\}_2)(\eta^5\text{-}Cp^{Me4H}))_2(\mu\text{-}\eta^1\text{:}\eta^2\text{-}^{13}CO_3)]$ and $[(U(\eta^8\text{-}C_8H_6\{Si^iPr_3\text{-}1,4\}_2)(\eta^5\text{-}Cp^{Me4H}))_2(\mu\text{-}\eta^1\text{:}\eta^2\text{-}^{13}C_4O_4)]$ were detected by $^{13}C\{^1H\}$ NMR. This is the first example of an oxocarbon synthesised from CO_2.

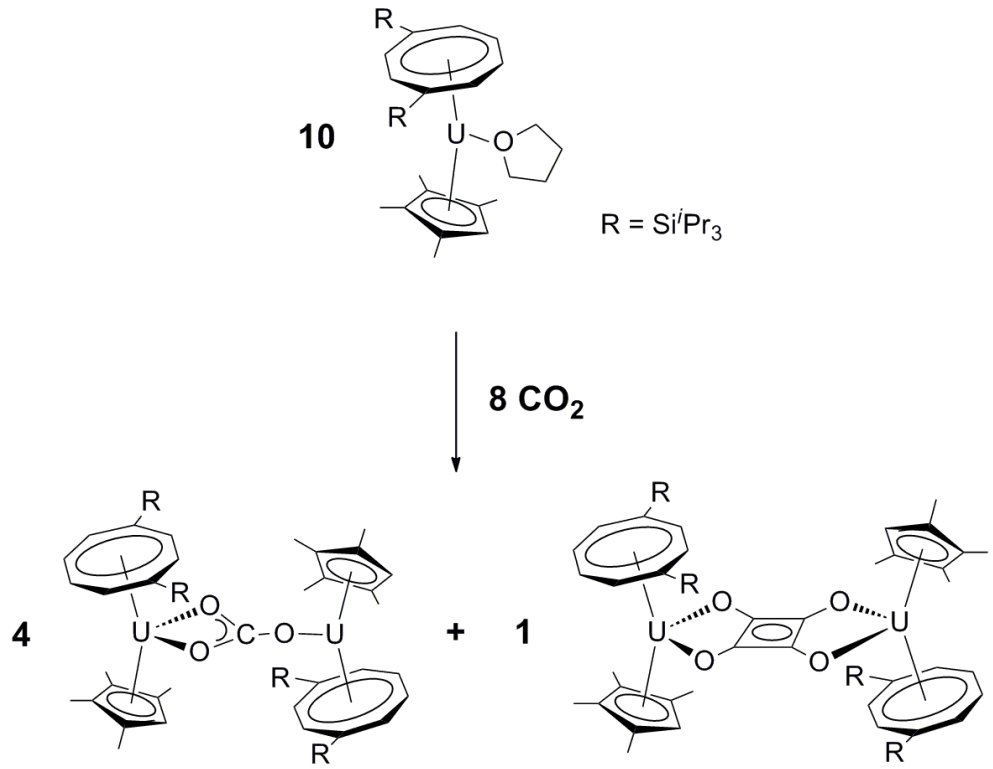

Figure 36: Stoichiometric reaction to form carbonate and squarate from CO_2

A variety of reactivity is observed for low-valent f-block complexes with CO_2, including deoxygenation,[60,140] reductive coupling[130] and reductive disproportionation.[149,151,152] In particular, the first examples of the η^1-OCO coordination mode[64] and $C_4O_4^{2-}$ synthesis[149] highlight the relevance of this chemistry. The binding of the CO_2 and its activation is not fully understood but some mechanistic insight [130,151,152] has been provided, and as seen before the ligand environment plays an important role.[60,149,151]

1.3 Scope of thesis

Complexes of the low-valent f-elements, and in particular uranium(III), provide a combination of high reduction potential with sterically demanding, robust ligands and they have been shown to bind, activate and reductively couple small molecules. However, to effect these transformations cleanly well-defined molecular complexes are required. The stabilisation of the metal centre in a low oxidation state, while maintaining its accessibility towards the substrate is challenging. A small change in ligand environment may result in significant difference in reactivity, which cannot be predicted.

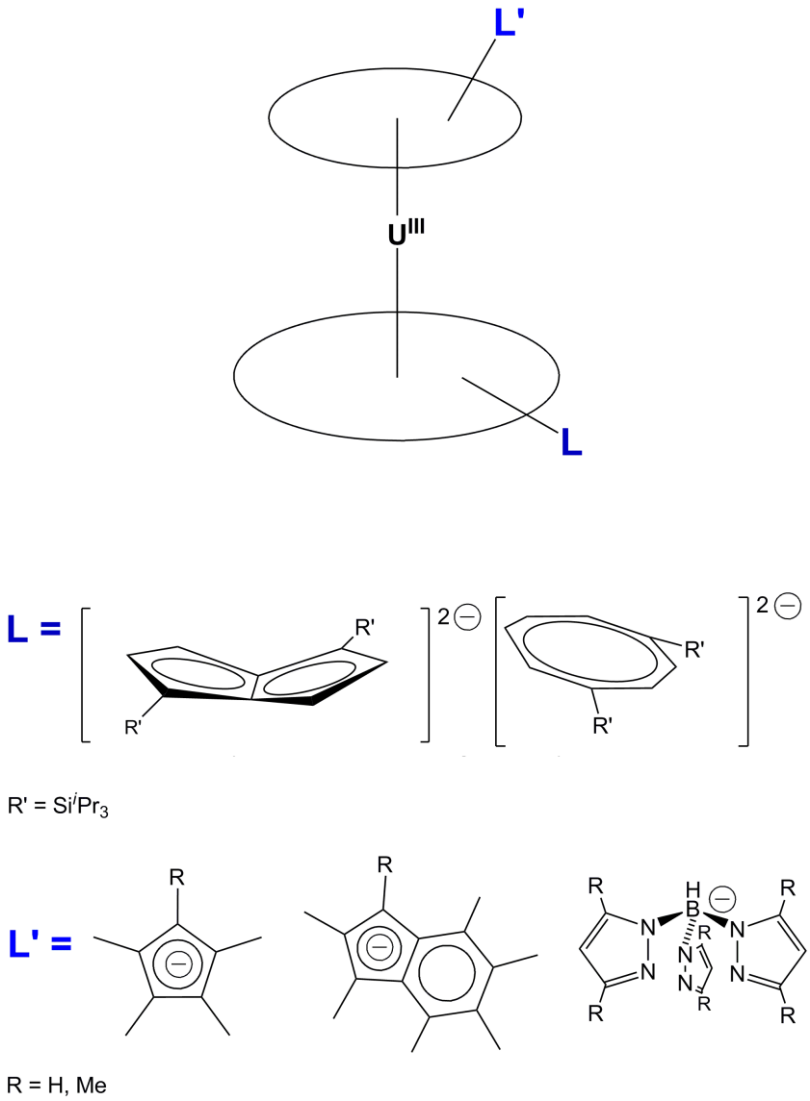

R = H, Me

Figure 37: Template for U(III) mixed-sandwich complexes

The low-valent uranium mixed-sandwich system shown diagrammatically in Figure 37, where L' = $(\eta^5\text{-}Cp^{Me5})^-$ or $(\eta^5\text{-}Cp^{Me4H})^-$ and L = $(\eta^8\text{-}C_8H_6\{Si^iPr_3\text{-}1,4\}_2)^{2-}$ or $(\eta^8\text{-}C_8H_4\{Si^iPr_3\text{-}1,4\}_2)^{2-}$ demonstrates versatile reactivity with small molecules and the products of the reactions have been fully characterised. This thesis examines some further reactivity of the previously synthesised complexes $[U(\eta^8\text{-}C_8H_6\{Si^iPr_3\text{-}1,4\}_2)(\eta^5\text{-}Cp^R)(THF)]$ (R = Cp^{Me5}, Cp^{Me4H}) with small molecules and the chemical abstraction of

the labelled oxocarbon from $[(U(\eta^8\text{-}C_8H_6\{Si^iPr_3\text{-}1,4\}_2)(\eta^5\text{-}Cp^{Me4H}))_2(\mu\text{-}\eta^2\text{:}\eta^2\text{-}^{13}C_4O_4)]$ in Chapter 2. Chapters 3 and 4 detail the syntheses of novel uranium(III) mixed-sandwich complexes using the template shown above but substituting the cyclopentadienyl ligands for other monoanionic ligands, Tp^R (Tp = trispyrazolyl borate, R = Me, H) and the Ind^R (Ind = indenyl, R= Me_6, Me_7). The reactivity of the novel complexes with CO, CO_2 and methyl isocyanide is investigated. Chapter 5 presents the conclusions of the research in Chapters 2-4.

1.4 References:

[1] N. N. Greenwood and A. Earnshaw, The Chemistry of The Elements, 2nd edn., Butterworth-Heinemann, Oxford, 1997.

[2] T. J. Marks and R. D. Ernst, in G. Wilkinson, F. G. A. Stone and E. W. Abel Eds *Comprehensive Organometallic Chemistry*, Pergamon, Press, Oxford, 1982, Vol. 3, Chap. 21 p. 173 and references therein.

[3] J. J. Katz, G. T. Seaborg and L. R. Morss, *The Chemistry of the Actinide Elements*, Vols. 1 and 2, 2nd edn, Chapman and Hall Ltd., 1986.

[4] N. Kaltsoyannis, *Chem. Soc. Rev.*, 2003, **32**, 9.

[5] O. P. Lam, C. Anthon and K. Meyer, *Dalton Trans*., 2009, 9677.

[6] D. E. Morris, R. E. Da Re, K. C. Jantunen, I. Castro-Rodriguez and J. L. Kiplinger, *Organometallics*, 2004, **23**, 5142.

[7] a) D. C. Sonnenberger and J. G. Gaudiello, *Inorg. Chem.*, 1988, **27**, 2747. b) D. Hauchard, M. Cassir, J. Chivot, D. Baudry and M. Ephritikhine, *J. Electroanal. Chem.*, 1993, **347**, 399. c) C. Clappe, D. Leveugle, D. Hauchard and G. Durand, *J. Electroanal. Chem*., 1998, **448**, 95.

[8] L. R. Avens, D. M. Barnhart, C. J. Burns, S. D. Mckee and W. H. Smith, *Inorg. Chem.*, 1994, **33**, 4245.

[9] L. T Reynolds and G. Wilkinson, *J. Inorg. Nucl. Chem.*, 1956, 21, 246.

[10] a) J. M. Birmingham and G. Wilkinson, *J. Am. Chem. Soc*., 1954, **76**, 6210. b) J. M. Birmingham and G. Wilkinson, *J. Am. Chem. Soc*., 1956, **78**, 422

[11] T. J. Katz, *J. Am. Chem. Soc.*, 1960, **82**, 3784.

[12] R. D. Fischer, *Theor. Chim. Acta*, 1963, **1**, 418

[13] A. Streitweiser Jr. and U. Muller-Westerhoff, *J. Am. Chem. Soc.*, 1968, **90**, 7364.

[14] A. Zalkin and K. N. Raymond, *J. Am. Chem. Soc.*, 1969, **91**, 5667.

[15] D. Seyferth, *Organometallics*, 2004, **23**, 3562.

[16] J. M. Manriquez, P. J. Fagan and T. J. Marks, *J. Am. Chem. Soc.*, 1978, **100**, 3939.

[17] T. J. Marks, *Science*, 1982, **217**, 990.

[18] C. J. Burns, D. L. Clark and A. P. Sattelberger, *Actinides: Organometallic Chemistry*, Los Alamos National Laboratory, Los Alamos, NM, USA.

[19] a) J. C. Taylor and P. W. Wilson, *Acta. Crystallogr*., 1974, **B30**, 2803. b) J. H. Levy, J. C. Taylor and P. W. Wilson, *Acta. Crystallogr*., 1975, **B31**, 880.

[20] B. Kanellakopulos, E. O. Fischer, E. Dornberger and F. Baumgartner, *J. Organomet. Chem.*, 1970, **24**, 507.

[21] I. Santos, N. Marques and A. P. De Matos, *Inorg. Chim. Acta*, 1985, **110**, 149.

[22] R. A. Anderson, *Inorg. Chem.*, 1979, **18**, 1507.

[23] a) K. W. Bagnall, D. Brown, P. J. Jones and J. G. H. du Preez, *J. Chem. Soc.*, 1965, 350. b) J. G. H. du Preez and B. Zeelie, *J. Chem. Soc. Chem. Comm*., 1986, 743.

[24] a) D. L. Clark, A. P. Sattelberger, S. G. Bott and N. R. Vrtis, *Inorg. Chem.*, 1989, **28**,1771. b) $[UI_3(THF)_4]$ was first reported as "green-black" solid in a 72 % yield and characterised by elemental analysis and I.R. spectroscopy in G. B. Deacon and T. D. Tuong, *Polyhed.*, 1988, **7**, 249.

[25] a) W. J. Evans, S. A. Kozimor and J. W. Ziller, *J. Am. Chem. Soc.*, 2003, **125**, 14264. b) L. R. Avens, D. M. Barnhart, C. J. Burns and S. D. McKee, *Inorg. Chem.*, 1996, **35**, 537. c) C. Boisson, J. C. Berthet, M. Lance, M. Nierlich and M. Ephritikhine, *Chem. Comm*., 1996, 2129.

[26] L. R. Avens, S. G. Bott, D. L. Clark, A. P. Sattelberger, J. G. Watkin and B. D. Zwick, *Inorg. Chem.*, 1994, **33**, 2248.

[27] F. G. Cloke and P. B. Hitchcock, *J. Am. Chem. Soc.*, 2002, **124**, 9352. For greater detail see: G. K. B. Clentsmith, F. G. N. Cloke, M. D. Francis, J. R. Hanks, P. B. Nixon and J. F. Nixon, *J. Organomet. Chem.*, 2008, **693**, 2287.

[28] J. D. Corbett, *Inorg. Synth.*, 1983, **22**, 31.

[29] W. J. Evans, S. A. Kozimor, J. W. Ziller, A. A. Fagin and M. N. Bochkarev, *Inorg. Chem.*, 2005, **44**, 3993.

[30] M. N. Bocharev and A. A. Fagin, *Chem. –Eur. J.*, 1999, **5**, 2990.

[31] C. D. Carmichael, N. A. Jones and P. A. Arnold, *Inorg. Chem.*, 2008, **47**, 8577.

[32] M. Sharma and M. S. Eisen, *Structure and Bonding: Organometallic and Coordination Chemistry of the Actinides*, 2008, Springer-Verlag Berlin, Heidelberg.

[33] a) M. Ephritikhine, *Dalton Trans.*, 2006, 2501. b) W. J. Evans and S. A. Kozimor, *Coord. Chem. Rev.*, 2006, **250**, 911. c) O. P. Lam, C. Anthon and K. Meyer, *Dalton Trans.*, 2009, 9677.

[34] a) A. R. Fox, S. C. Bart, K. Meyer and C. C. Cummins, *Nature*, 2008, **455**, 341. b) T. Andrea and M. S. Eisen, *Chem. Soc. Rev.*, 2008, **37**, 550.

[35] a) R. H. Crabtree, *The Organometallic Chemistry Of The Transition Metals*, 2nd edn, Wiley Interscience, 1994. b) C. Elschenbroich and A. Saltzer, *Organometallics: A Concise Introduction*, 2nd edn, VCH, 1992.

[36] a) M. J. S. Dewar, *Bull. Soc. Chim. Fr.*, 1951, **18**, C71. b) J. Chatt and L. A. Duncanson, *J. Chem. Soc.*, 1953, 2939.

[37] Handbook of Chemistry and Physics, 89th edn., CRC Press, 2008.

[38] J. E. Ellis and W. Beck, *Angew. Chem. Int. Ed. Engl.*, 1995, **34**, 2489.

[39] J. L. Slater, R. K. Sheline, K. C. Lin and W. Weltner Jr, *J. Chem. Phys*.,1971, **55**, 5129.

[40] J. G. Brennan, R. A. Anderson and J. L. Robbins, *J. Am. Chem. Soc.*, 1986, **108**, 335.

[41] J. G. Brennan, S. D. Stults, R. A. Anderson and A. Zalkin, *Organometallics*, 1988, **7**, 1329.

[42] J. G. Brennan, S. D. Stults, R. A. Anderson and A. Zalkin, *Inorg. Chim. Acta*, 1987, **139**, 201.

[43] J. S. Parry, E. Carmona, S. Coles and M. Hursthouse, *J. Am. Chem. Soc.*, 1995,**117**, 2649.

[44] F. G. N. Cloke, S. A. Hawkes, P. B. Hitchcock and P. Scott, *Organometallics*, 1994, **13**, 2895.

[45] D. J. Sikora, M. D. Rausch, R. D. Rogers and J. L. Atwood, *J. Am. Chem. Soc.*, 1981, **103**, 1265.

[46] M. del Mar Conejo, J. S. Parry, E. Carmona, M. Schultz, J. G. Brennan, S. M. Beshouri, R. A. Anderson, R. D. Rogers, S. Coles and M. Hursthouse, *Chem. Eur. J.*, 1999, **5**, 3000.

[47] W. J. Evans, S. A. Kozimor, G. W. Nyce and J. W. Ziller, *J. Am. Chem. Soc.*, 2003, **125**, 13831.

[48] a) L. Maron, L. Perrin, O. Eisenstein and R. A. Anderson, *J. Am. Chem. Soc*., 2002, **124**, 5614. b) P. Selg, H. H. Brintzinger, M. Schultz and R. A. Anderson, *Organometallics*, 2002, **21**, 3100.

[49] B. E. Bursten and R. J. Strittmatter, *J. Am. Chem. Soc.*, 1987, **109**, 6606.

[50] W. J. Evans,G. W. Nyce, M. A. Johnston and J. W. Ziller, *J. Am. Chem. Soc*., 2000, **122**, 12019.

[51] F. A. Cotton and G. W. Wilkinson, *Advanced Inorganic Chemistry*, 6th edn, Wiley Interscience, 1999.

[52] a) C. E. Zachmanoglou, A. Docrat, B. M. Bridgewater, G. Parkin, C. G. Brandow, J. E. Bercaw, C. N. Jardine, M. Lyall, J. C. Green and J. B. Keister, *J. Am. Chem. Soc.*, 2002, **124**, 9525. b) J. W. Lauher and R. Hoffmann, *J. Am. Chem. Soc*., 1976, **98**, 1729.

[53] J. C. Green, *Chem. Soc. Rev*., 1998, **27**, 263.

[54] L. Maron, O. Eisenstein and R. A. Anderson, *Organometallics*, 2009, **28**, 3629.

[55] S. D. Stults, unpublished results.

[56] a) L. Seijo, Z. Barandiáran and E. Haraguindey, *J. Chem. Phys.*, 2001, **114**, 118. b) H. M. Crosswhite, H. Crosswhite, W. T. Carnall and P. A. Paszek, *J. Chem. Phys.*, 1980, **72**, 5103.

[57] R. A. Anderson, *Inorg. Chem.*, 1979, **18**, 1507.

[58] I. Castro-Rodriguez, H. Nakai and K. Meyer, *Chem. Commun.*, 2006, 1353.

[59] I. Castro-Rodriguez, K. Olsen, P. Gantzel and K. Meyer, *Chem. Comm.*, 2002, 2764.

[60] I. Castro-Rodriguez and K. Meyer, *J. Am. Chem. Soc.*, 2005, **127**, 11242 and supporting information.

[61] I. Castro-Rodriguez, K. Olsen, P. Gantzel and K. Meyer, *J. Am. Chem. Soc.*, 2003, **125**, 4565.

[62] a) T. D. Tilley and R. A. Anderson, *J. Chem. Soc.Chem. Comm*, 1981, 985. b) T. D. Tilley and R. A. Anderson, *J. Am. Chem. Soc.*, 1982,**104**, 1772.

[63] H. Nakai, X. Hu, L.N. A. L. Rheingold and K. Meyer, *Inorg. Chem.*, 2004, **43**, 855.

[64] I. Castro-Rodriguez, H. Nakai, L. N. Zakharov, A. L. Rheingold and K. Meyer, *Science*, 2004, **305**, 1757 and supporting information.

[65] I. Castro-Rodriguez, H. Nakai and K. Meyer, *Angew. Int. Ed. Eng.*, 2006, **45**, 2389.

[66] J. E. Bercaw, R. H. Marvich, L. G. Bell and H. H. Brintzinger, *J. Am. Chem. Soc.*, 1972, **94**, 1219.

[67] J. M. Manriquez, D. M. McAlister, R. D. Sanner and J. E. Bercaw, *J. Am. Chem.Soc.*, 1976, **98**, 6733.

[68] P. T. Wolczanski and J. E. Bercaw, *Acc. Chem. Res.*, 1980, **13**, 121.

[69] a) R. P. Planalp and R. A. Anderson, *J. Am. Chem. Soc.*, 1983, **105**, 7774. b) C. D. Wood and R. R. Schrock, *J. Am. Chem. Soc.*, 1979, **101**, 5421.

[70] E. M. Carnahan, J. D. Protasiewicz and S. J. Lippard, *Acc. Chem. Res.*, 1993, **26**, 90.

[71] a) V. L. Coffin, W. Brennan and B. B. Wayland, *J. Am. Chem. Soc*., 1988, **110**, 6063. b) B. B. Wayland, A. E. Sherry, G. Poszmik and A. G. Bunn, *J. Am. Chem. Soc.*, 1992, **114**, 1673.

[72] T. J. Marks, *Science*, 1982, **217**, 989.

[73] a) R. E. Cramer, R. B. Maynard, J. C. Maw and J. W. Gllje, *Organometallics*, 1982, **1**, 869. b) G. Paolucci, G. Rossetto, P. Zanella, K. Yunlue and R. D. Fischer, *J. Organomet. Chem.*, 1984, **272**, 363. c) K. Moloy and T. J. Marks, *J. Am. Chem. Soc.*, 1984, **106**, 7051. d) M. Weydert, J. G. Brennan, R. A. Anderson and R. G. Bergman, *Organometallics*, 1995, **14**, 3942.

[74] M. R. Leonov and G. V. Solov'yova, *Metallorg. Khim.*, 1993, **6**, 198. See: J. Richter and F. T. Edelmann, *Coord. Chem. Rev.*, 1996, **147**, 373.

[75] W. J. Evans, K. J. Forrestal and J. W. Ziller, *J. Am. Chem. Soc.*, 1995, **117**, 12635.

[76] W. J. Evans, I. Bloom, W. E. Hunter and J. L. Atwood, *J. Am. Chem. Soc.*, 1981, **103**, 6507.

[77] W. J. Evans, J. W. Grate, L. A. Hughes, H. Zhang and J. L. Atwood, *J. Am. Chem. Soc.*, 1985, **107**, 3728.

[78] F. R. Kreissel, A. Frank, U. Schubert, L. L. Lindner and G. Huttner, *Angew. Chem. Int. Ed. Engl.*, 1976, **15**, 632.

[79] W. J. Evans, D. S. Lee, J. W. Ziller and N. Kaltsoyannis, *J. Am. Chem. Soc.*, 2006, **128**, 14176.

[80] P. Selg, H. H. Brintzinger, M. Schultz and R. A. Anderson, *Organometallics*, 2002, **21**, 3100 and supportinginformation.

[81] C. K. Rofer-De-Poorter, *Chem. Rev.*, 1981, **81**, 447.

[82] H. Sabzyan and M. R. Noorbala, *J. Mol. Struct. Theochem.*, 2003, **262**, 143.

[83] O. T. Summerscales, F. G. N. Cloke, P. B. Hitchcock, J. C. Green and N. Hazari, *Science*, 2006, **311**, 829.

[84] F. G. N. Cloke and P. B. Hitchcock, *J. Am. Chem. Soc.*, 2002, **124**, 9352.

[85] K. B. Wiberg, *Acc. Chem. Res.*, 1996, **29**, 229.

[86] R. West, *Oxocarbons*, 1980, Academic, New York.

[87] a) G. Seitz and P. Imming, *Chem. Rev.*, 1992, **92**, 1227. b) P. v. R. Schleyer, K. Najafian, B. Kiran and H. Jiao, *J. Org. Chem.*, 2000, **65**, 426. c) B. B. Wayland and X. Fu, *Science*, 2006, **311**, 790.

[88] P. W. Lednor and P. C. Versloot, *J. Chem. Soc. Chem. Commun.*, 1983, 284.

[89] a) G. Silvestri, S. Gambino, G. Filardo, M. Guainazzi and R. Ercoli, *Gazz. Chim. Ital.*, 1972, **102**, 818. b) G. Silvestri, S. Gambino, G. Filardo, G. Spardaro and L. Palmisano, *Electrochim. Acta.*, 1978, **23**, 413.

[90] M. Shibata, D. Omori and N. Furyra, *Electrochemistry*, 1999, **67**, 335.

[91] G. Bockmair and H. P. Z. Fritz, *Z. Naturforsch. B*, 1975, **30**, 330.

[92] a) W. J. Evans, G. W. Nyce and J. W. Ziller, *Ang. Chem. Int. Ed. Engl.*, 2000, **39**, 240. b) W. J. Evans, S. A. Korimor and J. W. Ziller, *J. Am. Chem. Soc.*, 2003, **125**, 14264.

[93] O. T. Summerscales, F. G. N. Cloke, P. B. Hitchcock, J. C. Green and N. Hazari, *J. Am. Chem. Soc.*, 2006, **128**, 9602.

[94] O. T. Summerscales and F. G. N. Cloke, *Structure and Bonding: Organometallic and Coordination Chemistry of the Actinides*, 2008, Springer-Verlag Berlin Heidelberg.

[95] J. C. Green and N. Hazari, unpublished results.

[96] O. T. Summerscales, DPhil thesis, University of Sussex, 2007.

[97] L. Gemlin, *Ann. Phys. Leipzig*, 1825, **4**, 31.

[98] J. Liebig, *Ann. Chem. Pharm.*, 1834, **11**, 182.

[99] a) A. Joannis, *C. R. Acad. Sci. Paris.*, 1893, **116**, 1518. b) A. Joannis, *C. R. Acad. Sci. Paris.*, 1914, **158**, 874.

[100] F. Calderazzo, *Coord. Chem. Rev.*, 2005, **249**, 873.

[101] W. Buechner and E. Weiss, *Chem. Ber*, 1965, **98**, 126.

[102] E. Weiss and W. Buechner, *Z. Allorg. Allgem. Chem.*, 1964, **330**, 251.

[103] W. Buechner, *Helv. Chim. Acta.*, 1964, **46**, 2111.

[104] W. Buechner and E. Weiss, *Helv. Chim. Acta*., 1964, **47**, 1415.

[105] W. F. Sager, A. Fatiadi, P. C. Parks, D. G. White and T. P. Perros, *J. Inorg. Nucl. Chem.*, 1963, **25**, 187.

[106] F. A. Uribe, P. R. Sharpe and A. J. Bard, *J. Electroannal. Chem.*, 1983, **152**, 173.

[107] A. S. P. Frey, F. G. N. Cloke, P. B. Hitchcock, I. J. Day, J. C. Green and G. Aitken, *J. Am. Chem. Soc*., 2008, **138**, 13816.

[108] a) M. D. Fryzuk and S. A. Johnson, *Coord. Chem. Rev.*, 2000, **200-202**, 379. b) B. A. MacKay and M. D. Fryzuk, *Chem. Rev.*, 2004, **104**, 385. c) M. Hidaia and Y. Mizobe, *Chem. Rev.*, 1995, **95**, 1115. d) S. Gambarotta, *J. Organomet. Chem.*, 1995, **500**, 117.

[109] W. J. Evans, T. A. Ulibarri and J. W. Ziller, *J. Am. Chem. Soc.*, 1988, **110**, 6877.

[110] a) W. J. Evans, D. S. Lee and J. W. Ziller, *J. Am. Chem. Soc.*, 2004, **126**, 454. b) W. J. Evans, D. S. Lee, D. B. Rego, J. M. Perotti, S. A. Kozimor, E. K. Moore and J. W. Ziller, *J. Am. Chem. Soc.*, 2004, **126**, 14574. See also: E. A. MacLachlan and M. D. Fryzuk, *Organometallics*, 2006, **25**, 1530.

[111] W. J. Evans, S. E. Lorenz and J. W. Ziller, *Inorg. Chem.*, 2009, **48**, 2001.

[112] a) J. Jubb and S. Gambarotta, *J. Am. Chem. Soc.*, 1994, **116**, 4477. b) M. Ganesan, S. Gambarotta and G. P. A. Yap, *Angew. Chem. Int. Ed. Engl.*, 2001, **40**, 766. c) C. D. Bérubé, M. Yazdanbakhsh, S. Gambarotta and G. P. Yap, *Organometallics*, 2003, **22**, 3742. d) E. Campazzi, E. Solari, C. Floriani and R. Scopelliti, *Chem. Commun.*, 1998, 2603.

[113] I. Korobkov, S. Gambarotta and G. P. A. Yap, *Ang. Chem. Int. Ed. Engl.*, 2002, **41**, 3433.

[114] F. Haber, Ammonia, German Patent, DE 229126, 1909

[115] a) P. Roussel and P. Scott, *J. Am. Chem. Soc.*, 1998, **120**, 1070. b) P. Roussel, N. D. Tinker and P. Scott, *J. Alloys and Comp.*, 1998, **271**, 150.

[116] N. Kaltsoyannis and P. Scott, *Chem. Commun.*, 1998, 1665.

[117] P. Roussel, W. Errington, N. Kaltsoyannis and P. Scott, *J. Organomet. Chem.*, 2001, **635**, 69.

[118] C. Morton, N. W. Alcock, M. R. Lees, I. J. Munslow, C. J. Saunders and P. Scott, *J. Am. Chem. Soc.*, 1999, **121**, 11255.

[119] R. Boaretto, P. Roussel, N. W. Alcock, A. J. Kingsley, I. J. Munslow, C. J. Saunders and P. Scott, *J. Organomet. Chem.*, 1999, **591**, 174.

[120] A. L. Odom, P. L. Arnold and C. C. Cummins, *J. Am. Chem. Soc.*, 1998, **120**, 5836.

[121] C. E. Laplaza, M. J. A. Johnston, J. C. Peters, A. L. Odom, E. Kim, C. C. Cummins, C. J. George and I. J. Pickering, *J. A. Chem. Soc.*, 1996, **118**, 8623.

[122] This intermediate has since been characterised. See: J. J. Curley, T. R. Cook, S. Y. Reece, P. Mueller and C. C. Cummins, *J. Am. Chem. Soc.*, 2008, **130**, 9394.

[123] F. G. N. Cloke, J. C. Green and N. Kaltsoyannis, *Organometallics*, 2004, **23**, 832.

[124] W. J. Evans and S. A. Kozimor, *Coord. Chem. Rev.*, 2006, **250**, 911.

[125] a) J. A. Pool, E. Lobkovsky and P. J. Chirik, *Nature*, 2004, **427**, 527. b) J. A. Pool, W. H. Bernskoetter and P. J. Chirik, *J. Am. Chem. Soc.*, 2004, **126**, 14326.

[126] a) J. M. Manriquez and J. E. Bercaw, *J. Am. Chem. Soc.*, 1974, **96**, 6229. b) J. M. Manriquez, R. D. Sanner, R. E. Marsh and J. E. Bercaw, *J. Am. Chem. Soc.*, 1976, **98**, 3042.

[127] D. H. Gibson, *Chem. Rev*., 1996, **96**, 2063.

[128] a) W. Leitner, *Ang. Chem. Int. Ed. Engl.*, 1995, **34**, 2207. b) G. Leigh, *J. Chem. Sco. Chem. Commun.*, 1974, 1033.

[129] X. Yin and J. R. Moss, *Coord. Chem. Rev.*, 1999, **181**, 27.

[130] W. J. Evans, C. A. Seibel and J. W. Ziller, *Inorg. Chem.*, 1998, **37**, 770.

[131] a) W. J. Evans, D. S. Lee, C. Lie and J. W. Ziller, *Angew. Chem. Int. Ed. Engl.*, 2004, **43**, 5517. b) W. J. Evans, D. S. Lee, M. A. Johnston and J. W. Ziller, *Organometallics*, 2005, **24**, 6393.

[132] W. J. Evans, D. B. Rego, J. W. Ziller, A. G. DiPasquale and A. L. Rheingold, *Organometallics*, 2007, **26**, 4737.

[133] K. G. Moloy and T. J. Marks, *Inorg. Chim. Acta.*, 1985, **110**, 127.

[134] C. Lescop, T. Arliguie, M. Lance, M. Nierlich and M. Ephritikhine, *J. Organomet. Chem.*, 1999, **580**, 137.

[135] S. Bart, C. Anthon, F. Heinemann, E. Bill, N. Edelstein and K. Meyer, *J. Am. Chem. Soc.*, 2008, **130**, 12536.

[136] F. Calderazzo, G. Dell'Amico, R. Netti and R. Pasguali, *Inorg. Chem.*, 1978, **17**, 471.

[137] W. J. Evans, N. A. Siladke and J. W. Ziller, *Comp. Rend. Chim.*, in press.

[138] J. G. Brennan, R. A. Anderson and A. Zalkin, *Inorg. Chem.*, 1986, **25**, 1756.

[139] J. G. Brennan, R. A. Anderson and A. Zalkin, *Inorg. Chem.*, 1986, **25**, 1761.

[140] J. C. Berthet, J. F. Maréchal, M. Nierlich, M. Lance, J. Vigner and M. Ephritikhine, *J. Organomet. Chem.*, 1991, **408**, 335.

[141] F. Bottomly, I. J. B. Lin and M. Mukaida, *J. Am. Chem. Soc.*, 1980, **102**, 5238. See also for the reactivity with NO: F. Bottomley and I. J. B. Lin, *J. Chem. Soc. Dalton Trans.*, 1981, 271.

[142] W. J. Evans, J. W. Grate, I. Bloom, W. E. Hunter and J. L. Atwood, *J. Am. Chem. Soc.*, 1985, **107**, 405 and references therein.

[143] M. R. Spirlet, J. Rebizant, C. Apostolidis, E. Dornberger, B. Kanellakopulos and B. Powietzka, *Polyhedron*, 1996, **15**, 1503.

[144] W. Beeckman, J. Goffart, J. Rebizant and M. R. Spirlet, *J. Organomet. Chem.*, 1986, **307**, 23.

[145] L. R. Avens, D. M. Barnhart, C. J. Burns, S. D. McKee and W. H. Smith, *Inorg. Chem.*, 1994, **33**, 4245.

[146] G. Fachinetti, C. Floriani, A. Chiesi-Villa and C. Guastini, *J. Am. Chem. Soc.*, 1979, **101**, 1767.

[147] K. K. Pandey, *Coord. Chem. Rev.*, 1995, **140**, 37.

[148] a) H. Mauser, W. A. King, J. E. Gready and T. J. Andrews, *J. Am. Chem. Soc.*, 2001, **123**, 10821. b) H.-J. Lee, M. D. Lloyd, K. Harlos, I. J. Clifton, J. E. Baldwin and C. J. Schofield, *J. Mol. Biol.*, 2001, **308**, 937.

[149] O. T. Summerscales, A. S. P. Frey, F. G. N. Cloke and P. B. Hitchcock, *Chem. Commun.*, 2009, 198.

[150] S. C. Bart, C. Anthon, F.W. Heinemann, E. Bill, N. M. Edelstein and K. Meyer, *Inorg. Chem.*, 2009, **48**, 9419.

[151] O. P. Lam, S. C. Bart, H. Kameo, F. W. Heinemann and K. Meyer, *Chem. Commun.*, 2010, **46**, 3137 and supporting information.

[152] N. W. Davies, A. S. P. Frey, M. G. Gardiner and J. Wang, *Chem. Commun.*, 2006, 4853.

[153] J. Wang, A. K. J. Dick, M. G. Gardiner, B. F. Yates, E. J. Peacock, B. W. Skelton and A. H. White, *Eur. J. Inorg. Chem.*, 2004, 1992.

[154] N. W. Alcock, *J. Chem. Soc. Dalton Trans.*, 1973, 1610.

[155] J. Wang, M. G. Gardiner, B. W. Skelton and A. H. White, *Organometallics*, 2005, **24**, 815.

[156] W. J. Evans, J. M. Perotti and J. W. Ziller, *J. Am. Chem. Soc.*, 2005, **127**, 3894.

CHAPTER TWO: CYCLOPENTADIENYL CONTAINING MIXED-SANDWICH U(III) COMPLEXES

2.1 Reactivity of [U(η^5-Cp^R)(η^8-C_8H_6{Si^iPr_3-1,4}$_2$)(THF)] (R = Me_4H, Me_5) with small molecules.

2.1.1 Introduction:

The discovery of uranocene in 1968[1] was a watershed in organoactinide chemistry, though its reactivity proved to be limited. Whereas the half-sandwich complexes [Th(η^8-C_8H_8)X_2] (X = Cl, BH_4),[2] precursors to derivative chemistry, are readily synthesised from [Th(η^8-C_8H_8)$_2$], the chemistry of [U(η^8-C_8H_8)$_2$] is complicated by the accessibility of the trivalent oxidation state and the particular stability of [U(η^8-C_8H_8)$_2$].[3] The use of substituted cyclooctatetraenyl ligands is less common in organometallic chemistry than the use of substituted cyclopentadienyl ligands, though examples have been synthesised using alkyl, alkoxy and amino[4] or bulky silyl substituents.[5]

The chemistry of mono-cyclooctatetraenyl uranium complexes is well established.[6] The half-sandwich chemistry of U(IV) was pioneered and developed by the Ephritikhine group, from $[U(\eta^8\text{-}C_8H_8)I_2(THF)_2]$[7] and the polymeric $[U(\eta^8\text{-}C_8H_8)(BH_4)_2]_n$[8] precursors and includes the mixed ring complexes $[U(\eta^8\text{-}C_8H_8)(\eta^5\text{-}Cp)R]$ (R = $N(SiMe_3)_2$, CH_2SiMe_3).[9] It is interesting to note that the substituted cyclooctatetraenyl complex $[U(\eta^8\text{-}C_8H_6\{SiMe_3\text{-}1,4\}_2)(BH_4)_2]$[10] can be prepared from $[UCl_2(BH_4)_2]$ and $[Li_2(C_8H_6\{SiMe_3\text{-}1,4\}_2)]$ but that $[U(\eta^8\text{-}C_8H_8)_2]$ was the only isolable product of an analogous reaction using $[K_2(C_8H_8)]$, which suggests that the substituents on the cyclooctatetraene stabilise the half-sandwich complex with respect to redistribution reactions.

It was the synthesis of the trivalent starting material, $[UI_3(THF)_4]$[11] and with it $[U(\eta^5\text{-}Cp^{Me5})I_2(THF)_3]$[12] in 1989, that enabled the subsequent synthesis of the mixed-sandwich complex $[U(\eta^5\text{-}Cp^{Me5})(\eta^8\text{-}C_8H_8)(THF)]$.[13] The structure of the THF adduct was not determined but the bipyridine adduct, $[U(\eta^5\text{-}Cp^{Me5})(\eta^8\text{-}C_8H_8)(Me_2bpy)]$ (Me_2bpy = 4,4'-dimethyl-2,2'-bipyridine) revealed a bent sandwich structure, with a Cp-U-C_8H_8 centroid angle of 132.8°. No electron transfer to the bipyridine ligand was observed by UV/VIS and ^1H NMR and the complex was assigned as U(III). This was rationalised by the stability of the U(III) complex by comparison to the Yb(II) complex $[Yb(Cp^{Me5})_2(OEt_2)]$, which is oxidised by bipyridine. The relative oxidation potentials were determined by cyclic voltammetry to be E° - 0.69 V for U(III) and 1.40 V Yb(II). The only characterised reductive chemistry that has been reported for the unsubstituted cyclooctatetraenyl mixed-sandwich complex $[U(\eta^5\text{-}Cp^{Me5})(\eta^8\text{-}C_8H_8)(THF)]$ is the two

electron reduction of cyclooctatetraene to form the bridging [(U(η^5-Cp^{Me5})(η^8-C_8H_8))$_2$(μ-η^3:η^3-C_8H_8)] complex.[14]

The reductive coupling of CO[15] and the reductive disproportionation of CO_2[16] by the U(III) mixed-sandwich complexes [U(η^8-C_8H_6{Si^iPr_3-1,4}$_2$)(η^5-Cp^R)(THF)] (R = Me_5, Me_4H) has been described in Chapter One. This section details the reactions of [U(η^8-C_8H_6{Si^iPr_3-1,4}$_2$)(η^5-Cp^{Me4H})(THF)] (**2.1**) with high-pressure H_2/CO and selected small molecules and the reactivity of **2.1** and [U(η^8-C_8H_6{Si^iPr_3-1,4}$_2$)(η^5-Cp^{Me5})(THF)] (**2.2**) with methyl isocyanide.

*2.1.2 Synthesis of [U(η^8-C_8H_6{Si^iPr_3-1,4}$_2$)(η^5-Cp^R)(THF)] (R = Me_4H (**2.1**), Me_5 (**2.2**)).*

The [U(η^5-Cp^R)I_2(THF)$_3$] (R = Me_4H, Me_5) complexes were synthesised according to a modified literature preparation[11] in an 80 % yield. A solution of UI_3 in THF was stirred vigorously for 1 hr prior to the addition of a THF slurry of KCp^R (R = Me_4H, Me_5) and the resulting blue-green solution was stirred overnight. Volatiles were removed in vacuo, the green solids were extracted with toluene and the mixture was filtered and then stripped to dryness.

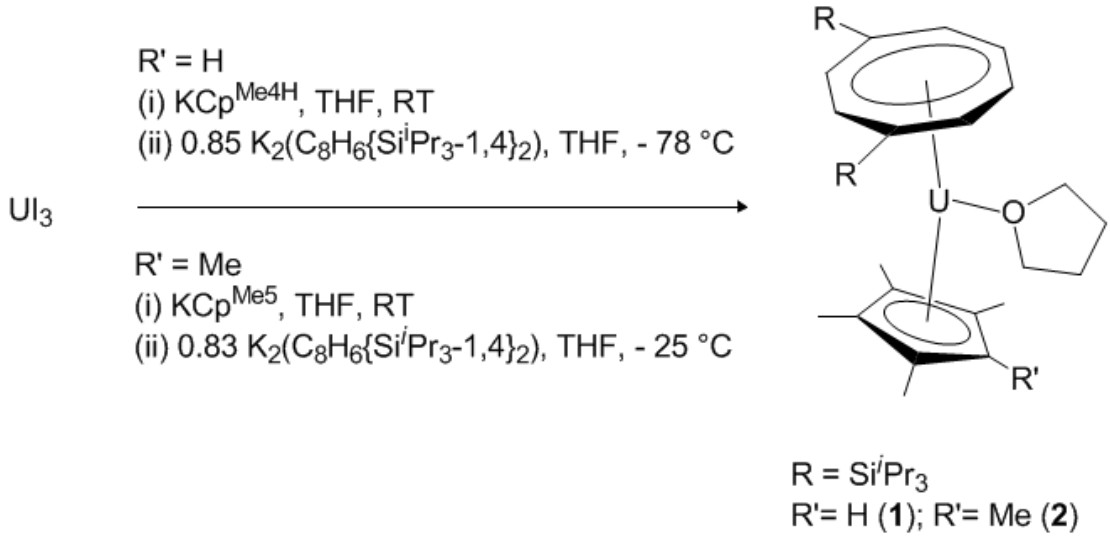

Scheme 1: Synthesis of $[U(\eta^8\text{-}C_8H_6\{Si^iPr_3\text{-}1,4\}_2)(\eta^5\text{-}Cp^R)(THF)]$ (R = Me_4H (**2.1**), Me_5 (**2.2**)).

The mixed-sandwich complexes were synthesised in a manner analogous to that described by Summerscales et al,[15] and the overall synthesis is shown above. Synthesis of **2.1**: green residues of $[U(\eta^5\text{-}Cp^{Me4H})I_2(THF)_3]$ were taken up in THF and to this was added dropwise at -78ºC over 2 hrs, 0.85 equivalents of $K_2(C_8H_6\{Si^iPr_3\text{-}1,4\}_2)$ in THF. The solution was allowed to warm to room temperature, upon which a colour change was observed from an emerald green to a dark brown with white precipitate, and this was stirred for a further 90 min. Pentane work-up and cooling to -30 °C overnight yielded black needle-like crystals of **2.1** (46 % w.r.t UI_3).

Synthesis of **2.2**: dark green residue of $[U(\eta^5\text{-}Cp^{Me5})I_2(THF)_3]$ was taken up in THF and cooled to -25 °C, to this 0.83 equivalents of $K_2(C_8H_6\{Si^iPr_3\text{-}1,4\}_2)$ in THF was added dropwise over 90 min. The solution was observed to change from a bright green to a

dark brown with the appearance of a white precipitate, and warmed to room temperature with stirring overnight. Pentane work-up and cooling to -30 °C overnight yielded black needle-like crystals of **2.2** (55 % w.r.t UI_3).

It was found that the synthesis of **2.2** at -25 °C, as described above, rather than at room temperature as is described in the literature,[15a] resulted in a 10 % increase in the yield. The ^{1}H NMR data and mass spectra of **2.1** and **2.2** were in good agreement with in the literature.[15]

*2.1.3 Reaction of [U(η^8-C_8H_6{Si^{i}Pr$_3$-1,4}$_2$)(η^5-Cp^{Me4H})(THF)] (**2.1**) with 10 bar H_2 /CO:*

Complex **2.1** was found to have no reactivity with H_2 under mild conditions.[17] It was reacted with 10 bar H_2/CO to determine whether at the increased pressure it would show reactivity towards the mixture of gases.

Complex **2.1** was dissolved in toluene, to this was added 10 bar H_2 /CO from a pre-pressurised bomb. The colour of the solution changed from brown to red with the formation of a brown precipitate. The solution was stirred under pressure of gas overnight. Samples of the reaction mixture, under nitrogen and hydrolysed were submitted for GCMS and blanks of toluene, ethylene glycol, diethylene glycol, pentane and hexane were run for comparison. Unfortunately the instrument was unable to differentiate between the solvent peaks and potential products of low molecular weight,

for example, ethylene glycol. The only peaks visible in the mass spectrum correspond to the ligands present, both deprotonated and neutral. The volatiles were removed *in vacuo* leaving red solids but no crystalline material was able to be isolated and ^{1}H NMR spectrum displayed a mixture of products. The EI mass spectrum of the red solids shows at peak at m/z = 1072 and a peak at m/z = 777 likely corresponding to the M^{+} of $[U(\eta^{8}\text{-}C_8H_6\{Si^{i}Pr_3\text{-}1,4\}_2)_2]$ (m/z = 1070) and base-free **2.1** (m/z = 775), though both peaks are 2 amu heavier than expected. This does not appear significant as no evidence for a uranium hydride or reactivity with hydrogen has been observed in our laboratory using U(III) mixed-sandwich complexes and may be a result of the EI process.

*2.1.4 Reactivity of $[U(\eta^{8}\text{-}C_8H_6\{Si^{i}Pr_3\text{-}1,4\}_2)(\eta^{5}\text{-}Cp^{Me4H})(THF)]$ (**2.1**) with CS_2 and ^{t}BuNCO:*

The trivalent metallocenes $[U(\eta^{5}\text{-}Cp^{Me})_3(THF)]$ and $[U(\eta^{5}\text{-}Cp^{SiMe3})_3]$ react with CS_2 to form the binuclear U(IV) complexes $[(\eta^{5}\text{-}Cp^{R})_3U]_2[\mu\text{-}\eta^{1}\text{:}\eta^{2}\text{-}CS_2]$ (R = Me, $SiMe_3$).[18] As CS_2 is isoelectronic with CO_2 and **2.1** reacts with 0.8 equivalents of CO_2 to form a mixture of carbonate and squarate products, the same stoichiometery was used.[16]

Complex **2.1** was dissolved in a minimum amount of toluene and to this was added 0.8 equivalents of CS_2 via a gas-tight syringe at -78 ºC. The solution was allowed to warm to room temperature and stir overnight. The colour of the solution changed from dark brown to red and solids were seen to precipitate. Volatiles were removed *in vacuo* and the red-brown solids extracted with THF. The ^{1}H NMR spectrum at room temperature

showed a mixture of products. It was not possible to separate the products or obtain material suitable for X-ray analysis from a range of solvents. The mass spectrum shows no peak for the M^+ of **2.1** but is dominated by the product of ligand redistribution, $[U(\eta^5\text{-}C_8H_6\{Si^iPr_3\text{-}1,4\}_2)_2]$.

The reaction of **2.2** with ^{i}PrNCO led to the observation of free ^{i}PrNC by GCMS and an unidentified oxidized uranium complex.[17] The reaction of PhNCO with $[U(\eta^5\text{-}Cp^{Me})_3(THF)]$ resulted in the reduction of the PhNCO and the formation of a bridging U(IV) species $[((\eta^5\text{-}Cp^{Me})_3U)_2(\mu\text{-}\eta^1\text{:}\eta^2\text{-}OCNPh)]$[19] with an η^1 U-O interaction and an η^2 U'-NC interaction. This complex did not liberate CO on heating to 80 ºC.

Complex **2.1** was dissolved in toluene and to this were added 2 equivalents of ^{t}BuNCO via a gas-tight syringe. There was an immediate colour change from brown to red. Volatiles were removed in vacuo and the sticky red solids extracted with THF. As in the reaction with CS_2, the ^{1}H NMR spectrum at room temperature showed a mixture of products and it was not possible to separate the products or obtain crystalline material suitable for characterisation. The EI mass spectrum did not contain a peak for $[U(\eta^8\text{-}C_8H_6\{Si^iPr_3\text{-}1,4\}_2)_2]$, however, the peaks at m/z = 849, 771, 728 cannot be unambiguously assigned and there is no direct evidence for the uranium(IV) oxo species.

*2.1.5 Synthesis and characterisation of [U(η^8-C_8H_6{Si^{i}Pr$_3$-1,4}$_2$)(η^5-Cp^{Me4H})(η^1-NCMe)] (**2.3**):*

The reductive coupling of alkyl[20] and aryl[21] nitriles and cross coupling with CO[22] is known for the early transition metals. Complexes of divalent lanthanides have provided examples of both reductive coupling of acetonitrile[23] and C-C bond cleavage.[24] The reaction of the uranium hydride complex [(η^5-Cp^{Me5})$_2$UH)$_2$] with acetonitrile resulted in the isolation of [{(η^5-Cp^{Me5})$_2$U(CH_3C(NH)=CHC=(NH)=CHCN)}$_2$], the product of the reductive coupling of three acetonitrile molecules to form a diaminocyanopentadienyl dianion with concomitant loss of H_2. The reaction with CD_3CN resulted in a fully deuterated coupled product, suggesting no incorporation of uranium hydrides.[25] The uranium nitrile complexes [(η^5-Cp)$_3$U(NCR)] (R = Me, ^{n}Pr, ^{i}Pr or ^{t}Bu) have been synthesised from the reaction of [(η^5-Cp)$_3$U(THF)] with the corresponding nitrile.[26]

The reaction of **2.1** in toluene with 1 equivalent of acetonitrile at room temperature, followed by work-up and crystallisation from THF at – 50 °C resulted in the isolation of [U(η^5-Cp^{Me4H})(η^8-C_8H_6{Si^{i}Pr$_3$-1,4}$_2$)(η^1-NCMe)] (**2.3**) in a 50 % yield. The spectroscopic data and elemental analysis are in agreement with the molecular formation. Complex **2.3** proved sparingly soluble in common solvents and can be stored under inert atmosphere in the solid state. The ^{1}H NMR spectrum in d_8-thf at 30 °C, displays a similar pattern to that observed in complex **2.1**, indicative of a monomeric structure and single ligand environments rendered by mirror plane symmetry on the NMR timescale, with resonances which are significantly shifted from those of **2.1**.

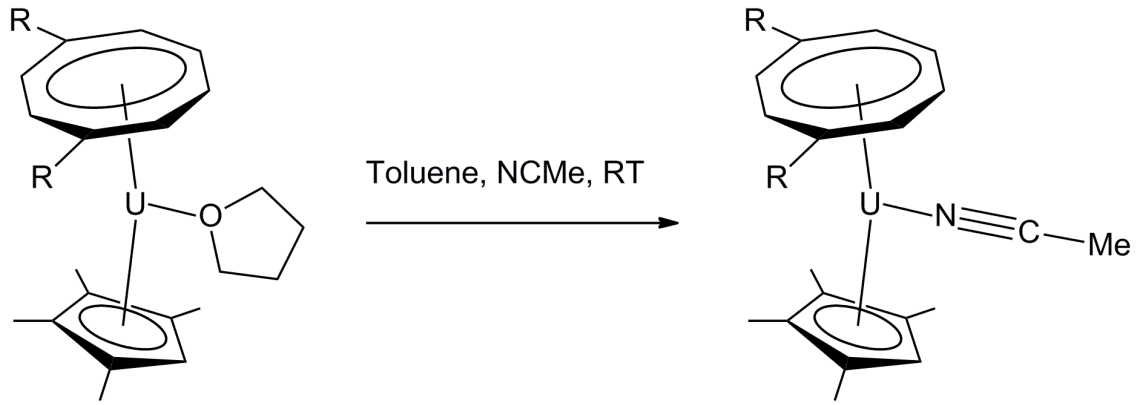

R = $Si^{i}Pr_3$

Scheme 2: Synthesis of [U(η^5-Cp^{Me4H})(η^8-C_8H_6{$Si^{i}Pr_3$-1,4}$_2$)(η^1-NCMe)] (**2.3**)

The paramagnetic nature of the uranium centre results in a wide spectral range and anisotropic chemical shifts, however, the signals themselves are well defined, which allows the NMR shifts to be assigned on the basis of relative integration. The bulky triisopropyl silyl groups on the cycloctatetraenyl ligand provide a useful spectroscopic handle in the ^{1}H NMR, as they appear in a ratio of 18:18:6 for the two sets of ^{i}Pr-CH_3 protons and the ^{i}Pr-CH protons, respectively, though multiplicity is not necessarily observed. In the ^{1}H NMR spectrum of **2.3**, neither the Cp^{Me4H}-CH resonance nor the coordinated acetonitrile could be identified. In the case of the Cp^{Me4H}-CH resonance, this is most likely a result of an increase in linewidth. The Cp^{Me4H}-CH resonance is significantly broadened in complex **2.1**; the resonances of the ring protons of both the cyclopentadienyl and the cycloctatetraenyl ligands are much broader than those of the ring substituents, presumably as a consequence of being π-bound to the uranium centre. The nitrile resonances were observed by ^{1}H NMR in the U(III) complexes [(η^5-

$Cp)_3U(NCR)]$ (R = Me, ^{n}Pr, ^{i}Pr or ^{t}Bu),[26] but not in the uranium(III) adduct $[U(\{ArO\}_3tacn)(\eta^1\text{-}NCMe)]$[27] (Ar = 3,5-di-tert-butylbenzyl, tacn = 1,4,7-triazacyclononane).

Single crystals of **2.3** were grown from a saturated THF solution at – 50 °C. The structure is shown in Figure 1 and selected structural parameters are given. For the structural and refinement data see Appendix Two. The molecule lies of on a crystallographic mirror plane with the 'missing' methyl group of the Cp^{Me4H} ring disordered between the two positions related by the mirror plane.

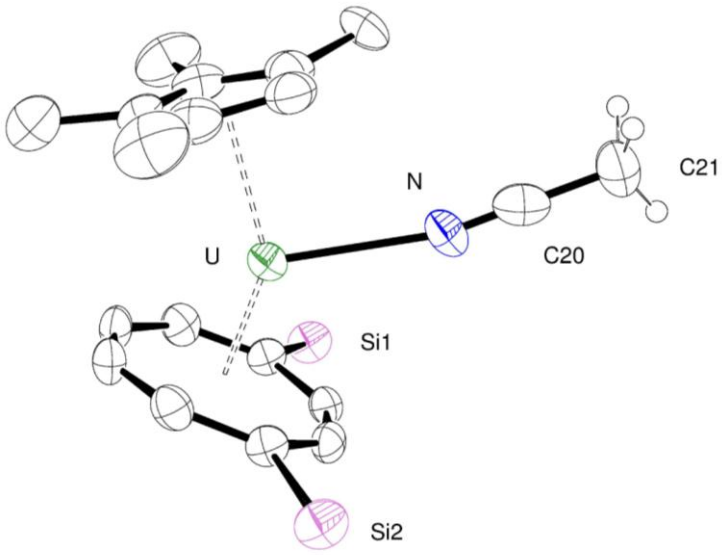

Figure 1: $[U(\eta^5\text{-}Cp^{Me4H})(\eta^8\text{-}C_8H_6\{Si^iPr_3\text{-}1,4\}_2)(\eta^1\text{-}NCMe)]$ (**2.3**) ellipsoids at 50 % probability, ^{i}Pr groups and H atoms, except MeCN, omitted for clarity. Selected bond distances (Å) and angles (°): U-M1 1.972(6), U-M2 2.502(6), U-N 2.586(8), N-C 1.133(13), U-N-C 167.6(8), M1-U-M2 145.5(2) (M1 is the centroid of the $[C_8H_6\{Si^iPr_3\text{-}1,4\}_2]^{2-}$ ring and M2 the centroid of the $(Cp^{Me4H})^-$ ring).

The bent-sandwich structure of **2.3** is comparable to that of complex **2.1** [U(η^8-$C_8H_6\{Si^iPr_3\text{-}1,4\}_2$)($\eta^5$-$Cp^{Me4H}$)(THF)], in which the M1-U-M2 angle is 141.8(2)° and the uranium centroid distances in the two complexes are identical within esds, U-M1 1.977(5) Å and U-M2 2.506(6) Å in **2.1**. The U-N bond distance of 2.586(8) Å in **2.3** is shorter than the U-N(NCMe) of 2.66 Å in the bulky [U($\{ArO\}_3$tacn)(η^1-NCMe)][27] complex and falls between the values of U-N(NCR) 2.61(1) Å and 2.551(9) Å for the examples of [(η^5-Cp)$_3$U(NCR)] (R = ^{n}Pr or ^{i}Pr),[26] which were structurally characterized. The U-NCMe interaction is not unusual and the N-C distance in **2.3** is not lengthened from that in the free nitrile 1.158(2) Å.[28]

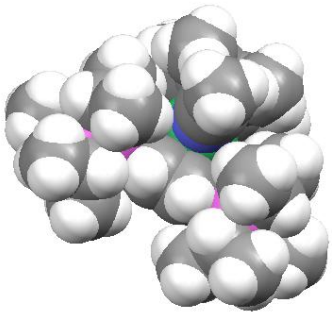

Figure 2: Spacefilling representation of [U(η^5-Cp^{Me4H})(η^8-$C_8H_6\{Si^iPr_3\text{-}1,4\}_2$)($\eta^1$-NCMe)] (2.3) with the uranium atom in green, nitrogen atom in blue, silicon atoms in pink, carbon atoms in grey and hydrogen atoms in white.

The U-N-C angle in the bulkier NC^{i}Pr adduct, [(η^5-Cp)$_3$U(NC^{i}Pr)] deviates less from linear at 172.1(8)° than the 167.6(8)° in **2.3**. This may may be due to the steric crowding, as seen in the spacefilling representation of **2.3** shown in Figure 2, the acetonitrile is surrounded by the methyl groups of the cyclopentadienyl ligand above

and the isopropyl groups of the triisopropyl silyl cyclooctatentraenyl ligand below. It is possible that the bulky steric environment may prevent an oxidative kinetic pathway from occurring or that the activation and/or coupling of acetonitrile by **2.1** is not entropically favoured at room temperature.

*2.1.6 Attempted thermolysis of [U(η^8-C_8H_6{Si^iPr_3-1,4}$_2$)(η^5-Cp^{Me4H})(η^1-NCMe)] (**2.3**):*

Interestingly, the reaction of [(η^5-Cp)$_3$U(THF)] with benzonitrile at room temperature or thermolysis of the adducts [(η^5-Cp)$_3$U(NCR)] (R = Me or ^{n}Pr) resulted in equimolar amounts of the uranium(IV) complexes [(η^5-Cp)$_3$U(CN)] and [(η^5-Cp)$_3$U(R)] (R = Me, ^{n}Pr or Ph).[26] It was proposed that **2.1** might show similar reactivity to the *tris*-cyclopentadienyl complexes of uranium(III) or that the mixed-sandwich ligand environment might confer sufficient stability to isolate the benzonitrile adduct. The addition of the benzonitrile to **2.1** at -55 ºC resulted in a colour change from brown to bright green. However, upon warming to room temperature the colour of the solution returned to brown. Volatiles were removed *in vacuo* and red solids were extracted with pentane and separated from the remaining green solids. The green solids were taken up in toluene but no characterisation data were obtained and the green solution was observed to change colour to red after subsequent manipulation.

When **2.3** was heated in d_8- toluene at 80 °C, the ^{1}H NMR obtained showed a mixture of products and three ^{29}Si environments were observed by ^{29}Si{^{1}H} NMR. The EI mass spectrum of the reaction mixture displayed a range of products, consistent with a single

uranium centre but which were unable to be unambiguously assigned. The thermolysis of **2.3** was repeated in d_8-thf at 50 ºC, in the hope that the improved solubility and lower heating temperature might result in a more controlled reaction. However, after heating for 3 days the ^{1}H NMR spectrum showed a mixture of products and five resonances were observed by ^{29}Si{^{1}H} NMR, which do not correspond to those of free ligand. The EI mass spectrum of the reaction mixture was more complex, including the M^{+} for **2.3** and some of the products observed after heating in d_8- toluene. There are three other sets of peaks, each related to the other by the loss of the $(Cp^{Me4H})^{-}$ ligand, but they have not been unambiguously assigned.

*2.1.7 Reactivity of [U(η^{8}-C$_8$H$_6${Si^{i}Pr$_3$-1,4}$_2$)(η^{5}-Cp^{R})(THF)] (R = Me$_4$H (**2.1**), Me$_5$ (**2.2**)) with MeNC:*

Isocyanides are isoelectronic with CO and have been used to model CO reactivity.[29,30] The first reported isocyanide complex of uranium(III) was [U(η^{5}-Cp)$_3$(CNC$_6$H$_{11}$)], also the first example of a U-C σ-single bond.[31] Anderson et al. also synthesised and structurally characterised [U(η^{5}-Cp^{SiMe3})$_3$(η^{1}-CNEt)], when they reported the first molecular CO complex [U(η^{5}-Cp^{SiMe3})$_3$(CO)], which eluded structural characterization.[32] The complex [U(O-2,6-t-Bu$_2$C$_6$H$_3$)$_3$] reacts to form either the 1:1 or 1:2 adduct with CN^{t}Bu, [U(O-2,6-t-Bu$_2$C$_6$H$_3$)$_3$(η^{1}-CN^{t}Bu)$_n$] (n = 1, 2), the latter identified by ^{1}H NMR at low temperature.[33] This is the also the only example of a low-valent uranium isocyanide complex that is not supported in a *tris*-cyclopentadienyl ligand environment.

Carmona and co-workers have synthesised a range of isocyanide metallocene complexes [U(η^5-Cp^R)$_3$(η^1-CNR')] (R = H, Me, Me_4H, ^{t}Bu, $SiMe_3$, 1,3-$(SiMe_3)_2$, R' = Me, Et, ^{i}Pr, ^{t}Bu, MeO-p-C_6H_4, 2,6-$Me_2C_6H_3$) from the reaction of the base-free metallocene with an excess of CNR.[34] The 1:1 adduct was formed in all cases, except [U(η^5-Cp^{Me4H}){η^1-CN(2,6-$Me_2C_6H_3$)}] for which both the 1:1 and 1:2 were synthesised. Not all of the isocyanide complexes could be isolated. It was found that in [U(η^5-Cp^{Me4H})$_3$(η^1-CNR)] (R = Me, ^{i}Pr, ^{t}Bu) were unstable in solution and decompostition to [U(η^5-Cp^{Me4H})$_3$(CN)] was proposed. The aromatic isocyanide complexes, where R = MeO-p-C_6H_4 or 2,6-$Me_2C_6H_3$ were thermally stable and the molecular structure of [U(η^5-Cp^{Me4H})$_3$(η^1-CNMeO-p-C_6H_4)] was determined. The reactivity of **2.1** and **2.2** with methyl isocyanide is of interest in the context of the reactivity with CO[15] to form the deltate and squarate dianions. Pseudo-oxocarbons are known but their synthesis is non-trivial.[35]

Complex **2.1** was reacted with 1 equivalent of MeNC under the conditions used in the synthesis of **2.3**. On addition the colour of the solution remained brown and a brown precipitate was formed upon addition. The solvent was removed *in vacuo* and the dark brown solids extracted with THF. After several days in THF the colour of the solution was observed to change colour from brown to red. It has not been possible to obtain solid material suitable for characterisation from a range of solvents. The ^{1}H NMR spectrum of the reaction mixture is consistent with the formation of a major and a minor product. This is supported by the two resonances observed by ^{29}Si{^{1}H} NMR, one of which is significantly more intense than the other. However, the EI mass spectrum does not show anything other than the fragmentation of the solvated parent ion **2.1**.

Complex **2.2** was reacted in toluene at - 78 °C with 2 equivalents of MeNC. After warming to ambient temperature overnight, the colour of the solution was observed to be red/brown and no precipitate was visible. The solvent was removed *in vacuo* and the red/brown matrix extracted with diethyl ether. It has not been possible to obtain solid material suitable for characterisation from a range of solvents. The ^{1}H NMR spectrum of the reaction mixture is consistent with the formation of a major product. Free THF is also visible in the ^{1}H NMR, indicating its lability in this reaction, as the only THF present is that which was previously coordinated to the uranium centre. The EI mass spectrum also does not show anything other than the fragmentation of the solvated parent ion **2**, however the unsolvated M+ does not appear (the peak at 809 amu corresponds to $[U(\eta^5\text{-}Cp^{Me5})(\eta^8\text{-}C_8H_6\{Si^iPr_3\text{-}1,4\}_2)(F)]$ from the defluorination of the calibrant used in the EI[17]). This is curious following the observed lability of the THF in solution but it is not indicative either of reaction or no reaction.

The product of the reaction of MeNC with **2.2** or major product in the case of the reaction with **2.1**, have similar ^{1}H NMR spectra. However, in the absence of further characterising data, it is unclear what the formulation of the product(s) of this reaction might be. Given the difficulty of isolating crystalline material, *in situ* solution IR spectroscopy, after desolvation of **2.1** and **2.2**, might be a more effective way of studying these reactions.

*2.1.8 Structure of [U(η^5-Cp^{Me5})(η^8-C_8H_6{Si^iPr_3-1,4}$_2$)(η^1-CNMe)] (**2.4**):*

Small crystals were grown from an NMR scale reaction of **2.2** with MeNC in d_6-benzene over several months at room temperature. The structure was determined as [U(η^5-Cp^{Me5})(η^8-C_8H_6{Si^iPr_3-1,4}$_2$)(η^1-CNMe)] (**2.4**) and the disordered benzene solvate was modelled as a rigid body over two orientations.

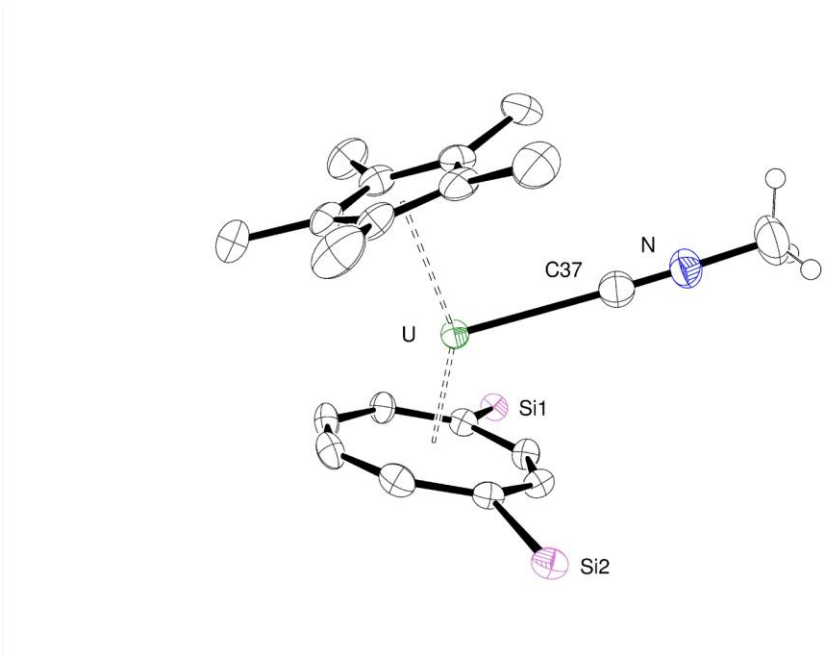

Figure 3: [U(η^5-Cp^{Me5})(η^8-C_8H_6{Si^iPr_3-1,4}$_2$)(η^1-CNMe)] (**2.4**) ellipsoids at 50 % probability, ^{i}Pr groups and H atoms, except MeNC, omitted for clarity. Selected bond distances (Å) and angles (°): U-M1 1.947(5), U-M2 2.482(5), U-C37 2.660(4), N-C37 1.142(5), M1-U-M2 148.3(2), U-C37-N 178.4 (M1 is the centroid of the [C_8H_6{Si^iPr_3-1,4}$_2$]$^{2-}$ ring and M2 the centroid of the (Cp^{Me5})$^-$ ring).

As in the case of **2.3** the bent-sandwich structure of **2.4** is comparable to that of the parent complex **2.2**[15a] and the N-C(Me) distance in **2.4** is essentially identical to that found in **2.3**.The U-C37 distance in **2.4** is significantly longer than that found in either [U(η^5-Cp^{SiMe3})(η^1-CNEt)],[32] 2.57(3) Å or [U(η^5-Cp^{Me4H})(η^1-CNMeO-p-C_6H_4)],[34] 2.464(4) Å. The U-C37-N angle in **2.4** is closer to 180° than **2.3** or either of the aforementioned U(III) complexes, which have very similar U-C-N angles of 173.6(2)° and 173.7(9)°, respectively. The U-C(NR) distance is longer in [U(η^5-Cp^{Me4H})(η^1-CNMeO-p-C_6H_4)] than the U-C(CO) 2.383(6) Å in [U(η^5-Cp^{Me4})$_3$(η^1-CO)],[36] the only directly comparable structurally characterised example.

The metal to ligand back-bonding in the [U(η^5-Cp^{Me4H})$_3$(η^1-CNMeO-p-C_6H_4)] complex is based on a ν_{CNR} stretch of 2072 cm^{-1}, which is shifted by -50 cm^{-1} from the free isocyanide, though the C-N(R) distance is not significantly lengthened. Carmona found that the ν_{CNR} of the uranium(III) aryl isocyanide adducts shifted to lower wavenumbers but that the alkyl isocyanide adducts shifted to higher wavenumbers, relative to their respective free ν_{CNR} and that the shift was dependant on the substituents on the Cp rings[34]. It is interesting to note that in the complexes [U(η^5-Cp^{Me4H})$_3$(η^1-CNR)] (R = Me, ^{i}Pr, ^{t}Bu), the shift in ν_{CNR} on complexation is < 10 cm^{-1}.

As there was insufficient material for further characterisation, any discussion of the U-CNMe interaction in **2.4** would be premature and indeed the isolation of **2.4** does not provide evidence of reactivity, necessarily, though the ^{1}H NMR of the reaction of **2.2** with MeNC is consistent with the formation of a single product. It is interesting that **2.4**,

in contrast to Carmona's uranium(III) alkyl isocyanides, is stable in solution, *vide supra*. The long U-C bond and the almost linear U-C-N angle in **2.4** are not indicative of a strong interaction between the uranium(III) centre and the MeNC. The uranium centre in **2.4** appears more exposed in the spacefilling representation shown in Figure 4, relative to that of **2.3** in Figure 2 this may be a result of the Van der Waals radius of the carbon atom and the long U-C distance, though there is no significant change to the overall uranium-ligand bonding parameters between **2.2** and **2.4**.

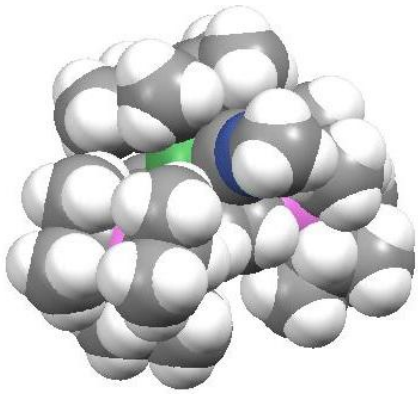

Figure 4: Spacefilling representation of [U(η^5-Cp^{Me5})(η^8-C_8H_6{Si^iPr_3-1,4}$_2$)(η^1-CNMe)] (**2.4**) with the uranium atom in green, nitrogen atom in blue, silicon atoms in pink, carbon atoms in gray and hydrogen atoms in white.

2.1.9 Conclusion:

The uranium(III) complexes [U(η^5-Cp^R)(η^8-C_8H_6{Si^iPr_3-1,4}$_2$)(THF)] (R = Me_4H (**2.1**), Me_5 (**2.2**)) were successfully synthesised and the yield of **2.2** was improved from that reported in the literature. The reactions of **2.1** with high-pressure H_2/CO and other small molecules did not lead to the isolation of new products with the exception of the reaction of **2.1** with one equivalent of acetonitrile, which resulted in the isolation and full characterisation of the acetonitrile adduct of complex **2.1**, [U(η^5-Cp^{Me4H})(η^8-C_8H_6{Si^iPr_3-1,4}$_2$)(η^1-NCMe)] (**2.3**). Complex **2.3** undergoes thermolysis when heated in either d_8-thf or d_8-toluene to form a number of products, the formulation of which were not able to be elucidated.

Complexes **2.1** and **2.2** were reacted with methylisocyanide and the ^{1}H NMR data suggest a major and minor product in the case of **2.1** and a single product in the case of **2.2**. A structure was obtained from an NMR scale reaction of **2.2** with methylisocyanide and shown to be the isocyanide adduct [U(η^5-Cp^{Me5})(η^8-C_8H_6{Si^iPr_3-1,4}$_2$)(η^1-CNMe)] (**2.4**), which has a long U-C interaction.

2.2 Oxocarbon Extraction: the reactivity of [(U(η^8-C_8H_6{Si^{i}Pr$_3$-1,4}$_2$)(η^5-Cp^{Me4H}))$_2$(μ-η^2:η^2-$^{13}C_4O_4$)] (2.5) with halogen containing reagents and pseudo-halides.

2.2.1 Introduction:

The cyclooligomerisation of CO by the uranium mixed-sandwich complexes [U(η^8-C_8H_6{Si^{i}Pr$_3$-1,4}$_2$)(η^5-Cp^R)(THF)] (R = Me$_4$H (**2.1**), Me$_5$ (**2.2**)) is the first example of oxocarbon synthesis from CO under mild conditions.[15] These reactions demonstrate C-C bond formation from a C_1 source and carbocycles are of synthetic importance as they are often incorporated in pharmaceutically active molecules.[37] The production of completely ^{13}C-enriched carbocycles from ^{13}CO under mild conditions may also be of commercial value as fully labelled molecules are often very expensive. However, to be practically applicable the substrate must be able to be removed from the metal centre, for example as shown in Scheme 3. In which the $^{13}C_4O_4^{2-}$ unit is chemically removed from the uranium centres by reaction with an organic halide or pseudohalide, yielding the uranium(IV) halide or pseudohalide and the functionalised $^{13}C_4$-unit. To complete the cycle the uranium(IV) halide or pseudohalide could then be reduced back to U(III) and reacted with further CO.

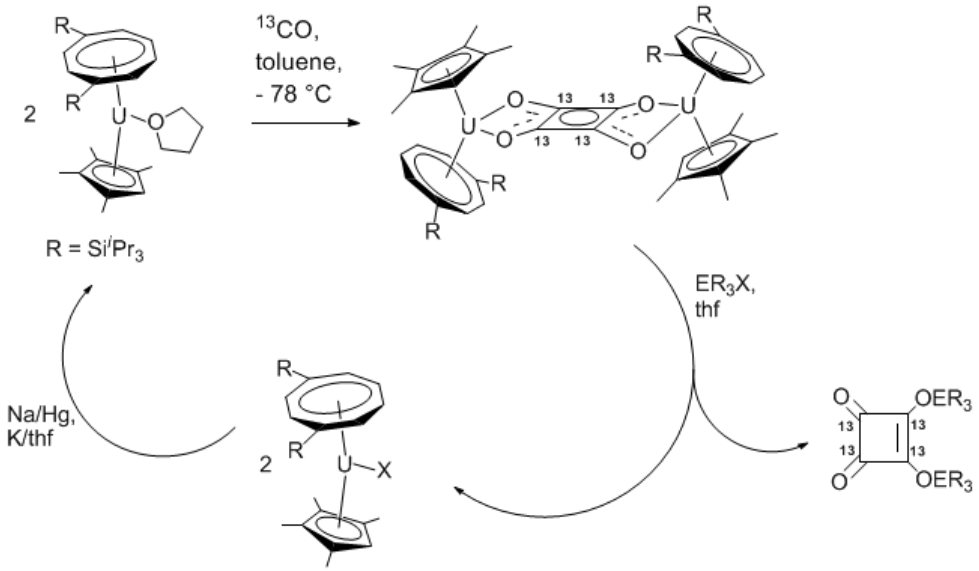

Scheme 3: Proposed cycle for the conversion of ^{13}CO to functionalised squarate.

*2.2.2 Synthesis of [(U(η⁸-C₈H₆{Si^{i}Pr₃-1,4}₂)(η⁵-Cp^{Me4H}))₂(μ-η²:η²-^{13}C₄O₄)] (**2.5**)*

A solution of **2.1** was freeze-thaw degassed in toluene, and whilst frozen and under static vacuum was exposed to an excess of ^{13}CO via the Toepler line. The solution was then transferred to a -78 ºC bath and allowed to warm to room temperature overnight; upon which the deeply coloured black solution was observed to have changed to a dark red colour with visible precipitate. Volatiles were removed in vacuo and the red solids were taken up in Et_2O with a very little THF. Filtration and cooling to -50 ºC for 3 days gave **2.5** as a dark red crystalline solid in 3 % yield.

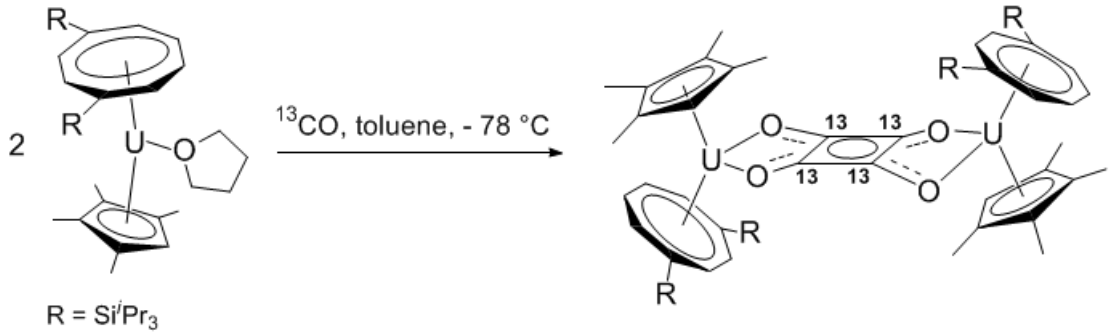

Scheme 4: Synthesis of [(U(η^8-C_8H_6{Si^{i}Pr$_3$-1,4}$_2$)(η^5-Cp^{Me4H}))$_2$(μ-η^2:η^2-$^{13}C_4O_4$)] (**2.5**)

The reaction between **2.1** and an overpressure of CO is reported to produce [(U(η^8-C_8H_6{Si^{i}Pr$_3$-1,4}$_2$)(η^5-Cp^{Me4H}))$_2$(μ-η^2:η^2-C_4O_4)] in a 66 % isolated yield);[15b] there is no recorded yield for **2.5** that pre-dates this work. The extremely low yield of **2.5** seen here, is due in part to the difficulty of isolating crystalline material. Complex **2.5** is sparingly soluble in Et_2O and very soluble in THF, but it was found that an 8:1 ratio of Et_2O to THF was effective. It is quite possible the yield of **2.5** is a result of the lower reaction pressure. There is a significant pressure disparity between the larger scale reaction at ca. 1 atm and the smaller scale reaction with labelled ^{13}CO. It is not economic to 'waste' ^{13}CO in doing these reactions, as the squarate dianion is the product of the 2 molecules of CO per uranium(III) centre. Doubling the amount of ^{13}CO used (in mmHg) did not improve the yield of **2.5**.

It is significant that the maximum pressure the Toepler pump can pressurise to is 0.85 atm. The reaction of [U(η^8-C_8H_6{Si^{i}Pr$_3$-1,4}$_2$)(η^5-Cp^{Me5})] with a sub-stoichiometric 0.9 equivalents of ^{13}CO added *via* the Toepler line to yield [U(η^8-C_8H_6{Si^{i}Pr$_3$-1,4}$_2$)(η^5-

Cp^{Me5})]$_2$(μ-η^1:η^1-$^{13}C_2O_2$)], also yields small amounts of the deltate complex[38] and indeed the analogous reaction to form the labelled deltate complex also yields the ynediolate complex.[39] The relationship between the specific pressure of the low-pressure system and the yields of the various carbocycles has not been fully rationalised. Pressure of the reaction vessel was seen to be important in the isolation of the coupled CO product in the reaction of [Sm(η^5-Cp^{Me5})$_2$(THF)$_2$] with CO.[40]

The $^{13}C\{^1H\}$ NMR spectrum of **2.5** in d_8-thf room temperature exhibits the characteristically broad singlet assigned to the enriched squarate fragment at δ –106.2 ppm and is shown in

Figure 5. The ^1H NMR spectrum of **2.5** displays no evidence for restricted rotation on the NMR timescale and the Cp^{Me4H}-C*H* resonance cannot be identified (see Section 2.1.5). As

Figure 5 shows, labelling of the $C_4O_4^{2-}$ unit enables the observation of the $^{13}C_4O_4^{2-}$ unit in **2.5** by $^{13}C\{^1H\}$ NMR in a very few scans and therefore provides a very useful spectroscopic handle for the reactivity of **2.5** with organic halides and pseudohalides.

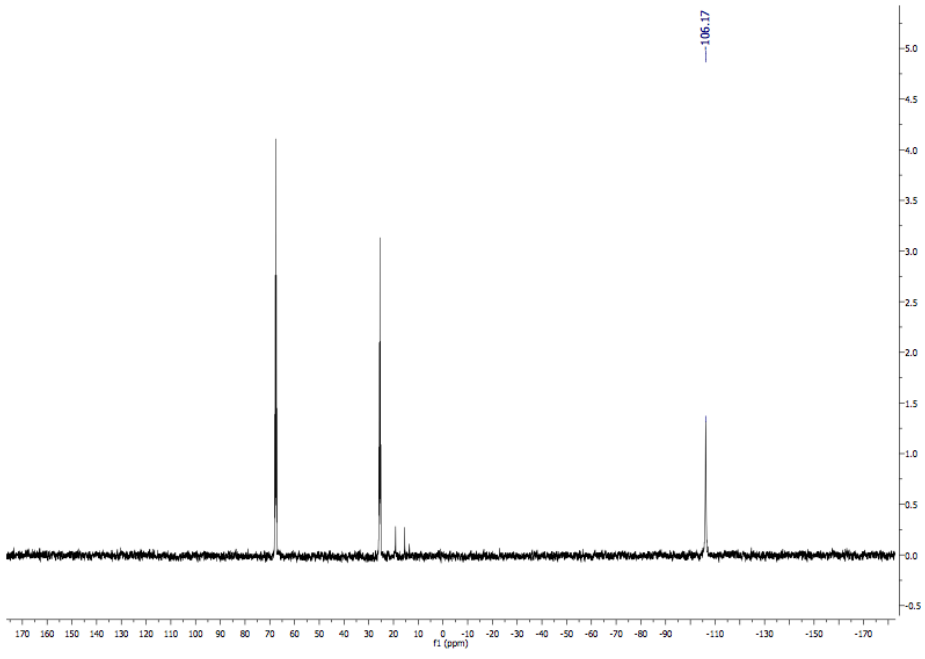

Figure 5: $^{13}C\{^{1}H\}$ NMR spectrum of **2.5,** 11 mgs in d_8-thf, 100.45 MHz, 30 ºC, 64 scans, lb = 5.

*2.2.3 Reactivity of [(U(η⁸-C₈H₆{Si^{i}Pr₃-1,4}₂)(η⁵-Cp^{Me4H}))₂(μ-η²:η²-^{13}C₄O₄)] (**2.5**) with SiR₃X (R = Me, Ph, X = I, Cl, OTf):*

The complex [(U(η^8-C_8H_6{Si^{i}Pr$_3$-1,4}$_2$)(η^5-Cp^{Me5}))$_2$(μ-η^1:η^2-$^{13}C_3O_3$)] was shown to react with $SiMe_3Cl$ to give [(U(η^8-C_8H_6{Si^{i}Pr$_3$-1,4}$_2$)(η^5-Cp^{Me5})(Cl)] by ^{1}H NMR but the functionalised $^{13}C_3O_3$ unit was not detected by $^{13}C\{^1H\}$ NMR. The reaction of [(U(η^8-C_8H_6{Si^{i}Pr$_3$-1,4}$_2$)(η^5-Cp^{Me4H}))$_2$(μ-η^2:η^2-$^{13}C_4O_4$)] (**2.5**) in d_8-thf with 2.5 equivalents of $SiMe_3Cl$ at room temperature resulted in the complete disappearance of the bound $^{13}C_4O_4$ unit and the appearance of the silylated squarate unit $^{13}C_4O_2(OSiMe_3)_2$

by $^{13}C\{^{1}H\}$ NMR at δ = 189.1, 189.7, 190.4, 195.7, 196.3 and 197.0 ppm and the observation of the chloride complex $[(U(\eta^{8}\text{-}C_8H_6\{Si^{i}Pr_3\text{-}1,4\}_2)(\eta^{5}\text{-}Cp^{Me4H})(Cl)]$ by ^{1}H NMR.[17] No fully ^{13}C-labelled squarate derivatives have been synthesised other than that reported by Summerscales *et al*[15,17] however a range of substituted squarate derivatives have been synthesised and their $^{13}C\{^{1}H\}$ NMR shifts recorded.[41] The $^{13}C\{^{1}H\}$ NMR spectrum of $C_4O_2(OMe)_2$ displays two resonances at δ 188.9 and 184.3 ppm.[42] In the ^{13}C NMR spectrum the resonance at δ 184.3 ppm is split into a quartet J_{CH} = 4 Hz and this was assigned to the β-carbon. In $C_4O_2(OSiMe_3)_2$ no coupling was observed by NMR between the ring carbons and the $SiMe_3$.[43] In all examples of substituted squarate derivatives the carbonyl resonance is found upfield from that of the β-carbon and the difference in chemical shift between the two resonances depends on the substituent groups on the oxygen atoms bonded to the β-carbon.

The NMR scale reaction between **2.5** and 2.5 equivalents of $SiMe_3I$ (stored at -20 ºC) in d_6-benzene at room temperature resulted in a darkening of the solution from orange to red on addition and red solids were visible. The $^{13}C\{^{1}H\}$ NMR spectrum was run within 10 min of addition and showed labelled broad multiplets at δ 194.0 and 188.1 ppm in the region expected for the $^{13}C_4O_2(OSiMe_3)_2$ product.[17,41,43] When complex **2.5** was reacted with 1 equivalent of $SiMe_3OTf$, in an analogous manner to the reaction of **2.5** with $SiMe_3I$, the physical observations were the same and the $^{13}C\{^{1}H\}$ NMR spectrum showed more intense labelled muliplets for the $^{13}C_4O_2(OSiMe_3)_2$ product at the same chemical shifts. The reactions of **2.5** with $SiMe_3I$ and $SiMe_3OTf$ were undertaken in d_6-benzene, to avoid side reactions with a more coordinating solvent. As **2.5** is sparingly soluble in d_6-benzene and solids were present, the samples were placed in a NMR

heating block set at 70 ºC. The $^{13}C\{^1H\}$ NMR spectra after heating each displayed a small amount of **2.5** but neither resonances in the product region nor other enriched resonances could be reliably identified.

The combination of the limited solubility and the incomplete nature of the reaction of $SiMe_3I$ and $SiMe_3OTf$ with **2.5** prevent any unambiguous conclusions from being drawn. The $^{13}C\{^1H\}$ NMR data indicates that the reaction does occur but why it does not go to completion and why the product resonances disappear on heating remains unclear, the $^{13}C_4O_2(OSiMe_3)_2$ product should be thermally stable up to 170 ºC.[43] There are several factors to consider; $C_4O_2(OSiMe_3)_2$ was found to undergo rapid intermolecular silyl migration by VT $^{13}C\{^1H\}$ NMR and the observation of the crossover product by MS EI after the mixing of $C_4O_2(OSiR_3)_2$ (R = Me, CD_3) at room temperature, though the mechanism is unknown and also the T_1 of the squarate carbons in $C_4O_2(OMe)_2$ are long.[41] It is also not clear what effect being in solution with the paramagnetic U(IV) centre will have on the $^{13}C\{^1H\}$ NMR spectrum of $^{13}C_4O_2(OSiMe_3)_2$.

To avoid the difficulty associated with measuring small quantities of volatile liquids and to further test the stoichiometery of the reaction the bulkier $SiPh_3Cl$ was reacted with **2.5**. To a solution of **2.5** in d_8-thf 2 equivalents of $SiPh_3Cl$ was added in an NMR tube. The solution was shaken manually and allowed to react overnight, after which the colour of the solution was observed to lighten from dark red to orange. The initial $^{13}C\{^1H\}$ NMR spectrum indicated that incomplete reaction had taken place and an overnight $^{13}C\{^1H\}$ spectrum of the $^{13}C_4O_2(OSiPh_3)_2$ (**2.6**) product shown in Figure 6.

The NMR tube was heated at 50 ºC to encourage further reaction but no change to the spectrum was observed. However, the addition of excess Ph_3SiCl (10 equivalents) did result in the complete disappearance of bound squarate peak of **2.5**.

The incomplete reaction of **2.5** with 2 equivalents of Ph_3SiCl suggests the reaction does not proceed stoichiometrically. It is unclear why this should be, although this was also the case in the reaction of **2.5** with $SiMe_3Cl$, which required at least 2.5 equivalents of $SiMe_3Cl$ to go to completion.[17] Larger scale reactions would be needed to test the stoichiometry of the reaction, most likely using the unlabelled complex $[(U(\eta^8\text{-}C_8H_6\{Si^iPr_3\text{-}1,4\}_2)(\eta^5\text{-}Cp^{Me4H}))_2(\mu\text{-}\eta^2\text{:}\eta^2\text{-}C_4O_4)]$ and GC-MS rather than NMR spectroscopy.

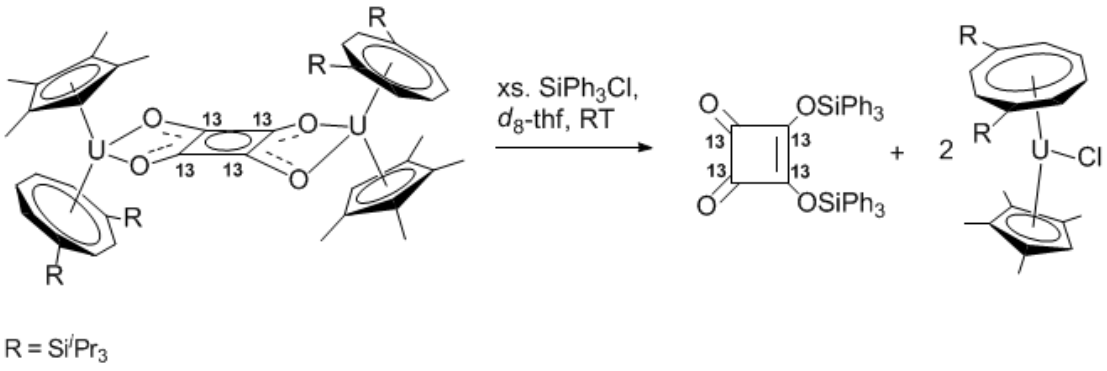

Scheme 5: Synthesis of $^{13}C_4O_4(SiPh_3)_2$ (**2.6**)

The $^{13}C\{^1H\}$ spectrum of **2.6** (Figure 6) shows second order effects resulting from the coupling of the ^{13}C labelled carbons, result in an AA'BB' system of 12 lines.[44] The second order nature of the spectrum can be seen in the roofing of the outer signals. The

$^{13}C\{^{1}H\}$ spectrum of **2.6**, appears as two apparent triplets of doublets at δ = 187.1, 187.7, 188.4, 193.4, 194.0 and 195.7 ppm, however, owing to the mixing of spin-states that results from the values δ and the J being similar in magnitude, the apparent multiplicity in the second-order spectrum of **2.6** cannot be assigned. The chemical shifts in **2.6** are very similar to those observed for $^{13}C_4O_2(OSiMe_3)_2$, at δ = 189.1, 189.7, 190.4, 195.7, 196.3 and 197.0 ppm, the $^{13}C\{^{1}H\}$ spectrum of which displays the same second order pattern.[17]

In $^{13}C_4O_2(OSiR_3)_2$ (R = Me, Ph) the value of the coupling constants will depend on the amount of s-character in the hybridisation of the bonding orbitals[45], however, couplings in conjugated systems[46] or between ^{13}C-labelled atoms[47] can be much larger than predicted, as they result from a combination of π-character and contributions from other coupling mechanisms.[48] Data on ^{13}C-^{13}C coupling constants is not available for direct comparison in most cases[49] and the solution of the specific contributions of the $^{1}J_{CC}$, $^{2}J_{CC}$ and $^{3}J_{CC}$ or the sign of $^{2}J_{CC}$ cannot be experimentally determined because the experimentally observed couplings are the product of the mixing of spin states. The spectrum may be able to be either simulated, either from experimental data or from a calculated structure. The $^{13}C\{^{1}H\}$ NMR spectrum of $^{13}C_4O_2(OSiMe_3)_2$ was simulated from the calculated structure by Nilay Hazari at the University of Oxford and is shown in Figure 7.

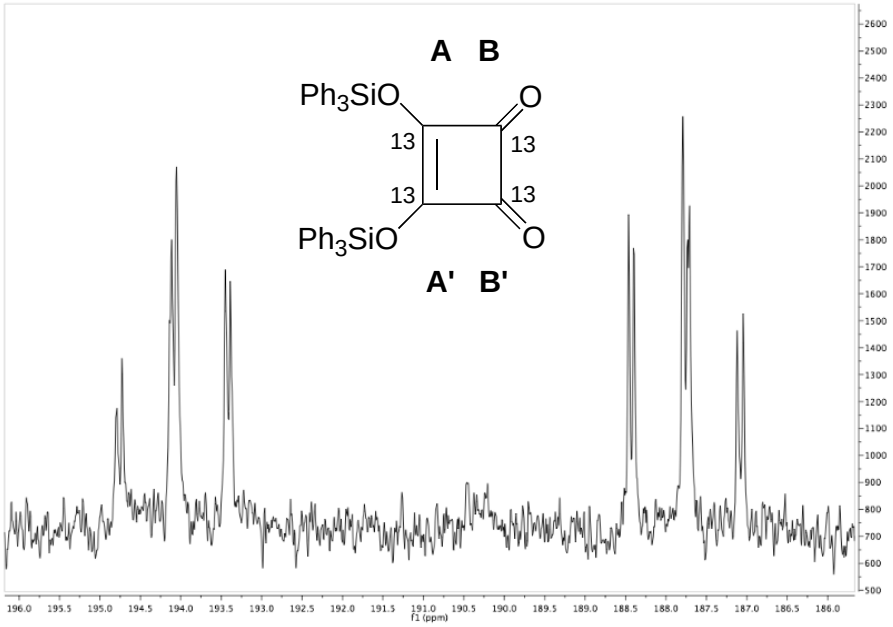

Figure 6: $^{13}C\{^{1}H\}$ NMR spectrum of $^{13}C_4O_2(OSiPh_3)_2$ (**2.6**) (d_8-thf, selected data, 100.45 MHz, 30 ºC, 10000 scans, lb = 5)

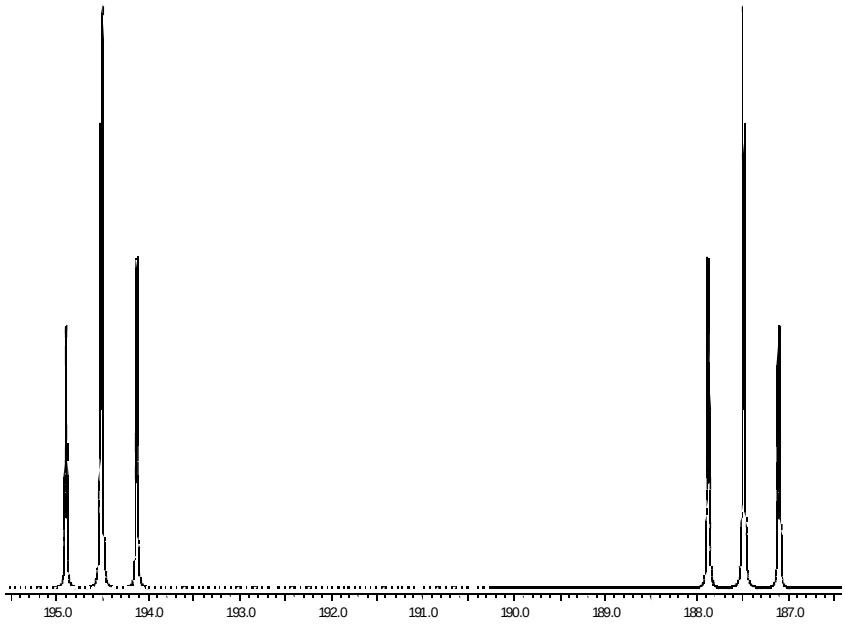

Figure 7: Simulated $^{13}C\{^{1}H\}$ spectrum of $^{13}C_4O_2(OSiMe_3)_2$. $J_{AA'}$ = 93.4 Hz, $J_{BB'}$ = 90.0 Hz, $J_{AB} = J_{A'B'}$ = 49. 1 Hz and $J_{AB'} = J_{A'B}$ = 48. 3 Hz.

*2.2.4 Reaction of [(U(η^8-C_8H_6{Si^iPr_3-1,4}$_2$)(η^5-Cp^{Me4H}))$_2$(μ-η^2:η^2-C_4O_4)] (**2.5**) with other halogenated reagents:*

The reaction of **2.5** with 2 equivalents of benzyl chloride in d_6-benzene showed only starting material in the $^{13}C\{^1H\}$ NMR, even after heating at 70 ºC for 3 days. This is presumed to because the formation of a carbon-oxygen bond provides an insufficient driving force to break the uranium-oxygen bonds, even in combination with the formation of the uranium-halogen bond. For this reason **2.5** was reacted with reagents containing heteroatoms known to form strong bonds to oxygen.

Complex **2.5** did not react with an excess (7 equivalents) of isopropylphenylchloro phosphine by $^{31}P\{^1H\}$ and $^{13}C\{^1H\}$ NMR. The NMR scale reaction of **2.5** with 2 equivalents of dimethyl aluminium chloride in thf/d_6-benzene was observed to lighten in colour from dark red to orange. The overnight $^{13}C\{^1H\}$ NMR spectrum of the reaction mixture showed a small peak for complex **2.5** and an ill-defined bump in the baseline of the spectrum in the region of δ 180-210 ppm. The only uranium complex seen in the MS EI of the reaction mixture was the chloride complex [(U(η^8-C_8H_6{Si^iPr_3-1,4}$_2$)(η^5-Cp^{Me4H})(Cl)], that the M+ and the fragments thereof contain the chloride ion is evident from the isotopic distribution. The data again point to the reaction having taken place but are insufficient to draw any clear conclusions.

2.2.5 Conclusion:

The uranium(IV) ^{13}C-labelled complex [(U(η^8-C_8H_6{Si^{i}Pr$_3$-1,4}$_2$)(η^5-Cp^{Me4H}))$_2$(μ-η^2:η^2-$^{13}C_4O_4$)] (**2.5**) was synthesised from the reaction of [U(η^8-C_8H_6{Si^{i}Pr$_3$-1,4}$_2$)(η^5-Cp^{Me4H})(THF)] with ^{13}CO, but was only able to be isolated in a very low yield. The reactions of **2.5** with halides or pseudohalides were monitored by ^{13}C{^{1}H} NMR spectroscopy. Complex **2.5** reacts with SiR_3X (R = Me, X = I, OTf or R = Ph, X = Cl), but the only functionalised product reliably observed by ^{13}C{^{1}H} NMR was $^{13}C_4O_2(OSiPh_3)_2$ (**2.6**), which has a AA'BB' spin-system and displays second-order effects. Reactions of **2.5** with benzyl chloride or isopropylphenylchloro phosphine did not proceed, whereas the reaction of **2.5** with dimethyl aluminium chloride led to the observation of the uranium(IV) chloride complex [(U(η^8-C_8H_6{Si^{i}Pr$_3$-1,4}$_2$)(η^5-Cp^{Me4H})(Cl)] by mass spectrometry.

Although ^{13}C{^{1}H} NMR spectroscopy does provide a means of following these reactions, neither has the stoichiometry of the reaction been rationalised nor have the products been fully characterised. The reactions need to be repeated on a larger scale, for which using ^{13}CO would not be cost effective, and focus both on increasing the yield of [(U(η^8-C_8H_6{Si^{i}Pr$_3$-1,4}$_2$)(η^5-Cp^{Me4H}))$_2$(μ-η^2:η^2-C_4O_4)] and on the recovery of the organic fragment. Since these reactions were undertaken, other work in the group has shown that the removal of the oxocarbon and reduction of the uranium centre may be achieved electrochemically.

2.3 Experimental Details For Chapter Two

General details are given in Appendix One.

*2.3.1 Synthesis of [U(η^5-Cp^{Me4H})(η^8-C_8H_6{Si^iPr_3-1,4}$_2$)(THF)] (**2.1**)*

To a solid equimolar mixture of UI_3 (1.86 g, 3.00 mmol) and KCp^{Me4H} (0.48 g, 3.00 mmol), was added THF (150 mL) and the resulting blue-green solution was stirred for 24 hr. Volatiles were removed in vacuo, the green solids were extracted with 2 x 45 mL toluene, filtered through Celite® and stripped to dryness. The green residues were taken up in THF (50 mL) and to this was added dropwise at -78ºC over 2 hrs, a solution of $K_2(C_8H_6\{Si^iPr_3\text{-}1,4\}_2)$ (1.28 g, 2.58 mmol, 0.86 equivalents) in THF (20 mL). The solution was allowed to warm to room temperature, upon which a colour change was observed from an emerald green to a dark brown with white precipitate, and was stirred for a further 90 minutes at this temperature. The solvent was removed *in vacuo* and the solids extracted with 3 x 40 ml pentane and filtered through Celite®. Concentration to ca. 50 mL and cooling to -30 °C overnight yielded **2.1** as black needle-like crystals.

Yield: 1.17 g (1.38 mmol), 46 % based on UI_3

^{1}H NMR (d_6-benzene, 293 K): δ 39.60 (v. br, s, 2H, COT ring-CH), 1.61 (br, s, 4H, THF-CH_2), 1.21 (v. br, s, 1H, Cp^{Me4H}-CH), 0.59 (br, s, 4H, THF-CH_2), -2.08 (s, 6H, ^{i}Pr-CH), -5.95 (s, 18H, ^{i}Pr-CH_3), -10.26 (s, 18H, ^{i}Pr-CH_3), -12.79 (br, s, 6H, Cp^{Me4H}-CH_3), -21.23 (br, s, 6H, Cp^{Me4H}-CH_3), -80.48 (v. br, s, 2H, COT ring-CH), -116.53 (v. br, s, 2H, COT ring-CH)

MS (EI): m/z = 775 (M^+ - THF)

2.3.2 Synthesis of [U(η^5-Cp^{Me5})(η^8-C_8H_6{Si^iPr_3-1,4}$_2$)(THF)] (**2.2**)

A solution of UI_3 (1.42 g, 2.29 mmol) in THF ca. 100 ml was stirred vigorously for 1 hr prior to the addition of a THF slurry of KCp^{Me5} (0.40 g, 2.29 mmol) and the resulting blue-green solution was stirred for 24 hr. Volatiles were removed in vacuo, the green solids were extracted with toluene, filtered and stripped to dryness. The dark green residues were taken up in THF (50 mL) and cooled to -25 °C, to this a solution of $K_2(C_8H_6\{Si^iPr_3\text{-}1,4\}_2)$ (0.940 g, 1.90 mmol, 0.83 equivalents) in THF (15 mL) was added dropwise over 90 min. The solution was observed to change from a bright green to a dark brown with the appearance of a white precipitate, and was warmed to room temperature with stirring overnight. The solvent was removed *in vacuo* and the brown solids extracted with 2 x 40 ml pentane and filtered through Celite®. Concentration of the dark green solution to ca. 40 ml and cooling to -50 °C overnight yielded the **2.2** as black needle-like crystals, which were washed with cold pentane before drying in vacuo.

Yield: 1.08 g (1.25 mmol), 55 % based on UI_3

^{1}H NMR (d_8-toluene, 293 K): δ 50.6 (s, br, 2H, COT ring-CH), 2.8 (s, br, 4H, THF-CH_2), 1.1 (s, br, 4H, THF-CH_2), -1.0 (s, br, 6H, ^{i}Pr-CH), -4.9 (s, br, 18H, ^{i}Pr-CH_3), -8.8 (s, br, 18H, ^{i}Pr-CH_3), -16.5 (s, br, 15H, Cp-CH_3), -86.5 (s, br, 2H, COT-CH), - 125.2 (s, br, 2H, COT ring-CH)

MS (EI): m/z = 789 (M^+ - THF)

*2.3.3 Reaction of [U(η^5-Cp^{Me4H})(η^8-$C_8H_6\{Si^iPr_3\text{-}1,4\}_2$)(THF)] (**2.1**) with 10 bar H_2/CO*

Complex **2.1** (50 mg, 0.06 mmol) was dissolved in toluene (10 ml) and transferred to a high-pressure vessel. To this was added 10 bar H_2/CO from a pre-pressurised bomb and the colour of the solution changed from brown to red and a brown precipitate formed. The solution was stirred overnight and volatiles were removed *in vacuo* leaving red solids. It was not possible to obtain material suitable for X-ray analysis from a range of solvents.

MS (EI) toluene solution: m/z = 417 ($C_8H_7\{Si^iPr_3\text{-}1,4\}_2$), 374 ($C_8H_7\{Si^iPr_3\}$), 157 ($^iPr_3Si$)

MS (EI) solids: m/z = 1071 [$U(C_8H_6\{Si^iPr_3\text{-}1,4\}_2)_2$], 777 M+ **2.1**

^{1}H NMR (d_6-benzene, 293 K): Resonances cannot be assigned.

*2.3.4 Reaction of [U(η^5-Cp^{Me4H})(η^8-$C_8H_6\{Si^iPr_3\text{-}1,4\}_2$)(THF)] (**2.1**) with CS_2*

Complex **2.1** (100 mg, 0.12 mmol) was dissolved in toluene (1 ml). To this was added CS_2 (5.7 µL, 0.10 mmol, 0.83 equivalents) via a gas-tight syringe at -78 ºC. The solution warmed to room temperature overnight and its colour changed from brown to red and solids were seen to precipitate. Volatiles were removed *in vacuo* and the red-

brown solids were extracted with THF. It was not possible to obtain material suitable for X-ray analysis from a range of solvents.

MS (EI): m/z = 1070 [$U(C_8H_6\{Si^iPr_3\text{-}1,4\}_2)_2$], 914 [$U(C_8H_6\{Si^iPr_3\text{-}1,4\}_2)_2$] – $^iPr_3Si$

^{1}H NMR (d_6-benzene, 293 K): Resonances cannot be assigned.

*2.3.5 Reaction of [U(η^5-Cp^{Me4H})(η^8-$C_8H_6\{Si^iPr_3\text{-}1,4\}_2$)(THF)] (**2.1**) with ^{t}BuNCO*

Complex **2.1** (93 mg, 0.11 mmol) was dissolved in toluene (1 ml) to this was added ^{t}BuNCO (25 µL, d = 0.87, 0.22 mmol, 2 equivalents) via a gas-tight syringe. There was an immediate colour change from brown to red. Volatiles were removed *in vacuo* and the sticky red solids were extracted with THF. It was not possible to obtain material suitable for X-ray analysis.

MS (EI): m/z = 849, 771, 728

^{1}H NMR (d_6-benzene, 293 K): Resonances cannot be assigned.

*2.3.6 Synthesis of [U(η^5-Cp^{Me4H})(η^8-$C_8H_6\{Si^iPr_3\text{-}1,4\}_2$)($\eta^1$-NCMe)] (**2.3**)*

Complex **2.1** (100 mg, 0.12 mmol) was dissolved in toluene (ca. 5 ml). To this brown solution was added acetonitrile (6.2 µL, 0.12 mmol) via a gas-tight syringe. Brown solids were seen to precipitate and the solution was stirred overnight. Volatiles were removed *in vacuo* and the brown solids were extracted with THF. Black crystals were obtained by slow-cooling of the concentrated solution to – 50 °C.

Yield: 45 mg (0.06 mmol), 50 %

Anal. Calc. (found) for $C_{37}H_{64}Si_2NU$: C 54.37 (54.31), H 7.90 (7.93), N 1.83 (1.89)

MS (EI): m/z = 815 (M+), 775 (M^+ - CH_3CN)

^{1}H NMR (d_8-thf, 303 K): δ 12.60 (v. br, s, 2H, COT ring-CH), -1.43 (br, s, 6H, Cp^{Me4H}-CH_3), -3.13 (s, 18H, ^{i}Pr-CH_3), -3.88 (v. br, s, 6H, ^{i}Pr-CH), -4.45 (s, 18H, ^{i}Pr-CH_3), -13.72 (br, s, 6H, Cp^{Me4H}-CH_3), -75.37 (v. br, s, 2H, COT ring-CH), -90.75 (v. br, s, 2H, COT ring-CH)

*2.3.7 Thermolysis of [U(η^5-Cp^{Me4H})(η^8-C$_8$H$_6${Si^{i}Pr$_3$-1,4}$_2$)(η^1-NCMe)] (**2.3**)*

A brown solution of **2.3** (14 mg, 0.017 mmol) was heated at 80 °C in d_8- toluene for 2 weeks.

^{29}Si{^{1}H} NMR (d_8-thf, 303 K): δ -125.02, -128.65, -130.72

MS (EI): m/z = 727, 775 (M+ **2.1**/**2.3** -THF), 794, 815 (M+ **2.3**), 831, 848, 902.

A brown solution **2.3** (23 mgs, 0.03 mmol) in d_8-thf was heated at 50 °C for 5 days. The colour of the solution was observed to change to red.

^{29}Si{^{1}H} NMR (d_8-thf, 303 K): δ -104.15, -127.07, -134.47, -136.31, -141.74

MS (EI): m/z = 673 (794 - Cp^{Me4H}), 727 (848 - Cp^{Me4H}), 735 (857 - Cp^{Me4H}), 751, 775 (M+ **2.1** -THF), 794, 815 (M+- **2.1**), 831, 848, 857

*2.3.8 Reaction of [U(η^5-Cp^{Me4H})(η^8-C_8H_6{Si^iPr_3-1,4}$_2$)(THF)] (**2.1**) with MeNC*

An ampoule was charged with **2.1** (0.16 g, 0.19 mmol) and dissolved in toluene in the glovebox. To this, MeNC (10 μL, 0.19 mmol, 1 equivalent) was added by gas-tight syringe. The colour of the solution remained brown and a brown precipitate was formed upon addition. The solvent was removed *in vacuo* and the dark brown solids were extracted with THF. After several days in THF the colour of the solution was observed to redden. It has not been possible to obtain material suitable for X-ray analysis from a range of solvents.

^{1}H NMR (d_6-benzene, 303 K, selected data): δ -7.20 (s, 18H, ^{i}Pr-CH_3), -14.34 (s, 18H, ^{i}Pr-CH_3), -17.55 (br, s, 6H, ^{i}Pr-CH).

Further signals: δ -3.41, -4.47, -14.84, -16.63 integrate to between 4H and 6H.

^{29}Si{^{1}H} NMR (d_6-benzene, 303 K): δ -136.95, -138.82

MS (EI): m/z = 848 (M+), 776 (M+ -THF), 728 (M+ -Cp^{Me4H})

*2.3.9 Reaction of [U(η^5-Cp^{Me5})(η^8-C_8H_6{Si^iPr_3-1,4}$_2$)(THF)] (**2.2**) with MeNC*

A solution of **2.2** (0.15 g, 0.18 mmol) in toluene (15 ml) was cooled to - 78 °C. To this a solution of MeNC (18.50 μL, 0.36 mmol, 2 equivalents) in toluene (5 ml) was added dropwise over 35 min. The solution was warmed to ambient temperature overnight, after which the colour of the solution was observed to be red/brown and no precipitate

was visible. The solvent was removed in vacuo and the red/brown matrix was taken up in diethyl ether and filtered.

^{1}H NMR (d_6-benzene, 303 K, selected data): δ 3.55 (s, br, 8H, THF-CH_2), 1.47 (s, br, 8H, THF-CH_2), -6.26 (s, 6H, Cp^{Me5}-CH_3), -7.70 (s, 18H, ^{i}Pr-CH_3), -14.33 (s, 18H, ^{i}Pr-CH_3), -17.61 (br, s, 6H, ^{i}Pr-CH).

Further signals: δ 141.29, 113.15, 55.84, 30.00, 16.50, 2.00, -39.49, -88.73 integrate to between 1H and 2H.

MS (EI): m/z = 863 (M+), 809 [U(η^5-Cp^{Me5})(η^8-C_8H_6{Si^iPr_3-1,4}$_2$)(F)], 728 (M+ - Cp^{Me5})

*2.3.10 Synthesis of [(U(η^5-Cp^{Me4H})(η^8-C_8H_6{Si^iPr_3-1,4}$_2$))$_2$(μ-η^2:η^2-$^{13}C_4O_4$)] (**2.5**)*

A solution of **2.1** (240 mg, 0.28 mmol) was freeze-thaw degassed in toluene (15 mL), and, whilst frozen and under static vacuum was exposed to ^{13}CO (210 mmHg) via the Toepler line. The solution was transferred to a -78 ºC bath and allowed to warm to room temperature overnight, after which the deeply coloured black solution was observed to have changed to a dark red colour with visible precipitate. Volatiles were removed *in vacuo* and the red solids were taken up in Et_2O (4 mL) and THF (0.5 mL). Filtration and cooling to -50 ºC for 3 days gave the labelled product as a dark red crystalline solid.

Yield: 7 mg (0.004 mmol), 3 % w.r.t **2.1**

^{1}H NMR (d_8-THF, 303 K): δ 55.47 (br, s, 4H, COT ring-CH), 17.36 (s, 12H, Cp^{Me4H}-CH_3), 1.27 (s, 12H, Cp^{Me4H}-CH_3), -4.46 (s, 36H, ^{i}Pr-CH_3), -5.24 (s, 12H, ^{i}Pr-CH), -6.46 (s, 36H, ^{i}Pr-CH_3), -79.90 (br, s, 4H, COT ring-CH), -84.35 (br, s, 4H, COT ring-CH).

^{13}C NMR (d_8-THF, 303 K, selected data): δ –106.2 (br, s, $^{13}C_4O_4$)

^{29}Si NMR (d_8-THF, 303 K): δ -74.9

MS (EI): m/z = 1666 (M+)

*2.3.11 NMR scale reaction of [(U(η^5-Cp^{Me4H})(η^8-C_8H_6{Si^{i}Pr$_3$-1,4}$_2$))$_2$(μ-η^2:η^2-$^{13}C_4O_4$)] (**2.5**) with $SiMe_3I$*

A Youngs NMR tube was charged with **2.5** (10 mg, 0.06 mmol). To this was added C_6D_6 and Me_3SiI (2.14 μL, d = 1.40, 0.015 mmol, 2.5 equivalents). The tube was shaken and the colour observed to change from orange to red. The $^{13}C\{^{1}H\}$ NMR spectrum was run within 10 min of addition, after which red solids were visible.

$^{13}C\{^{1}H\}$ NMR (C_6D_6, 293 K): δ 194.0, (v. br, m, $^{13}C_4O_4(SiMe_3)_2$) 188.1(v. br, m, $^{13}C_4O_4(SiMe_3)_2$)

After heating the sample in a NMR heating block set at 70 ºC for 20 hrs.

$^{13}C\{^{1}H\}$ NMR (C_6D_6, 293 K): δ -115.3 (**2.5**)

*2.3.12 NMR scale reaction of [(U(η^5-Cp^{Me4H})(η^8-C_8H_6{Si^iPr_3-1,4}$_2$))$_2$(μ-η^2:η^2-$^{13}C_4O_4$)] (**2.5**) with $SiMe_3OTf$*

A Youngs NMR tube was charged with **2.5** (10 mg, 0.06 mmol). To this was added C_6D_6 and $Me_3SiSO_3CF_3$ (11 µL of a 10 % solution in C_6D_6, 0.006 mmol, 1 equivalent). The tube was shaken and the colour observed to change from orange to red and red solids were visible. The $^{13}C\{^1H\}$ NMR spectrum was run within 10 min of addition.

$^{13}C\{^1H\}$ NMR (C_6D_6, 293 K): δ 194.0, (v. br, m, $^{13}C_4O_4(SiMe_3)_2$) 188.1(v. br, m, $^{13}C_4O_4(SiMe_3)_2$)

*2.3.13 Synthesis of $^{13}C_4O_4(SiPh_3)_2$ (**2.6**)*

To a solution of **2.5** (10 mg, 0.006 mmol) in d_8-thf was added Ph_3SiCl (3.5 mg, 0.012 mmol, 2 equivalents), weighed on an analytical balance. The solution was shaken manually and allowed to react overnight, after which the colour of the solution was observed to change from dark red to orange.

^1H NMR (d_8-thf, 293 K): Resonances could not be assigned.

$^{13}C\{^1H\}$ NMR (d_8-thf, 293 K, overnight): δ 187.1 (d), 187.6 (d), 188.3 (d), 193.3 (d), 194.1 (d), 194.6 (d), –106.2 (br, s, $^{13}C_4O_4$)

After addition of further Ph_3SiCl (17.5 mg, 0.06 mmol, 10 equivalents):

$^{13}C\{^1H\}$ NMR (d_8-thf, 293 K, overnight): δ 187.1 (d), 187.6 (d), 188.3 (d), 193.3 (d), 194.1 (d), 194.6 (d).

*2.3.14 NMR scale reaction of [(U(η^5-Cp^{Me4H})(η^8-C_8H_6{Si^iPr_3-1,4}$_2$))$_2$(μ-η^2:η^2-$^{13}C_4O_4$)] (**2.5**) with benzyl chloride*

Benzyl chloride (2 µL, 0.018 mmol, 2.5 equivalents) was added to a Youngs NMR tube containing **2.5** (11 mg, 0.007 mmol) in d_6-benzene and heated at 70 ºC for 3 days.

$^{13}C\{^1H\}$ NMR (C_6D_6, 293 K): δ -115.3 (**2.5**)

*2.3.15 NMR scale reaction of [(U(η^5-Cp^{Me4H})(η^8-C_8H_6{Si^iPr_3-1,4}$_2$))$_2$(μ-η^2:η^2-$^{13}C_4O_4$)] (**2.5**) with {(^{i}Pr)PhPCl}*

Isopropylphenylchloro phosphine (9.1 mg, 0.049 mmol, 7 equivalents) was added to a Youngs NMR tube containing **2.5** (11 mg, 0.007 mmol) in d_6-benzene.

$^{13}C\{^1H\}$ NMR (C_6D_6, 293 K): δ -115.3 (**2.5**)

$^{31}P\{^1H\}$ NMR (C_6D_6, 293 K): δ 99.1 {(^{i}Pr)PhPCl}

*2.3.16 NMR scale reaction of [(U(η^5-Cp^{Me4H})(η^8-C_8H_6{Si^iPr_3-1,4}$_2$))$_2$(μ-η^2:η^2-$^{13}C_4O_4$)] (**2.5**) with $AlMe_2(Cl)$*

A Youngs NMR tube was charged with **2.5** (11 mg, 0.007 mmol) and dissolved in thf. A few drops of d_6-benzene and $AlMe_2(Cl)$ in hexanes (13 µL, 1 M, 0.013 mmol, 2

equivalents) were added the colour of the solution was observed to lighten in colour from dark red to orange.

^{1}H NMR (d_6-benzene, 293 K): Resonances could not be assigned.

^{13}C{^{1}H} NMR (d_6-benzene, 293 K): δ 180-210 (broad resonance in baseline)

MS EI: *m/z* = 809 [(U(η^{5}-Cp^{Me4H})(η^{8}-C_8H_6{Si^{i}Pr$_3$-1,4}$_2$)Cl], 766 [(U(η^{5}-Cp^{Me4H})(η^{8}-C_8H_6{Si^{i}Pr$_3$-1,4}$_2$)Cl]-iPr, 688 [(U(η^{5}-Cp^{Me4H})(η^{8}-C_8H_6{Si^{i}Pr$_3$-1,4}$_2$)Cl]-CpMe$_4$H

2.4 References:

[1] A. Streitwieser Jr. and U. Muller-Westerhoff, *J. Am. Chem. Soc.*, 1968, **90**, 7364.

[2] C. Le Vanda, J. P. Solar and A. Streitwieser, Jr., *J. Am. Chem. Soc.*, 1980, **102**, 2128.

[3] T. R. Boussie, R. M. Moore, A. Streitwieser, Jr., A. Zalkin, J. Brennan and K. A. Smith, *Organometallics*, 1990, **9**, 2010.

[4] a) C. A. Harmon and A. Streitweiser Jr., *Inorg. Chem.*, 1973, **12**, 1102. b) C. A. Harmon, D. P. Bauer, S. R. Berryhill, K. Hagiwara and A. Streitweiser Jr., *Inorg. Chem.*, 1977, **16**, 2143.

[5] a) N. C. Burton, F. G. N. Cloke, S. C. P. Joseph, H. Karamallakis and A. A. Sameh, *J. Organomet. Chem.*, 1993, **426**, 39. b) U. Kilimann, R. Herbst-Irmer, D. Stalke and F. T. Edelmann, *Angew. Chem. Int. Ed. Engl.*, 1994, **33**, 1618.

[6] D. Seyferth, *Organometallics*, 2004, **23**, 3562.

[7] J. -C. Berthet, J. -F. Le Maréchal and M. Ephritikhine, *J. Organomet. Chem*, 1990, **393**, C47.

[8] D. Baudry, E. Bulot, M. Ephritikhine, M. Nielich, M. Lance and J. Vigner, *J. Organomet. Chem*, 1990, **388**, 279.

[9] J. -C. Berthet, J. -F. Le Maréchal and M. Ephritikhine, *J. Organomet. Chem*, 1994, **155**, 155.

[10] N. C. Burton, F. G. N. Cloke, P. B. Hitchcock, H. de Lemos and A. A. Sameh, *J. Chem. Soc. Chem. Commun.*, 1989, 1462.

[11] D. L. Clark, A. P. Sattelberger, S. G. Bott and N. R. Vrtis, *Inorg. Chem.*, 1989, **28**,1771.

[12] L. R. Avens, C. J. Burns, R. J. Butcher, D. L. Clark, J. C. Gordon, A. R. Schake, B. L. Scott, J. G. Watkin and B. D. Zwick, *Organometallics*, 2000, **19**, 451.

[13] A. R. Schake, L. R. Avens, C. J. Burns, D. L. Clark, A. P. Sattelberger and W. H. Smith, *Organometallics*, 1993, **12**, 1497.

[14] W. J. Evans, G. W. Nyce and J. W. Ziller, *Angew. Chem. Int. Ed. Engl.*, 2000, **39**, 240.

[15] a) O. T. Summerscales, F. G. N. Cloke, P. B. Hitchcock, J. C. Green and N. Hazari, *Science*, 2006, **311**, 829. b) O. T. Summerscales, F. G. N. Cloke, P. B. Hitchcock, J. C. Green and N. Hazari, *J. Am. Chem. Soc.*, 2006, **128**, 9602. c) A. S. P. Frey, F. G. N. Cloke, P. B. Hitchcock, I. J. Day, J. C. Green and G. Aitken, *J. Am. Chem. Soc.*, 2008, **138**, 13816.

[16] O. T. Summerscales, A. S. P. Frey, F. G. N. Cloke and P. B. Hitchcock, *Chem. Commun.*, 2009, 198.

[17] O. T. Summerscales, DPhil Thesis, University of Sussex, 2007

[18] J. G. Brennan, R. A. Andersen, A. Zalkin, *Inorg. Chem*, **1986,** 25, 1756.

[19] J. G. Brennan and R. A. Anderson, *J. Am. Chem. Soc.*, 1985, **107**, 514.

[20] a) E. J. M. De Boer and J. H. Teuben, *J. Organomet. Chem.*, 1977, **140**, 41. b) E. J. M. De Boer and J. H. Teuben, *J. Organomet. Chem.*, 1978, **153**, 53. c) R. Duchateau, A. J. Williams, S. Gambarotta and M. Y. Chaing, *Inorg. Chem.*, 1991, **30**, 4863. d) F. A. Cotton and W. T. Hall, *J. Am. Chem. Soc.*, 1979, **101**, 5094.

[21] F. Rehbaum and K. H. Thiele, *J. Organomet. Chem.*, 1991, **410**, 327.

[22] S. A. Cohen and J. E. Bercaw, *Organometallics*, 1985, **4**, 1006.

[23] M. N. Bochkarev, G. V. Khoroshenkov, H. Schumann and S. Dechert, *J. Am. Chem. Soc.*, 2003, **125**, 2894.

[24] W. J. Evans, E. Montalvo, S. E. Foster, K. A. Harada and J. W. Ziller, *Organometallics*, 2007, **26**, 2904.

[25] W. J. Evans, K. A. Miller and J. W. Ziller, *Angew. Chem. Int. Ed.*, 2008, **47**, 589.

[26] R. Adam, C. Villiers, M. Ephritikhine, M. Lance, M. Nierlich and J. Vigner, *J. Organomet. Chem.*, 1993, **445**, 99.

[27] I. Castro-Rodriguez, K. Olsen, P. Gantzel and K. Meyer, *J. Am. Chem. Soc*, 2003, **125**, 4565.

[28] Handbook of Chemistry and Physics, 89rd edn., CRC Press, 2008.

[29] T. J. Marks, *Science*, 1982, **217**, 989.

[30] E. M. Carnahan, J. D. Protasiewicz and S. J. Lippard, *Acc. Chem. Res.*, 1993, **26**, 90.

[31] B. Kanellakopulos, E. O. Fischer, E. Dornberger and F. Baumgartner, *J. Organomet. Chem.*, 1970, **24**, 507.

[32] J. G. Brennan, R. A. Anderson and J. L. Robbins, *J. Am. Chem. Soc.*, 1986, **108**, 335.

[33] W. G. Van Der Sluys and A. P. Sattleberger, *Inorg. Chem.*, 1989, **28**, 2496.

[34] M. del Mar Conejo, J. S. Parry, E. Carmona, M. Schultz, J. G. Brennan, S. M. Beshouri, R. A. Anderson, R. D. Rogers, S. Coles and M. Hursthouse, *Chem. Eur. J.*, 1999, **5**, 3000.

[35] G. Seitz and P. Imming, *Chem. Rev.*, 1992, **92**, 1227.

[36] J. S. Parry, E. Carmona, S. Coles and M. Hursthouse, *J. Am. Chem. Soc.*, 1995,**117**, 2649.

[37] B. B. Wayland and X. Fu, *Science*, 2006, **311**, 790.

[38] A. S. P. Frey, F. G. N. Cloke, P. B. Hitchcock, I. J. Day, J. C. Green and G. Aitken, *J. Am. Chem. Soc.*, 2008, **138**, 13816.

[39] A. S. P. Frey, personal communication.

[40] W. J. Evans, J. W. Grate, L. A. Hughes, H. Zhang and J. L. Atwood, *J. Am. Chem. Soc.*, 1985, **107**, 3728.

[41] N. C. Lim, M. D. Morton, H. A. Jenkins and C. Brueckner, J. Org. Chem., 2003, **68**, 9233.

[42] a) G. Neumeier, Diplomarbeit, University of Magedeburg, 1975 b) G. Neumeier, Dissertation, University of Magedeburg. 1978.

See also: S. Cohen and S. G. Cohn, J. Am. Chem. Soc., 1966, **88**, 1533.

[43] M. T. Reetz and G. Neumeier, Liebigs Ann. Chem., 1981, 1234.

[44] H. Friebolin, *Basic One- and Two-Dimensional NMR Spectroscopy*, 3rd edn., 1998, Wiley-VCH.

[45] F. W. Wehrli, A. P. March and S. Wehrli, *Interpretation of carbon-13 NMR spectra*, 2nd edn., J. Wiley and Sons Ltd., 1988, Chichester, New York.

[46] a) M. Karplus and J. A. Pople, *J. Chem. Phys*, 1963, **38**, 2803. b) J. M. Schulman and M. D. Newton, *J. Am. Chem. Soc.*, 1974, **96**, 6295.

[47] a) H. M. McConnell, *J. Mol. Spectrosc.*, 1957, 1, 11. b) G. A. Gray, P. D. Ellis, D. D. Traficante and G. E. Maciel, *J. Magn. Res.*, 1969, 1, 41.

[48] H-O. Kalinowski, S. Berger and S. Braun, *Carbon-13 NMR spectroscopy*, J. Wiley and Sons Ltd., 1988, Chichester, New York.

[49] F. J. Weigert and J. D. Roberts, *J. Am. Chem. Soc*., 1972, **94**, 6021. See also for $^{1}J_{CC}$ in aromatic compounds: P. E. Hansen, *Org. Mag. Reson.*, 1979, **12**, 109.

CHAPTER THREE: TRISPYRAZOLYLBORATE CONTAINING U(III) HALF-SANDWICH COMPLEXES

3.1 Synthesis and characterisation of [U(κ^3-Tp^{Me2})(η^8-C_8H_6{Si^{i}Pr$_3$-1,4}$_2$)] and [U(κ^3-Tp^{Me2})(η^8-C_8H_4{Si^{i}Pr$_3$-1,4}$_2$)].

3.1.1 Introduction

Recent years have seen a move away from the domination of the cyclopentadienyl ligand in d- and f-block chemistry, as other ligand systems have emerged as viable alternatives.[1] One such class is the scorpionate ligand, pioneered by Trofimenko.[2] A number of half-sandwich complexes of the general formula [Ln(η^8-C_8H_8)(Tp)] (Tp = hydrotris(pyrazolyl)borate, Ln = Ce, Pr, Nd, Sm) were synthesised by Edelmann *et al.* who found that the use of the bulkier Tp^{Me2}, with substituents on the 3- and 5- positions of the pyrazolyl ring, improved handling and solubility. These complexes have been used to study the bonding between the metal centre and the cyclooctatetrenyl ring.[3] Poly(pyrazolyl)borate complexes of uranium have been studied since the early 1980s, with a range of first and second generation scorpionates.[4] The size and the electronic properties of substituents on the pyrazolyl ring have a profound influence upon molecular structure, solution behaviour and reactivity.[5]

Takats *et al.* reported the synthesis and full characterisation of [U(κ^3-Tp^{Me2})I_2(THF)$_2$][6] and [U(κ^3-Tp^{Me2})(κ^2-η^2-Tp^{Me2})I], the latter displaying an unusual structure in the solid

state with an interaction between the uranium and the N=N double bond of one of the pyrazolyl rings on one of the Tp^{Me2} ligands.[7] These complexes provided a clean, high-yielding entry into both amido and hydrocarbyl derivative chemistry of low-valent uranium. In particular, the complex $[U(\kappa^3\text{-}Tp^{Me2})(CH\{SiMe_3\}_2)_2(THF)]$ was shown to display reactivity towards H_2 and CO under mild conditions, though the reaction products were not characterised.[8] More recently the derivatisation of $[U(\kappa^3\text{-}Tp^{Me2})(\kappa^4\text{-}Tp^{Me2})I]$ was also demonstrated including the structures of $[U(\kappa^3\text{-}Tp^{Me2})_2(N\{C_6H_5\}_2)]$ and $[U(\kappa^3\text{-}Tp^{Me2})_2(N\{SiMe_3\}_2)]$.[9]

Section 3.1 details the synthetic route to the trispyrazolylborate half-sandwich complexes of uranium(III), $[U(\kappa^3\text{-}Tp^{Me2})(\eta^8\text{-}C_8H_6\{Si^iPr_3\text{-}1,4\}_2)]$ (**3.1**) and $[U(\kappa^3\text{-}Tp^{Me2})(\eta^8\text{-}C_8H_4\{Si^iPr_3\text{-}1,4\}_2)]$ (**3.2**), and their characterisation.

*3.1.2 Synthetic route to $[U(\kappa^3\text{-}Tp^{Me2})(\eta^8\text{-}C_8H_6\{Si^iPr_3\text{-}1,4\}_2)]$ (**3.1**) and $[U(\kappa^3\text{-}Tp^{Me2})(\eta^8\text{-}C_8H_4\{Si^iPr_3\text{-}1,4\}_2)]$ (**3.2**)*

The reaction of UI_3 in THF with KTp^{Me2}, separation of KI by toluene work-up, and the subsequent slow addition of 0.75 equivalents of $[K_2(C_8H_6\{Si^iPr_3\text{-}1,4\}_2)]$ at 0 °C in THF followed by extraction with pentane yielded $[U(\kappa^3\text{-}Tp^{Me2})(\eta^8\text{-}C_8H_6\{Si^iPr_3\text{-}1,4\}_2)]$ (**3.1**) as a dark red microcrystalline solid in a moderate yield (30 % w.r.t UI_3). Using the synthetic strategy described for **3.1** and 0.8 equivalents of $[K_2\ (C_8H_4\{Si^iPr_3\text{-}1,4\}_2)]$ it was possible to synthesise $[U(\kappa^3\text{-}Tp^{Me2})(\eta^8\text{-}C_8H_4\{Si^iPr_3\text{-}1,4\}_2)]$ (**3.2)** as a purple crystalline solid in a poor isolated yield (11 % w.r.t UI_3). This isolated yield reflects the

difficulty of separating **3.2** from attendant side-products of similar solubility. The elemental analysis and spectroscopic data for both complexes are in agreement with the molecular formation. Complexes **3.1** and **3.2** are stable at room temperature under inert atmosphere over a period of months, both in the solid state and in solution.

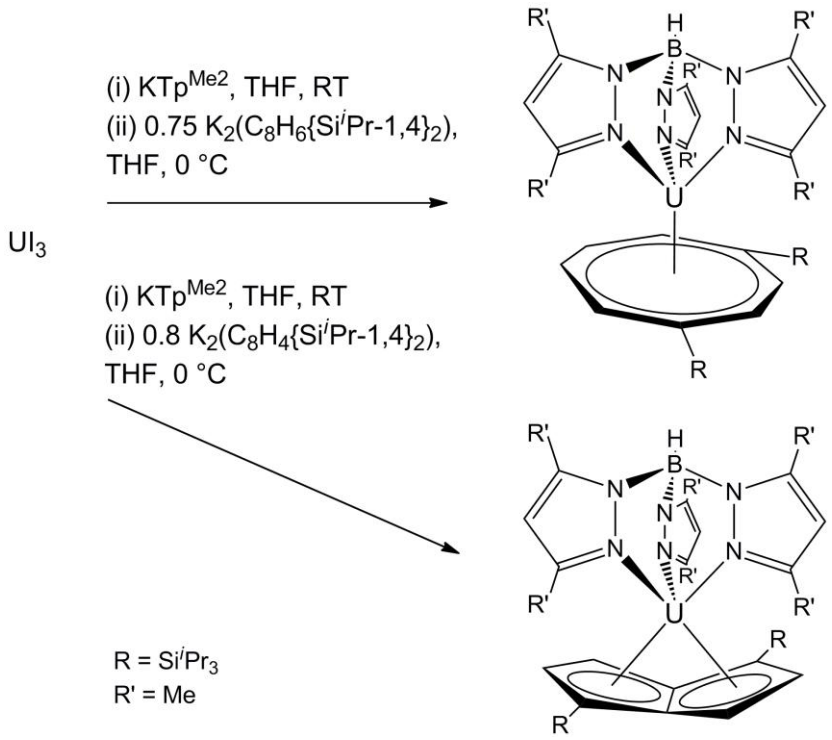

Scheme 1: Synthesis of [U(κ^3-Tp^{Me2})(η^8-$C_8H_6\{Si^iPr_3\text{-}1,4\}_2$)] (**3.1**) and [U($\kappa^3$-$Tp^{Me2}$)($\eta^8$-$C_8H_4\{Si^iPr_3\text{-}1,4\}_2$)] (**3.2**)

*3.1.3 Characterisation of [U(κ³-Tp^{Me2})(η⁸-C$_8$H$_6${Si^{i}Pr$_3$-1,4}$_2$)] (**3.1**) and [U(κ³-Tp^{Me2})(η⁸-C$_8$H$_4${Si^{i}Pr$_3$-1,4}$_2$)] (**3.2**)*

The ^{1}H NMR spectrum of **3.1** in polar and non-polar solvents at room temperature is not in accordance with a 9:9:3 ratio for the 3-Me, 5-Me and 4-H proton environments of a fully equilibrated Tp^{Me2} ligand[2] but rather was consistent with an idealised pseudo-staggered conformation, where only two of the pyrazolyl rings are magnetically equivalent giving rise to a 3:3:1:6:6:2 ratio. This static conformation remains well defined up to 80 °C, above which the 3-Me, 5-Me and 4-H resonances were seen to broaden, though the high-temperature limiting spectra were not able to be obtained. In contrast the ^{1}H NMR spectrum of **3.2** at room temperature does exhibit a 9:9:3 ratio for the bound Tp^{Me2}. The range over which the resonances associated with both complexes are observed is broad, spanning 74 ppm for **3.1** and 41 ppm for **3.2**, expected for the paramagnetic U(III) centre. The ^{1}H and ^{29}Si{^{1}H} NMR resonances associated with the [C$_8$H$_6${Si^{i}Pr$_3$-1,4}$_2$]$^{2-}$ and [C$_8$H$_4${Si^{i}Pr$_3$-1,4}$_2$]$^{2-}$ ligands are consistent with a single Si^{i}Pr$_3$ environment rendered by mirror plane symmetry on an NMR time scale.

The B-H resonance is also clearly identifiable in the room temperature ^{1}H NMR spectra as a very broad multiplet, at 18.9 ppm for **3.1** and 18.0 ppm for **3.2**. Though the integration of this resonance is complicated by its broadness, the assignment was confirmed by the loss of multiplicity of this resonance in the ^{1}H{^{11}B} spectrum. ^{11}B NMR spectroscopy is a useful tool for looking at such complexes and can provide important information about the co-ordination environment of the boron.[10] The ^{11}B{^{1}H} NMR spectrum at room temperature displays a broad resonance at 32.8 ppm for **3.1** and 38.2 ppm for **3.2**. A combination of paramagnetic and quadrupolar broadening produces

a larger line-width and the coupling of this signal is not resolved in the ^{1}H coupled spectrum.

Due to the limited solubility of **3.1** in common solvents it was difficult to obtain crystals suitable for X-ray diffraction. However, eventually suitable crystals were grown from a saturated solution of diethylether at 5 °C over ten days. Crystals of **3.2** were grown from a saturated pentane solution at -20 °C over 48 hrs.

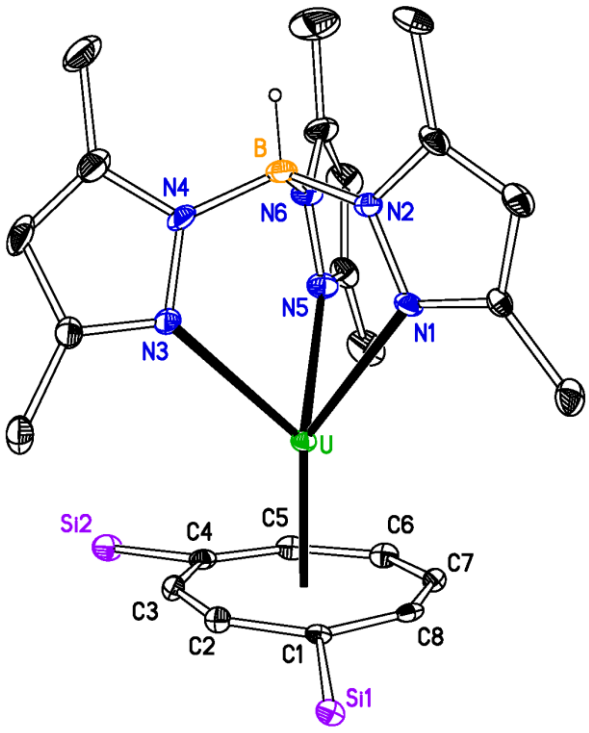

Figure 1: Molecular structure of $[U(\kappa^3\text{-}Tp^{Me2})(\eta^8\text{-}C_8H_6\{Si^iPr_3\text{-}1,4\}_2)]$ (**3.1**), ellipsoids at 50 % probability, ^{i}Pr groups and H atoms, except B-H, omitted for clarity. M1 is the centroid of the $[(C_8H_6\{Si^iPr_3\text{-}1,4\}_2)]^{2-}$ ring.

Table 1: Selected bond distances (Å) and angles (°) for [U(κ^3-Tp^{Me2})(η^8-C_8H_6{Si^{i}Pr$_3$-1,4}$_2$)] (**3.1**) (M1 is the centroid of the [(C_8H_6{Si^{i}Pr$_3$-1,4}$_2$)]$^{2-}$ ring; M2 is the centroid defined by N1, N3 and N5) and [U(κ^3-Tp^{Me2})(η^8-C_8H_4{Si^{i}Pr$_3$-1,4}$_2$)] (**3.2**) (M1 is the mid-point of the C4-C5 bond; M2 is the centroid defined by N1, N3 and N5).

Parameter	**3.1**	**3.2**
U-N1	2.573(5)	2.604(7)
U-N3	2.647(4)	2.611(7)
U-N5	2.652(5)	2.572(7)
U-N_{ave}	-	2.596(12)
U-M1	2.000(5)	2.417(7)
U-M2	1.841(5)	1.804(7)
U-C1	-	2.775(7)
U-C3	-	2.736(7)
U-C6	-	2.791(7)
U-C8	-	2.755(7)
M1-U-M2	176.18(1)	166.60(2)

In **3.1** U-N1 is slightly shorter than U-N3 and U-N5, it is not different enough to be considered structurally significant. The U-N distances in **3.1** and **3.2** are comparable to those found other U(III) complexes and can cover a large range, for example U-N (2.480(6) Å – 2.802(6) Å) in [U(κ^3-Tp^{Me2})$_2$(N{SiMe$_3$}$_2$)].[9] The U-N_{ave} in **3.2** is shorter than those found in **3.1**, this is presumably the result of the fold around the bridgehead

in the pentalene ligand *vide infra*, thus easing the steric crowding. The U-M1 distance in **3.1**, however, is essentially identical to that observed in [U(η^8-C_8H_6{Si^{i}Pr$_3$-1,4}$_2$)(η^5-Cp^{Me5})] U-M1 (1.975(6) Å).[14] The U-N distances in both **3.1** and **3.2** are longer than the U-N_{ave} (2.53(3) Å) found in the [U(κ^3-Tp^{Me2})I_2(THF)$_2$] precursor. [6,8]

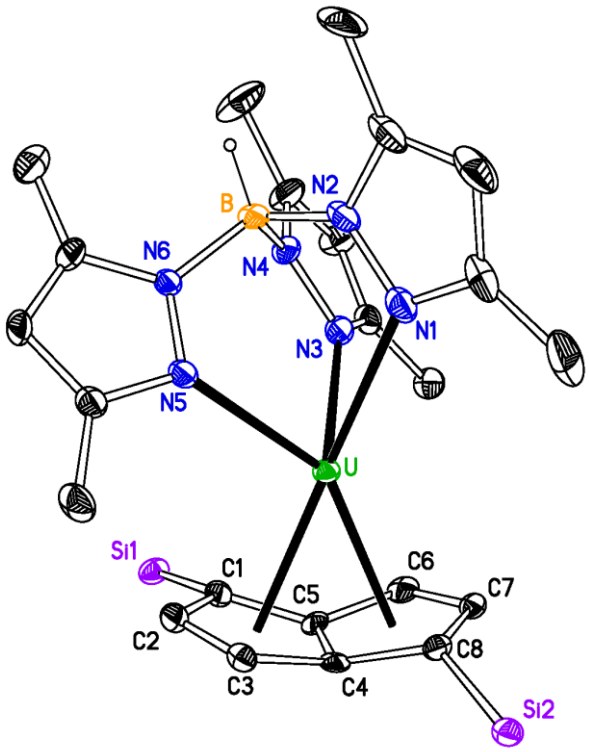

Figure 2: Molecular structure of [U(κ^3-Tp^{Me2})(η^8-C_8H_4{Si^{i}Pr$_3$-1,4}$_2$)] (**3.2**), ellipsoids at 50 % probability, ^{i}Pr groups and H atoms, except B-H, omitted for clarity.

The fold angle between least squares planes defined by C_5-rings of the pentalene ligand is 24.2(6)°, this is closer to the value of 24° observed in the sterically crowded [Th(η^8-

$C_8H_4\{Si^iPr_3\text{-}1,4\}_2)_2]$,[11] than the 26° of $[U(\eta^8\text{-}C_8H_4\{Si^iPr_3\text{-}1,4\}_2)(\eta^5\text{-}Cp^{Me5})]$.[16] The U-C1, C3, C6, C8 distances that represent the major bonding interactions[12] are likewise longer than those found in $[U(\eta^8\text{-}C_8H_4\{Si^iPr_3\text{-}1,4\}_2)(\eta^5\text{-}Cp^{Me5})]$ U-C1 (2.733(7) Å), U-C3 (2.721(7) Å), U-C6 (2.683(7) Å) and U-C8 (2.722(7) Å). Both the $[C_8H_6\{Si^iPr_3\text{-}1,4\}_2]^{2-}$ and $[C_8H_4\{Si^iPr_3\text{-}1,4\}_2]^{2-}$ ligands are substituted in the 1 and 4 positions, in $[C_8H_6\{Si^iPr_3\text{-}1,4\}_2]^{2-}$ case the bulky substituents are on the same side of the ring, whereas they are on opposite sides of the bridgehead in the $[C_8H_4\{Si^iPr_3\text{-}1,4\}_2]^{2-}$ case. This allows the staggered conformation found in **3.1** but in **3.2** the positioning of the N3-N4 and N5-N6 rings either side of Si1 brings the N1-N2 ring and Si2 into proximity and their mutual repulsion results in a M1-U-M2 angle which is significantly more acute than that in **3.1**.

The complexes are both base-free, unlike their cyclopentadienyl analogues, although the preparation of all complexes was undertaken in THF. The substitution of Tp^{Me2} for Cp^{Me5} is reflected by a less acute fold angle and by a lengthening of the U-C interactions in **3.2** but not by a lengthening of the U-M1 in **3.1**. The solution NMR spectra of unsolvated Tp lanthanide complexes have been shown to approximate closely to their solid state structures.[13,10a] In complex **3.1** the positioning of the Tp^{Me2} ligand prevents the free rotation of the $[C_8H_6\{Si^iPr_3\text{-}1,4\}_2]^{2-}$ ligand even in solution. The longer bonding interactions between the uranium centre and the $[C_8H_4\{Si^iPr_3\text{-}1,4\}_2]^{2-}$ and the positioning of the Si^iPr_3 groups in **3.2** may lead to it being fluxional in solution. Thus the solution behaviour observed would seem to be a reflection of their solid state molecular structures.

3.2 Reactivity of [U(κ^3-Tp^{Me2})(η^8-C$_8$H$_6${Si^{i}Pr$_3$-1,4}$_2$)] and [U(κ^3-Tp^{Me2})(η^8-C$_8$H$_4${Si^{i}Pr$_3$-1,4}$_2$)] with small molecules

3.2.1 Introduction

It has been demonstrated that uranium(III) complexes of the type [U(η^8-C$_8$H$_6${Si^{i}Pr$_3$-1,4}$_2$)(η^5-Cp^R)(THF)] (Cp^R= Cp^{Me5} or Cp^{Me4H}) display high reactivity towards small molecules. The reaction of these complexes with CO to form $C_3O_3^{2-}$ and $C_4O_4^{2-}$ respectively, was the first example of selective, spontaneous, low-temperature, reductive homologation of CO.[14] The related mixed-sandwich complex [U(η^8-C$_8$H$_4${Si^{i}Pr$_3$-1,4}$_2$)(η^5-Cp^{Me5})], which utilises the relatively less studied silylated dianionic pentalene ligand[15] [C$_8$H$_4${Si^{i}Pr$_3$-1,4}$_2$]$^{2-}$, has been shown to reversibly bind N_2; the resultant U(IV) complex contains a bridging, sideways-bound N_2^{2-} unit.[16] The reactivity of **3.1** and **3.2** with small molecules is detailed in Section 3.2.

*3.2.2 Reactivity of [U(κ^3-Tp^{Me2})(η^8-C$_8$H$_6${Si^{i}Pr$_3$-1,4}$_2$)] (**3.1**)*

In marked contrast to [U(η^8-C$_8$H$_6${Si^{i}Pr$_3$-1,4}$_2$)(η^5-Cp^{Me5})] (**2.2**), **3.1** displays no reactivity towards CO, CO_2 or MeNC under mild conditions by ^{1}H, ^{13}C{^{1}H}, ^{11}B{^{1}H} and ^{29}Si{^{1}H} NMR and MS. The reaction of **3.1** with an overpressure of CO, although accompanied by a colour change, did not yield any material suitable for X-ray diffraction studies and showed only decomposition products by mass spectrometry. As has been seen in section *3.1.3*, complex **3.1** maintains its static conformation in solution by ^{1}H NMR spectroscopy even at elevated temperature, the bulky and interlocking

nature of the steric environment may prevent access of the small molecule to the uranium(III) centre. The lack of reactivity of **3.1** is similar to that of complexes [Ln(Tp^{Me2})$_2$] (Ln = Sm, Yb), which in spite of the reducing nature of divalent lanthanides, display no reactivity towards CO, isocyanides or alkynes.[17] This lack of reactivity was attributed to the lack of an available oxidative reaction pathway.

There is no relative eletronic trend that describes the electron donating properties of the Tp^{Me2} and Cp^{Me5} ligands across the periodic table.[18] The donation is dependent rather on the overall composition of the specific complex. The bonding modes adopted by the two ligands are quite different, the Tp is a σ donor, whereas the Cp ligand is capable of σ, π and δ donation.[2b] The unsubstituted Tp and Cp^{Me5} are of similar steric bulk,[19] though the larger Tp^{Me2} is often used as an alternative to Cp^{Me5}, its Tolman cone angle of 236°[20] is significantly larger than that of Cp^{Me5} (182°).[21] A futher difference is that the Tp ligand adopts octahedral geometry preferentially, whereas the Cp ligand is capable of several hapticities.[2]

*3.2.3 DFT analysis of [U(κ^3-Tp^{Me2})(η^8-C_8H_6{Si^iPr_3-1,4}$_2$)] (**3.1**)*

Binding of CO to [U(η^8-C_8H_6{Si^iPr_3-1,4}$_2$)(η^5-Cp^{Me5})] involves a high degree of reduction of the CO ligand, with two unpaired electrons partially occupying the CO π* orbitals.[14a] One possible reason for the lack of reactivity of **3.1** with CO might be that the uranium centre is less reducing than **2.2**. In order to test this hypothesis, DFT was used to estimate the relative reducing power of the two compounds. The DFT study was

carried out by Prof. J. C. Green and Dr G. Aitken at the University of Oxford. In order to make the two systems computationally accessible the $Si^{i}Pr_3$ groups attached to the cyclooctatetraenyl ligands were replaced by SiH_3 groups, but full methylation of both Cp^{Me5} and Tp^{Me2} was maintained. The calculated structures [U(η^8-C_8H_6{SiH_3-1,4}2)(η^5-Cp^{Me5})] **I** and [U(η^8-C_8H_6{SiH_3-1,4}$_2$)(κ^3-Tp^{Me2})] **II** were optimised with S=3/2 and are shown in Figure 3, with selected structural parameters listed in Table 2. The energies of the singularly occupied 5f orbitals were higher for the Tp^{Me2} complex than the Cp^{Me5} complex. The three unpaired electrons occupied 5f orbitals in both cases with the spin density on the uranium being 3.0. The calculated structures of the CO adducts, [U(η^8-C_8H_6{SiH_3-1,4}$_2$)(η^5-Cp^{Me5})(η^1-CO)] **III** and [U(η^8-C_8H_6{SiH_3-1,4}$_2$)(κ^3-Tp^{Me2})(η^1-CO)] **IV**, were optimised; selected structural parameters and spin densities are given in Table 2.

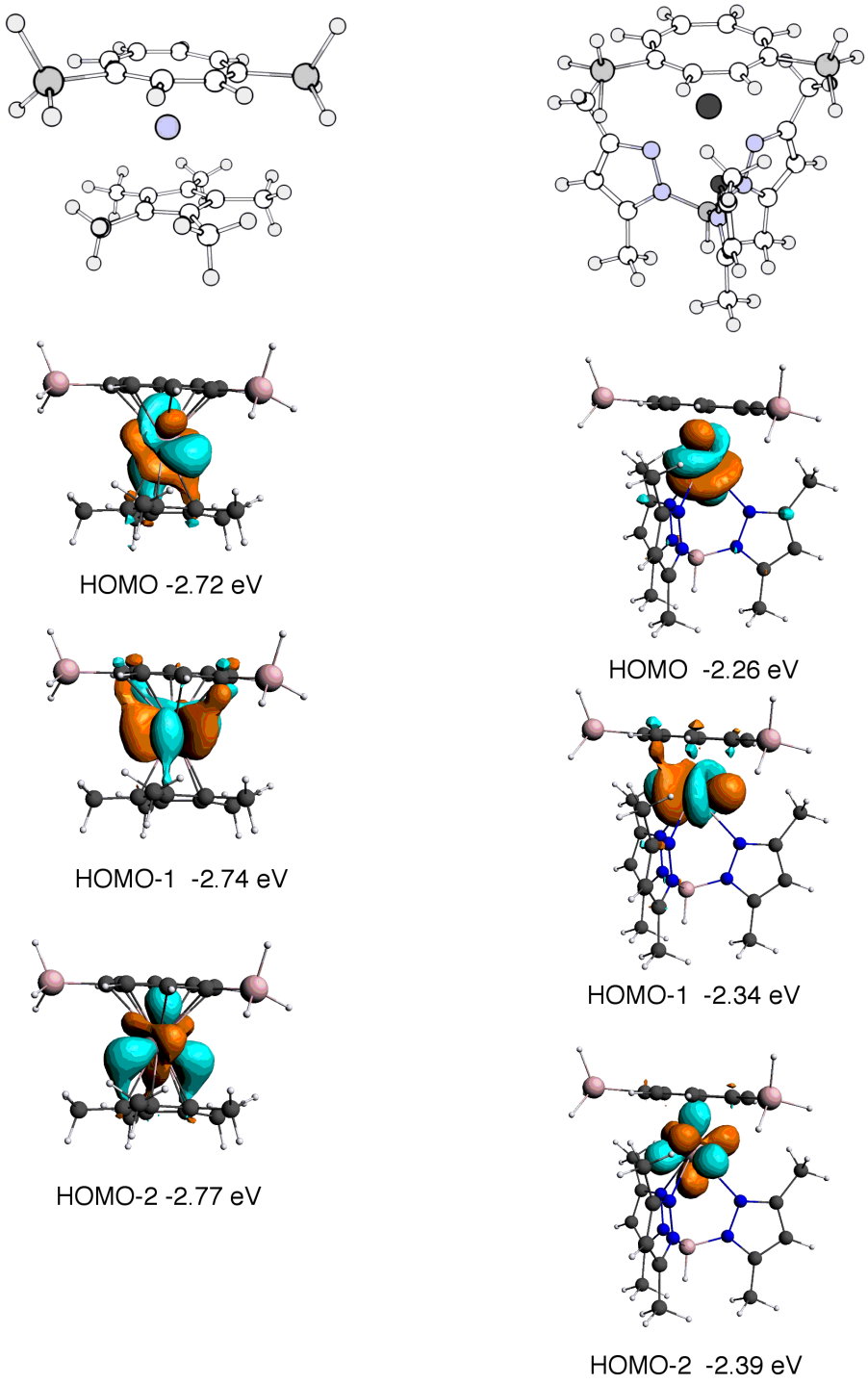

Figure 3: Calculated structures and singularly occupied 5f orbitals α-spin of [U(η^8-$C_8H_6\{SiH_3\text{-}1,4\}_2$)($\eta^5$-$Cp^{Me5}$)] **I** and [U($\eta^8$-$C_8H_6\{SiH_3\text{-}1,4\}_2$)($\kappa^3$-$Tp^{Me2}$)] **II**

The CO SCF binding energies were calculated as 1.02 eV for **III** and 0.84 eV for **IV**. Thus, in spite of the higher f orbital energies for the Tp^{Me2} complex, the CO is less tightly bound. This is confirmed by the U-C distance which is longer in **IV** (2.4 Å) than **III** (2.35 Å). The distances between the uranuim and the supporting ligands increase on CO binding for both complexes. In **III** less unpaired spin density is transferred to the CO group than in **IV**. For the bulkier Tp^{Me2} group the energetic cost appears to be too great to support the entropic barrier to CO binding.

Thermodynamic driving forces for the reaction of **3.1** with CO might include the U(III)/U(IV) oxidation, breaking of π-bonds and the formation of σ-bonds and the formation of U-O bonds. However, if there is no kinetic pathway available the reaction cannot proceed. There is insufficient data to determine whether that is the case for the reaction of **3.1** with CO. The static structure of **3.1** by ^{1}H in solution suggests that the steric environment may prevent access of the CO to the uranium centre or the dimerisation of reaction products. It is unclear whether the sterics would have a kinetic or thermodynamic effect on the reaction.

Table 2: Selected structural parameters (Å) and spin densities calculated for structures [U(η^8-$C_8H_6\{SiH_3\text{-}1,4\}_2$)($\eta^5$-$Cp^{Me5}$)] **I**, [U($\eta^8$-$C_8H_6\{SiH_3\text{-}1,4\}_2$)($\kappa^3$-$Tp^{Me2}$)] **II**, [U($\eta^8$-$C_8H_6\{SiH_3\text{-}1,4\}_2$)($\eta^5$-$Cp^{Me5}$)($\eta^1$-CO)] **III** and [U($\eta^8$-$C_8H_6\{SiH_3\text{-}1,4\}_2$)($\kappa^3$-$Tp^{Me2}$)($\eta^1$-CO)] **IV**.

	I	II	III	IV
U-C ($C_8H_6\{SiH_3\text{-}1,4\}_2$)	2.65-2.70	2.71-2.75	2.66-2.82	2.72-2.82
U-C (Cp*)	2.62-2.76		2.70-2.77	
U-N (Tp^{Me2})		2.57-2.59		2.55-2.72
U-C (CO)			2.35	2.40
C-O (CO)			1.17	1.17
U spin density	3.0	3.0	2.72	2.79
C spin density			0.26	0.22
O spin density			0.14	0.19

*3.2.4 Synthesis of [U(η^8-$C_8H_6\{Si^iPr_3\text{-}1,4\}_2$)($\eta^2$-dmpz)$_2$($\eta^1$-CNMe)] (**3.3**)*

However, **3.1** reacts in the presence of a tenfold excess of MeNC when heated at 80 °C on an NMR scale in d_8-toluene to yield [U(η^8-$C_8H_6\{Si^iPr_3\text{-}1,4\}_2$)($\eta^2$-dmpz)$_2$($\eta^1$-CNMe)] (**3.3**). The elemental analysis and mass spectrum of **3.3** are in agreement with the molecular formation of [U(η^8-$C_8H_6\{Si^iPr_3\text{-}1,4\}_2$)($\eta^2$-dmpz)$_2$], after loss of the coordinated isocyanide.

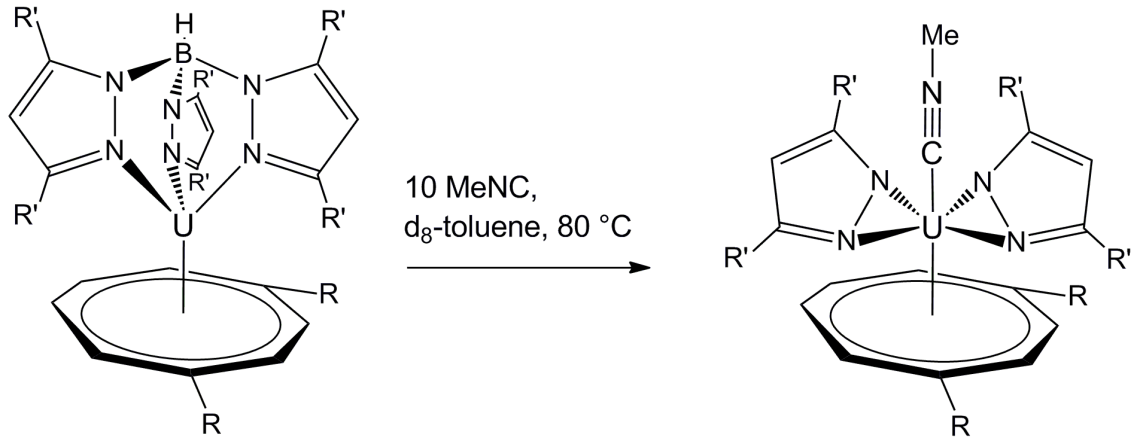

R = Si^{i}Pr$_3$
R' = Me

Scheme 2: Synthesis of [U(η^8-C$_8$H$_6${Si^{i}Pr$_3$-1,4}$_2$)(η^2-dmpz)$_2$(η^1-CNMe)] (**3.3**)

The U-M1 distance in **3.3** and in **3.1** are essentially identical within esds. That the change in formal oxidation state from U(III)/U(IV) is not necessarily accompanied by a change in structural parameters has been observed for other mixed-sandwich complexes and attributed to steric congestion.[14,16] The two pyrazolide rings are bound in an endo-bidentate fashion to the metal centre, the distances in **3.3** are closer to those found in [U(Cp^{Me5})$_2$(η^2-pz)$_2$] and [U(Cp)$_3$(η^2-pz)] U-N (2.4 Å) and (2.36 Å),[22] than the longer averaged distances in [U(κ^3-Tp^{Me2})(N{SiMe$_3$}$_2$)(η^2-dmpz)] U-N$_{ave}$ (2.440(8) Å) and [U(κ^3-Tp^{Me2})$_2$(η^2-dmpz)] U-N$_{ave}$ (2.444(11) Å).[8] This endo-bidentate binding mode was first observed in [U(Cp)$_3$(η^2-pz)] and considered a consequence of the more ionic bonding in the actinides as opposed to the bridging mode observed in the d-block elements, which allows for directional covalent bonding.

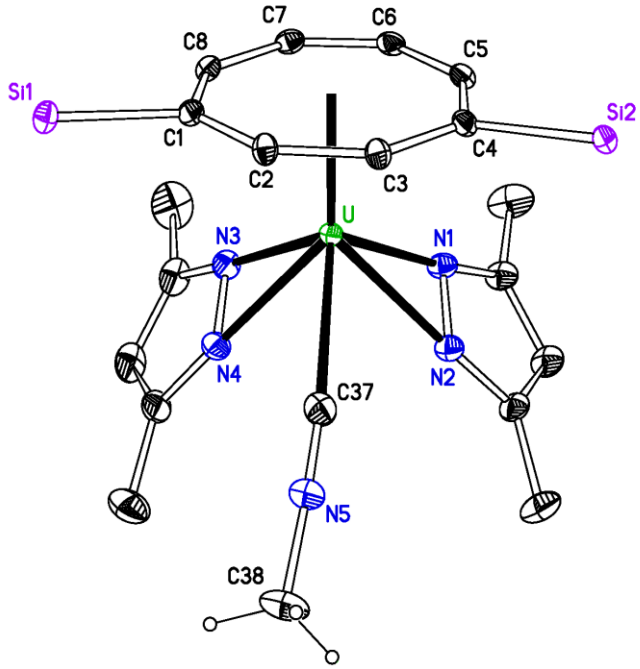

Figure 4: Molecular structure of [U(η^8-C_8H_6{Si^{i}Pr$_3$-1,4}$_2$)(η^2-dmpz)$_2$(η^1-CNMe)] (**3.3**), ellipsoids at 50 % probability, ^{i}Pr groups and H atoms, except MeNC, omitted for clarity. Selected bond distances (Å) and angles (°): U-N1 2.353(2), U-N2 2.397(2), U-N3 2.360(2), U-N4 2.387(2), U-M1 1.987(7) Å, U-C37 2.675(3), C37-N5 1.140(3), N5-C37-U 170.0(2) (M1 is the centroid of the [C_8H_6{Si^{i}Pr$_3$-1,4}$_2$]$^{2-}$ ring).

The relevant bonding interaction between the metal centre and the (η^1-CNMe) in **3.3** are essentially identical within esds to those found in the [U(η^8-C_8H_6{Si^{i}Pr$_3$-1,4}$_2$)(η-Cp*)(η^1-CNMe)] (**2.5**), though the U-C-N angle (178.4°), deviates more from linear than that observed in **3.3**. This U-C distance in **3.3** is significantly longer than those found in the literature; much longer than the U-C (2.464(4) Å) observed for [U(Cp^{Me4H})$_3$(CNC_6H_4-*p*-OMe)] in which π-back-bonding is thought to occur.[23] These

observations are in keeping with an unactivated, loosely coordinated isocyanide in **3.3**. The ^{1}H NMR spectrum of complex **3.3** at room temperature is unexpectedly complex, showing two Si^{i}Pr$_3$ environments and significant broadening and merging of the dmpz resonances. It has not been possible to determine whether this reflects different conformations in solution, or fast association and dissociation of the isocyanide, or a mixture of **3.3** and [U(η^8-C_8H_6{Si^{i}Pr$_3$-1,4}$_2$)(η^2-dmpz)$_2$] resulting from partial loss of the isocyanide on drying **3.3** *in vacuuo*. The isocyanide resonance cannot be identified, this would not be surprising in itself as it is a small molecule σ-bonded to a paramagnet, or it may be broadened out as a result of an exchange process. It is worth mentioning that the carbonyl resonance in the known range of uranium(III) monocarbonyl complexes has never been observed by ^{13}C{^{1}H}NMR.[23,24,25]

The fragility of the B-N bond is well documented and fragmentation of the Tp^{Me2} ligand especially when coordinated to an electropositive metal is a recurrent problem in lanthanide chemistry,[26] though in some cases this fragmentation is the result of adventitious water or oxygen;[27] in most instances the mechanistic details of the fragmentation pathway have been neither investigated or reported. Fragmentation, however, is not usually accompanied by redox behaviour. When [Sm(κ^3-Tp^{Me2})(κ^2-Tp^{Me2})(η-Cp)] was heated to 165 °C under vacuum overnight it yielded [Sm(κ^3-Tp^{Me2})$_2$(dmpz)] and [Sm(HB(dmpz)$_2$(C_5H_4))(κ^3-Tp^{Me2})].[28]

For low-valent uranium, the availability of the +4 oxidation state has led to a few examples of redox behaviour: the themolysis of [U(κ^3-Tp^{Me2})(κ^2- Tp^{Me2})(Cp)] at 160

°C, under vacuum for 3 days resulted in the oxidation of the metal centre to yield $[U(Cp)_3(dmpz)]$, $[U(Tp^{Me2})(dmpz)_3]$ and $[(HB(dmpz)_2)_2]$.[29] Redox behaviour was also observed during the thermal decomposition of $[U(\kappa^3\text{-}Tp^{Me2})(N\{SiMe_3\}_2)_2]$.[8] In both of these examples there is more than one U(IV) species produced and the mechanism is unclear, but B-N cleavage is proposed to dominate. The observed reactivity for **3.1**, mediated by a combination of heating and the excess isocyanide, results in the single U(IV) species **3.3,** suggesting that it is the oxidation of the uranium centre, that takes precedence over B-N cleavage.

*3.2.5 Reactivity of $[U(\kappa^3\text{-}Tp^{Me2})(\eta^8\text{-}C_8H_4\{Si^iPr_3\text{-}1,4\}_2)]$ (**3.2**)*

The reactions of **3.2** with MeNC, CO or CO_2 result in a colour change from pink/purple to brown/red. No material suitable for X-ray analysis was obtained from a range of solvents. The reaction of **3.2** with 4.5 equivalents of ^{13}CO added at low temperature *via* the Toepler pump resulted in a single product resonance at -71.5 ppm by $^{11}B\{^1H\}$ NMR, two product resonances at -128.2 and -99.5 ppm by $^{29}Si\{^1H\}$ NMR and a very broad resonance at 235.5 ppm by $^{13}C\{^1H\}$NMR. Addition of further ^{13}CO (4.5 equivalents) to the same sample resulted in an increase in intensity of the product resonances at -71.5 ppm and -99.5 ppm by $^{11}B\{^1H\}$ NMR and $^{29}Si\{^1H\}$ NMR, and the disappearance of the product resonance at -128.2 ppm by $^{29}Si\{^1H\}$ NMR. The ^{13}C-labelled product resonance was observed to have shifted upfield to 204.7 ppm by $^{13}C\{^1H\}$ NMR. No free ^{13}CO was observed by $^{13}C\{^1H\}$ NMR, in spite of the huge excess of labelled gas. This and the upfield shift in the ^{13}C-product resonance are perhaps indicative of a equilibrium, possibly involving the coordination of multiple ^{13}CO units to the uranium centre. The

reaction of **3.2** with $^{13}CO_2$, also resulted in the observation of multiple product resonances by $^{11}B\{^1H\}$ (-82.9, 89.4, -94.5 ppm) and $^{13}C\{^1H\}$ NMR (167 and 175 ppm) and free ^{13}CO (185 ppm) and $^{13}CO_2$ (123 ppm). In the $^{11}B\{^1H\}$ spectrum after a week at room temperature only the resonance at -94.5 ppm was still visible and the resonance at 175 ppm shifted to 173 ppm in the $^{13}C\{^1H\}$ NMR spectrum. These early results are very interesting but in the absence of data, which confirms the molecular formulation, no more can be elucidated at this stage.

3.2.6 Conclusion

The substitution of the Cp^R ligand for the Tp^{Me2} ligand has led to the synthesis of two novel uranium(III) half-sandwich complexes, **3.1** and **3.2**. The X-ray structures of these complexes reveal that the increase in steric congestion resulting from the use of the Tp^{Me2} ligand, in place of Cp^{Me5}, is not reflected in an increase in the U-centroid distance to the $(C_8H_6\{Si^iPr_3\text{-}1,4\}_2)^{2-}$ ligand in **3.1** but in **3.2** results in a lengthening of the U-C distances to the pentalene ligand. This is corroborated by the solution NMR behaviour of the complexes: **3.1** retains a static structure up to 80 °C, whereas **3.2** is fully fluxional at room temperature. The ability of the pentalene ligand to fold around the bridgehead allows greater access to the metal centre in **3.2**. Complex **3.1** displays no reactivity towards CO, CO_2, MeNC under mild conditions, though initial reactivity studies on **3.2** show it is reactive towards small molecules under the same conditions. DFT calculations on the model systems $[U(\eta^8\text{-}C_8H_6\{SiH_3\text{-}1,4\}_2)(\eta^5\text{-}Cp^{Me5})]$ **I** and $[U(\eta^8\text{-}C_8H_6\{SiH_3\text{-}1,4\}_2)(\kappa^3\text{-}Tp^{Me2})]$ **II** show that **II** is more reducing than its cyclopentadienyl analogue. However, for the bulkier system, CO binding is more thermodynamically

unfavourable. When heated at 80 °C in the presence of a tenfold excess of MeNC **3.1** reacts to yield [U(η^8-C_8H_6{Si^{i}Pr$_3$-1,4}$_2$)(η^2-dmpz)$_2$(η^1-CNMe)] (**3.3)**.

3.2.7 Attempted syntheses of [U(κ^3-Tp^{Me2})(η^8-C_8H_6{SiMe$_3$-1,4}$_2$)]and [U(κ^3-Tp)(η^8-C_8H_4{Si^{i}Pr$_3$-1,4}$_2$)].

Using the synthetic route described for **3.1** and **3.2** and $K_2(C_8H_6\{SiMe_3\text{-}1,4\}_2)$ it was possible to synthesise [U(κ^3-Tp^{Me2})(η^8-C_8H_6{SiMe$_3$-1,4}$_2$)] but as the reaction was low yielding and it was not possible to separate the desired U(III) species from the [U(η^8-$C_8H_6\{SiMe_3\text{-}1,4\}_2)_2$] side product, this was not pursued further. It is interesting to note that using the less bulky $(C_8H_6\{SiMe_3\text{-}1,4\}_2)^{2-}$ resulted in a ^{1}H NMR spectrum of [U(κ^3-Tp^{Me2})(η^8-$C_8H_6\{SiMe_3\text{-}1,4\}_2$)] at ambient temperature, which is consistent with single ligand environments rendered by mirror plane symmetry on an NMR time scale.

The reaction of UI_3 with unsubstituted KTp, followed by the addition of $K_2(C_8H_4\{Si^iPr_3\text{-}1,4\}_2)$ resulted in the isolation of a green/black micocrystalline material in a moderate yield. However, single crystals suitable for X-ray analysis were not obtained from a range of solvents and the elemental analysis was not found to be correct for either [U(κ^3-Tp)(η^8-C_8H_4{Si^{i}Pr$_3$-1,4}$_2$)] or [U(κ^3-Tp)(η^8-C_8H_4{Si^{i}Pr$_3$-1,4}$_2$)I]. The ^{1}H NMR spectrum of the product at ambient temperature, was consistent with restricted rotation on an NMR time scale. This is a curious result, given the reduction of bulk on moving to the unsubstituted KTp from KTp^{Me2}. The vapour diffusion of pentane into a saturated thf solution at ambient temperature after two weeks, resulted in the structure

shown in Figure 5, which incorporates a bridging oxo unit and the η^5-hydropentalenyl ligand. The refinement of the data is not sufficient to confirm more than the basic connectivity. It is possible that this structure arises from the ring opening of thf by [U(κ^3-Tp)(η^8-C_8H_4{Si^{i}Pr$_3$-1,4}$_2$)I]. This is a known reaction of uranium complexes with thf[30] and diethyl ether.[31] There are also examples in Sm(II)[32,33] chemistry, of particular relevance is the reaction of $K_2(C_8H_4\{Si^iPr_3\text{-}1,4\}_2)$ with [Sm(η^5-Cp^{Me5})(μ-I)(THF)$_2$] which yields the Sm(III) complexes [Sm(η^5-Cp^{Me5})(η^8-C_8H_4{Si^{i}Pr$_3$-1,4}$_2$)] and [Sm(η^8-C_8H_4{Si^{i}Pr$_3$-1,4}$_2$)(η^5-C_8H_5{Si^{i}Pr$_3$-1,4}$_2$)] and a mixed-valence Sm(II)/Sm(III) cluster, [Sm$_6$(η^5-Cp^{Me5})$_6$(OMe)$_8$O][K(THF)$_6$] *via* solvent activation.[33]

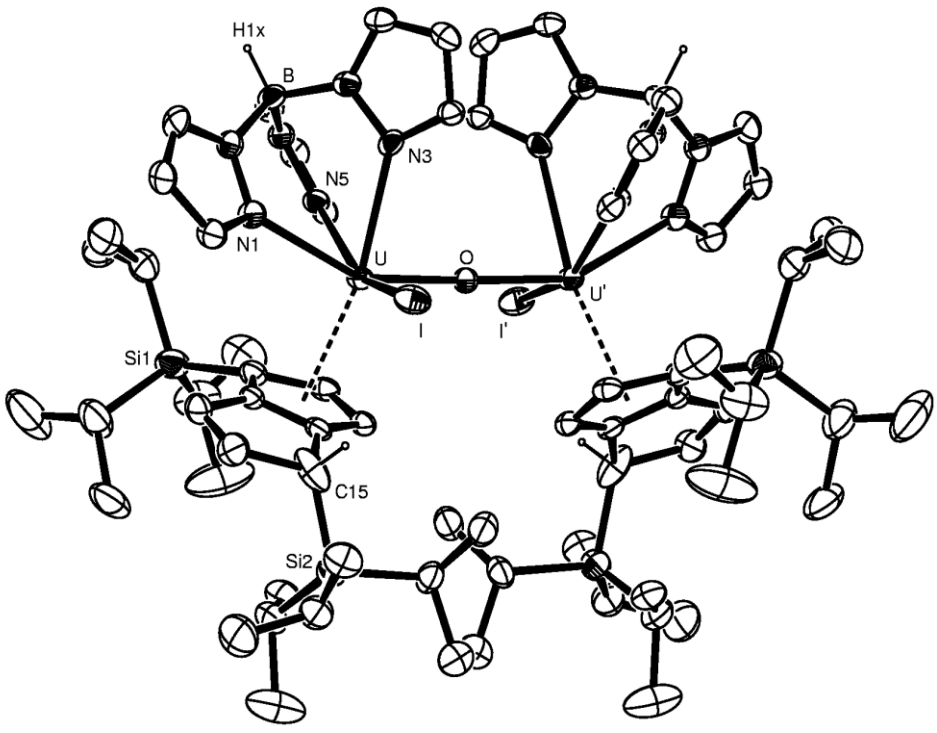

Figure 5. Representation of [(U(κ^3-Tp)(η^5-C_8H_5{Si^{i}Pr$_3$-1,4}$_2$)I)$_2$(μ-O)]

3.3 Experimental details for Chapter Three

General details are given in Appendix One.

*3.3.1 Synthesis of [U(κ^3-Tp^{Me2})(η^8-C$_8$H$_6${Si^{i}Pr$_3$-1,4}$_2$)] (**3.1**)*

An ampoule was charged with UI_3 (0.39 g, 0.62 mmol) and THF (*ca.* 50 ml) added, the dark purple solution was stirred overnight at ambient temperature. To this a colourless solution of KTp^{Me2} (0.21 g, 0.62 mmol) in THF (*ca.* 20 ml) was added drop-wise over 45 min and the reaction mixture stirred for a further 2 h 30 min after which time a white precipitate was observed. Volatiles were removed at reduced pressure, solids extracted with toluene and filtered on a frit through dry Celite®. The dark purple solution was stripped to dryness, taken up in THF (*ca.* 60 ml) and cooled to 0 °C. To this a yellow solution of K_2(C$_8$H$_6${Si^{i}Pr$_3$-1,4}$_2$) (0.75 equivalents, 0.23 g, 0.47 mmol) in THF (25 ml) was added dropwise over the course of an hour. The solution was warmed to ambient temperature overnight under a partial vacuum after which the colour of the solution was observed to be a deep red and a white precipitate was observed. Volatiles were removed at reduced pressure and solids extracted with pentane and filtered on a frit through dry Celite®.

Yield: 175 mg, 29.4 %

^{1}H NMR (d_8-toluene, 303 K): δ_H 18.9 (br, m, 1H, B-*H*), 10.1 (s, 2H, Tp^{Me2}-C*H*), 4.1 (s, 1H, Tp^{Me2}-C*H*), 3.5 (s, 6H, Tp^{Me2}-C*H$_3$*), -0.2 (s, 3H, Tp^{Me2}-C*H$_3$*), -1.8 (d, J_{HH} = 5.2 Hz, 18H, ^{i}Pr-C*H$_3$*), -2.3 (d, J_{HH} = 5.3 Hz, 18H, ^{i}Pr-C*H$_3$*), -2.8 (br, s, 6H, ^{i}Pr-C*H*), -15.4 (s,

3H, Tp^{Me2}-C*H*$_3$), -17.5 (s, 6H, Tp^{Me2}-C*H*$_3$), -22.0 (br, s, 2H, COT ring C*H*), -50.3 (br, s, 2H, COT ring C*H*) , -54.8 (br, s, 2H, COT ring C*H*).

$^{11}B\{^1H\}$ NMR (d_8-toluene, 328 K): δ_B 32.8

$^{29}Si\{^1H\}$ NMR (d_8-toluene, 328 K): δ_{Si} -115.6

MS (EI): m/z = 951 (M+)

*3.3.2 Synthesis of [U(κ^3-Tp^{Me2})(η^8-C$_8$H$_4${Si^{i}Pr$_3$-1,4}$_2$)] (**3.2**)*

In an analogous manner to that described in 3.3.1 **3.2** was synthesised using UI_3 (0.77 g, 1.24 mmol), KTp^{Me2} (0.42 g, 1.24 mmol) and $K_2(C_8H_4\{Si^iPr_3\text{-}1,4\}_2)$ (0.80 equivalents, 0.49 g, 0.99 mmol).

Yield: 129 mg, 11 %

Analysis calculated (found) for $C_{41}H_{68}BN_6Si_2U$: % C 51.58 (51.91), % H 7.17 (7.12), % N 8.85 (8.81).

^1H NMR (d_8-toluene, 303 K): δ_H18.0 (br, m, 1H, B-*H*), 7.7 (s, 3H, Tp-C*H*), 7.3 (br, s, 2H, pentalene ring C*H*), 2.5 (s, 9H, Tp-C*H*$_3$), -5.3 (s, 18H, ^{i}Pr-C*H*$_3$), -9.9 (s, 18H, ^{i}Pr-C*H*$_3$), -11.6 (br, s, 6H, ^{i}Pr-C*H*), -17.1 (s, 9H, Tp-C*H*$_3$), -23.2 (br, s, 2H, pentalene ring C*H*). $^{11}B\{^1H\}$ NMR (d_8-toluene, 303 K): δ_B 38.2; ^{29}Si (d_8-toluene, 303 K): δ_{Si} -159.3

MS (EI): m/z = 949 (M+)

*3.3.3 Synthesis of [U(η^8-C_8H_6{Si^{i}Pr$_3$-1,4}$_2$)(κ^2-dmpz)$_2$(η^1-CNMe)] (**3.3**)*

Complex **3.1** (61 mgs, 6.41 mmol) was dissolved in d_8-toluene and placed in an NMR tube. MeNC (34 µL, 64.1 mmol) was added by syringe and the tube inverted to aid mixing. The dark red solution was heated at 80 °C in a heating block and monitored by ^{1}H and ^{11}B NMR. After 24 hrs the colour of the solution was observed to lighten to a dark orange colour and bright red crystals were visible. The solution was heated for a further 24 hrs after which time the reaction was observed to be complete. Crystalline material for characterisation was washed into a schlenk, cooled, washed with cold toluene and dried *in vacuuo*.

Analysis calculated (found) for $C_{38}H_{65}N_4Si_2U$: % C 51.18 (51.38), % H 7.35 (7.29), % N 6.64 (6.59).

^{1}H NMR (d_8-toluene, 303 K): δ_H 1.1 (m, 6H, COT ring C*H*, dmpz-*H*), -1.9 (v br, m, 12H, dmpz-C*H*$_3$), -4.8 (br, s, 9H, ^{i}Pr-C*H*$_3$), -5.0 (br, s, 3H, ^{i}Pr-C*H*), -5.46 (br, s, 9H, ^{i}Pr-C*H*$_3$), -9.0 (br, s, 9H, ^{i}Pr-C*H*$_3$), -10.0 (br, s, 3H, ^{i}Pr-C*H*), -31.4 (s, 2H, COT ring C*H*). One ^{i}Pr-C*H*$_3$ resonance is obscured by solvent.

MS (EI): m/z = 844 (M+ - MeNC)

*3.3.4 Reaction of [U(κ^3-Tp^{Me2})(η-C_8H_4{Si^{i}Pr$_3$-1,4}$_2$)](**3.2**) with excess ^{13}CO*

^{13}CO (4.5 equivalents) was added by Toepler pump to a degassed pink/purple solution of [U(κ^3-Tp^{Me2})(η-C_8H_4{Si^{i}Pr$_3$-1,4}$_2$)] (16 mg, 0.02 mmol) in d_8-toluene (0.5 ml) at -78

°C. There was an immediate colour change to red/brown and the sample left to warm to room temperature overnight.

$^{11}B\{^{1}H\}$ NMR (d_8-toluene, 303 K, selected data): δ_B -71.5 ppm

$^{29}Si\{^{1}H\}$ (d_8-toluene, 303 K, selected data): δ_{Si} -128.2, -99.5 ppm

$^{13}C\{^{1}H\}$ (d_8-toluene, 303 K, selected data): δ_C 235.5 ppm

In a manner analogous to that described in 3.3.4 further ^{13}CO (4.5 equivalents) was added to the sample of [U(κ^3-Tp^{Me2})(η-$C_8H_4\{Si^iPr_3\text{-}1,4\}_2$)].

$^{11}B\{^{1}H\}$ NMR (d_8-toluene, 303 K, selected data): δ_B -71.5 ppm

$^{29}Si\{^{1}H\}$ (d_8-toluene, 303 K, selected data): δ_{Si} -99.3 ppm

$^{13}C\{^{1}H\}$ (d_8-toluene, 303 K, selected data): δ_C 204.7 ppm

*3.3.5 Reaction of [U(κ^3-Tp^{Me2})(η-$C_8H_4\{Si^iPr_3\text{-}1,4\}_2$)](**3.2**) with $^{13}CO_2$*

In a manner analogous to that described in 3.3.4, $^{13}CO_2$ (3.6 equivalents) was added to [U(κ^3-Tp^{Me2})(η-$C_8H_4\{Si^iPr_3\text{-}1,4\}_2$)] (21 mg, 0.022 mmol) in d_8-toluene.

$^{11}B\{^{1}H\}$ NMR (d_8-toluene, 303 K, selected data): δ_B -82.9, 89.4, -94.5 ppm

$^{13}C\{^{1}H\}$ (d_8-toluene, 303 K, selected data): δ_C 185 (^{13}CO), 123 ($^{13}CO_2$), 167 and 175 ppm

After a week at room temperature:

$^{11}B\{^{1}H\}$ NMR (d_8-toluene, 303 K, selected data): δ_B -94.5 ppm

$^{13}C\{^{1}H\}$ (d_8-toluene, 303 K, selected data): δ_C 185 (^{13}CO), 123 ($^{13}CO_2$), 167 and 173 ppm

3.3.6 Isolation of [U(κ³-Tp^{Me2})I$_2$(THF)$_2$]

A colourless solution of KTp^{Me2} (0.27 g, 0.81 mmol) in THF (20 ml) was added over an hour to a dark purple solution of UI_3 (0.50 g, 0.81 mmol) in THF (70 ml). The dark purple solution was filtered by filter canula, reduced to *ca.* 35 ml and crystals suitable for X-ray analysis were obtained by slow cooling to – 50 °C for 4 days.

Yield: 310 mgs, 0.33 mmol, 41 %

MS (EI): m/z = 789 (M+ - THF)

^{1}H NMR (d_8-toluene, 293 K): δ 13.45 (v. br, m, B-*H*), 7.90 (s, 3H, Tp^{Me2}-*H*), 2.29 (s, 9H, Tp^{Me2}-C*H*$_3$), 2.01 (br, s, 8H, THF-C*H*$_2$), 0.62 (br, s, 8H, THF-C*H*$_2$), -13.39 (br, s, 9H, Tp^{Me2}-C*H*$_3$).

3.3.7 Attempted synthesis of [U(κ³-Tp^{Me2})(η-C$_8$H$_6${SiMe$_3$-1,4}$_2$)]

[U(κ^3-Tp^{Me2})I$_2$(THF)$_2$] (0.24 g, 0.26 mmol) in THF (100 ml) was cooled to – 10 °C and an orange solution of K$_2$(C$_8$H$_6${SiMe$_3$-1,4}$_2$) (0.085 g, 0.26 mmol, 1 equivalent) in THF (20 ml) was added dropwise over 35 min. After half the addition was complete the

colour of the solution changed from deep purple to red and a white precipitate was observed. The solution was warmed to ambient temperature overnight under a partial vacuum, volatiles were removed *in vacuo*, solids extracted with pentane and filtered on a frit through dry Celite®. The red solution was reduced in volume (30 ml); slow cooling to - 50 °C yielded red and green microcrystalline material.

Yield: 20 mgs, 0.03 mmol, 12 %

^{11}B NMR VNMR 600: 33.3 ppm (s, B-H)

^{29}Si NMR VNMR 600: - 111.3 ppm (s, $SiMe_3$)

MS (EI): m/z = 784, 734

^{1}H NMR (C_6D_6, 303 K): δ 19.70 (v. br, m, B-*H*), 8.71 (v. br, s, 3H, Tp^{Me2}-*H*), 2.22 (br, s, 9H, Tp^{Me2}-C*H*$_3$), -6.84 (s, 18H, SiC*H*$_3$), -18.89 (s, 9H, Tp^{Me2}-C*H*$_3$), -29.24 (s, 2H, COT ring-C*H*), -48.85 (s, 2H, COT ring-C*H*), -52.69 (s, 2H, COT ring-C*H*).

3.3.8 Attempted synthesis of [U(κ^3-Tp)(C_8H_4{Si^{i}Pr$_3$-1,4}$_2$)]

An ampoule was charged with UI_3 (0.60 g, 0.97 mmol) and THF (*ca.* 50 ml) added, the dark purple solution was stirred vigorously for 40 min before being cooled to 0 °C. To this a colourless solution of KTp (0.24 g, 0.97 mmol) in THF (*ca.* 15 ml) was added drop-wise over 25 min during which time a white precipitate was observed and the reaction mixture warmed to room temperature and stirred overnight. Volatiles were removed at reduced pressure, solids extracted with toluene and filtered. The dark purple solution was stripped to dryness, taken up in THF (*ca.* 30 ml) and cooled to -10 °C. To this a yellow solution of $K_2(C_8H_6${Si^{i}Pr$_3$-1,4}$_2$) (0.80 equivalents, 0.38 g, 0.78 mmol) in

THF (25 ml) was added dropwise over the course of an hour, the colour of the solution changed to red/brown and a white precipitate was formed. The solution was warmed to ambient temperature overnight under a partial vacuum, volatiles were removed at reduced pressure and solids extracted with pentane and filtered on a frit through dry Celite®. Concentration of the brown pentane solution to (20 ml) and cooling to -50 °C, yielded a black crystalline material. Single crystals suitable for X-ray analysis were not obtained from a range of solvents.

Yield: 175 mg, 21 %

^{1}H NMR (d_8-toluene, 303 K): δ_H 35.47 (s, 1H), 28.01 (s, 1H), 22.82 (s, 1H), 20.49 (s, 1H), 15.51 (s, 1H), 15.10 (br, m, 1H, B-*H*), 12.32 (s, 1H), 9.13 (s, 1H), 7.38 (s, 1H), 2.32 (s, 1H), -0.59 (s, 9H, ^{i}Pr-C*H*$_3$), -2.09 (s, 9H, ^{i}Pr-C*H*$_3$), -3.09 (s, 1H), -3.14 (s, 9H, ^{i}Pr-C*H*$_3$), -4.09 (s, 9H, ^{i}Pr-C*H*$_3$), -6.28 (s, 1H), -6.60 (s, 3H, ^{i}Pr-C*H*), -14.11 (s, 3H, ^{i}Pr-C*H*), -21.87 (s, 1H), -35.90 (s, 1H), -40.72 (s, 1H).

^{11}B{^{1}H} NMR (d_8-toluene, 328 K): δ_B ; 25.9 ppm

^{29}Si NMR (d_8-toluene, 328 K): δ_{Si} -121.7, -127.6 ppm

MS (EI): m/z = 865 (M+), 1002

3.4 References:

[1] F. T. Edelmann, D. M. M. Freckmann and H. Schumann, *Chem. Rev.*, 2002, **102**, 1851.

[2] a) S. Trofimenko, *J. Am. Chem. Soc.*, 1966, **88**, 1842. b) S. Trofimenko, *Chem. Rev.*, 1993, 93, 943.

[3] a) U. Kilimann and F. T. Edelmann, *J. Orgmet. Chem.*, 1993, **444**, C15. b) H-D. Amberger, F. T. Edelmann, J. Gottfriedsen, R. Herbst-Irmer, S. Jank, U. Kilimann, M. Noltemeyer, H. Reddmann and M. Schaefer, *Inorg. Chem.* 2009, **48**, 760.

[4] A. Paulo, J. D. G. Correia, M. P. C. Campello and I. Santos, *Polyhedron*, 2004, **23**, 331.

[5] M. P. C. Campello, A. Domingos, A. Galvao, A. Pires de Matos and I. Santos, *J Organomet. Chem.*, 1999, **579**, 5.

[6] See also: S. J. Kraft, P. E. Fanwick and S. C. Bart, *Inorg. Chem.*, 2010, **49**, 1103.

[7] a) Y. Sun, R. McDonald, J. Takats, V. W. Day and T. A. Eberspacher, *Inorg. Chem.*, 1994, **33**, 4433. b) R. McDonald, Y. Sun, J. Takats, V. W. Day and T. A. Eberspacher, *J. Alloys and Comp.*, 1994, **8-10**, 4041

[8] Y. Sun, PhD Thesis, University of Alberta, 1995.

[9] M. A. Antunes, G. M. Ferrence, A. Domingos, R. McDonald, C. J. Burns, J. Takats, and N. Marques, *Inorg. Chem.*, 2004, **43**, 6640.

[10] a) N. Marques, A. Pires de Matos and K.W. Bagnall, *Inorg. Chim. Acta*, 1984, **95**, 75. b) I. Santos, N. Marques and A. Pires de Matos, *Inorg. Chim. Acta*, 1985, **110**, 149. c) M. V. R. Stainer and J. Takats, *J. Am. Chem. Soc.*, 1985, **105**, 410.

[11] F. G. N. Cloke and P. B. Hitchcock, *J. Am. Chem. Soc.*, 1997, **119**, 7899

[12] F. G. N. Cloke, J. C. Green and C. N. Jardine, *Organometallics*, 1999, 18, 1080.

[13] a) D. L. Reger, J. A. Lindemann and L. Lebioda, *Inorg. Chim. Acta*, 1987, **139**, 71. b) D. P. Long, A. Chandrasekaran, R. O. Day, P. A. Bianconi and A. L. Rheingold, *Inorg. Chem.*, 2000, **39**, 4476.

[14] a) O. T. Summerscales, F. G. N. Cloke, P. B. Hitchcock, J. C. Green and N. Hazari, *Science*, 2006, **311**, 829. b) O. T. Summerscales, F. G. N. Cloke, P. B. Hitchcock, J. C. Green and N. Hazari, *J. Am. Chem. Soc.*, 2006, **128**, 9602.

[15] O. T. Summerscales and F. G. N. Cloke, *Coord. Chem. Rev.*, 2006, **250**, 1122.

[16] F. G. N. Cloke and P. B. Hitchcock, *J. Am. Chem. Soc.*, 2002, **124**, 9352

[17] A. C. Hillier, X. W. Zhang, G. H. Maunder, S. Y. Liu, T. A. Eberspacher, M. V. Metz, R. McDonald, A. Domingos, N. Marques, V. W. Day, A. Sella and J. Takats, *Inorg. Chem.*, 2001, 40, 5106.

[18] a) D. M. Tellers, S. J. Skoog, R. G. Bergman, T. B. Gunnoe and W. D. Harman, *Organometallics*, 2000, **19**, 2428. (b) F. T. Edelmann, *Angew. Int. Ed.*, 2001, **40**, 1656.

[19] N. Hitajima, W. B. Tolman, *Prog. Inorg. Chem.*, 1995, **43**, 418.

[20] A. L. Rheingold, R. L. Ostrander, B. S. Haggerty and S. Trofimenko, *Inorg. Chem.* 1994, **33**, 3666.

[21] P. M. Maitlis, *Chem. Soc. Rev.* 1981, **10**, 1.

[22] a) C. W. Eigenbrot, Jr. and K. N. Raymond, *Inorg. Chem.*, 1981, **20**, 1553. b) *Ibid.*, 1982, **21**, 2653.

[23] M. D. Conejo, J. S. Parry, E. Carmona, M. Schultz, J. G. Brennann, S. M. Beshouri, R. A. Anderson, R. D. Rogers, S. Coles and M. Hursthouse, *Chem . Eur. J.*, 2000, **5**, 3000.

[24] a) J. G. Brennan, R. A. Anderson and J. L. Robbins, *J. Am. Chem. Soc.*, 1986, **108**, 335. b) J. S. Parry, E. Carmona, S. Coles and M. Hursthouse, *J. Am. Chem. Soc.*, 1995,**117**, 2649.

[25] A. S. P. Frey, F. G. N. Cloke, P. B. Hitchcock, I. J. Day, J. C. Green and G. Aitken, *J. Am. Chem. Soc*., 2008, **138**, 13816.

[26] a) N. Marques, A. Sella and J. Takats, *Chem. Rev.*, 2002, **102**, 2137. b) M. Ephritikhine, *Angew. Int. Ed.*, 2009, **48**, 4898.

[27] A. Domingos, M. R. J. Elsegood, A. C. Hillier, G. Y. Lin, S. Y. Liu, I. Lopes, N. Marques, G. H. Maunder, R. McDonald, A. Sella, J. W. Steed and J. Takats, *Inorg. Chem.*, 2002, **41**, 6761.

[28] I. Lopes, G. Y. Lin, A. Domingos, R. McDonald, N. Marques and J. Takats, *J. Am. Chem. Soc.*, 1999, **121**, 8110.

[29] M. A. Antunes, A. Domingos, I. Cordeiro dos Santos, N. Marques and J. Takats, *Polyhedron*, 2005, 24, 3038.

[30] a) C. Boisson, J. C. Berthet, M. Lance. M. Nierlich and M. Epthritikhine, *Chem. Commun.*, 1996, 2129. b) L. R. Avens, D. M. Barnhart, C. J. Burns and S. D. McKee, *Inorg. Chem.*, 1996, **35**, 537. c) W. J. Evans, S. A. Korimor and J. W. Ziller, *J. Am. Chem. Soc.*, 2003, **125**, 14264.

[31] C. P. Larch, F. G. N. Cloke and P. B. Hitchcock, *Chem. Commun.*, 2008, 82.

[32] W. J. Evans, J. T. Leman and J. W. Ziller, *Inorg. Chem.*,1996, **35**, 4283.

[33] O. T. Summerscales, D. R. Johnston, F. G. N. Cloke and P. B. Hitchcock, *Organometallics*, 2008, **27**, 5612.

CHAPTER FOUR: INDENYL CONTAINING U(III) MIXED-SANDWICH COMPLEXES

4.1 Synthesis and characterisation of [U(η^5-Ind^R)(η^8-C_8H_6{Si^{i}Pr$_3$-1,4}$_2$)] (R = Me$_6$, Me$_7$).

4.1.1 Introduction

The indenyl ligand class (Ind$^-$) is widely used in organometallic chemistry as an alternative to the Cp$^-$ ligands.[1] It is much more closely related chemically to the Cp$^-$ than the scorpionate ligands described in the previous chapter. Substitution of Cp$^-$ ligands for Ind$^-$ ligands has been shown to enhance the reactivity of complexes, the so-called 'indenyl effect', for example by an increase in the rate of associative substition.[2] The indenyl effect is not fully understood but is thought to be a consequence of the ability of the indenyl ligand to slip from η^5 to η^3 hapticity;[3] the haptotrophic flexibility resulting in a gain in aromaticity of the benzo ring and the freeing of a coordination site at the metal centre. More recently a theoretical examination of the indenyl effect has suggested that it is directly correlated to the strength of the M-L bond,[4] the M-(η^5-Cp) bond being stronger than the M-(η^5-Ind) bond and the M-(η^3-Ind) bond being stronger than the M-(η^3-Cp) bond. The difference in energy of the η^3-bound state in comparison to the η^5-bound state for the indenyl complex is small, leading to lower activation energies and faster reaction rates for reactions in which the haptotrophic shift occurs in the rate-determining step.

Group IV *ansa*-indenyl complexes have been shown to be effective catalysts for the stereospecific polymerisation of α-olefins.[5] The first η^9-indenyl complexes [Zr(η^5-$Ind^{1,3R}$)(η^5,η^9-$Ind^{1,3R}$)] (R = $CHMe_2$, Si^tBuMe_2) were structurally characterised by Chirik *et al*..[6] The η^9,η^5-bound rings were observed to interconvert rapidly in solution by NMR spectroscopy and theoretical studies supported the existence of an η^5,η^5-zirconocene intermediate.[4] These observations and the parallel of the dinitrogen activation chemistry of bis(cyclopentadienyl) Zr and Hf complexes,[7] led to the exploration of the reactivity of the bis(indenyl) zirconocenes with N_2, and the isolation of a range of dinitrogen complexes, including the isolation of rare examples of side-on, end-on dinitrogen compounds.[8] It is also of note that the choice of 1,3-substituents has an effect on the stability of the η^9-bound state. Complexes with 1,3-alkyl substituents are stable in coordinating solvents but 1,3-silyl-substituted complexes undergo rapid haptotrophic rearrangement on addition of THF or DME.[9]

Of the range of coordination modes available to the indenyl ligand, the most common is the η^5, but η^3, η^6, η^9 and η^1 are known.[3,6,10] The most common coordination mode observed in the indenyl chemistry of the f-block is η^5 and the factors affecting which coordination mode is adopted have been studied theoretically.[11,12] Tris(indenyl) lanthanide complexes [Ln$(Ind)_3$(THF)] (Ln = La, Sm, Gd, Tb, Dy, Yb)[13] were synthesied in the late 1960s and there was spectroscopic evidence for covalent bonding in the [Sm$(Ind)_3$(THF)] complex.[13,14] Evans *et al.* reported the synthesis of the Sm(II) indenyl complex [Sm(η^5-$Ind)_2$(THF)],[15] which has a more open coordination environment, but reactivity that is directly comparable to the reactivity of Sm(II)

cyclopentadienyl complexes.[16] Substitution of the indenyl ligand is necessary for the stabilisation of half-sandwich dialkyl complexes of the lanthanides,[17] which show catalytic activity. The only crystalographically characterised examples of f-block mixed-sandwich complexes are the $[Ln(\eta^5\text{-Ind})(\eta^8\text{-}C_8H_6)(THF)_2]$ (Ln = Pr, Nd) complexes[18] synthesised by Wen *et al*, but there have been no reports of the reactivity of these complexes.

The uranium(IV) complex $[U(\eta^5\text{-Ind})_3Cl]$[19] was structurally characterised in 1971. The complex has a tetrahedral geometry, and the orientation of the rings and the U-C bonding distances ruled out η^1-coordination to the metal centre. The IR data indicated that the C_5 ring of the indenyl was aromatic but the NMR data was ambiguous. The tris-indenyl $[U(\eta^5\text{-Ind})_3]$[20] is known but there are very few examples of indenyl containing uranium(III) complexes.[21] It has been suggested that methylation of the indenyl ligand would confer the advantages seen in the chemistry of methylated cyclopentadienyl organometallics. The permethylated indenyl ligand (Ind^{Me7})[22,23] is synthesised from the Frediel-Crafts acylation of prehnitene.[24] As prehnitene is not readily available, the permethylated indenyl ligand used in this work was generously donated by Prof. D. O'Hare of Oxford University. Examples of methyl substituted indenyl complexes of the lathanides[25] and actinides are few.[26,27,28,29] A range of derivative chemistry has been demonstrated for $[Th(\eta^5\text{-}Ind^{Me7})_2Cl_2]$,[28] which is similar to that displayed by the analogous $[Th(\eta^5\text{-}Cp^{Me5})_2Cl_2]$[30] complex.

Section 4.1 details the synthesis, characterisation and electrochemistry of the uranium(III) complexes [U(η^5-Ind^{Me6})(η^8-C_8H_6{Si^{i}Pr$_3$-1,4}$_2$)] (**4.1**) and [U(η^5-Ind^{Me7})(η^8-C_8H_4{Si^{i}Pr$_3$-1,4}$_2$)] (**4.2**), which incorporate the hexamethyl indenyl and permethyl indenyl ligands, respectively. The reactivity of **4.1** and **4.2** with CO and CO_2 is reported in Section 4.2.

*4.1.2 Synthetic route to [U(η^5-Ind^{Me6})(η^8-C_8H_6{Si^{i}Pr$_3$-1,4}$_2$)] (**4.1**) and [U(η^5-Ind^{Me7})(η^8-C_8H_6{Si^{i}Pr$_3$-1,4}$_2$)] (**4.2**)*

The addition of KInd^{Me6} to a cooled pre-stirred solution of UI_3, in THF, separation of KI by toluene work-up, and the slow addition of 0.8 equivalents of K_2(C_8H_6{Si^{i}Pr$_3$-1,4}$_2$) in THF at – 78 °C, followed by stirring at room temperature and pentane work-up yielded [U(η^5-Ind^{Me6})(η^8-C_8H_6{Si^{i}Pr$_3$-1,4}$_2$)] (**4.1**) as a dark red crystalline solid in a 20 % yield. Using the synthetic strategy described for **4.1** but maintaining the yellow suspension of KInd^{Me7} at -90 °C during the addition to UI_3 to prevent side-reactions with the solvent, [U(η^5-Ind^{Me7})(η^8-C_8H_4{Si^{i}Pr$_3$-1,4}$_2$)] (**4.2**) was isolated as a brown crystalline solid in a 24 % yield.

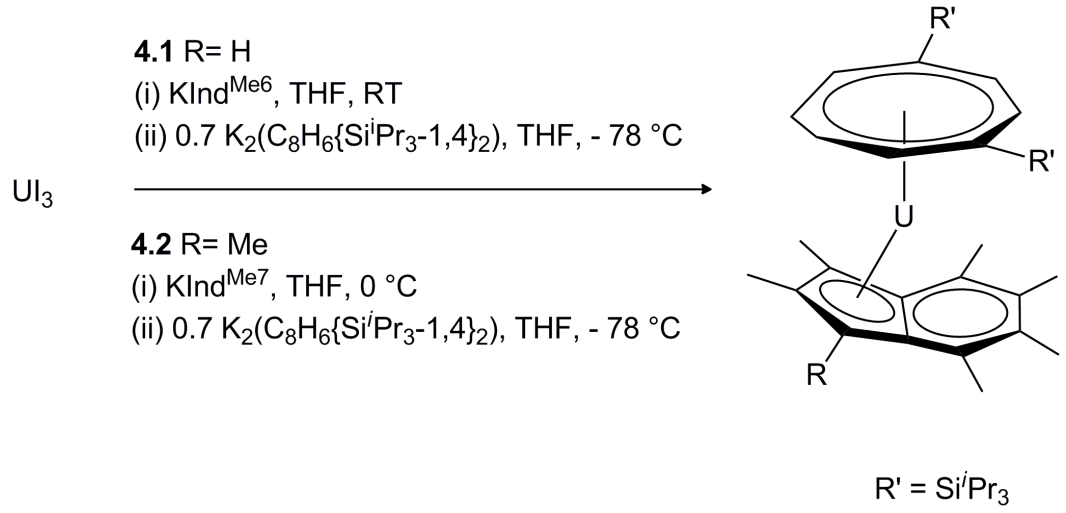

Scheme 1: Synthesis of $[U(\eta^5\text{-Ind}^R)(\eta^8\text{-}C_8H_6\{Si^iPr_3\text{-}1,4\}_2)]$ (R = Me_6 (**4.1**), Me_7 (**4.2**))

The elemental analysis and spectroscopic data for both complexes are in agreement with their molecular formation. **4.1** and **4.2** are stable at room temperature under inert atmosphere over a period of months, both in the solid state and in solution.

*4.1.3 Characterisation of $[U(\eta^5\text{-Ind}^R)(\eta^8\text{-}C_8H_6\{Si^iPr_3\text{-}1,4\}_2)]$ (R = Me_6 (**4.1**), Me_7 (**4.2**))*

In complex **4.2** the ^1H and $^{29}Si\{^1H\}$ NMR resonances associated with the $[C_8H_6\{Si^iPr_3\text{-}1,4\}_2]^{2-}$ and $[\eta^5\text{-Ind}^{Me7}]^-$ ligands in d_8-toluene at room temperature are consistent with a single Si^iPr_3 environment and 4 Ind-CH_3 environments in a 2:2:2:1 ratio, rendered by mirror plane symmetry on an NMR time scale. The ^1H spectrum of **4.1** in d_8-toluene at room temperature is consistent with the magnetic inequivalence of the ligand environments on an NMR timescale, resulting in two Si^iPr_3 environments and 6 Ind-CH_3 environments of equal integration, two of which are overlapping. The Ind-C*H*

resonance could not be identified, most likely as a result of broadening (see Section *2.1*).

The ^{1}H NMR data is in keeping with the observation of two resonances in the ^{29}Si{^{1}H} NMR of **4.1** in d_8-toluene at room temperature at δ - 110.8, -138.1 ppm. The ^{29}Si{^{1}H} NMR shift of **4.2** in d_8-toluene at room temperature appears at δ -122.2 ppm, between those observed in **4.1**. The ^{29}Si{^{1}H} shifts observed for **4.1** and **4.2** are in a similar spectral region to those observed for the previously reported mixed-sandwich complexes. The spectral range over which the resonances of complexes **4.1** and **4.2** are observed by ^{1}H NMR is broad, expected for the paramagnetic U(III) centre. VT ^{1}H NMR studies of **4.1** did not display coalescence at high temperature, however, the very linear relationship between chemical shift and temperature is shown in Figure .

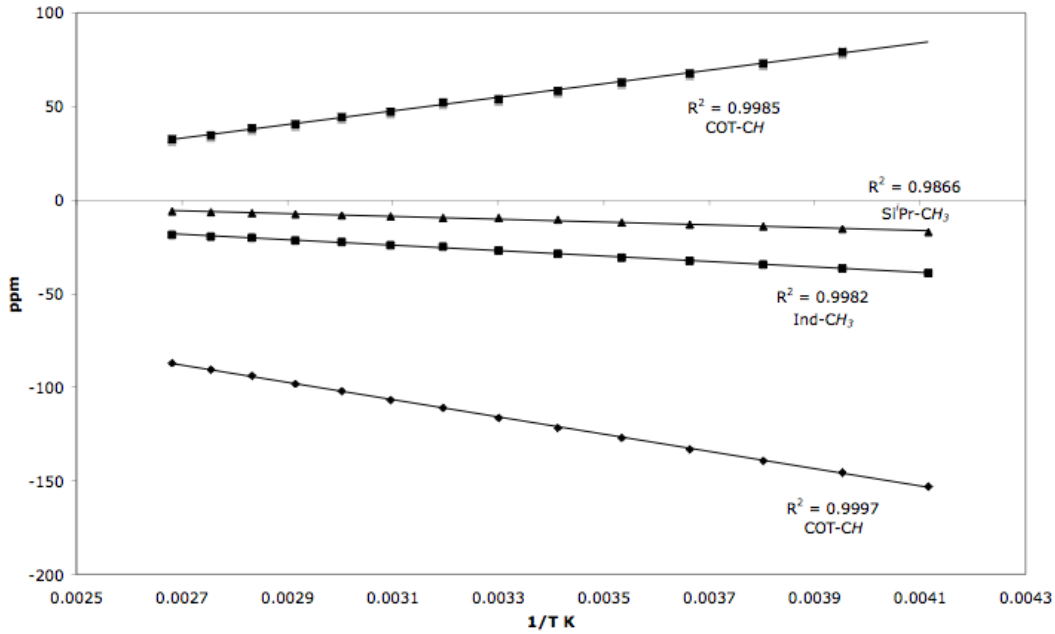

Figure 1: Plot showing the linear relationship between chemical shift and 1/T in **4.1.**

Crystals of **4.1** and **4.2** were grown from pentane and Et_2O, respectively, from slow-cooling of saturated solutions to -50 °C and their molecular structures were determined by single crystal x-ray diffraction. The complexes were found to be isomorphous, with a unit cell consisting of two independent molecules of essentially the same geometry.

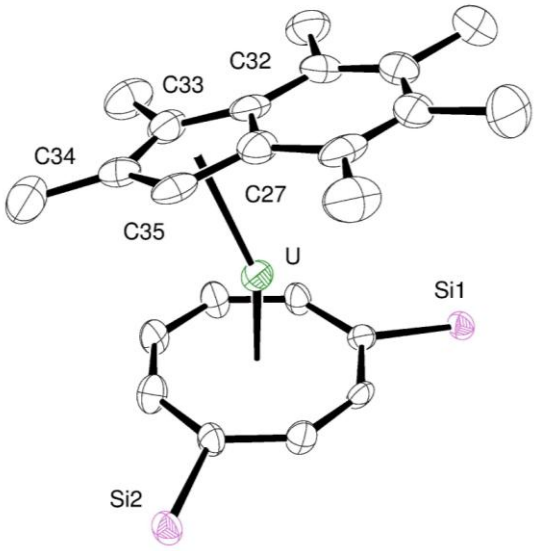

Figure 2: Structure(s) Molecular structure of [U(η^5-Ind^{Me6})(η^8-C_8H_6{Si^{i}Pr$_3$-1,4}$_2$)] (**4.1**), ellipsoids at 50 % probability, ^{i}Pr groups and H atoms, omitted for clarity.

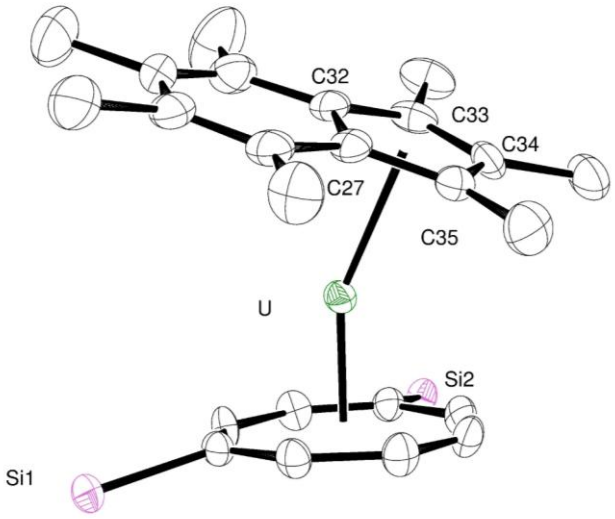

Figure 3: Structure(s) Molecular structure of [U(η^5-Ind^{Me7})(η^8-C_8H_6{Si^{i}Pr$_3$-1,4}$_2$)] (**4.2**), ellipsoids at 50 % probability, ^{i}Pr groups and H atoms, omitted for clarity.

Table 1: Selected bond distances (Å) and angles (°) for [U(η^5-Ind^{Me6})(η^8-C_8H_6{Si^{i}Pr$_3$-1,4}$_2$)] (**4.1**), and [U(η^5-Ind^{Me7})(η^8-C_8H_4{Si^{i}Pr$_3$-1,4}$_2$)] (**4.2**). M1 is the centroid of the [(C_8H_6{Si^{i}Pr$_3$-1,4}$_2$)]$^{2-}$ ring and M2 the centroid of the [η^5-Ind^R]$^-$ (R = Me_6, Me_7).

Parameter	**4.1**	**4.2**
U-M(1)	1.907(8)	1.917(16)
U-M(2)	2.459(8)	2.460(9)
U-C(27)	2.659(8)	2.705(5)
U-C(32)	2.688(8)	2.661(5)
U-C(33)	2.764(8)	2.753(5)
U-C(35)	2.753(8)	2.775(5)
U-C(34)	2.842(8)	2.814(5)
M1-U-M2	154.6(3)	154.3(4)

There is no direct structural comparison for complexes **4.1** and **4.2**, however, in the two related complexes [Pr(η^5-Ind)(η^8-C_8H_8)(THF)$_2$] and [Pr(η^5-Cp)(η^8-C_8H_8)(THF)$_2$], the Pr-C_8H_8 bond distance and angles were seen to be identical and the average Pr to ligand distances comparable, at 2.607 Å for Pr-Ind$_{ave}$ and 2.530 Å for Pr-Cp$_{ave}$.[18] Complexes **4.1** and **4.2** both display a bent sandwich structure in which the [C_8H_6{Si^{i}Pr$_3$-1,4}$_2$]$^{2-}$ and [Ind^{Me7}]$^-$ ligands exhibit η^5 (*vide infra*) and η^8 coordination modes, respectively. The U-M1 and U-M2 distances in **4.1** and **4.2** are essentially identical, as in also the case of the uranium(III) complexes [U(η^8-C_8H_6{Si^{i}Pr$_3$-1,4}$_2$)(η^5-Cp^{Me4H})(THF)] (**2.1)**

and [U(η^8-C_8H_6{Si^{i}Pr$_3$-1,4}$_2$)(η^5-Cp^{Me5})(THF)] (**2.2**). The U-M1 and U-M2 distances in **4.1** and **4.2** are slightly shorter than those found in the cyclopentadienyl mixed-sandwich complexes **2.1** and **2.2** (U-M1 1.977(5) Å and U-M2 2.506(6) Å in **2.1**).[31]

Unlike **2.1** and **2.2**, there is no THF coordinated to the uranium centre in **4.1** and **4.2** which are thus base-free, although the syntheses of the complexes are undertaken in THF. This may be a result of the increase in steric stabilisation imparted by the substituted indenyl ligands, *vs.* the cyclopentadienyl ligands and results in the increase in the M1-U-M2 angle from 141.8(2)° in **2.1**. The range of U-C(Ind) distances in **4.1** and **4.2** (2.659(8) - 2.842(8) Å) are comparable to those found in both the uranium(III) complex [U(η^5-Ind)$_3$][20] (2.73 – 2.85 Å) and the uranium (IV) complexes [U(η^5-Ind)$_3$Cl][19] (2.67 – 2.89 Å) and [U(η^5-Ind$^{1,4,7\text{-}Me3}$)$_3$Cl][29] (2.66 – 2.93 Å), with the oxidation state of the uranium or the substitution resulting in little change to the range of U-C(Ind) distances observed.

In sterically crowded complexes such as [U(η^5-Ind)$_3$Cl][19] the U-C(Ind) distances to the bridging carbons atoms (C27 and C32 in **4.1**) are longer than the U-C(Ind) distances to the wing-tip carbon atoms (C33 and C35 in **4.1**). This is not the case in complexes **4.1** and **4.2**. There are three parameters that are important in metal-indenyl bonding (Figure 4): the slip parameter, defined as the difference between the average U-C(bridgehead) and U-C(wingtip) ($\Delta_{M\text{-}C}$), the hinge angle (HA) and the fold angle (FA).[3,28 ,32] Most indenyl complexes display a small distortion in bonding.[33] An η^5 indenyl complex is defined as having an HA of less than 10° and a $\Delta_{M\text{-}C}$ of up to 0.25 Å,[3a] whereas an η^3

complex is defined as having an HA of 20-30° and a Δ_{M-C} of 0.69-0.8 Å.[34] The structural distortions in η^5 cyclopentadienyl complexes are smaller, a HA of less than 5° and a Δ_{M-C} of up to 0.15 Å,[3a] but similar in η^3 complexes, a HA of 20° and a Δ_{M-C} of 0.60 Å.[35]

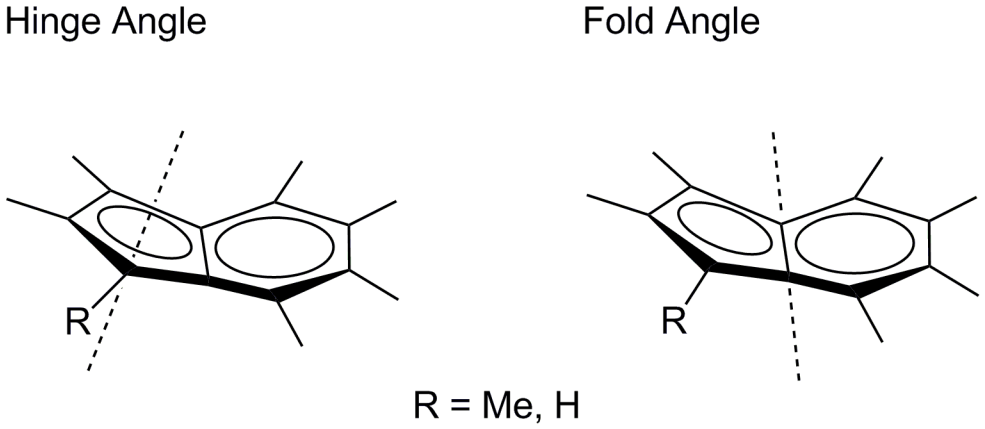

Figure 4: Distortion parameters in M-Ind bonding.

Table 2: Structural distortions in **4.1** and **4.2**.

Complex	Δ_{M-C}/Å	HA/°	FA/°
4.1	-0.09	2.8	2.8
4.2	-0.08	2.6	3.0

The structural distortions for complexes **4.1** and **4.2** are well within in the range of η^5-indenyl bonding and comparable to those found in the thorium complexes [Th(η^5-Ind^{Me7})$_2$$Me_2$] and [Th($\eta^5$-$Ind^{Me7}$)$_2$$Cl_2$] ($\Delta_{M-C}$ = 0.08, -0.06, HA = 2.8, 1.8 and FA = 4.2). The non-planarity of the Ind^{Me7} ligand, has been attributed to steric repulsion, in the case of the thorium complexes, between proximal methyl groups on the two Ind^{Me7} ligands[28] and in **4.1** and **4.2** between the Ind^{R} (R = Me_6, Me_7) and the bulky triisopropyl sily groups on the cyclooctatetraenyl ligand. A result of the molecular geometry is that substrate access to the uranium centre is increased, illustrated in Figure 5.

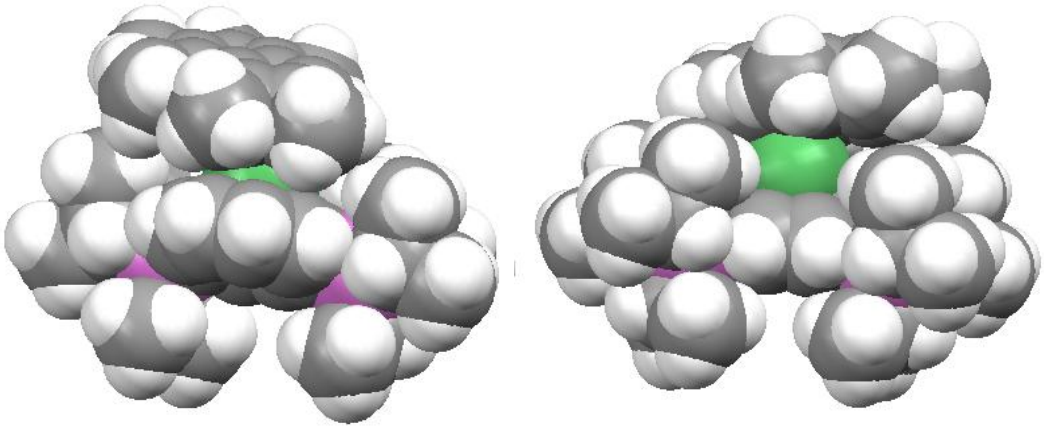

Figure 5: Spacefilling representations of **4.1** showing the access to the uranium centre from different sides of the complex.

*4.1.4 Electrochemistry of [U(η^5-Ind^R)(η^8-C_8H_6{Si^{i}Pr$_3$-1,4}$_2$)] (R = Me$_6$ (**4.1**), Me$_7$ (**4.2**)).*

Analytical electrochemical studies (cyclic voltammetry) were carried out on complexes **4.1** and **4.2** to determine their redox potentials and identify any electronic effects between the indenyl mixed-sandwich complexes and how they compare electronically to the cyclopentadienyl complexes. The potentials are shown in Table 3 and the cyclic voltammograms in Figure 7 and Figure 6. The studies were conducted by Dr R. J. Blagg of the University of Sussex/NNL and details of the experimental set-up are given in Appendix One.

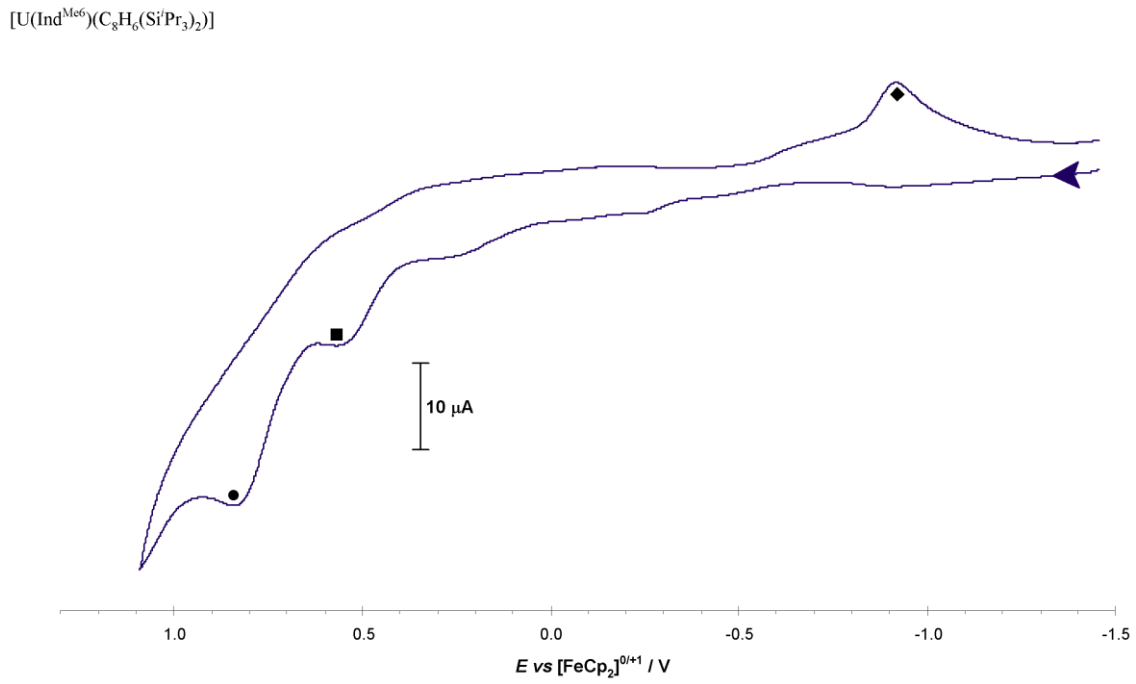

Figure 6: Cyclic Voltammogram of [U(η^5-Ind^{Me6})(η^8-C_8H_4{Si^{i}Pr$_3$-1,4}$_2$)] (**4.1**), showing the irreversible oxidation wave and the by-product reduction wave.

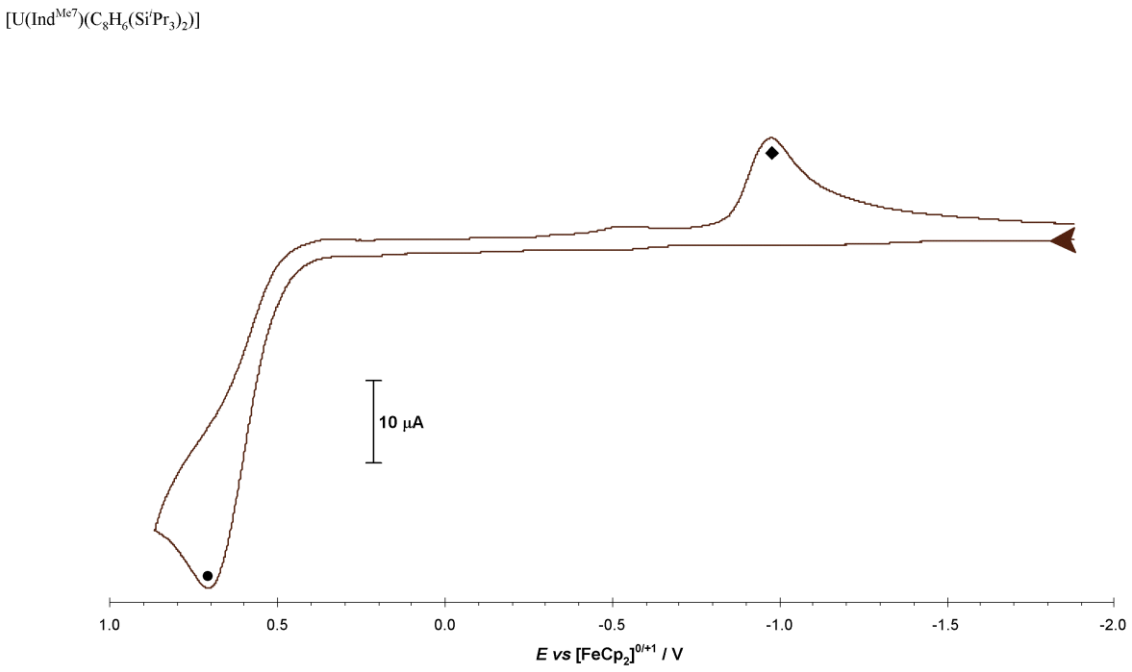

Figure 7: Cyclic Voltammogram of [U(η^5-Ind^{Me7})(η^8-C_8H_4{Si^{i}Pr$_3$-1,4}$_2$)] (**4.2**), showing the irreversible oxidation wave and the by-product reduction wave.

Table 3: Electrochemical data for uranium(III) mixed-sandwich complexes [U(η^8-C_8H_6{Si^{i}Pr$_3$-1,4}$_2$)(η^5-Cp^{Me4H})(THF)] (**2.1**), [U(η^8-C_8H_6{Si^{i}Pr$_3$-1,4}$_2$)(η^5-Cp^{Me5})(THF)] (**2.2**), [U(η^5-Ind^{Me6})(η^8-C_8H_6{Si^{i}Pr$_3$-1,4}$_2$)] (**4.1**) and [U(η^5-Ind^{Me7})(η^8-C_8H_4{Si^{i}Pr$_3$-1,4}$_2$)] (**4.2**).

Complex	E_p(ox) {U}/V	E_p(red) {U'}/V
2.1	+0.65	-
2.2	+0.62	-0.80
4.1	+0.84	-0.88
4.2	+0.71	-0.87

The one electron U^{III}/U^{IV} oxidation is observed as an irreversible wave at +0.84 V in **4.1** and +0.71 V in **4.2** *vs.* ferrocene. The irreversibility of the oxidation wave indicates that the oxidised but structurally similar uranium(IV) species are not stable on the electrochemical timescale (*ca.* 1 sec.).[36] The reduction waves in **4.1** and **4.2** at -0.88 V and -0.87 V, respectively, *vs.* ferrocene are due to a unknown single product from the decomposition of the U(IV) species generated, which is both redox active and stable on a timescale of *ca.* 10 sec.

The lower the value for the oxidation potential of the uranium(III) species, the stronger a reducing agent it is,[37] but as the reduction potential was not observed it is not possible to compare it with the literature values for the U(IV)/U(III) redox couple.[38,39] Electrochemical studies on uranium(III) complexes are not numerous and the oxidation potentials observed vary greatly. The complexes, $[U(\eta^5\text{-}Cp^{Me5})_2Cl(THF)]$ and $[U(\eta^5\text{-}Cp)_3(THF)]$ display irreversible oxidations at -0.71 V[40] and +0.32 V,[41] respectively; the irreversibility is attributed to the reactivity of the coordinatively unsaturated cation. Whereas the cyclic voltammogram of $[U(OAr)_3]$ (OAr = 2,6-di-*tert*-butylphenoxide) shows a reversible one-electron oxidation of $[U(OAr)_3]$ with a $E_{1/2}$ of -1.22 V.[42] It should also be mentioned that in the electrochemical study of U(IV) cyclopentadienyl complexes,[39] all complexes exhibited irreversible oxidative processes at potentials greater than +0.5 V *vs.* ferrocene, which were attributed to cyclopentadienyl-localised processes.[43]

The ease of reduction across the series of U(IV) complexes, $[U(\eta^5\text{-}Cp^R)_3Cl]$ ($R = SiMe_3 < H < C(CH_3)_3 < CH_3$)[44] was found to approximate to the electron donating ability of

the Cp^{R-} ligand, except for the reversal of the positions of the H and $C(CH_3)_3$ groups. In complexes **2.1** and **2.2** the change in substitution appears to have no significant effect on the oxidation potential. However, the oxidation potentials of **4.1** (+0.84 V) and **4.2** (+0.71 V) are significantly different and this may result from substitution in the 1/3 position of the indenyl ligand, for which sigma effects have been found to be large and generally additive. Substitution in the 1/3 position has been seen to cause a 97 mV decrease in oxidation potential per methyl group per indenyl ligand per ferrocene in Fe(II) indenyl complexes.[45]

Complexes **2.1** and **2.2** are easier to oxidise and therefore are stronger reducing agents than **4.1** and **4.2**. The greater stability of the trivalent state of the uranium centre in complexes **4.1** and **4.2** in comparison to complexes **2.1** and **2.2** may result from the electronic differences between the ligands. In general the bonding in indenyl transition metal complexes[46] will approximate to the bonding in transition metal cyclopentadienyl complexes.[47] However, the coordination of the ligands to a metal centre differs as a result of the nodal properties of their respective π orbitals. In the indenyl complexes, π-overlap is decreased as symmetric overlap is prevented, resulting in longer M-C distances to the bridgehead.[48] The indenyl ligand is a better σ-donor than the cyclopentadienyl ligand in the d^6 complexes: $[M(\eta^5\text{-Ind})_2]$, $[M(\eta^5\text{-}Cp^R)_2]$ (M = Ru, Fe, R = H, Me) but a weaker donor than Cp^{Me5} ligand.[46] When $[M(\eta^5\text{-}Cp^{Me5})_2]$ (M = Fe, Co) were compared to $[M(\eta^5\text{-}Ind^{Me7})_2]$ (M = Fe, Co) the permethylated indenyl ligand was found to be more electron donating than Cp^{Me5} in the iron complex but less in the cobalt complex.[23]

4.2 Reactivity of [U(η^5-Ind^R)(η^8-C_8H_6{Si^{i}Pr$_3$-1,4}$_2$)] (R = Me$_6$, Me$_7$) with small molecules.

4.2.1 Introduction:

The reactivity of the cyclopentadienyl mixed-sandwich complexes of uranium(III) has been discussed in Chapters One[49] and Two and contrasted with the reactivity of the trispyrazolylborate half-sandwich complexes in Chapter Three. The syntheses of **4.1** and **4.2** and their structural and electronic differences to complexes **2.1** and **2.2** have been established in Section 4.1. The reactivity of **4.1** and **4.2** with CO and CO_2 is investigated in this Section.

*4.2.2 Reactivity of [U(η^5-Ind^{Me6})(η^8-C_8H_6{Si^{i}Pr$_3$-1,4}$_2$)] (**4.1**) with ^{13}CO:*

Exposure of a degassed solution of **4.1** in d_8-toluene at - 78 °C to *ca.* 4.7 equivalents of ^{13}CO *via* the Toepler line and subsequent warming to ambient temperature with shaking resulted in a colour change from red to a brown and the appearance of two ^{13}C-labelled product resonances at δ 272.3 and – 63.5 ppm in the ^{13}C{^{1}H} NMR spectrum. The spectrum is shown in Figure 8. It is notable that there is no free ^{13}CO present in solution (δ 186 ppm in d_8-toluene).[50] Further addition of ^{13}CO to the reaction did not result in a further reaction by ^{13}C{^{1}H} NMR spectroscopy.

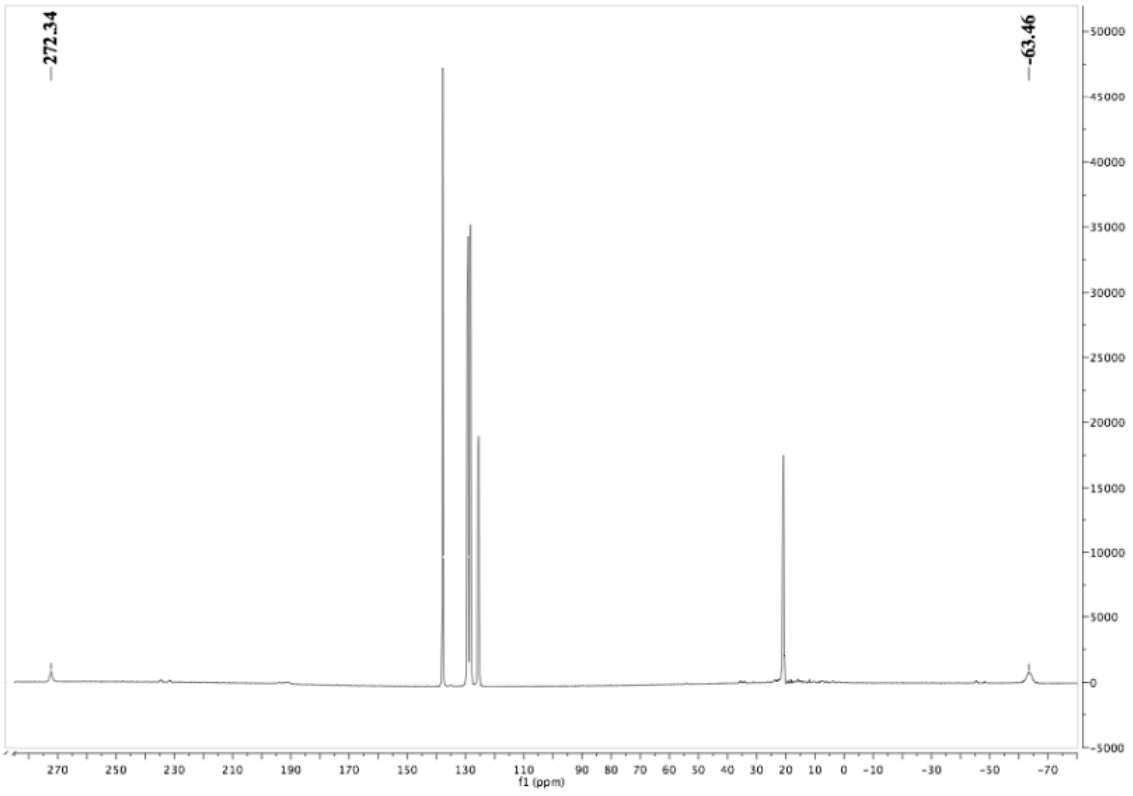

Figure 8: $^{13}C\{^{1}H\}$ NMR spectrum (150 MHz, d_8-toluene, 298 K) of the NMR scale reaction of **4.1** with 4.7 ^{13}CO

The difference in chemical shift between the product resonances (335 ppm) is large, but is similar to the 339 ppm difference in chemical shift between the labelled deltate and squarate complexes in d_8-thf, $[(U(\eta^8\text{-}C_8H_6\{Si^iPr_3\text{-}1,4\}_2)(\eta^5\text{-}Cp^{Me5}))_2(\mu\text{-}\eta^1\text{:}\eta^2\text{-}^{13}C_3O_3)]$ at 225 ppm and $[(U(\eta^8\text{-}C_8H_6\{Si^iPr_3\text{-}1,4\}_2)(\eta^5\text{-}Cp^{Me4H}))_2(\mu\text{-}\eta^2\text{:}\eta^2\text{-}^{13}C_4O_4)]$ – 111.4 ppm.[31] The resolution of the resonances was improved on by running the sample at a lower magnetic field (Figure 9). The reduction in the observed anisotropic effect is in agreement with the formation of aromatic products, such as the oxocarbon dianions. The spectrometers are set at different temperatures, which accounts for the difference in chemical shifts between the spectra in Figure 9. The two resonances have different line-

widths, $\nu_{1/2}$ 35 Hz for the resonances at 270 ppm and 80 Hz for the resonances at -58 ppm and are shifted by different amounts with temperature, 2.4 ppm for the resonances at 270 ppm and 5.4 ppm for the resonances at -58 ppm.

Unlike the resonances for the uranium-bound ^{13}C-labelled oxocarbons, the product resonances from the reaction of **4.1** with ^{13}CO possess multiplicity. This inequivalence may result from restricted rotation in a dimeric species or from different isomers of the product, resulting in resonances which are very similar in chemical shift. NMR experiments designed to determine the origins of the multiplicity proved inconclusive. A VT NMR experiment was undertaken and the multiplicity of the resonance at low frequency was not resolved by 80 °C, however, the composition of the sample was altered at high temperature.

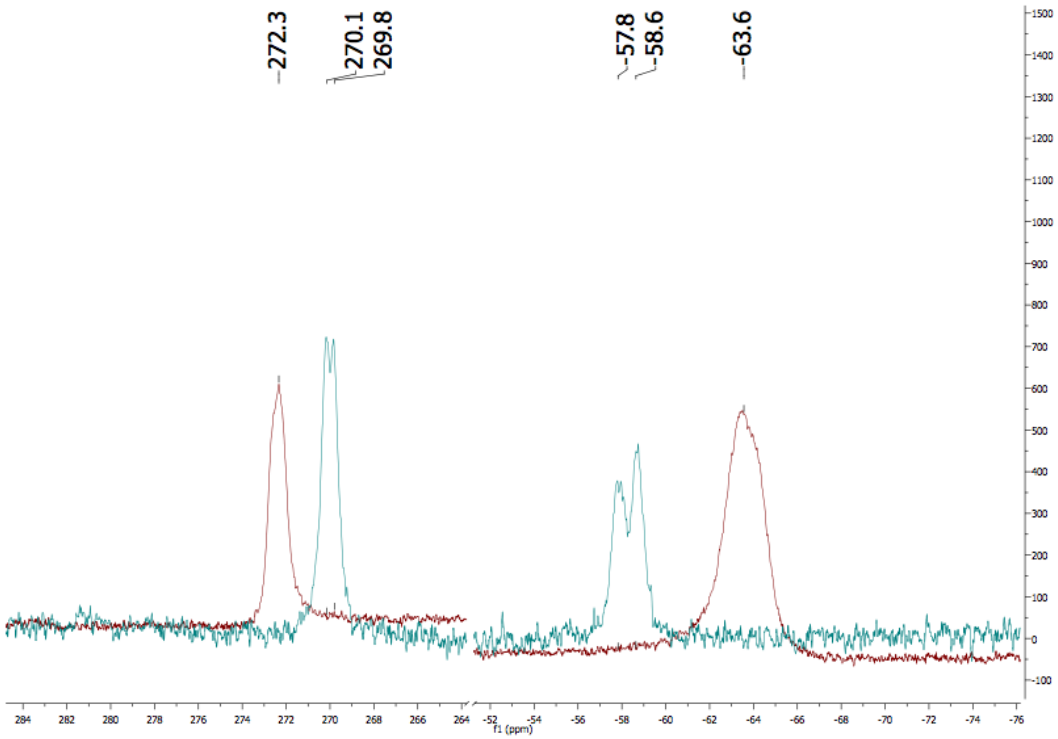

Figure 9: $^{13}C\{^{1}H\}$ NMR spectra of the ^{13}C-labelled products of the reaction of **4.1** with ^{13}CO. Red spectrum = 150 MHz, d_8-toluene, 298 K; green spectrum = 100 MHz, d_8-toluene, 303 K.

When the reaction between **4.1** and *ca.* 4.4 equivalents of ^{13}CO was repeated under approximately the same conditions a different result was obtained. The manner of addition and pressure of gas were constant between the reactions, the only difference was in the amount of shaking of the NMR tube. Instead of the mixture of ^{13}C-labelled products *vide supra*, the ^{13}C-labelled product at δ – 58 ppm and free ^{13}CO at 186 ppm were observed by $^{13}C\{^{1}H\}$ NMR. Extreme sensitivity to reaction conditions, be it temperature or reaction time or shaking/stirring has been previously noted during a study into the mechanism of the deltate formation.[51]

The reaction of **4.1** with a sub-stochiometric amount of ^{13}CO (0.5 equivalents) was found to yield the two ^{13}C-labelled product resonances at δ 270 and – 58 ppm, reproducibly by $^{13}C\{^{1}H\}$ NMR. It is also of note that the products are visible within 4 hours of the addition of ^{13}CO gas to **4.1**. This suggests that the energetic barrier to reaction for either species is low and VT NMR studies of the reaction of **4.1** with ^{13}CO at low-temperature would be useful.

Complex **4.1** was reacted with 0.5 equivalents of a 50/50 mixture of $^{12}CO/^{13}CO$, in the hope of observing a secondary isotopic shift by $^{13}C\{^{1}H\}$ NMR, indicative of carbon-carbon bond formation,[52] however, no new ^{13}C resonances were seen over the course of the experiment by $^{13}C\{^{1}H\}$ NMR. This is perhaps because of the sub-stochiometric amount of only partially labelled gas added or the formation of a number of isotopic species, preventing their observation over the timescale of the NMR experiment (18000 scans, *ca.* 11 hrs).

Another approach considered was to identify the products of the reaction of **4.1** with ^{13}CO by removing them from the uranium centre, particularly as the delate and squarate oxocarbon complexes were shown to have different reactivities with organic halides and the silyl functionalised squarate products exhibit a distinctive second order $^{13}C\{^{1}H\}$ spectrum (see Section 2.2). An NMR scale reaction of **4.1** with 0.5 ^{13}CO, containing the two ^{13}C-labelled ^{13}CO products, was reacted with excess Ph_3SiCl. The colour of the solution changed from brown to orange. The resonances at 270 ppm remained unchanged but the resonances at -58 ppm were seen to disappear over the course of 6

days, which implies they are distinct species. Nothing was observed in the 180-200 ppm region for $C_2O_2(OSiR_2)$ species.[53]

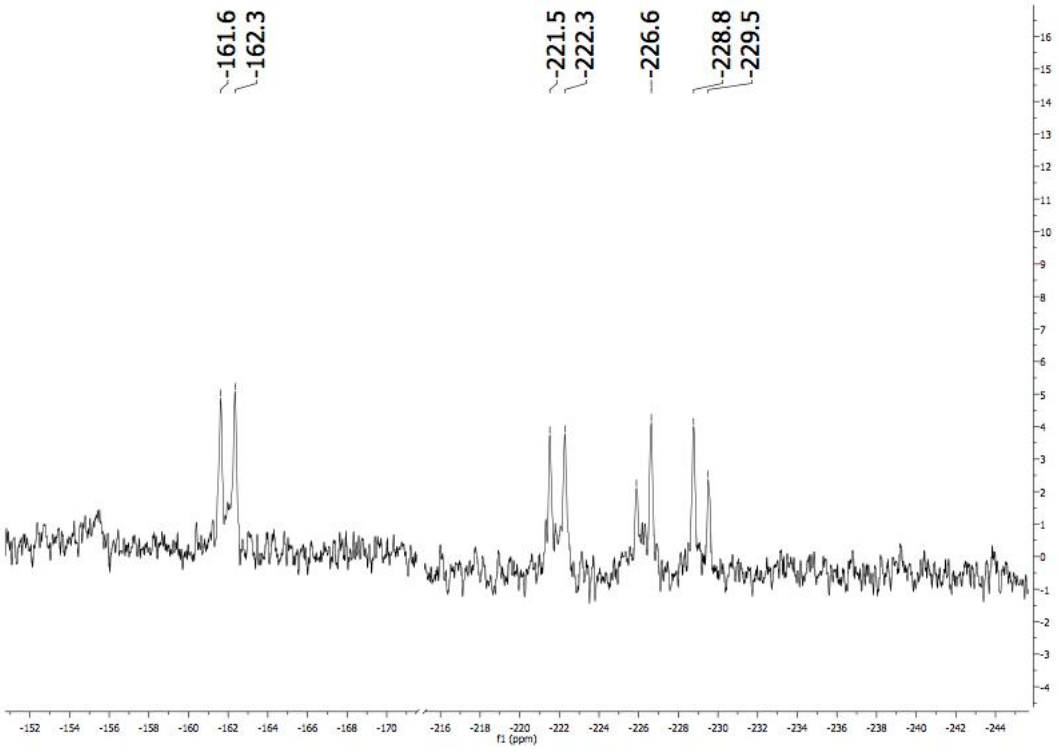

Figure 10: $^{13}C\{^1H\}$ NMR spectrum (100 MHz, d_8-toluene, 303 K, selected data) of the quenching of the NMR scale reaction of **4.1** with 0.5 ^{13}CO with excess $SiPh_3Cl$.

Instead, the disappearance of the resonances at -58 ppm was accompanied by the appearance of two apparent doublets centred at -161.9 and -221.9 and doublet of doublets centred at -228 ppm in the $^{13}C\{^1H\}$ spectrum shown above. The $^{29}Si\{^1H\}$ spectrum of the reaction mixture after 6 days displays five resonances between -80 and -136 ppm, the chemical shifts are consistent with being uranium-bound. The very low frequency of these new resonances is interesting as it is suggests that the product(s) of this reaction are uranium bound. The NMR data suggests that at least partial silylation

of the ^{13}CO reaction product at -58 ppm has taken place. It is unclear from the $^{13}C\{^{1}H\}$ NMR data whether the ^{13}CO product unit remains intact or whether the spectrum could arise from a ring-opening reaction. If any such products could be isolated, they might provide insight into the mechanism of removing the ^{13}CO product from the uranium centre.

*4.2.3 Synthesis of [(U(η⁵-Ind^{Me6})(η⁸-C₈H₆{Si^{i}Pr₃-1,4}₂))₂(μ-η²:η²-C₄O₄)] (**4.3**).*

A dark red solution of [U(η^5-Ind^{Me6})(η^8-C_8H_6{Si^{i}Pr$_3$-1,4}$_2$)] (**4.1**) in toluene was cooled to -78 °C, degassed and exposed to an overpressure of CO (5 psi). The reaction vessel was allowed to warm to room temperature slowly and volatiles were removed *in vacuo*, yielding a sticky red solid. Crystals suitable single crystal X-ray diffraction were grown by cooling a saturated pentane solution at -50 °C over several weeks. There was insufficient crystalline material for further characterisation. The structure was revealed as [(U(η^5-Ind^{Me6})(η^8-C_8H_6{Si^{i}Pr$_3$-1,4}$_2$))$_2$(μ-η^2:η^2-C_4O_4)] (**4.3**), shown in Figure 11. Selected structural parameters are presented in Table 4.

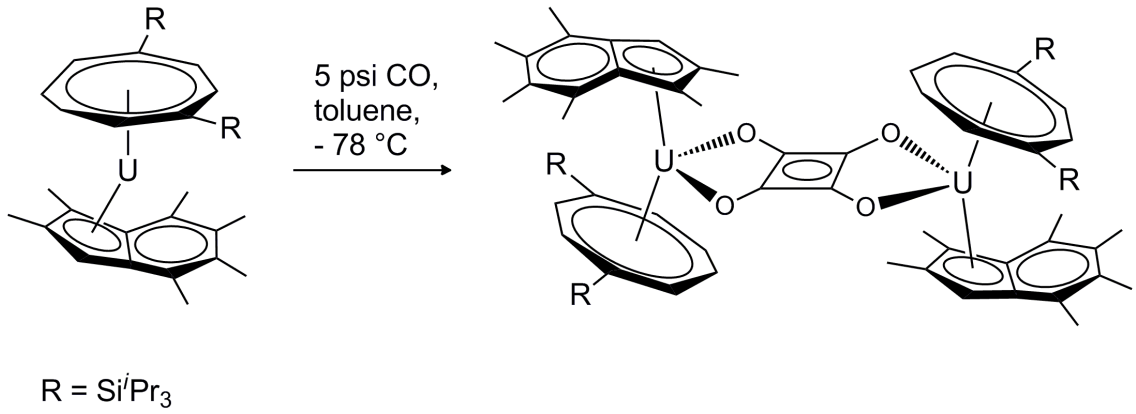

Scheme 2: Synthesis of [(U(η^5-Ind^{Me6})(η^8-C_8H_6{Si^{i}Pr$_3$-1,4}$_2$))$_2$(μ-η^2:η^2-C_4O_4)] (**4.3**).

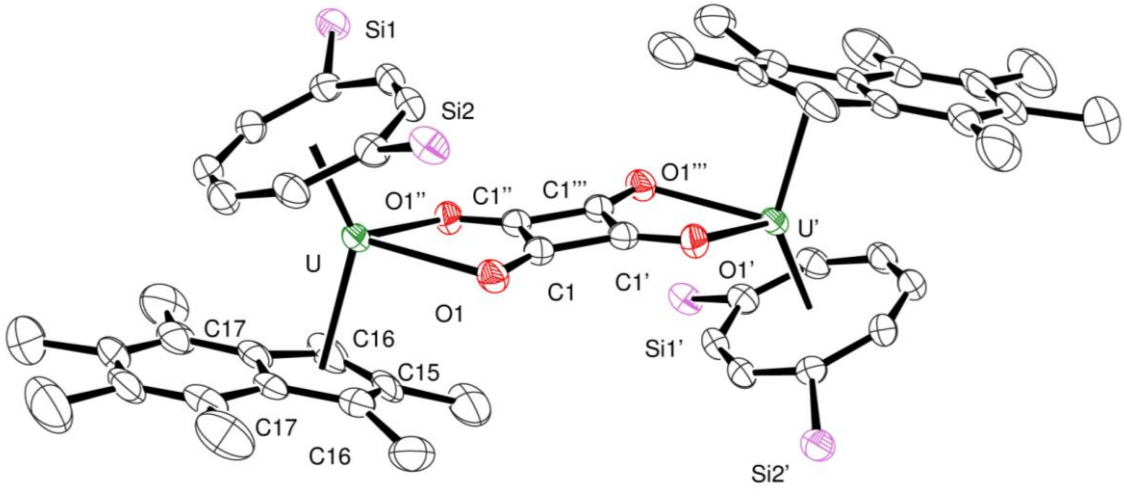

Figure 11: Molecular structure of [(U(η^5-Ind^{Me6})(η^8-C_8H_6{Si^{i}Pr$_3$-1,4}$_2$))$_2$(μ-η^2:η^2-C_4O_4)] (**4.3**) There is 50:50 Me/H occupancy at the C(16) position.

Table 4: Selected bond distances (Å) and angles (°) for [(U(η^5-Ind^{Me6})(η^8-C_8H_6{Si^{i}Pr$_3$-1,4}$_2$))$_2$(μ-η^2:η^2-C_4O_4)] (**4.3**). M1 is the centroid of the [(C_8H_6{Si^{i}Pr$_3$-1,4}$_2$)]$^{2-}$ ring and M2 the centroid of the [η^5-Ind^{Me6}]$^-$.

Parameter	**4.3**
U-M(1)	1.9475(5)
U-M(2)	2.496(5)
U-O(1)	2.472(3)
U-C(17)	2.820(5)
U-C(16)	2.730(5)
U-C(15)	2.758(5)
O(1)-C(1)	1.259(5)
C(1)-C(1)’	1.472(9)
C(1)-C(1)’’	1.442(9)
M(1)-U-M(2)	141.8(1)
O(1)-U-O(1)’’	73.87(14)
C(1)-O(1)-U	104.5(3)
O(1)-C(1)-C(1)’’	127.4(3)
O(1)-C(1)-C(1)’	142.6(3)
C(1)’’-C(1)-C(1)’	90.0

There is no significant lengthening of uranium-ligand bonding distances in **4.3**, either to the $[(C_8H_6\{Si^iPr_3\text{-}1,4\}_2)]^{2-}$ or the $[\eta^5\text{-}Ind^{Me6}]^-$ ligands, from those in **4.1**. That the oxidation of U(III) to U(IV) is not necessarily reflected in the bonding parameters, has been seen in the uranium(IV) oxocarbon complexes[49,52] and in the dinitrogen complex $[(U(\eta\text{-}C_8H_4\{Si^iPr_3\text{-}1,4\}_2)(\eta\text{-}Cp^{Me5}))_2(\mu\text{-}\eta^2\text{:}\eta^2\text{-}N_2)]$.[54] The bond lengths and angles of the U-C_4O_4-U core are directly comparable to those found in $[(U(\eta^8\text{-}C_8H_6\{Si^iPr_3\text{-}1,4\}_2)(\eta^5\text{-}Cp^{Me4H}))_2(\mu\text{-}\eta^2\text{:}\eta^2\text{-}C_4O_4)]$.[49b]

The structural distortions to the bonding of the indenyl ligand in **4.3** are more pronounced than in **4.1**. The U-C(16) distance is shorter than the U-C(17) distance to the bridging carbon atoms but the ring slip of $\Delta_{M\text{-}C}$ = 0.09 Å is well-within the $\Delta_{M\text{-}C}$ of up to 0.25 Å observed for η^5 complexes,[3a] though larger than the $\Delta_{M\text{-}C}$ = -0.09 Å in **4.1**. The disparity in U-C lengths, though not significant in terms of hapticity, does indicate the level of steric crowding in **4.3**. This is also seen in the increase of the hinge angle (HA) of 6.2° and the fold angle (FA) of 6.6° in **4.3** from those found in **4.1** (2.8°). The methyl substituents on the η^5-indenyl are inclined away above the plane of the ring by 4.2° in **4.3**, as defined by the angle between the plane of the ring and the plane of the three (due to the disorder) methyl carbons, this is greater than the 2.6° displacement seen in **4.2**.

This is a valuable result as it demonstrates that the reductive coupling of CO is not limited to the Cp-containing mixed-sandwich complexes of uranium(III). It is also likely that **4.3** corresponds to the product of the reaction of **4.1** with ^{13}CO that appears

in the $^{13}C\{^{1}H\}$ NMR at δ – 58 ppm on the basis of its chemical shift. Unfortunately further characterisation was not achieved within the timeframe of this work. The synthesis of **4.3** and multiple products from the reaction of **4.1** with CO suggest that complex **4.1** is a strong candidate for further research as it might prove possible to gain mechanistic and/or kinetic insight into the factors affecting product formation. This is an interesting point because the selectivity of formation of either the squarate complex from $[U(\eta^8\text{-}C_8H_6\{Si^iPr_3\text{-}1,4\}_2)(\eta^5\text{-}Cp^R)(THF)]$ where R = Me_4H and the deltate complex where R = Me_5, is thought to be a direct result of steric constraints in the proposed Zig-Zag intermediate[52] (see *Section 1.2.2*). However, the increased stability of the η^3-indenyl ligand, relative to the Cp ligand, might enable alternative pathways.

*4.2.4 Reactivity of [U(η⁵-Ind^Me7)(η⁸-C₈H₄{Si^iPr₃-1,4}₂)] (**4.2**) with CO.*

Complex $[U(\eta^5\text{-}Ind^{Me7})(\eta^8\text{-}C_8H_6\{Si^iPr_3\text{-}1,4\}_2)]$ (**4.2**) in d_8-toluene was cooled to -78 °C, degassed and ^{13}CO (*ca.* 2 equivalents) was added *via* the Toepler line. After addition of the gas, the colour of the solution was observed to darken from red to brown. The tube was warmed to room temperature overnight. The ^{1}H NMR spectrum of the reaction mixture was found to display the same number and ratios of ligand resonances as seen in **4.2** but with a significant difference in chemical shift, the spectra are overlaid in Figure 12. The indenyl ligands resonances in the ^{1}H NMR spectrum of the reaction mixture are also significantly broadened, over double the line-width at half-height, in comparison to those in **4.2**. The observed difference in chemical shift and broadening could be the result of an exchange process, between **4.2** and the product of the reaction of ^{13}CO, for example a carbonyl species.

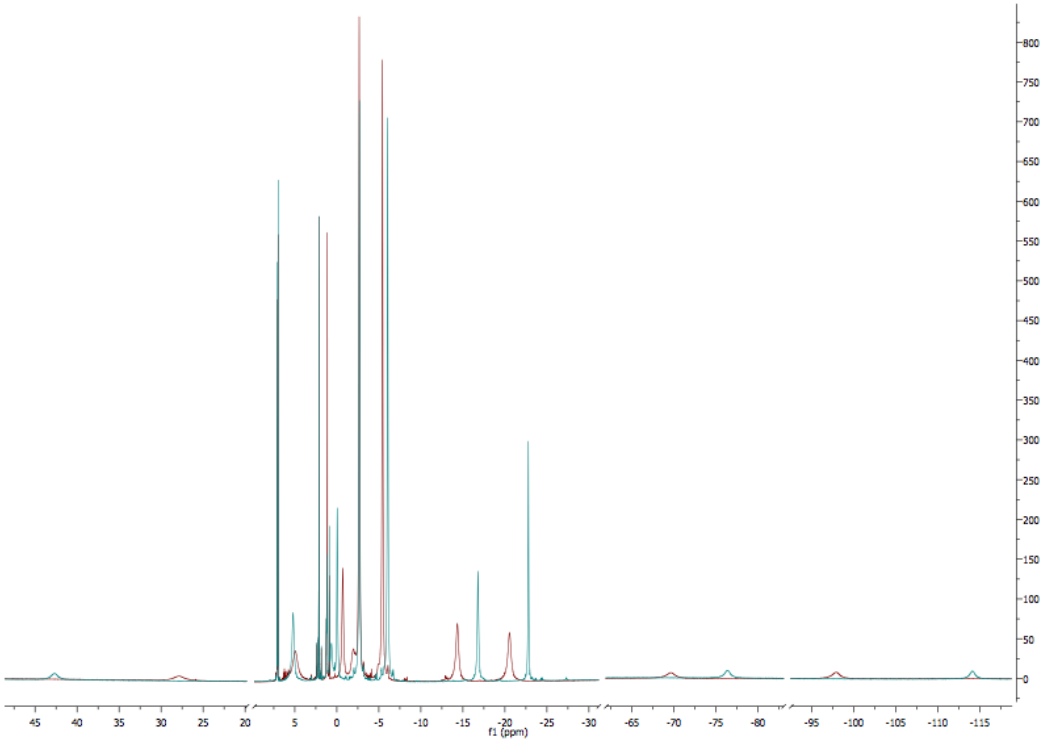

Figure 12: ^{1}H NMR (100 MHz, d_8-toluene, 303 K) of **4.2** (green) and the reaction of **4.2** with ^{13}CO (*ca.* 2 equivalents) (red).

The ^{13}C{^{1}H} NMR spectrum of the reaction of **4.2** with ^{13}CO showed neither a labelled product or free ^{13}CO after 24 hours but after a week a single ^{13}C-labelled product resonance was observed at δ 395 ppm (Figure 13). Further addition of ^{13}CO to the reaction mixture did not result in a further reaction by ^{13}C{^{1}H} NMR. The ^{1}H NMR spectrum associated with the δ 395 ppm product was observed to be distinct from either **4.2** or the initial ^{1}H spectrum on coordination of ^{13}CO. The resonances associated with the $[C_8H_6\{Si^iPr_3\text{-}1,4\}_2]^{2-}$ ligand are consistent with a single Si^iPr_3 environment rendered

by mirror plane symmetry but the Ind-CH_3 are no longer symmetry equivalent, perhaps indicative of restricted rotation or a dimeric structure in solution. It is also of note that while four of the Ind-CH_3 resonances appear as sharp singlets, the other three are significantly broadened. However, in the absence of structural characterisation or VT NMR studies, it would be premature to speculate about the hapticity of the indenyl ligand in this complex or possible fluxionality in solution. No dimeric parent ion was observed by mass spectrometry of the crude reaction mixture and the only crystalline material isolated from the reaction was determined by X-ray crystallography to be **4.2**.

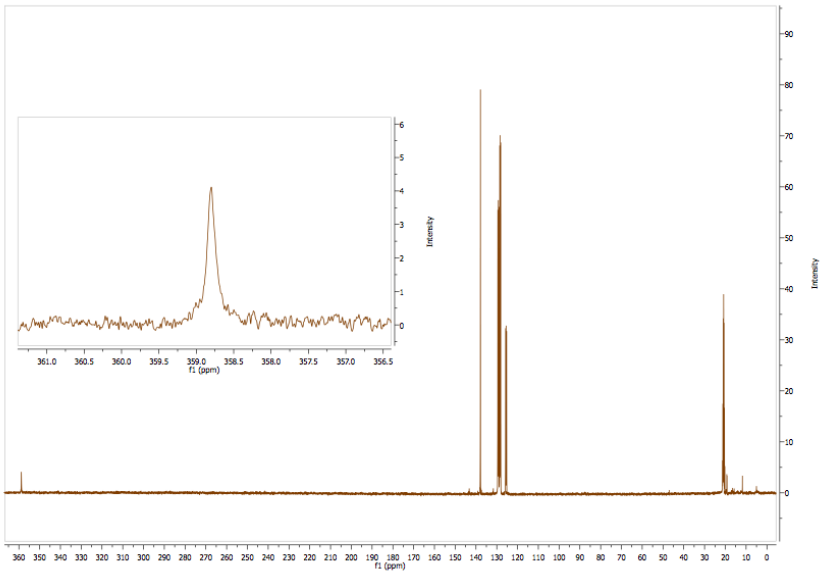

Figure 13: $^{13}C\{^{1}H\}$ NMR (100 MHz, d_8-toluene, 303 K) after a week of the reaction of **4.2** with ^{13}CO (*ca.* 2 equivalents), showing the product at δ 395 ppm.

The $^{13}C\{^{1}H\}$ chemical shift of the product of the reaction of **4.2** with ^{13}CO, (δ 395 ppm in d_8-toluene at room temperature) is at a higher frequency than either the products of the reaction of **4.1** with ^{13}CO or the uranium oxocarbon complexes,[49] the closest to it in

chemical shift is the ynediolate complex, $[U(\eta^8\text{-}C_8H_6\{Si^iPr_3\text{-}1,4\}_2)(\eta^5\text{-}Cp^{Me5})]_2[(\mu\text{-}\eta^1\text{:}\eta^1\text{-}^{13}C_2O_2)]$[52] at δ 313 ppm in d_8-toluene at room temperature. The ynediolate complex is the thermodynamic product of the reaction of $[U(\eta^8\text{-}C_8H_6\{Si^iPr_3\text{-}1,4\}_2)(\eta^5\text{-}Cp^{Me5})]$ with 0.9 equivalents of CO, which proceeds *via* the short-lived $[U(\eta^8\text{-}C_8H_6\{Si^iPr_3\text{-}1,4\}_2)(\eta^5\text{-}Cp^{Me5})(CO)]$ species, as observed by IR only. None of the known uranium(III) carbonyls has been observed by $^{13}C\{^1H\}$ NMR.[55,56] The ^1H NMR observation of an initial product, on coordination of ^{13}CO to **4.2**, which is $^{13}C\{^1H\}$ silent and then reacts further over time to form a second product with a very high frequency in the $^{13}C\{^1H\}$ NMR are suggestive of a similar reactivity of **4.2** with ^{13}CO to that described for the formation of the ynediolate complex.

The initial coordination of CO to **4.2** was found to be reversible, on exposure to vacuum or if not maintained under a positive pressure of ^{13}CO by ^1H NMR, IR and X-ray crystallography. The product resonance observed at δ 395 ppm by $^{13}C\{^1H\}$ NMR is stable once formed but the amount of time required for its formation at room temperature is not known. It was subsequently discovered, from the reaction of **4.2** with a 50/50 mixture of $^{12}CO/^{13}CO$, that the addition of a sub-stoichiometric amount of CO gas, *ca.* 0.7 equivalents in this case, does not result in a reaction by ^1H and $^{13}C\{^1H\}$ NMR.

Other work in our laboratory has shown that although the complex $[U(\eta^8\text{-}C_8H_6\{Si^iPr_3\text{-}1,4\}_2)(\eta^5\text{-}Cp^{Me5})]_2[(\mu\text{-}\eta^1\text{:}\eta^1\text{-}^{13}C_2O_2)]$ displays no reactivity towards H_2, it is possible to functionalise the $C_2O_2^{2-}$ unit. The reaction of $[U(\eta^8\text{-}C_8H_6\{Si^iPr_3\text{-}1,4\}_2)(\eta^5\text{-}Cp^{Me5})]$ in

d_8- toluene at -78 °C, with 1 equivalent of ^{13}CO, followed by the addition of 1.5 equivalents of H_2 resulted in the isolation of the uranium methoxide complex [U(η^8-C_8H_6{Si^{i}Pr$_3$-1,4}$_2$)(η^5-Cp^{Me5})(OMe)],[57] readily resolved as a quartet by ^{13}C NMR. However, when complex **4.2** was reacted under analogous conditions, there was no evidence of methoxide formation by $^{13}C\{^1H\}$ or ^{13}C NMR. This result and the reversibility of the initial coordination of the CO to **4.2** indicate that the mechanism of the reaction of **4.2** differs from that proposed for the reaction of [U(η^8-C_8H_6{Si^{i}Pr$_3$-1,4}$_2$)(η^5-Cp^{Me5})] with either CO or CO/H_2. The steric bulk in **4.2** and the higher oxidation potential observed may mean that reduction of the CO and the formation of a dimeric product are energetically less favourable in the case of **4.2** than either **4.1** or the uranium(III) cyclopentadienyl mixed-sandwich complexes.

The [U(η^8-C_8H_6{Si^{i}Pr$_3$-1,4}$_2$)(η^5-Cp^{Me5})(CO)] species was observed by IR by quickly transferring the reaction mixture to a high-integrity solution IR cell.[52] In the case of the reaction of **4.2** with ^{13}CO, perhaps because of the reversibility of the reaction, this technique did not result in the observation of a carbonyl species. The reaction of **4.2** with 2.5 equivalents of ^{13}CO at -50 ºC in methylcyclohexane was monitored by *in situ* IR spectroscopy, using a React IR™ instrument, and selected spectra are shown below.

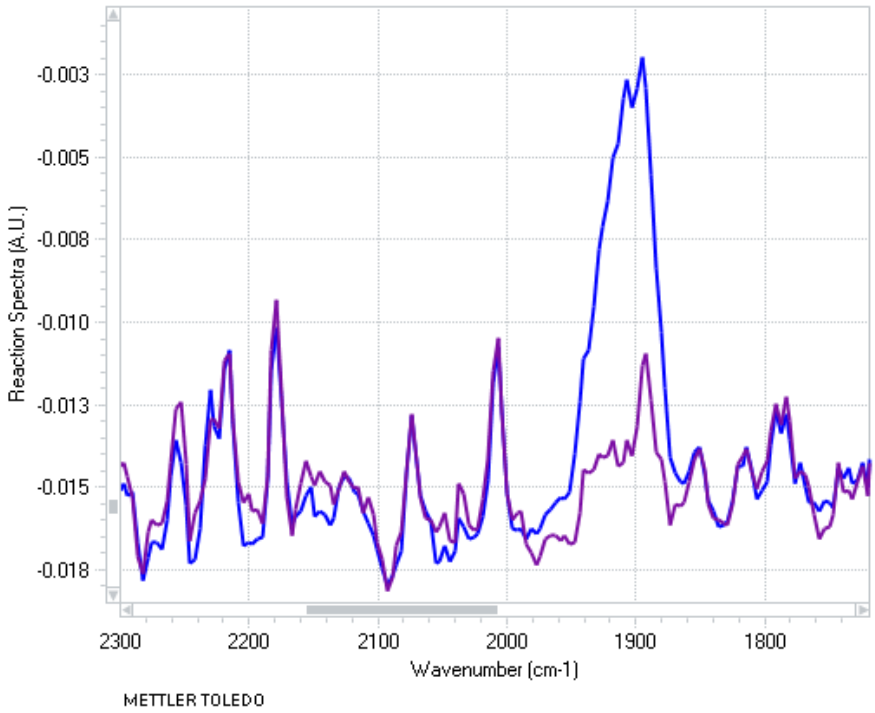

Figure 14: FTIR spectra of the reaction of **4.2** with 2.5 equivalents of ^{13}CO in methylcyclohexane at -50 ºC: before (purple) and after (blue) the addition of ^{13}CO.

The absorption at 1905 cm^{-1} is consistent with the low-temperature binding of CO to form [U(η^5-Ind^{Me7})(η^8-C_8H_6{Si^iPr_3-1,4}$_2$)(^{13}CO)] (**4.4**) and is in the range (1880 - 1976 cm^{-1}) associated with uranium(III) monocarbonyls.[55,56] There was no evidence of free ^{13}CO in solution. The assignment was confirmed by the shift to 1945 cm^{-1} on the addition of ^{12}CO. The isotopic shift is in agreement with that predicted by theory.[58]

That the reaction between **4.2** and CO at low temperature is best described as an equilibrium is illustrated in Figure 15, which shows the shift to higher wavenumbers on the addition of excess ^{12}CO. Complex **4.4** was seen to be long-lived as the absorption at 1905 cm^{-1} was observed after the reaction had been stirring for 12 hrs at room

temperature. This is in contrast to [U(η^8-C_8H_6{Si^{i}Pr$_3$-1,4}$_2$)(η^5-Cp^{Me5})(CO)], which is very short-lived (15 min). The ν_{CO} of **4.4** is only 15 cm^{-1} higher than the 1920 cm^{-1} in [U(η^8-C_8H_6{Si^{i}Pr$_3$-1,4}$_2$)(η^5-Cp^{Me5})(CO)],[52] but as has been previously mentioned, the reduction in ν_{CO} from free CO does not signify the reactivity of the carbonyl species.

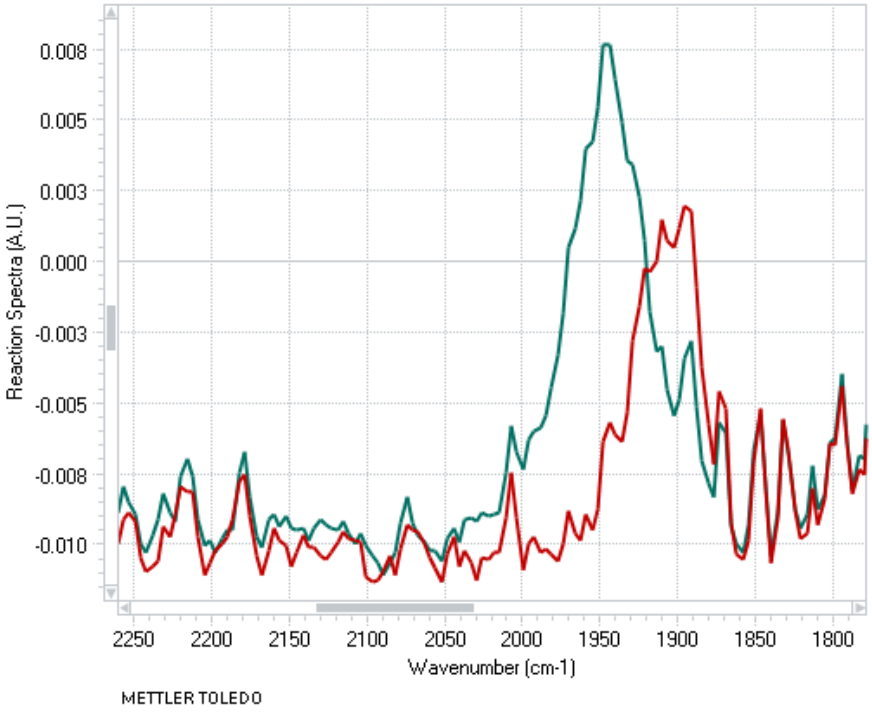

Figure 15: FTIR spectra of the reaction of **4.2** with CO in methylcyclohexane at -50 ºC, showing carbonyl exchange on the spectrum of [U(η^5-Ind^{Me7})(η^8-C_8H_6{Si^{i}Pr$_3$-1,4}$_2$)(^{13}CO)] (**4.4**) (red) on the addition of excess ^{12}CO (green).

The experimental observations from the reaction of **4.2** with ^{13}CO are consistent with the initial formation of a long-lived species by ^{1}H NMR, confirmed by *in situ* IR spectroscopy to be the U(III) carbonyl species [U(η^5-Ind^{Me7})(η^8-C_8H_6{Si^{i}Pr$_3$-1,4}$_2$)(^{13}CO)] (**4.4**). Over time this is followed by the formation of a single ^{13}C-labelled

product at δ 395 ppm by $^{13}C\{^{1}H\}$ NMR. It has not been possible within the timeframe of this work to establish the molecular formation of this product.

*4.2.5 Reactivity of [U(η^5-Ind^{Me6})(η^8-C$_8$H$_6${Si^{i}Pr$_3$-1,4}$_2$)] (**4.1**) and [U(η^5-Ind^{Me7})(η^8-C$_8$H$_4${Si^{i}Pr$_3$-1,4}$_2$)] (**4.2**) with $^{13}CO_2$.*

The low-valent mixed-sandwich complexes [U(η^8-C$_8$H$_6${Si^{i}Pr$_3$-1,4}$_2$)(η^5-Cp^R)(THF)] (R = Me$_5$ (**2.1**), Me$_4$H (**2.2**)) react *via* reductive disproportionation with excess CO_2 at -30 °C to yield the [(U(η^8-C$_8$H$_6${Si^{i}Pr$_3$-1,4}$_2$)(η^5-Cp^R))$_2$(μ-η^1:η^2-CO$_3$)] (R = Me$_5$, Me$_4$H) carbonate complexes. The ^{13}C-labelled carbonate resonances appear in d_8-toluene at 111.7 ppm for [(U(η^8-C$_8$H$_6${Si^{i}Pr$_3$-1,4}$_2$)(η^5-Cp^{Me5}))$_2$(μ-η^1:η^2-^{13}CO$_3$)] and 137.6 ppm for [(U(η^8-C$_8$H$_6${Si^{i}Pr$_3$-1,4}$_2$)(η^5-Cp^{Me4H}))$_2$(μ-η^1:η^2-^{13}CO$_3$)] and in both cases free ^{13}CO was observed at 185 ppm.[59]

A solution of [U(η^5-Ind^{Me7})(η^8-C$_8$H$_6${Si^{i}Pr$_3$-1,4}$_2$)] (**4.2**) in d_8- toluene was cooled to -78 °C, degassed and $^{13}CO_2$ (*ca.* 2 equivalents) was added *via* the Toepler line. The colour of the solution changed from red/brown to bright red on the addition of gas and was accompanied by the appearance of a single product resonance in the $^{13}C\{^{1}H\}$ NMR spectrum at δ 180.8 ppm as well resonances at δ 184.8 and 123 ppm for free ^{13}CO and free $^{13}CO_2$, respectively. The experimental observation of free ^{13}CO and a single ^{13}C-labelled product suggest that **4.2** shares a similar reactivity with $^{13}CO_2$ to **2.1** and **2.2**. An excess of $^{13}CO_2$ in the $^{13}C\{^{1}H\}$ NMR spectrum is in keeping with carbonate formation as the reaction to form a U(IV)-CO_3^{2-}-U(IV) species and ^{13}CO is stoichiometric.

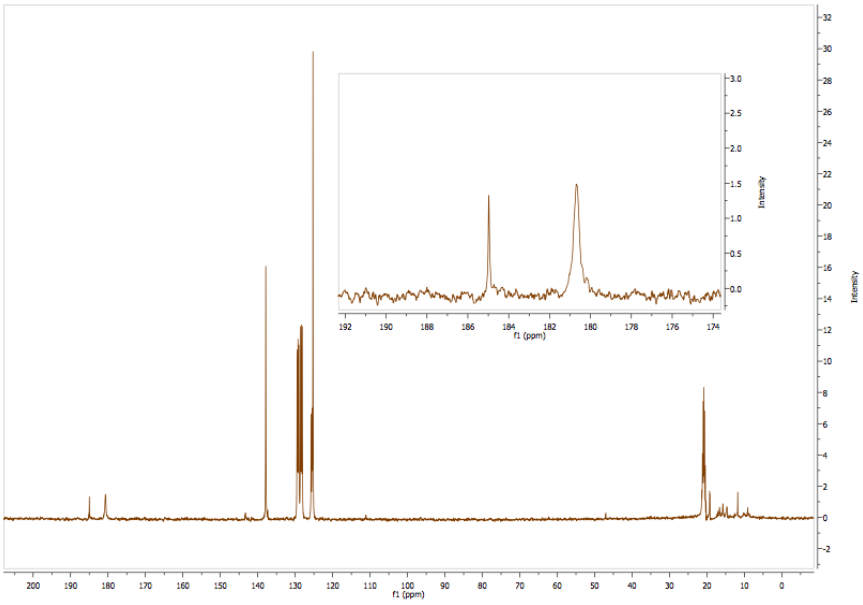

Figure 16: $^{13}C\{^{1}H\}$ NMR spectrum (d_8-toluene, 303 K) of the reaction of **4.2** with $^{13}CO_2$

Exposure of [U(η^5-Ind^{Me6})(η^8-$C_8H_6\{Si^iPr_3\text{-}1,4\}_2$)] (**4.1**) to 2.3 equivalents of $^{13}CO_2$ under analogous conditions resulted in a colour change from red/brown to bright red and the appearance of three product resonances in the $^{13}C\{^{1}H\}$ NMR as well as resonances at δ 184.8 and 123 ppm for free ^{13}CO and free $^{13}CO_2$, respectively. The $^{13}C\{^{1}H\}$ NMR spectrum is shown in Figure 17. Two of the ^{13}C-labelled products appear close together at δ 210.5 and 209.2 ppm and the third resonance is a broad multiplet centred at δ -58 ppm, at the same chemical shift as seen for one of the products of the reaction of **4.1** with ^{13}CO. The observation of ^{13}CO suggests that, unlike their reactivity with ^{13}CO, that complexes **4.1** and **4.2** display similar reactivity with $^{13}CO_2$.

The two ^{13}C-labelled products of the reaction of **4.1** with $^{13}CO_2$ are singlets but have chemical shifts, which are similar enough to allow for the possibility that the resonances are isomers of each other; there are two modes of bridging carbonate (μ-η^1:η^2-CO_3) and (μ-η^2:η^2-CO_3) that have been structurally characterised for uranium complexes.[59,60] The reaction of **4.1** with the ^{13}CO formed in the reaction, in the presence of excess $^{13}CO_2$ suggests the reaction of **4.1** with CO is significantly faster than the reaction with CO_2.

The $^{13}C\{^1H\}$ NMR spectrum of the reaction of [U(η^8-C_8H_6{Si^{i}Pr$_3$-1,4}$_2$)(η^5-Cp^{Me4H})(THF)] (**2.1**) with excess $^{13}CO_2$ also revealed a peak at δ 112.4 ppm in d_8-toluene assigned to the labelled squarate complex.[59] The resonance, centred at δ -58 ppm, product of the reaction of **4.1** and ^{13}CO, has not been definitively proved as the squarate complex **4.3**. The mass spectrum of the reaction of **4.1** with $^{13}CO_2$ does display peaks at above the amu of a dimeric species but these peaks have not been rationalised.

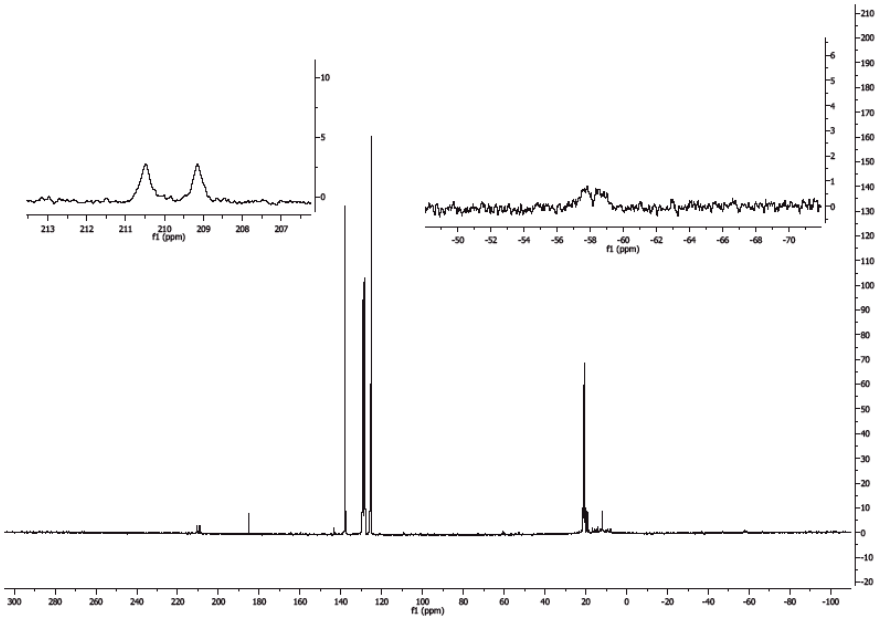

Figure 17: $^{13}C\{^{1}H\}$ NMR spectrum (d_8-toluene, 303 K) of the reaction of **4.1** with $^{13}CO_2$

4.2.6 Conclusions

Complexes **4.1** and **4.2** have been shown to possess interesting reactivity with ^{13}CO and $^{13}CO_2$. The products of these reactions have not been fully rationalised or characterised, however, the ^{1}H and $^{13}C\{^{1}H\}$ NMR data and the structure of **4.3**, indicate that the reactivity of the indenyl mixed-sandwich complexes of uranium(III) is both comparable and complementary to the reactivity of the cyclopentadienyl mixed-sandwich complexes.

4.3 Experimental details for Chapter 4

General details are given in Appendix One.

*4.3.1 Synthesis of [U(η^5-Ind^{Me6})(η^8-C_8H_6{Si^{i}Pr$_3$-1,4}$_2$)] (**4.1**).*

A yellow solution of KInd^{Me6} (0.61 g, 2.50 mmol) in THF (15 ml) was added dropwise over 15 min to a cooled to 0 °C, pre-stirred solution of UI_3 (1.60 g, 2.50 mmol) in THF (100 ml) and the colour of the solution was observed to change from purple to a dark green with the formation of a white precipitate. The solution was stirred overnight, stripped to dryness and the dark green solids extracted with toluene and filtered. The solids were taken up in THF (50 ml) and the dark green solution cooled to – 78 °C, to this a yellow solution of $K_2(C_8H_6\{Si^iPr_3\text{-}1,4\}_2)$ (1.03 g, 2.08 mmol, 0.83 equivalents) in THF (20 ml) was added dropwise over 1 hr 15 min and the solution was stirred for a further 30 min at this temperature. The reaction vessel was then removed from the cold bath and stirred for 2 hrs 30 min. The colour of the solution was observed to have changed to a dark red and a white precipitate was observed about 20 minutes after the vessel was removed from the cold bath. Volatiles were removed *in vacuo* and solids extracted with toluene and the red/brown solution filtered. The solution was stripped to dryness and dissolved in the minimum amount of pentane.

Yield: 445 mg, 20 %

Analysis calculated (found) for $C_{41}H_{67}Si_2U$: % C 57.50 (57.57), % H 7.71 (7.77)

^{1}H NMR (399.5 MHz, d_8-toluene, 303 K): δ_H 53.98 (v. br, s, 1H, COT ring-C*H*), 19.40 (v. br, m, COT ring-C*H*), 5.53 (br, m, 6H, Ind-CH_3), 0.45 (br, s, 3H, Ind-CH_3), -1.05 (s, 9H, ^{i}Pr-CH_3), -3.55 (s, 9H, ^{i}Pr-CH_3), -5.60 (s, 9H, ^{i}Pr-CH_3), -6.70 (s, 3H, ^{i}Pr-C*H*), -10.58 (s, 9H, ^{i}Pr-CH_3), -15.10 (br, s, 3H, Ind-CH_3), -17.40 (br, s, 3H, Ind-CH_3), -19.30 (s, 9H, ^{i}Pr-CH_3), -27.96 (br, s, 3H, Ind-CH_3), -50.88 (v. br, s, 1H, COT ring-C*H*), -94.14 (v. br, s, 1H, COT ring-C*H*), -103.58 (v. br, s, 1H, COT ring-C*H*), -117.06 (v. br, s, 1H, COT ring-C*H*).

^{29}Si{^{1}H}(d_8-toluene, 303 K): δ - 110.8, -138.08 ppm

MS (EI): m/z = 853 (M+)

*4.3.2 Synthesis of [U(η^5-Ind^{Me7})(η^8-C_8H_6{Si^{i}Pr$_3$-1,4}$_2$)] (**4.2**)*

A yellow suspension of KInd^{Me7} (0.49 g, 1.94 mmol) in THF (15 ml) at –90 °C was added dropwise over 45 min to the pre-stirred solution of UI_3 (1.20 g, 1.94 mmol) in THF (100 ml) at 0 °C and the colour of the solution was observed to change from purple to a dark green with the formation of a white precipitate. The solution was stirred overnight, stripped to dryness and the dark green solids extracted with toluene and filtered. The solids were taken up in THF (50 ml) and the dark green solution cooled to –78 °C, to this a yellow solution of $K_2(C_8H_6\{Si^{i}Pr_3\text{-}1,4\}_2)$ (0.78 g, 1.57 mmol, 0.81 equivalents) in THF (30 ml) was added dropwise over 1 hr and the solution was stirred for a further hour at this temperature. The reaction vessel was then removed from the cold bath and stirred for 1 hr 15 min. The colour of the solution was observed to have changed to a dark red and a white precipitate was observed about 20 minutes after the vessel was removed from the cold bath. Volatiles were removed *in vacuo* and the sticky

red/brown solids extracted with pentane, sonicated and filtered on a frit through dry Celite® and recrystalised from minimum pentane.

Yield: 405 mg, 24 %

Analysis calculated (found) for $C_{42}H_{69}Si_2U$: % C 58.13 (58.12), % H 6.46 (6.49)

^{1}H NMR (399.5 MHz, d_8-toluene, 303 K): δ_H 42.59 (v. br, s, 2H, COT ring-C*H*), 5.22 (br, s, 6H, Ind-C*H*$_3$), 0.65 (br, s, 3H, Ind-C*H*$_3$), -0.05 (br, s, 6H, Ind-C*H*$_3$), -2.70 (s, 18H, ^{i}Pr-C*H*$_3$), -6.05 (s, 18H, ^{i}Pr-C*H*$_3$), -16.79 (br, s, 6H, Ind-C*H*$_3$), -22.79 (s, 6H, ^{i}Pr-C*H*), -76.35 (v. br, s, 2H, COT ring-C*H*), -114.10 (v. br, s, 2H, COT ring-C*H*).

^{29}Si{^{1}H}(d_8-toluene, 303 K): -122.2

MS (EI): m/z = 867 (M+)

*4.3.3 NMR scale reaction of [U(η^5-Ind^{Me6})(η^8-C$_8$H$_6${Si^{i}Pr$_3$-1,4}$_2$)] (**4.1**) with ^{13}CO*

A red solution of [U(η^5-Ind^{Me6})(η-C$_8$H$_6${Si^{i}Pr$_3$-1,4}$_2$)] (**4.1**) (19 mg, 0.022 mmol) in d_8-toluene (0.5 ml) was cooled to - 78 °C, degassed, and ^{13}CO (*ca.* 4.7 equivalents) was added *via* the Toepler line. After addition of the gas the tube was inverted and warmed to room temperature in the supernatant of the cold bath over 3 hrs, with shaking every 30 min. The colour of the solution was observed to darken to a brown colour.

^{13}C{^{1}H} NMR (150 MHz, d_8-toluene, 303 K): δ 272.3 (m, br, ^{13}C-labelled) – 63.5 (m, br, ^{13}C-labelled).

^{29}Si{^{1}H}(d_8-toluene, 303 K): -78.8, -79.1, -86.71

*4.3.4 NMR scale reaction of [U(η^5-Ind^{Me6})(η^8-C_8H_6{Si^{i}Pr$_3$-1,4}$_2$)] (**4.1**) with ^{13}CO*

Reaction described in 4.3.3 was repeated using [U(η^5-Ind^{Me6})(η^8-C_8H_6{Si^{i}Pr$_3$-1,4}$_2$)] (**4.1**) (14 mg, 0.016 mmol) and ^{13}CO (*ca.* 4.4 equivalents).

^{13}C{^{1}H} NMR (150 MHz, d_8-toluene, 303 K): δ 186 (s, ^{13}CO), -63.5 (m, br, ^{13}C-labelled)

*4.3.5 NMR scale reaction of [U(η^5-Ind^{Me6})(η^8-C_8H_6{Si^{i}Pr$_3$-1,4}$_2$)] (**4.1**) with 0.5 ^{13}CO*

Reaction described in 4.3.3 was repeated using [U(η^5-Ind^{Me6})(η-C_8H_6{Si^{i}Pr$_3$-1,4}$_2$)] (**4.1**) (27 mg, 0.032 mmol) and ^{13}CO (*ca.* 0.5 equivalents).

^{13}C{^{1}H} NMR (150 MHz, d_8-toluene, 303 K): δ 186 (s, ^{13}CO), -63.5 (m, br, ^{13}C-labelled).

*4.3.6 Quenching reaction with Ph_3SiCl of [U(η^5-Ind^{Me6})(η^8-C_8H_6{Si^{i}Pr$_3$-1,4}$_2$)] (**4.1**) with 0.5 ^{13}CO*

To the reaction described in 4.3.5 Ph_3SiCl (21.6 mg, 0.07 mmol, 2.3 equivalents, w.r.t. [U(η^5-Ind^{Me6})(η-C_8H_6{Si^{i}Pr$_3$-1,4}$_2$)] (**4.1**)) was added. The solution was observed to lighten in colour to orange.

^{13}C{^{1}H} NMR (150 MHz, d_8-toluene, 303 K, selected data): δ 270, -161.6, 162.3, -221.2, -222.3, -225.9, -226.6, -228.8, -229.5

29Si{^{1}H} (d_8-toluene, 303 K): δ -81.5, -90.0, -100.4, -134.2, -136.0

MS (EI): m/z = 1204, 1071[U(η^{8}-C_8H_6{Si^{i}Pr$_3$-1,4}$_2$)$_2$] 913, 889, 788, 689.

*4.3.7 Synthesis of [(U(η^{5}-Ind^{Me6})(η-C_8H_6{Si^{i}Pr$_3$-1,4}$_2$))$_2$(μ-η^{2}:η^{2}-C_4O_4)] (**4.3**)*

A dark red solution of [U(η^{5}-Ind^{Me6})(η-C_8H_6{Si^{i}Pr$_3$-1,4}$_2$)] (**4.1**) (100 mg, 0.12 mmol) in toluene (15 ml) was cooled to -78 °C, after an hour the solution was degassed and CO (5 psi) added. The reaction was allowed to warm to room temperature slowly: after 4 hours the reaction vessel was removed from the -10 °C cold bath, and a red/brown precipitate observed. The mixture was stirred vigorously for a further 20 min, after which no solids were visible. The volatiles were removed *in vacuo*, yielding a sticky red matrix. Crystals suitable for X-ray analysis were grown by slow cooling to -50 °C of a pentane solution over several weeks, however, there was insufficient material for further characterisation.

*4.3.8 Reaction of [U(η^{5}-Ind^{Me7})(η-C_8H_6{Si^{i}Pr$_3$-1,4}$_2$)] (**4.2**) with ^{13}CO*

A red solution of [U(η^{5}-Ind^{Me7})(η-C_8H_6{Si^{i}Pr$_3$-1,4}$_2$)] (**4.2**) (30 mg, 0.035 mmol) in d_8-toluene (0.5 ml) was cooled to -78 °C, degassed and ^{13}CO (*ca.* 2 equivalents) was added *via* the Toepler line. After addition of the gas the tube was warmed to room temperature overnight. The colour of the solution was observed to darken to brown.

^{1}H NMR (399.5 MHz, d_8-toluene, 303 K): δ_H 27.51 (v. br, s, 2H, COT ring-C*H*), 4.89 (br, s, 6H, Ind-CH_3), -0.64 (br, s, 6H, ^{i}Pr-C*H*), -2.10 (br, s, 3H, Ind-CH_3), -2.65 (s, 18H,

^{i}Pr-CH_3), -5.39 (s, 18H, ^{i}Pr-CH_3), -14.37 (br, s, 6H, Ind-CH_3), -20.62 (br, s, 6H, Ind-CH_3), -69.59 (v. br, s, 2H, COT ring-C*H*), -97.62 (v. br, s, 2H, COT ring-C*H*).

After a week at room temperature:

$^{13}C\{^{1}H\}$ NMR (150 MHz, d_8-toluene, 303 K): δ 395 (s, ^{13}C-labelled)

^{1}H NMR (399.5 MHz, d_8-toluene, 303 K): δ_H -81.70 (v. br, s, 2H, COT ring-C*H*), 25.81 (br, s, 6H, Ind-CH_3), 14.51 (br, s, 6H, Ind-CH_3), 2.40 (s, 6H, Ind-CH_3), 2.20 (s, 6H, Ind-CH_3), 1.82 (s, 6H, Ind-CH_3), -3.53 (s, 18H, ^{i}Pr-CH_3), -3.86 (s, 6H, Ind-CH_3), -8.38 (s, 18H, ^{i}Pr-CH_3), -13.08 (br, s, 6H, ^{i}Pr-C*H*), -18.44 (br, s, 3H, Ind-CH_3), -45.24 (v. br, s, 2H, COT ring-C*H*), -53.40 (v. br, s, 2H, COT ring-C*H*).

*4.3.9 Reaction of [U(η^5-Ind^{Me6})(η^8-C$_8$H$_6${Si^{i}Pr$_3$-1,4}$_2$)] (**4.1**) with $^{13}CO_2$*

A red solution of [U(η^5-Ind^{Me7})(η-C$_8$H$_6${Si^{i}Pr$_3$-1,4}$_2$)] (26 mg, 0.03 mmol) in d_8-toluene was cooled to -78 °C, degassed, and $^{13}CO_2$ (*ca.* 2.3 equivalents) was added *via* the Toepler line. After addition of the gas the tube was warmed to room temperature overnight. The colour of the solution was observed to redden on addition of gas.

$^{13}C\{^{1}H\}$ NMR (150 MHz, d_8-toluene, 303 K): δ 184.8 (s, ^{13}CO), 123 (s, $^{13}CO_2$). 210.5 (^{13}C-labelled product), 209.2 (^{13}C-labelled product)

MS (EI): m/z = 1814, 1697, 1235, 1098,

*4.3.10 Reaction of [U(η^5-Ind^{Me7})(η-C_8H_6{Si^{i}Pr$_3$-1,4}$_2$)] (**4.2**) with $^{13}CO_2$*

A red solution of [U(η^5-Ind^{Me7})(η-C_8H_6{Si^{i}Pr$_3$-1,4}$_2$)] (**4.2**) (32 mg, 0.037 mmol) in d_8-toluene was cooled to -78 °C, degassed and $^{13}CO_2$ (*ca.* 2 equivalents) was added *via* the Toepler line. After addition of the gas the tube was warmed to room temperature overnight. The colour of the solution was observed to redden on addition of gas.

$^{13}C\{^1H\}$ NMR (150 MHz, d_8-toluene, 303 K): δ 186 (s, ^{13}CO), 180.8 (^{13}C-labelled product) 123 (s, $^{13}CO_2$)

4.4 References:

[1] a) R. H. Crabtree, *The Organometallic Chemistry Of The Transition Metals*, 2nd edn, Wiley Interscience, 1994. b) C. Elschenbroich and A. Saltzer, *Organometallics: A Concise Introduction*, 2nd edn, VCH, 1992.

[2] M. E. Rerek, L. N. Ji and F. Basolo, *J. Chem. Soc. Chem. Comm*. 1983, 1208.

[3] a) J. W. Faller, R. H. Crabtree and A. Habib, *Organometallics*, 1985, **4**, 929. b) J. M. O'Connor and C. P. Casey, *Chem. Rev.*,1987, **87**, 307.

[4] M. J. Calhorda, C. C. Romão and L. F. Verios, *Chem. Eur. J.*, 2002, **8**, 868.

[5] H. H. Brintzinger, D. Fischer, R. Muelhaupt, B. Rieger and R. M. Waymouth, *Angew. Chem. Int. Ed. Engl.*, 1995, **34**, 1143.

[6] C. A. Bradley, I. Keresztes, E. Lobkovsky, V. G. Young and P. J. Chirik, *J. Am. Chem. Soc.*, 2004, **126**, 16937.

[7] P. J. Chirik, *Dalton Trans.*, 2007, 16.

[8] D. Pun, E. Lobkovsky and P. J. Chirik, *J. Am. Chem. Soc.*, 2008, **130**, 6047.

[9] a) L. F. Veiros, *Organometallics*, 2006, **25**, 4698. b) C. A. Bradley, E. Lobkovsky, I. Keresztes and P. J. Chirik, *J. Am. Chem. Soc.*, 2005, **127**, 10291.

[10] a) F. A. Cotton, A. Musco and G. Yagupusky, *J. Am. Chem. Soc.*, 1967, **89**, 6136. b) A. Davidson and P. E. Rakita, *J. Organomet. Chem.*, 1970, **23**, 407.

[11] F. T. Edlemann, *Comprehensive Organometallic Chemistry III*, Vol. 4, Elsevier Ltd., Oxford, 2007.

[12] M. J. Calhorda, V. Felix and L. F. Verios, *Coord. Chem. Rev*. 2002, **230**, 49.

[13] M. Tsutsui and H. J. Gysling, *J. Am. Chem. Soc.*, 1969, **91**, 3175.

[14] M. Tsutsui and H. J. Gysling, *J. Am. Chem. Soc.*, 1968, **90**, 6880.

[15] W. J. Evans, T. S. Gummmersheimer, T. J. Boyle and J. W. Ziller, *Organometallics*, 1994, **13**, 1281.

[16] W. J. Evans, T. S. Gummerscheimer, and J. W. Ziller, *Appl. Organomet. Chem.* 1995, **9**, 437.

[17] X. Xu, Y. Chen, J. Feng, G. Zou and J. Sun, *Organometallics*, 2010, **29**, 549.

[18] K. Wen, J. Zhongsheng and C. Wenqi, *J. Chem. Soc., Chem. Comm.*, 1991, **10**, 680.

[19] a) P. G. Laubereau, L. Ganguly, J. H. Burns, B. M. Benjamin, J. L. Atwood and J. Selbin, *Inorg. Chem.*, 1971, **10**, 2274. b) J. H. Burns and P. G. Laubereau, *Inorg. Chem.*, 1971, **12**, 2789.

[20] J. Meunier-Piret, J. P. Declercq, G. Germain and M. Van Meerssche, *Bull. Chim. Soc. Bel.*, 1980, **89**, 121.

[21] a) S. Bettonville, J. Goffart and J. Fuger, *J. Organometallic Chem.*, 1990, **393**, 205.

b)X. Jermine, J. Goffart, S. Bettonville and J. Fuger, *J. Organometallic Chem.*, 1991, **415**, 363.

[22] T. K. Miyamoto, M. Tsutsui and L-B. Chen, *Chem. Lett.*, 1981, 729.

[23] D. O'Hare, J. C. Green, T. Marder, S. Collins, G. Stringer, A. K. Kakkar, N. Kaltsoyannis, A. Kuhn, R. Lewis, C. Mehnert, P. Scott, M. Kurmoo and S. Pugh, *Organometallics*, 1992, **11**, 48.

[24] A. D. Andreou, R. V. Bulbulian and P. H. Gore, *Tetrahedron*, 1980, **36**, 2101.

[25] M. Tsutsui, L-B. Chen and D. E. Bergbreiter, *J. Am. Chem. Soc.*, 1982, **104**, 855.

[26] W. Beeckman, J. Goffart, J. Rebizant and M. R. Spirlet, *J. Orgmet. Chem.* 1986, **307**, 23.

[27] J. Goffart, J. F. Desreux, B. P. Gilbert, J. L. Delsa, J. M. Renkin and G. Duyckaerts, *J. Organomet. Chem.*, 1981, **209**, 281.

[28] T. M. Trnka, J. B. Bonanno, B. M. Bridgewater and G. Parkin, *Organometallics*, 2001, **20**, 3255.

[29] J. Meunier-Piret and M. Van Meerssche, *Bull. Soc. Chim. Belg.*, 1984, **93**, 299.

[30] a) J. M. Manriquez, P. J. Fagan and T. J. Marks, *J. Am. Chem. Soc.*, 1978, **100**, 3939. b) T. J. Marks, *Science*, 1982, **217**, 990.

[31] O. T. Summerscales, DPhil Thesis, University of Sussex, 2007

[32] See for a different definition of FA: S. A. Westcottt, A. K. Kakkar, G. Stringer, N. Taylor and T. B. Marder, *J. Organomet. Chem.*, 1990, **394**, 777.

[33] V. Cadierno, J. Diaz, M. P. Gamsa, J. Gimeno and E. Lastra, *Coord. Chem. Rev.*, 1999, **193-195**, 147.

[34] A. K. Kakkar, S. J. Jones, N. J. Taylor, S. Collins and T. B. Marder, *J. Chem. Soc. Chem. Commun.*, 1989, **19**, 1454.

[35] G. Huttner, H. H. Brintzinger, L. G. Bell, P. Friedrich, V. Bejenke and D. Neugebauer, *J. Organomet. Chem.*, 1978, **145**, 329. See also: B. J. Grimmond, J. Y. Corey and N. P. Rath, *Organometallics*, 1999, **18**, 404.

[36] P. T. Kissinger and W. R. Heineman, *J. Chem. Ed.*, 1983, **60**, 702.

[37] N. G. Connelly and W. E. Geiger, *Chem. Rev.*, 1996, **96**, 877.

[38] S. Cotton, *Lathanide and Actinide Chemistry*, John Wiley and Sons Ltd., Chichester, 2006.

[39] D. E. Morris, R. E. Da Re, K. C. Jantunen, I. Castro-Rodriguez and J. L. Kiplinger, *Organometallics*, 2004, **23**, 5142.

[40] R. G. Finke, G. Gaughan and R. Voegeli, *J. Organomet. Chem.*, 1982, **229**, 179.

[41] F. Ossola, P. Zanella, P. Ugo and R. Seeber, *Inorg. Chim. Acta.*, 1988, **147**, 123.

[42] L. R. Avens, D. M. Barnhart, C. J. Burns, S. D. McKee and W. H. Smith, *Inorg. Chem.*, 1994, **33**, 4245.

[43] R. E. Da Re, C. J. Kuehl, M. G. Brown, R. C. Rocha, E. D. Bauer, K. D. John, D. E. Morris, A. P. Shreve and J. L. Sarrao, *Inorg. Chem.*, 2003, **42**, 5551.

[44] C. Clappe, D. Leveugle, D. hauchard and G. Durand, *J. Electroanal. Chem.*, 1998, **448**, 95.

[45] O. J. Curnow and G. M. Fern, *J. Organomet. Chem.*, 2005, **690**, 3018.

[46] N. S. Crossley, J. C. Green, A. Nagy and G. Stringer, *J. Chem. Soc. Dalton Trans.*, 1989, 2139.

[47] a) S. Evans, M. L. H. Green, B. Jewitt, A. F. Orchard and C. F. Pygall, *J. Chem Soc. Faraday Trans*, 1972, **2**, 1847. b) C. Cauletti, J. C. Green, R. M. Kelly, P. Powell, J. Van Tilborg, J. Robbins and J. Smart, *J. Electron Spectrosc. Relat. Phenom.*, 1980, **19**, 327.

[48] M. J. Calhorda and L. F. Veiros, *Coord. Chem. Rev.*, 1999, **186-187**, 37.

[49] a) O. T. Summerscales, F. G. N. Cloke, P. B. Hitchcock, J. C. Green and N. Hazari, *Science*, 2006, **311**, 829. b) O. T. Summerscales, F. G. N. Cloke, P. B. Hitchcock, J. C. Green and N. Hazari, *J. Am. Chem. Soc.*, 2006, **128**, 9602.

[50] V. L. Coffin, W. Brennan and B. B. Wayland, *J. Am. Chem. Soc.*, 1988, **110**, 6063.

[51] A. S. P. Frey, personal communication.

[52] A. S. P. Frey, F. G. N. Cloke, P. B. Hitchcock, I. J. Day, J. C. Green and G. Aitken, *J. Am. Chem. Soc.*, 2008, **138**, 13816.

[53] a) N. C. Lim, M. D. Morton, H. A. Jenkins and C. Brueckner, *J. Org. Chem.*, 2003, **68**, 9233. b) M. T. Reetz and G. Neumeier, *Liebigs Ann. Chem.*, 1981, 1234.

[54] F. G. N. Cloke and P. B. Hitchcock, *J. Am. Chem. Soc.*, 2002, **124**, 9352.

[55] M. del Mar Conejo, J. S. Parry, E. Carmona, M. Schultz, J. G. Brennan, S. M. Beshouri, R. A. Anderson, R. D. Rogers, S. Coles and M. Hursthouse, *Chem. Eur. J.*, 1999, **5**, 3000.

[56] a) J. G. Brennan, R. A. Anderson and J. L. Robbins, *J. Am. Chem. Soc.*, 1986, **108**, 335. b) W. J. Evans, S. A. Kozimor, G. W. Nyce and J. W. Ziller, *J. Am. Chem. Soc.*, 2003, **125**, 13831.

[57] A. S. P. Frey, F. G. N. Cloke, *in press*.

[58] J. A. Timney, Transition Metal Carbonyls: Infrared Spectra, *Encyclopedia of Inorganic Chemistry*, Ed. R. H. Crabtree, Wiley, 2008.

[59] O. T. Summerscales, A. S. P. Frey, F. G. N. Cloke and P. B. Hitchcock, *Chem. Commun.*, 2009, 198.

[60] O. P. Lam, S. C. Bart, H. Kameo, F. W. Heinemann and K. Meyer, *Chem. Commun.*, 2010, **46**, 3137.

CHAPTER FIVE: CONCLUSION

Chapter 2 builds on the novel reactivity demonstrated by the uranium(III) complexes [U(η^5-Cp^R)(η^8-C_8H_6{Si^{i}Pr$_3$-1,4}$_2$)(THF)] (R = Me_4H (**2.1**), Me_5 (**2.2**)) towards CO and CO_2 by reacting these complexes with other small molecules and by investigating the chemical removal of the coupled ^{13}CO product from the uranium centre. Chapters 3 and 4 examine the effect of ligand substitution on the stability and reactivity of mixed-sandwich complexes of uranium(III), with particular emphasis on the reactions with CO, CO_2 and MeNC.

Complexes **2.1** and **2.2** were successfully synthesised and the yield of **2.2** was improved from that reported in the literature. However, the reactions of **2.1** with high-pressure H_2/CO and other small molecules did not lead to the isolation of new products with the exception of the reaction of **2.1** with one equivalent of acetonitrile, which resulted in the isolation and full characterisation of [U(η^5-Cp^{Me4H})(η^8-C_8H_6{Si^{i}Pr$_3$-1,4}$_2$)(η^1-NCMe)] (**2.3**). The co-ordinated acetonitrile in **2.3** is unexceptional but the complex undergoes thermolysis when heated in either d_8-thf or d_8-toluene to form a number of products, the formulation of which were not able to be elucidated. Complexes **2.1** and **2.2** were reacted with MeNC and the ^{1}H NMR data suggest a major and minor product in the case of **2.1** and a single product in the case of **2.2**. A structure was obtained from an NMR scale reaction

of **2.2** with methylisocyanide and shown to be the isocyanide adduct [U(η^5-Cp^{Me5})(η^8-$C_8H_6\{Si^iPr_3\text{-}1,4\}_2$)($\eta^1$-CNMe)] (**2.4**). Complex **2.4** has a long U-C interaction and there is no lengthening of the C-N(Me) bond, indicative of no reduction.

The uranium(IV) ^{13}C-labelled complex [(U(η^8-$C_8H_6\{Si^iPr_3\text{-}1,4\}_2$)($\eta^5$-$Cp^{Me4H}$))$_2$($\mu$-$\eta^2$:$\eta^2$-$^{13}C_4O_4$)] (**2.5**) was synthesised but was only able to be isolated in a very low yield. The reactions of **2.5** with halides or pseudohalides were monitored by $^{13}C\{^1H\}$ NMR spectroscopy. Complex **2.5** reacts with SiR_3X (R = Me, X = I, OTf or R = Ph, X = Cl), but the only functionalised product reliably observed by $^{13}C\{^1H\}$ NMR was $^{13}C_4O_2(OSiPh_3)_2$ (**2.6**), which has a AA'BB' spin-system and displays second-order effects. Reactions of **2.5** with benzyl chloride or isopropylphenylchloro phosphine did not proceed, whereas the reaction of **2.5** with dimethyl aluminium chloride led to the observation of the uranium(IV) chloride complex [(U(η^8-$C_8H_6\{Si^iPr_3\text{-}1,4\}_2$)($\eta^5$-$Cp^{Me4H}$)(Cl)] by mass spectrometry.

The substitution of the Cp^R ligand for the Tp^{Me2} ligand has led to the synthesis of two novel uranium(III) half-sandwich complexes [U(κ^3-Tp^{Me2})(η^8-$C_8H_6\{Si^iPr_3\text{-}1,4\}_2$)] (**3.1**) and [U($\kappa^3$-$Tp^{Me2}$)($\eta^8$-$C_8H_4\{Si^iPr_3\text{-}1,4\}_2$)] (**3.2**). The X-ray structures of these complexes reveal that the increase in steric congestion resulting from the use of the Tp^{Me2} ligand, in place of Cp^{Me5}, is not reflected in an increase in the U-centroid distance to the $(C_8H_6\{Si^iPr_3\text{-}1,4\}_2)^{2-}$ ligand in **3.1** but in **3.2** results in a lengthening of the U-C distances to the pentalene ligand. This is corroborated by the solution NMR behaviour of the

complexes: **3.1** retains a static structure up to 80 °C, whereas **3.2** is fully fluxional at room temperature. The ability of the pentalene ligand to fold around the bridgehead allows greater access to the metal centre in **3.2**. Complex **3.1** displays no reactivity towards CO, CO_2, MeNC under mild conditions. DFT calculations suggest that for complex **3.1**, in spite of being highly reducing, the entropic cost of CO binding is too great for the reaction to proceed. When heated at 80 °C in the presence of a tenfold excess of MeNC **3.1** reacts to yield $[U(\eta^8\text{-}C_8H_6\{Si^iPr_3\text{-}1,4\}_2)(\eta^2\text{-}dmpz)_2(\eta^1\text{-}CNMe)]$ (**3.3)**. Initial reactivity studies on **3.2** show it is reactive towards small molecules under mild conditions but the reaction products were not able to be rationalised.

Complexes $[U(\eta^5\text{-}Ind^R)(\eta^8\text{-}C_8H_6\{Si^iPr_3\text{-}1,4\}_2)]$ (R = Me_6 (**4.1**), Me_7 (**4.2**)) were synthesised in a moderate yield and both display a base-free bent sandwich structure in which the $[C_8H_6\{Si^iPr_3\text{-}1,4\}_2]^{2-}$ and $[Ind^{Me7}]^-$ ligands exhibit η^8 and η^5coordination modes, respectively. The U-M1 and U-M2 centroid distances in **4.1** and **4.2** are essentially identical and are slightly shorter than those found in the cyclopentadienyl mixed-sandwich complexes **2.1** and **2.2**.

The reaction of **4.1** with ^{13}CO was found to yield two ^{13}C-labelled product resonances at δ 270 and – 58 ppm, reproducibly by $^{13}C\{^1H\}$ NMR spectroscopy when a sub-stochiometric amount of gas was used. From the reaction of **4.1** with an overpressure of CO, $[(U(\eta^5\text{-}Ind^{Me6})(\eta^8\text{-}C_8H_6\{Si^iPr_3\text{-}1,4\}_2))_2(\mu\text{-}\eta^2\text{:}\eta^2\text{-}C_4O_4)]$ (**4.3**) was isolated but there was

insufficient material for full characterization. There is no significant lengthening of uranium-ligand bonding distances in **4.3**, either to the $[(C_8H_6\{Si^iPr_3\text{-}1,4\}_2)]^{2-}$ or the $[\eta^5\text{-}Ind^{Me6}]^-$ ligand, from those in **4.1**. The U-C bond distances to the bridgehead carbon atoms in **4.3** are longer than those to the other carbon atoms that constitute the η^5 –bound $[\eta^5\text{-}Ind^{Me6}]^-$ ligands though the difference is not significant in terms of hapticity. The bond lengths and angles of the U-C_4O_4-U core are directly comparable to those found in $[(U(\eta^8\text{-}C_8H_6\{Si^iPr_3\text{-}1,4\}_2)(\eta^5\text{-}Cp^{Me4H}))_2(\mu\text{-}\eta^2\text{:}\eta^2\text{-}C_4O_4)]$. This result demonstrates that the reductive coupling of CO is not limited to the Cp-containing mixed-sandwich complexes of uranium(III). The synthesis of **4.3** and multiple products observed in the reaction of **4.1** with ^{13}CO suggest that it might prove possible to gain insight into the factors affecting the selectivity of product formation.

The reaction of **4.2** with ^{13}CO is consistent with the initial formation at low temperature of a long-lived species by ^1H NMR spectroscopy, confirmed by *in situ* IR spectroscopy to be the U(III) carbonyl species $[U(\eta^5\text{-}Ind^{Me7})(\eta^8\text{-}C_8H_6\{Si^iPr_3\text{-}1,4\}_2)(^{13}CO)]$ (**4.4**). The assignment was confirmed by an isotopic shift on the addition of ^{12}CO. Over time this is followed by the formation of a single ^{13}C-labelled product at δ 395 ppm by $^{13}C\{^1H\}$ NMR spectroscopy. These experimental observations are consistent with the reactivity of **2.2** with sub-stoichiometric CO to form the ynediolate complex but in the absence of further data on the molecular formation of the final ^{13}C-labelled product from the reaction of **4.2** with CO, the parallel is speculative at best.

The reaction of **4.2** with $^{13}CO_2$ resulted in a single product resonance in the $^{13}C\{^1H\}$ NMR spectrum at δ 180.8 ppm and the observance of free ^{13}CO. Exposure of **4.1** to $^{13}CO_2$ under analogous conditions resulted in three product resonances and free ^{13}CO by $^{13}C\{^1H\}$ NMR spectroscopy. Two of the ^{13}C-labelled products appear close together at δ 210.5 and 209.2 ppm and are possibly isomers and the third resonance is a broad multiplet centred at δ -58 ppm, at the same chemical shift as seen for one of the products of the reaction of **4.1** with ^{13}CO. The experimental observation of ^{13}C-labelled products and ^{13}CO suggests that the reaction of both **4.1** and **4.2** with $^{13}CO_2$ proceeds *via* reductive disproportionation, which is the reactivity displayed by **2.1** and **2.2** towards $^{13}CO_2$. The observance of the ^{13}CO product resonance in the reaction of **4.1** with $^{13}CO_2$ suggests that the reaction with ^{13}CO is faster than that with $^{13}CO_2$, which is also seen in the reaction of **2.1** with $^{13}CO_2$.

It was not possible to extend the chemistry of complexes **2.1** and **2.2** to include the activation of other small molecules. The choices of substrate and reaction conditions are non-trivial for these systems. Neither was it possible to satisfactorily rationalise the removal of the functionalised $^{13}C_4O_2(OSiPh_3)_2$ unit from complex **2.5**.

The synthesis and very different reactivity of the trispyrazolylborate complexes **3.1** and **3.2** illustrates the that changing either the monoanionic and dianionic components in the uranium(III) mixed sandwich system has a profound effect on the reactivity of the resultant complexes. The Tp^{Me2-} ligand is significantly different to the Cp^{R-} ligand and the lack of

reactivity with small molecules observed for complex **3.1** under mild conditions is significantly different to the reactivity of **2.1** or **2.2** under similar conditions. However, the relative contributions of the various factors, which result in no reactivity for **3.1** with small molecules, are unclear and complex **3.2** does exhibit facile and complex reactivity with small molecules under mild conditions.

The reactivity of complexes **4.1** and **4.2** with CO and CO_2 is comparable to that of **2.1** and **2.2** but the selectivity and rate of the reactions, particularly with CO, are different. It is significant that the reductive coupling of CO has been demonstrated in a non-Cp ligand environment. The differences in electronics, sterics and the more flexible hapticity of the indenyl ligand may result in alternative reaction pathways, which might provide further mechanistic insight into the reductive coupling of CO.

APPENDIX ONE: EXPERIMENTAL DETAILS

A1.1 General Experimental Details

The manipulation of air-sensitive compounds and their spectroscopic measurements were undertaken using standard high vacuum Schlenk-line techniques,[1] under an atmosphere of dry nitrogen or catalytically dried and deoxygenated argon, or under catalytically dried and deoxygenated nitrogen in an MBraun glove box < 1 ppm H_2O and < 3 ppm O_2. All glassware was dried by storage in an oven at 120 ^oC with subsequent cooling under 10^{-3} mbar vacuum followed by repeated alternate evacuation and purging with argon. Nitrogen and argon gases were supplied by BOC Gases UK. Celite 545 filter aid was flame dried *in vacuo* and filter canulae equipped with Whatman® 25 mm glass microfibre filters were dried in an oven at 120 °C prior to use.

A1.2 Purification of solvents

Solvents were purified by pre-drying over sodium wire prior to heating at reflux over the appropriate drying agent for a minimum of 72 hours before use. Toluene was dried by heating to reflux over sodium; hexane and THF were heated to reflux over potassium; diethyl ether and pentane were heated to reflux over sodium/potassium alloy. Dried solvents were collected, degassed and stored in potassium-mirrored ampoules, except THF, which was stored in an ampoule containing 4 Å molecular sieves, which had previously been flame-dried under vacuum. Deuterated NMR

solvents were purchased from GOSS Scientific Ltd. and purified by heating at reflux over the appropriate drying agent: d_1-chloroform and d_2-methylene dichloride over calcium hydride, d_6-benzene and d_8-thf and d_8-toluene over potassium. Vacuum transference to ampoules followed by freeze-thaw degassing was undertaken prior to storage under nitrogen.

A1.3 Instrumentation

NMR analysis was undertaken by the author using a Bruker Avance DPX-300 or Varian Direct Drive 400 MHz, 500 MHz or 600 MHz spectrometers. Chemical shifts are reported in parts per million (δ). In accordance with IUPAC convention downfield refers to a positive shift. ^{1}H NMR and ^{13}C{^{1}H} NMR spectra were internally referenced to residual protio solvent. ^{11}B{^{1}H} and ^{29}Si{^{1}H} were referenced externally to $BF_3.OEt_2$ and TMS. Elemental Analyses were carried out by Steven Boyer at the Elemental Analysis Service, London Metropolitan University. Mass spectra were recorded by Dr. A. Abdul-Sada using a VG Autospec Fisons instrument (electron ionisation at 70 eV) or a Kratos MS25 mass spectrometer. Single crystal x-ray diffraction analysis and data collection were performed by Dr P. B. Hitchcock or Dr M. P. Coles at 173 K on a Enraf-Nonius CAD4 diffractometer with graphite-monochromated Mo Kα radiation (λ = 0.71073 Å). Data collection was handled using KappaCCD software, final cell parameter calculations performed using program package WinGX. The data were corrected for absorption using the MULTISCAN program. Refinement was performed using SHELXL-97, and the thermal ellipsoid plots drawn using Shelxtl-XP. SADI restraints, isotropic C atoms, ^{i}Pr groups and H atoms omitted, except where specified.

Details of the structures in this thesis are given in Appendix Two or are available as cif files.

Analytical electrochemical studies (cyclic voltammetry) were carried out by Dr R. J. Blagg, University of Sussex/NNL using a three-electrode cell under an atmosphere of thf saturated argon, with data collection using a BASi Epsilon-EC potentiostat under computer control. The working electrode was a gold (2.0 mm^2) disc and the counter electrode a platinum wire. A second platinum wire was used as a *pseudo*-reference electrode, with potentials calibrated *in situ* by addition of ferocene and use of the $[FeCp_2]^{0/1+}$ redox couple as an internal standard. Sample solutions were *ca.* 1 $\mu mol.cm^{-3}$ in the test compound with 50 $\mu mol.cm^{-3}$ $[^nBu_4N][B(C_6F_5)_4]$ as the supporting electrolyte in thf solvent. Under these conditions the maximum solvent window is +1.5 to –2.9 V *vs.* $[FeCp_2]$.

Quantum chemical calculations were performed by Prof. J. C. Green and Dr G. Aitken of the University of Oxford using density functional methods of the Amsterdam Density Functional (Version ADF2008.01) package.[2] TZP basis sets were used with triple-ξ accuracy sets of Slater-type orbitals, with polarisation functions added to all atoms. Relativistic corrections were made using the ZORA (zero-order relativistic approximation) formalism[3] and the core electrons were frozen up to 1s for B, C and N, 2p for Si, and 5d for U. For U the 6p electrons were included in the valence set. The energies of the structures were calculated using the local density approximation (LDA)[4] due to Vosko *et al.* with the non-local exchange terms of Becke,[5] and the non-local correlation correction of Perdew[6] being applied to the calculated LDA densities (BP86).

A1.4 Commercially supplied reagents

The following materials were supplied by Aldrich: COD, HgI_2, 1,2,3,4 –tetramethyl-1,3-cyclopentadiene, triisopropyl silane and triflic acid, these reagents were used as received. The following materials were purchased from Aldrich and purified or dried prior to use[7] and stored under nitrogen: CS_2, ^{t}BuNCO, NCMe, $SiMe_3I$, $SiMe_3OTf$, $SiPh_3Cl$, $AlMe_2Cl$ in hexanes *n*BuLi, TMEDA and benzonitrile. $K(NTMS)_2$ was purchased from Fluka and recrystallised from toluene prior to use. Isotopically enriched gases ^{13}CO (99%) and $^{13}CO_2$ (99%) were supplied by Cambridge Isotopes, and added *via* Toepler line. Depleted uranium turnings were supplied by CERAC, and also kindly donated by BNFL.

A1.5 Synthesis of starting materials

$KInd^{Me6}$, $K_2(C_8H_6\{Si^iMe_3\text{-}1,4\}_2)$ and $K_2(C_8H_4\{Si^iPr_3\text{-}1,4\}_2)$ were donated by Prof. F. G. N. Cloke and Ind^{Me7} by Prof. D. O'Hare, Oxford University. KTp^{Me2} and $KTp^{tBu,Me}$ were generously donated by Dr Andrea Sella, University College London and KTp^{Me2} and KTp by Dr I. R. Crossley, University of Sussex. The neutral ligand species, Cp^{Me5}, Cp^{Me4H} and Ind^{Me7} were deprotonated using $K(N(SiMe_3)_2)$ in toluene and $C_8H_8\{Si^iPr_3\text{-}1,4\}_2$ was deprotonated by KNH_2 to give $K_2(C_8H_6\{Si^iPr_3\text{-}1,4\}_2)$. UI_3,[8] MeNC[9] and $C_8H_8\{Si^iPr_3\text{-}1,4\}_2$[10] were synthesised according to published procedure.

A1.6 References:

[1] D. F. Shriver, *The Manipulation of Air-Sensitive Compounds*, Mc-Graw-Hill, 1989.

[2] a) C. Fonseca Guerra, J. G. Snijder, G. Te Velde and E. J. Baerends, *Theor. Chem. Acc.*,1998, **99**, 391. b) G. Te Velde, F. M. Bickelhaupt, E. J. Baerends, C. Fonseca Guerra, S. J. A. Van Gisbergen, J. G. Snijders and T. Ziegler, *J. Comput. Chem*., 2001, **22**, 931. c) ADF2008.01, SCM, Theoretical Chemistry, Vrije Universiteit, Amsterdam, The Netherlands, http://www.scm.com.

[3] a) E. Vanlenthe, E. J. Baerends and J. G. Snijders, *J. Chem. Phys.*, 1993, **99**, 4597. b) *Ibid*., 1994, **101**, 9783. c) *Ibid.*,1996, **105**, 6505. d) E. Vanlenthe, A. Ehlers and E. J. Baerends, *J. Chem. Phys.*, 1999, **110**, 8943. e) E. Vanlenthe, R. VanLeeuwen, E. J. Baerends and J. G. Snijders, *Int. J. Quantum Chem.*, 1996, **57**, 281.

[4] S. H. Vosko, L. Wilk, and M. Nusair, *Can. J. Phys*., 1980, **58**, 1200.

[5] A. D. Becke, Physical Review A: Atomic, Molecular, and Optical Physics, 1988, **38**, 3098.

[6] J. P. Perdew, M. Levy, G. S. Painter and S. Wei, *Physical Review B: Condensed Matter and Materials Physics*, 1988, **37**, 838.

[7] W. L. F. Armarego, D. D. Perrin and D. R. Perrin, *Purification of Laboratory Chemicals*, Pergamon, 1985.

[8] F. G. Cloke and P. B. Hitchcock, *J. Am. Chem. Soc.*, 2002, **124**, 9352. For greater detail see: G. K. B. Clentsmith, F. G. N. Cloke, M. D. Francis, J. R. Hanks, P. B. Nixon and J. F. Nixon, *J. Organomet. Chem.*, 2008, **693**, 2287. See also: J. D. Corbett, *Inorg. Synth.*, 1983, **22**, 31.

[9] a) R. E. Schuster, J. E. Scott and J. Casanova J. Jr., *Organic Syntheses*, 1973, **5**, 772. b) *Ibid.*, 1966, **46**, 75.

[10] See: N. C. Burton, F. G. N. Cloke, P. B. Hitchcock, H. de Lemos and A. A. Sameh, *J. Chem. Soc. Chem. Commun.*, 1989, 1462.

Appendix Two: Crystallographic Data Tables And Full Crystallographic Data

Table 1.

Crystal structure and refinement data for Chapter Two: [U(η^5-Cp^{Me4H})(η^8-C_8H_6{Si^iPr_3-1,4}$_2$)(η^1-NCMe)] (**2.3**) and [U(η^5-Cp^{Me5})(η^8-C_8H_6{Si^iPr_3-1,4}$_2$)(η^1-CNMe)] (**2.4**).

Formula	$C_{37}H_{64}NSi_2U.(C_4H_8O)$	$C_{38}H_{66}NSi_2U.(C_6H_6)$
Formula weight	889.21	909.23
Temperature/ K	173(2)	173(2)
Wavelength/ Å	0.71073	0.71073
Crystal size/ mm	0.40×0.04×0.01	0.24×0.22×0.09
Crystal system	Monoclinic	Monoclinic
Space group	*P2$_1$*/m (No. 11)	*P2$_1$*/c (No. 14)
a/ Å	9.1365(4)	11.5001(2)
b/ Å	20.7810(11)	20.3108(2)
c/ Å	11.3353(5)	18.6771(2)
α/ °	90	90
β/ °	97.773(3)	93.6370(10)
γ/ °	90	90
V/ Å^3	2132.41(17)	4353.74(10)
Z	2	4
D_c/ Mg m^{-3}	1.39	1.39
Absorption coefficient / mm^{-1}	3.89	3.81
θ range for data collection	3.46 to 26.04	3.43 to 27.90

/ °

Reflections collected	11447	70468
Independent reflections	4255	10212
	[R_{int} = 0.077]	[R_{int} = 0.071]
Reflections with $I > 2\sigma(I)$	3458	8249
Data/ restraints/ parameters	4255 / 0 / 230	10212 / 0 / 410
Goodness-of-fit on F^2	1.075	1.056
Final R indices [$I > 2\sigma(I)$]	R_1 = 0.051	R_1 = 0.034
	wR_2 = 0.092	wR_2 = 0.058
R indices (all data)	R_1 = 0.072	R_1 = 0.052
	wR_2 = 0.092	wR_2 = 0.063
Largest peak/ hole/ e Å^{-3}	1.24 and –0.74*	0.10 and –0.75*

* close to uranium

Table 2.

Crystal structure and refinement data for Chapter Three: [U(κ^3-Tp^{Me2})(η^8-C_8H_6{Si^{i}Pr$_3$-1,4}$_2$)] (**3.1**), [U(κ^3-Tp^{Me2})(η^8-C_8H_4{Si^{i}Pr$_3$-1,4}$_2$)] (**3.2**) and [U(η^8-C_8H_6{Si^{i}Pr$_3$-1,4}$_2$)(κ^2-dmpz)$_2$(η^1-CNMe)] (**3.3**).

Formula	$C_{41}H_{70}BN_6Si_2U$	$C_{41}H_{68}BN_6Si_2U$	$C_{38}H_{65}N_5Si_2U$
Formula weight	952.05	950.03	886.16
Temperature/ K	173(2)	173(2)	173(2)
Wavelength/ Å	0.71073	0.71073	0.71073
Crystal size/ mm	0.18×0.16×0.05	0.30×0.28×0.02	0.28×0.14×0.08
Crystal system	Triclinic	Monoclinic	Monoclinic
Space group	$P\bar{1}$ (No. 2)	$P2_1/c$ (No. 14)	$P2_1/c$ (No. 14)
a/ Å	14.7539(3)	11.1026(2)	11.1426(1)
b/ Å	16.6976(3)	26.7178(6)	15.3770(2)
c/ Å	18.9057(3)	16.7781(3)	25.9618(3)
α/ °	78.877(1)	90	90
β/ °	80.450(1)	117.665(1)	109.926(1)
γ/ °	78.412(1)	90	90
V/ Å^3	4437.53(14)	4408.02(15)	4181.98(8)
Z	4	4	4
D_c/ Mg m^{-3}	1.43	1.43	1.41
Absorption coefficient / mm^{-1}	3.75	3.77	3.97
θ range for data collection / °	3.43 to 27.12	3.43 to 27.48	3.50 to 27.86
Reflections collected	79818	53016	68954
Independent reflections	19539 [R_{int} = 0.092]	9985 [R_{int} = 0.095]	9892 [R_{int} = 0.058]

Reflections with $I > 2\sigma(I)$	11968	8271	8796
Data/ restraints/ parameters	19539 / 7 / 959	9985 / 7 / 488	9892 / 0 / 420
Goodness-of-fit on F^2	1.019	1.239	1.097
Final R indices [$I > 2\sigma(I)$]	$R_1 = 0.045$	$R_1 = 0.064$	$R_1 = 0.025$
	$wR_2 = 0.084$	$wR_2 = 0.142$	$wR_2 = 0.050$
R indices (all data)	$R_1 = 0.097$	$R_1 = 0.081$	$R_1 = 0.032$
	$wR_2 = 0.099$	$wR_2 = 0.148$	$wR_2 = 0.052$
Largest peak/ hole/ e Å^{-3}	1.10 and –2.24*	4.14 and –2.78*	0.97 and –1.18

* close to uranium

Table 3.

Crystal structure and refinement data for Chapter Four: [U(η^5-Ind^{Me6})(η^8-C_8H_6{Si^{i}Pr$_3$-1,4}$_2$)] (**4.1**), [U(η^5-Ind^{Me7})(η^8-C_8H_4{Si^{i}Pr$_3$-1,4}$_2$)] (**4.2**) and [(U(η^5-Ind^{Me6})(η^8-C_8H_6{Si^{i}Pr$_3$-1,4}$_2$))$_2$(μ-η^2:η^2-C_4O_4)] (**4.3**).

Formula	$C_{41}H_{67}Si_2U$	$C_{42}H_{69}Si_2U$	$C_{86}H_{134}O_4Si_4U_2.(C_5H_{12})_4$
Formula weight	854.16	868.18	2108.94
Temperature/ K	173(2)	173(2)	173(2)
Wavelength/ Å	0.71073	0.71073	0.71073
Crystal size/ mm	0.20×0.03×0.01	0.22×0.15×0.06	0.25×0.1×0.05
Crystal system	Monoclinic	Monoclinic	Monoclinic
Space group	*P*2$_1$/n (No. 14)	*P*2$_1$/n (No. 14)	*C2*/m (No. 12)
a/ Å	15.2508(2)	15.2615(1)	25.7129(11)
b/ Å	26.5518(2)	26.6255(3)	20.1749(9)
c/ Å	19.8423(2)	20.1330(2)	12.0421(4)
α/ °	90	90	90
β/ °	96.332(1)	96.016(1)	116.292(2)
γ/ °	90	90	90
V/ Å^3	7985.8(2)	8135.89(13)	5600.6(4)
Z	8	8	2
D_c/ Mg m^{-3}	1.42	1.42	1.25
Absorption coefficient / mm^{-1}	4.15	4.08	2.98
θ range for data collection / °	3.46 to 26.01	3.41 to 27.48	3.47 to 26.04
Reflections collected	112708	113101	33000
Independent reflections	15662	18524	5653

	[R_{int} = 0.184]	[R_{int} = 0.087]	[R_{int} = 0.075]
Reflections with $I > 2\sigma(I)$	9603	13965	4855
Data/ restraints/ parameters	15662 / 0 / 829	18524 / 0 / 825	5653 / 12 / 256
Goodness-of-fit on F^2	1.036	1.041	1.133
Final R indices [$I > 2\sigma(I)$]	R_1 = 0.062	R_1 = 0.046	R_1 = 0.040
	wR_2 = 0.076	wR_2 = 0.077	wR_2 = 0.090
R indices (all data)	R_1 = 0.132	R_1 = 0.076	R_1 = 0.054
	wR_2 = 0.090	wR_2 = 0.085	wR_2 = 0.095
Largest peak/ hole/ e Å^{-3}	0.71 and –0.80	2.318 and –1.007*	0.90 and –0.98*

* close to uranium

Full Crystallographic Data:

Complex	Identification code	Page Number
[U(η^5-Cp^{Me4H})(η^8-C_8H_6{Si^{i}Pr$_3$-1,4}$_2$)(η^1-NCMe)] (**2.3**)	feb107	222
[U(η^5-Cp^{Me5})(η^8-C_8H_6{Si^{i}Pr$_3$-1,4}$_2$)(η^1-CNMe)] (**2.4**)	jun209	228
[U(κ^3-Tp^{Me2})(η^8-C_8H_6{Si^{i}Pr$_3$-1,4}$_2$)] (**3.1**)	nov609b	237
[U(κ^3-Tp^{Me2})(η^8-C_8H_4{Si^{i}Pr$_3$-1,4}$_2$)] (**3.2**)	apr709	253
[U(η^8-C_8H_6{Si^{i}Pr$_3$-1,4}$_2$)(κ^2-dmpz)$_2$(η^1-CNMe)] (**3.3**)	aug109	263
[U(η^5-Ind^{Me6})(η^8-C_8H_6{Si^{i}Pr$_3$-1,4}$_2$)] (**4.1**)	apr508	272
[U(η^5-Ind^{Me7})(η-C_8H_4{Si^{i}Pr$_3$-1,4}$_2$)] (**4.2**)	jul509	290
[(U(η^5-Ind^{Me6})(η^8-C_8H_6{Si^{i}Pr$_3$-1,4}$_2$))$_2$(μ-η^2:η^2-C_4O_4)] (**4.3**)	mar1308	307

CCDC 758454-758456 contain the supplementary crystallographic data for Chapter 3 (**3.1, 3.2, 3.3**). These can be obtained free of charge from The Cambridge

Crystallographic Data Centre via www.ccdc.cam.ac.uk/data_request.cif

Table 4.

Crystal data and structure refinement for **2.3**

[U(η^5-Cp^{Me4H})(η^8-C_8H_6{Si^{i}Pr$_3$-1,4}$_2$)(η^1-NCMe)]·THF

Identification code	feb107	
Empirical formula	C37 H64 N Si2 U . C4 H8 O	
Formula weight	889.21	
Temperature	173(2) K	
Wavelength	0.71073 Å	
Crystal system	Monoclinic	
Space group	$P2_1/m$ (No.11)	
Unit cell dimensions	a = 9.1365(4) Å	α= 90°.
	b = 20.7810(11) Å	β= 97.773(3)°.
	c = 11.3353(5) Å	γ = 90°.
Volume	2132.41(17) Å^3	
Z	2	
Density (calculated)	1.39 Mg/m^3	
Absorption coefficient	3.89 mm^{-1}	
F(000)	906	
Crystal size	0.40 x 0.04 x 0.01 mm^3	
Theta range for data collection	3.46 to 26.04°.	
Index ranges	-9<=h<=11, -19<=k<=25, -13<=l<=12	
Reflections collected	11447	
Independent reflections	4255 [R(int) = 0.077]	
Reflections with I>2sigma(I)	3458	
Completeness to theta = 26.04°	98.5 %	
Tmax. and Tmin.	0.9602 and 0.7676	
Refinement method	Full-matrix least-squares on F^2	
Data / restraints / parameters	4255 / 0 / 230	
Goodness-of-fit on F^2	1.075	
Final R indices [I>2sigma(I)]	R1 = 0.051, wR2 = 0.092	

R indices (all data) R1 = 0.072, wR2 = 0.099

Largest diff. peak and hole 1.24 and -0.74 e.Å^{-3} (near U)

The molecule lies on a crystallographic mirror plane with the 'missing' methyl; group of the Me4C5H ring disordered between the two C(17) positions related by the mirror plane.

Data collection KappaCCD , Program package WinGX , Abs correction analytical ,

Refinement using SHELXL-97 , Drawing using ORTEP-3 for Windows

Table 5.

Atomic coordinates (x 10^4) and equivalent isotropic displacement parameters (Å^{2}x 10^3)

for feb107. U(eq) is defined as one third of the trace of the orthogonalized U^{ij} tensor.

	x	y	z	U(eq)
U	8164(1)	2500	526(1)	33(1)
Si	7212(2)	4180(1)	2572(2)	44(1)
N	10738(9)	2500	1794(8)	47(2)
C(1)	6822(7)	3353(3)	1895(6)	33(1)
C(2)	5982(7)	3325(3)	750(6)	38(2)
C(3)	5341(6)	2843(3)	-9(6)	38(2)
C(4)	7374(6)	2842(3)	2683(6)	33(1)
C(5)	9152(9)	4464(4)	2431(8)	61(2)
C(6)	9426(11)	4476(5)	1131(9)	95(3)
C(7)	10367(8)	4063(4)	3166(9)	73(3)
C(8)	7080(8)	4142(3)	4237(7)	52(2)
C(9)	7390(12)	4788(4)	4861(9)	86(3)
C(10)	5657(9)	3835(4)	4556(7)	67(2)
C(11)	5867(9)	4778(3)	1730(7)	54(2)
C(12)	4240(10)	4648(4)	1803(8)	76(3)
C(13)	6232(13)	5491(4)	2051(10)	98(4)
C(14)	10112(8)	2836(3)	-1000(6)	51(2)
C(15)	8751(8)	3051(4)	-1605(7)	50(2)

C(16)	7925(11)	2500	-1973(8)	48(3)
C(17)	11377(14)	3304(8)	-596(14)	58(4)*
C(18)	8319(11)	3736(4)	-1934(8)	77(3)
C(19)	6487(13)	2500	-2788(11)	75(4)
C(20)	11957(13)	2500	2156(10)	55(3)
C(21)	13507(11)	2500	2624(11)	76(4)
O(1S)	3101(13)	2500	5484(13)	136(4)
C(1S)	2343(17)	1987(7)	5926(17)	167(7)
C(2S)	802(15)	2154(7)	5787(13)	171(9)

*** occupancy 0.5**

Table 6.

Bond lengths [Å] and angles [°] for feb107.

U-M(1)	1.972(6)
U-M(2)	2.502(6)
U-N	2.586(8)
U-C(3)	2.665(6)
U-C(2)	2.667(6)
U-C(14)	2.735(6)
U-C(4)	2.736(6)
U-C(1)	2.751(6)
Si-C(5)	1.895(8)
Si-C(1)	1.897(6)
Si-C(8)	1.909(8)
Si-C(11)	1.911(7)
N-C(20)	1.133(13)
C(1)-C(2)	1.417(9)
C(1)-C(4)	1.434(8)
C(2)-C(3)	1.397(9)
C(3)-C(3)’	1.426(12)
C(4)-C(4)’	1.423(12)

C(5)-C(6)	1.527(12)
C(5)-C(7)	1.540(12)
C(8)-C(9)	1.525(10)
C(8)-C(10)	1.534(10)
C(11)-C(12)	1.524(11)
C(11)-C(13)	1.551(10)
C(14)-C(14)’	1.395(14)
C(14)-C(15)	1.409(10)
C(14)-C(17)	1.533(15)
C(15)-C(16)	1.403(9)
C(15)-C(18)	1.511(10)
C(16)-C(15)’	1.403(9)
C(16)-C(19)	1.500(15)
C(20)-C(21)	1.444(16)
O(1S)-C(1S)	1.402(12)
C(1S)-C(2S)	1.437(18)
C(2S)-C(2S)’	1.44(3)

M(1)-U-M(2)	145.5(2)
M(1)-U-N	119.3(2)
M(2)-U-N	95.2(2)
C(5)-Si-C(1)	112.0(3)
C(5)-Si-C(8)	106.4(4)
C(1)-Si-C(8)	109.2(3)
C(5)-Si-C(11)	107.5(4)
C(1)-Si-C(11)	108.3(3)
C(8)-Si-C(11)	113.5(3)
C(20)-N-U	167.6(8)
C(2)-C(1)-C(4)	129.9(6)
C(2)-C(1)-Si	117.2(5)
C(4)-C(1)-Si	112.8(5)
C(3)-C(2)-C(1)	136.3(6)

C(2)-C(3)-C(3)’	135.8(4)
C(4)’-C(4)-C(1)	137.7(4)
C(6)-C(5)-C(7)	109.3(8)
C(6)-C(5)-Si	111.3(6)
C(7)-C(5)-Si	113.6(5)
C(9)-C(8)-C(10)	111.5(6)
C(9)-C(8)-Si	112.9(6)
C(10)-C(8)-Si	114.8(6)
C(12)-C(11)-C(13)	109.8(7)
C(12)-C(11)-Si	115.0(5)
C(13)-C(11)-Si	113.6(6)
C(14)’-C(14)-C(15)	108.5(4)
C(14)’-C(14)-C(17)	129.4(7)
C(15)-C(14)-C(17)	121.6(9)
C(16)-C(15)-C(14)	106.8(7)
C(16)-C(15)-C(18)	125.7(8)
C(14)-C(15)-C(18)	127.1(7)
C(15)-C(16)-C(15)’	109.4(9)
C(15)-C(16)-C(19)	125.0(5)
C(15)’-C(16)-C(19)	125.0(5)
N-C(20)-C(21)	179.7(12)
C(1S)-O(1S)-C(1S)’	99.1(15)
O(1S)-C(1S)-C(2S)	107.5(12)
C(1S)-C(2S)-C(2S)’	104.0(8)

Symmetry transformations used to generate equivalent atoms: ‘ x,-y+1/2,z

M(1) and M(2) are the centroids of the 8 and 5 membered rings respectively

8.2522 (0.0087) x + 0.0000 (0.0004) y - 6.2050 (0.0211) z = 4.4396 (0.0089)

* 0.0142 (0.0047) C1_a

```
*    0.0321 (0.0049)  C2_a
*   -0.0268 (0.0034)  C3_a
*   -0.0194 (0.0033)  C4_a
*    0.0142 (0.0047)  C1_$1a
*    0.0321 (0.0049)  C2_$1a
*   -0.0268 (0.0034)  C3_$1a
*   -0.0194 (0.0033)  C4_$1a
     1.9709 (0.0028)  U
    -0.0839 (0.0047)  Si_a

Rms deviation of fitted atoms =   0.0241


 4.6487 (0.0378) x + 0.0000 (0.0002) y - 10.4487 (0.0211) z = 5.7453
(0.0317)

Angle to previous plane (with approximate esd) = 34.00 ( 0.37 )

*    0.0002 (0.0018)  C14_a
*   -0.0007 (0.0049)  C15_a
*    0.0008 (0.0061)  C16_a
*    0.0002 (0.0018)  C14_$1a
*   -0.0007 (0.0049)  C15_$1a
    -2.4995 (0.0041)  U
     0.1663 (0.0186)  C17_a
     0.1428 (0.0106)  C18_a
     0.1829 (0.0183)  C19_a

Rms deviation of fitted atoms =   0.0006
```

Table 7.

Crystal data and structure refinement for **2.4**

$[U(\eta^5\text{-}Cp^{Me5})(\eta^8\text{-}C_8H_6\{Si^iPr_3\text{-}1,4\}_2)(\eta^1\text{-}CNMe)]\cdot C_6H_6$

Identification code	jun209	
Empirical formula	C38 H66 N Si2 U, C6 H6	
Formula weight	909.23	
Temperature	173(2) K	
Wavelength	0.71073 Å	
Crystal system	Monoclinic	
Space group	P 21/c (No.14)	
Unit cell dimensions	a = 11.5001(2) Å	α= 90°.
	b = 20.3108(2) Å	β= 93.6370(10)°.
	c = 18.6771(2) Å	γ = 90°.
Volume	4353.74(10) $Å^3$	
Z	4	
Density (calculated)	1.39 Mg/m^3	
Absorption coefficient	3.81 mm^{-1}	
F(000)	1852	
Crystal size	0.24 x 0.22 x 0.09 mm^3	
Theta range for data collection	3.43 to 27.90°.	
Index ranges	-14<=h<=14, -26<=k<=26, -24<=l<=24	
Reflections collected	70468	
Independent reflections	10212 [R(int) = 0.071]	
Reflections with I>2sigma(I)	8249	
Completeness to theta = 27.90°	98.1 %	
Absorption correction	Semi-empirical from equivalents	
Tmax. and Tmin.	0.5823 and 0.4367	
Refinement method	Full-matrix least-squares on F^2	
Data / restraints / parameters	10212 / 0 / 410	
Goodness-of-fit on F^2	1.056	

Final R indices [I>2sigma(I)]	R1 = 0.034, wR2 = 0.058
R indices (all data)	R1 = 0.052, wR2 = 0.063
Largest diff. peak and hole	0.10 and -0.75 e.Å^{-3} (close to U)

The disordered benzene solvate was modeled as a rigid body over two orientations

Data collection KappaCCD , Program package WinGX , Abs correction MULTISCAN

Refinement using SHELXL-97 , Drawing using ORTEP-3 for Windows

Table 8.

Atomic coordinates (x 10^4) and equivalent isotropic displacement parameters (Å^{2}x 10^3)

for jun209. U(eq) is defined as one third of the trace of the orthogonalized U^{ij} tensor.

	x	y	z	U(eq)
U	5379(1)	2397(1)	6398(1)	20(1)
Si(1)	7391(1)	4150(1)	5939(1)	22(1)
Si(2)	7649(1)	727(1)	5954(1)	24(1)
N	7036(3)	2397(2)	8225(2)	35(1)
C(1)	6794(3)	3290(2)	5772(2)	22(1)
C(2)	7542(3)	2783(2)	6072(2)	22(1)
C(3)	7588(3)	2091(2)	6091(2)	23(1)
C(4)	6901(3)	1553(2)	5812(2)	22(1)
C(5)	5868(3)	1553(2)	5355(2)	26(1)
C(6)	5142(3)	2034(2)	5013(2)	27(1)
C(7)	5091(3)	2726(2)	5002(2)	26(1)
C(8)	5745(3)	3238(2)	5337(2)	24(1)
C(9)	7061(3)	4483(2)	6852(2)	34(1)
C(10)	5746(4)	4477(2)	6944(3)	58(1)
C(11)	7705(5)	4138(2)	7483(2)	54(1)
C(12)	9038(3)	4116(2)	5917(2)	29(1)
C(13)	9507(3)	3743(2)	5277(2)	38(1)

C(14)	9619(3)	4794(2)	5995(2)	40(1)
C(15)	6683(3)	4734(2)	5244(2)	27(1)
C(16)	6932(4)	4574(2)	4470(2)	41(1)
C(17)	6911(4)	5469(2)	5392(2)	47(1)
C(18)	8440(4)	679(2)	6878(2)	39(1)
C(19)	9306(5)	115(3)	6968(3)	77(2)
C(20)	7656(6)	694(3)	7506(3)	79(2)
C(21)	6606(3)	16(2)	5761(2)	35(1)
C(22)	5623(4)	-43(2)	6267(3)	60(1)
C(23)	7242(4)	-648(2)	5728(3)	55(1)
C(24)	8791(3)	665(2)	5266(2)	30(1)
C(25)	8242(4)	651(2)	4497(2)	44(1)
C(26)	9714(4)	1206(2)	5337(2)	45(1)
C(27)	2974(3)	2364(2)	6276(2)	30(1)
C(28)	3247(3)	2898(2)	6743(2)	29(1)
C(29)	3763(3)	2639(2)	7395(2)	30(1)
C(30)	3799(3)	1947(2)	7324(2)	32(1)
C(31)	3300(3)	1776(2)	6639(2)	31(1)
C(32)	2286(3)	2414(2)	5567(2)	44(1)
C(33)	2904(4)	3608(2)	6599(2)	44(1)
C(34)	4039(4)	3025(2)	8067(2)	45(1)
C(35)	4178(4)	1462(2)	7908(2)	50(1)
C(36)	3042(4)	1089(2)	6365(3)	52(1)
C(37)	6553(3)	2403(2)	7672(2)	36(1)
C(38)	7613(4)	2395(2)	8926(2)	55(1)
C(39)	815(7)	2707(5)	8722(4)	57(3)
C(40)	538(7)	3036(2)	8081(7)	72(3)
C(41)	486(6)	2692(5)	7436(4)	47(2)
C(42)	712(6)	2020(5)	7432(3)	35(2)
C(43)	989(6)	1691(2)	8073(6)	52(3)
C(44)	1040(6)	2034(5)	8718(3)	53(3)
C(39A)	725(6)	2435(5)	8820(2)	50(3)

C(40A)	477(6)	2987(3)	8396(5)	46(2)
C(41A)	418(6)	2933(4)	7653(5)	53(3)
C(42A)	607(7)	2328(6)	7333(2)	49(3)
C(43A)	854(7)	1776(3)	7756(6)	61(3)
C(44A)	913(7)	1830(3)	8500(6)	63(3)
M(1)	6334(4)	2409(16)	5557(2)	10
M(2)	3417(4)	2325(16)	6876(2)	10

M(1) = centroid of COT ring; M(2) = centroid of Cp* ring

Table 9.

Bond lengths [Å] and angles [°] for jun209.

U-M(1)	1.974(5)
U-M(2)	2.482(5)
U-C(37)	2.660(4)
U-C(8)	2.670(3)
U-C(5)	2.680(3)
U-C(6)	2.687(3)
U-C(7)	2.693(3)
U-C(3)	2.712(3)
U-C(2)	2.714(3)
U-C(4)	2.728(3)
U-C(30)	2.743(3)
U-C(1)	2.748(3)
Si(1)-C(9)	1.895(4)
Si(1)-C(1)	1.897(3)
Si(1)-C(12)	1.898(4)
Si(1)-C(15)	1.902(3)
Si(2)-C(21)	1.896(4)
Si(2)-C(4)	1.896(3)
Si(2)-C(24)	1.898(4)

Si(2)-C(18)	1.902(4)
N-C(37)	1.142(5)
N-C(38)	1.430(5)
C(1)-C(8)	1.414(5)
C(1)-C(2)	1.432(4)
C(2)-C(3)	1.406(4)
C(3)-C(4)	1.428(5)
C(4)-C(5)	1.419(5)
C(5)-C(6)	1.411(5)
C(6)-C(7)	1.408(4)
C(7)-C(8)	1.407(4)
C(9)-C(11)	1.521(6)
C(9)-C(10)	1.532(6)
C(12)-C(14)	1.532(5)
C(12)-C(13)	1.542(5)
C(15)-C(16)	1.525(5)
C(15)-C(17)	1.538(5)
C(18)-C(19)	1.519(6)
C(18)-C(20)	1.524(6)
C(21)-C(22)	1.525(5)
C(21)-C(23)	1.538(5)
C(24)-C(26)	1.529(5)
C(24)-C(25)	1.533(5)
C(27)-C(31)	1.414(5)
C(27)-C(28)	1.414(5)
C(27)-C(32)	1.503(5)
C(28)-C(29)	1.422(5)
C(28)-C(33)	1.515(5)
C(29)-C(30)	1.413(5)
C(29)-C(34)	1.497(5)
C(30)-C(31)	1.412(5)
C(30)-C(35)	1.512(5)

C(31)-C(36)	1.509(5)

M(1)-U-M(2)	148.3(2)
M(1)-U-C(37)	115.81(15)
M(2)-U-C(37)	95.77(12)
C(9)-Si(1)-C(1)	112.67(15)
C(9)-Si(1)-C(12)	106.83(17)
C(1)-Si(1)-C(12)	108.32(15)
C(9)-Si(1)-C(15)	106.90(16)
C(1)-Si(1)-C(15)	109.05(15)
C(12)-Si(1)-C(15)	113.13(16)
C(21)-Si(2)-C(4)	111.79(16)
C(21)-Si(2)-C(24)	106.11(16)
C(4)-Si(2)-C(24)	106.96(15)
C(21)-Si(2)-C(18)	113.21(18)
C(4)-Si(2)-C(18)	110.97(15)
C(24)-Si(2)-C(18)	107.37(18)
C(37)-N-C(38)	178.5(4)
C(8)-C(1)-C(2)	129.8(3)
C(8)-C(1)-Si(1)	116.7(2)
C(2)-C(1)-Si(1)	113.3(2)
C(3)-C(2)-C(1)	138.5(3)
C(2)-C(3)-C(4)	137.5(3)
C(5)-C(4)-C(3)	130.0(3)
C(5)-C(4)-Si(2)	116.0(2)
C(3)-C(4)-Si(2)	113.1(2)
C(6)-C(5)-C(4)	136.2(3)
C(7)-C(6)-C(5)	136.2(3)
C(8)-C(7)-C(6)	135.3(3)
C(7)-C(8)-C(1)	136.3(3)
C(11)-C(9)-C(10)	110.2(4)
C(11)-C(9)-Si(1)	114.7(3)

C(10)-C(9)-Si(1)	110.7(3)
C(14)-C(12)-C(13)	110.1(3)
C(14)-C(12)-Si(1)	113.2(3)
C(13)-C(12)-Si(1)	115.6(2)
C(16)-C(15)-C(17)	109.6(3)
C(16)-C(15)-Si(1)	114.6(2)
C(17)-C(15)-Si(1)	114.9(3)
C(19)-C(18)-C(20)	110.2(4)
C(19)-C(18)-Si(2)	114.3(3)
C(20)-C(18)-Si(2)	115.2(3)
C(22)-C(21)-C(23)	109.2(3)
C(22)-C(21)-Si(2)	115.3(3)
C(23)-C(21)-Si(2)	112.2(3)
C(26)-C(24)-C(25)	109.7(3)
C(26)-C(24)-Si(2)	113.6(3)
C(25)-C(24)-Si(2)	111.9(3)
C(31)-C(27)-C(28)	108.1(3)
C(31)-C(27)-C(32)	126.0(3)
C(28)-C(27)-C(32)	125.2(3)
C(27)-C(28)-C(29)	108.0(3)
C(27)-C(28)-C(33)	125.1(3)
C(29)-C(28)-C(33)	126.5(3)
C(30)-C(29)-C(28)	107.5(3)
C(30)-C(29)-C(34)	126.5(3)
C(28)-C(29)-C(34)	125.3(3)
C(31)-C(30)-C(29)	108.5(3)
C(31)-C(30)-C(35)	125.1(4)
C(29)-C(30)-C(35)	126.0(4)
C(30)-C(31)-C(27)	107.9(3)
C(30)-C(31)-C(36)	126.5(4)
C(27)-C(31)-C(36)	125.4(4)

Least-squares planes (x,y,z in crystal coordinates) and deviations from them

(* indicates atom used to define plane)

- 6.8474 (0.0084) x - 0.1797 (0.0182) y + 15.6798 (0.0092) z = 4.3325 (0.0115)

* 0.0060 (0.0026) C1

* -0.0266 (0.0026) C2

* -0.0161 (0.0026) C3

* 0.0279 (0.0026) C4

* 0.0191 (0.0027) C5

* -0.0297 (0.0027) C6

* -0.0245 (0.0027) C7

* 0.0439 (0.0027) C8

-0.1560 (0.0037) Si1

-0.2477 (0.0037) Si2

1.9735 (0.0012) U

Rms deviation of fitted atoms = 0.0264

- 10.6798 (0.0075) x - 1.2762 (0.0375) y + 7.9139 (0.0299) z = 1.4953 (0.0248)

Angle to previous plane (with approximate esd) = 32.09 (0.14)

* -0.0064 (0.0022) C27

* 0.0031 (0.0022) C28

* 0.0014 (0.0022) C29

* -0.0053 (0.0022) C30

* 0.0072 (0.0022) C31

0.1606 (0.0065) C32

0.1657 (0.0069) C33

0.1887 (0.0066) C34

0.1143 (0.0068) C35

0.1543 (0.0069) C36

Rms deviation of fitted atoms = 0.0052

Table 10.

Crystal data and structure refinement for **3.1**

$[U(\kappa^3\text{-}Tp^{Me2})(\eta^8\text{-}C_8H_6\{Si^iPr_3\text{-}1,4\}_2)]$

Identification code	nov609b	
Empirical formula	C41 H70 B N6 Si2 U	
Formula weight	952.05	
Temperature	173(2) K	
Wavelength	0.71070 Å	
Crystal system	Triclinic	
Space group	$P\bar{1}$ (No.2)	
Unit cell dimensions	a = 14.7539(3) Å	α= 78.877(1)°.
	b = 16.6976(3) Å	β= 80.450(1)°.
	c = 18.9057(3) Å	γ = 78.412(1)°.
Volume	4437.53(14) $Å^3$	
Z	4	
Density (calculated)	1.43 Mg/m^3	
Absorption coefficient	3.75 mm^{-1}	
F(000)	1932	
Crystal size	0.18 x 0.16 x 0.05 mm^3	
Theta range for data collection	3.43 to 27.12°.	
Index ranges	-18<=h<=18, -21<=k<=21, -24<=l<=24	
Reflections collected	79818	
Independent reflections	19539 [R(int) = 0.092]	
Reflections with I>2sigma(I)	11968	
Completeness to theta = 27.12°	99.6 %	
Absorption correction	Semi-empirical from equivalents	
Tmax. and Tmin.	0.7160and 0.5215	
Refinement method	Full-matrix least-squares on F^2	
Data / restraints / parameters	19539 / 7 / 959	
Goodness-of-fit on F^2	1.019	

Final R indices [I>2sigma(I)]	R1 = 0.045, wR2 = 0.084
R indices (all data)	R1 = 0.097, wR2 = 0.099
Largest diff. peak and hole	1.10 and -2.24 e.Å^{-3} (near to Uranium)

Two molecules in the unit cell; an iso-propyl groups of one of the COT rings is disordered

Data collection KappaCCD , Program package WinGX , Abs correction MULTISCAN

Refinement using SHELXL-97 , Drawing using ORTEP-3 for Windows

Table 11.

Atomic coordinates (x 10^4) and equivalent isotropic displacement parameters (Å^{2}x 10^3)

for nov609b. U(eq) is defined as one third of the trace of the orthogonalized U^{ij} tensor.

	x	y	z	U(eq)
U	2768(1)	5777(1)	3009(1)	17(1)
Si(1)	3219(1)	7767(1)	4129(1)	18(1)
Si(2)	5587(1)	4590(1)	2273(1)	30(1)
N(1)	997(3)	5924(3)	3415(2)	22(1)
N(2)	645(3)	5214(3)	3730(2)	22(1)
N(3)	2614(3)	4579(3)	4142(2)	24(1)
N(4)	1998(3)	4071(3)	4096(2)	26(1)
N(5)	2087(3)	4762(3)	2400(3)	26(1)
N(6)	1488(3)	4284(3)	2842(3)	26(1)
C(1)	3397(4)	7083(3)	3406(3)	15(1)
C(2)	4077(4)	6353(3)	3541(3)	19(1)
C(3)	4566(4)	5710(3)	3156(3)	21(1)
C(4)	4631(4)	5494(3)	2450(3)	21(1)
C(5)	4131(4)	5901(3)	1867(3)	22(1)
C(6)	3429(4)	6602(3)	1720(3)	22(1)
C(7)	2917(4)	7220(3)	2105(3)	20(1)
C(8)	2905(4)	7412(3)	2803(3)	18(1)

C(9)	4398(4)	7717(3)	4436(3)	24(1)
C(10)	5195(4)	7816(4)	3806(3)	36(2)
C(11)	4380(5)	8327(4)	4952(4)	39(2)
C(12)	2702(4)	8866(3)	3737(3)	27(1)
C(13)	3311(5)	9261(4)	3080(4)	41(2)
C(14)	2396(5)	9467(4)	4282(4)	44(2)
C(15)	2388(4)	7412(4)	4961(3)	28(2)
C(16)	2732(5)	6535(4)	5332(4)	48(2)
C(17)	1398(4)	7468(4)	4781(4)	36(2)
C(18)	5243(6)	3547(4)	2613(4)	53(2)
C(19)	4360(6)	3455(5)	2339(6)	88(3)
C(20)	5149(9)	3277(7)	3400(5)	118(5)
C(21)	6602(4)	4625(4)	2763(4)	41(2)
C(22)	7484(5)	3993(4)	2551(4)	49(2)
C(23)	6866(5)	5450(4)	2743(4)	43(2)
C(24)	5899(5)	4651(4)	1249(4)	45(2)
C(25)	6547(6)	3890(5)	986(5)	80(3)
C(26)	6256(6)	5458(5)	872(4)	63(2)
C(27)	282(4)	6561(3)	3458(3)	20(1)
C(28)	-515(4)	6269(4)	3812(3)	29(1)
C(29)	-285(4)	5440(4)	3973(3)	26(1)
C(30)	389(4)	7429(3)	3134(3)	31(2)
C(31)	-889(4)	4813(4)	4347(4)	42(2)
C(32)	3163(4)	4163(4)	4647(3)	28(1)
C(33)	2910(5)	3391(4)	4909(3)	39(2)
C(34)	2177(5)	3351(4)	4564(3)	35(2)
C(35)	3900(4)	4494(4)	4881(4)	37(2)
C(36)	1649(6)	2655(4)	4649(4)	58(2)
C(37)	2154(4)	4574(4)	1728(3)	30(1)
C(38)	1599(5)	3996(4)	1743(4)	41(2)
C(39)	1190(5)	3821(4)	2444(4)	37(2)
C(40)	2726(5)	4969(4)	1085(3)	43(2)

C(41)	498(6)	3257(5)	2746(5)	66(3)
B(1)	1182(5)	4341(4)	3648(4)	28(2)
U(1B)	2751(1)	10828(1)	8013(1)	19(1)
Si(1B)	762(1)	9616(1)	7391(1)	27(1)
Si(2B)	973(1)	12813(1)	9171(1)	23(1)
N(1B)	4146(3)	9827(3)	7382(3)	24(1)
N(2B)	4819(3)	9387(3)	7808(3)	28(1)
N(3B)	2989(3)	9596(3)	9105(3)	28(1)
N(4B)	3877(3)	9114(3)	9061(3)	29(1)
N(5B)	4272(3)	10998(3)	8407(2)	24(1)
N(6B)	4834(3)	10289(3)	8725(3)	26(1)
C(1B)	1221(4)	10552(3)	7507(3)	24(1)
C(2B)	917(4)	10761(3)	8210(3)	22(1)
C(3B)	984(4)	11401(3)	8581(3)	20(1)
C(4B)	1384(4)	12137(3)	8439(3)	19(1)
C(5B)	1955(4)	12460(3)	7813(3)	18(1)
C(6B)	2301(4)	12268(3)	7116(3)	21(1)
C(7B)	2215(4)	11647(3)	6740(3)	22(1)
C(8B)	1773(4)	10945(3)	6897(3)	19(1)
C(9B)	-497(4)	9704(4)	7858(3)	29(1)
C(10B)	-1074(4)	10581(4)	7780(4)	41(2)
C(11B)	-1060(5)	9129(5)	7648(4)	48(2)
C(12B)	858(5)	9573(4)	6392(4)	38(2)
C(13B)	276(5)	10325(5)	5969(3)	52(2)
C(14B)	653(6)	8774(5)	6215(5)	75(3)
C(15B)	1447(6)	8702(5)	7971(7)	31(3) [a]
C(16B)	2437(8)	8484(9)	7592(7)	47(4) [a]
C(17B)	1023(7)	7912(5)	8205(6)	42(3) [a]
C(15C)	1554(16)	8552(12)	7547(14)	43(9) [b]
C(16C)	2541(17)	8480(20)	7130(20)	63(12) [b]
C(17C)	1580(30)	8310(20)	8366(16)	92(16) [b]
C(18B)	1585(5)	12423(4)	10006(3)	34(2)

C(19B)	1520(5)	11522(5)	10337(4)	50(2)
C(20B)	2635(5)	12507(5)	9880(4)	51(2)
C(21B)	1189(5)	13897(3)	8783(3)	33(2)
C(22B)	1058(5)	14486(4)	9349(4)	56(2)
C(23B)	643(5)	14334(4)	8150(4)	45(2)
C(24B)	-314(4)	12788(4)	9483(3)	30(1)
C(25B)	-782(5)	13423(4)	9987(4)	46(2)
C(26B)	-911(4)	12861(4)	8866(3)	40(2)
C(27B)	4459(4)	9665(4)	6701(3)	30(1)
C(28B)	5309(4)	9137(4)	6690(4)	37(2)
C(29B)	5531(4)	8976(4)	7388(4)	35(2)
C(30B)	3924(5)	10016(4)	6076(3)	41(2)
C(31B)	6409(5)	8485(4)	7665(5)	51(2)
C(32B)	2435(5)	9144(4)	9600(3)	30(2)
C(33B)	2955(5)	8386(4)	9848(4)	41(2)
C(34B)	3855(5)	8376(4)	9512(4)	34(2)
C(35B)	1435(5)	9450(4)	9841(3)	40(2)
C(36B)	4695(5)	7711(4)	9596(4)	47(2)
C(37B)	4666(4)	11636(3)	8461(3)	24(1)
C(38B)	5451(4)	11361(4)	8812(3)	27(1)
C(39B)	5545(4)	10517(4)	8970(3)	27(1)
C(40B)	4292(4)	12503(3)	8148(3)	31(2)
C(41B)	6288(5)	9897(4)	9330(4)	44(2)
B(1B)	4757(5)	9421(4)	8623(4)	27(2)

***a* 71.6 %, *b* 28.4 %**

Table 12.

Bond lengths [Å] and angles [°] for nov609b.

U-N(1)	2.573(5)
U-N(3)	2.647(4)
U-N(5)	2.652(5)
U-C(3)	2.691(6)
U-C(6)	2.693(5)
U-C(7)	2.696(5)
U-C(5)	2.702(5)
U-C(2)	2.725(6)
U-C(8)	2.725(5)
U-C(4)	2.759(5)
U-C(1)	2.802(5)
Si(1)-C(12)	1.896(5)
Si(1)-C(1)	1.900(5)
Si(1)-C(15)	1.902(6)
Si(1)-C(9)	1.906(6)
Si(2)-C(18)	1.875(7)
Si(2)-C(4)	1.887(5)
Si(2)-C(24)	1.902(7)
Si(2)-C(21)	1.903(7)
N(1)-C(27)	1.343(7)
N(1)-N(2)	1.380(6)
N(2)-C(29)	1.372(7)
N(2)-B(1)	1.537(8)
N(3)-C(32)	1.351(7)
N(3)-N(4)	1.384(6)
N(4)-C(34)	1.355(7)
N(4)-B(1)	1.531(8)
N(5)-C(37)	1.350(7)
N(5)-N(6)	1.379(6)

N(6)-C(39)	1.351(7)
N(6)-B(1)	1.532(8)
C(1)-C(8)	1.416(7)
C(1)-C(2)	1.424(7)
C(2)-C(3)	1.421(7)
C(3)-C(4)	1.433(7)
C(4)-C(5)	1.414(7)
C(5)-C(6)	1.415(7)
C(6)-C(7)	1.400(7)
C(7)-C(8)	1.412(7)
C(9)-C(11)	1.533(8)
C(9)-C(10)	1.538(8)
C(12)-C(13)	1.529(9)
C(12)-C(14)	1.530(8)
C(15)-C(16)	1.523(8)
C(15)-C(17)	1.535(8)
C(18)-C(20)	1.461(11)
C(18)-C(19)	1.525(10)
C(21)-C(23)	1.497(9)
C(21)-C(22)	1.551(8)
C(24)-C(25)	1.542(9)
C(24)-C(26)	1.546(10)
C(27)-C(28)	1.384(8)
C(27)-C(30)	1.489(8)
C(28)-C(29)	1.344(8)
C(29)-C(31)	1.508(8)
C(32)-C(33)	1.390(8)
C(32)-C(35)	1.477(9)
C(33)-C(34)	1.372(9)
C(34)-C(36)	1.495(9)
C(37)-C(38)	1.378(9)
C(37)-C(40)	1.483(9)

C(38)-C(39)	1.365(9)
C(39)-C(41)	1.498(9)
U(1B)-N(5B)	2.563(5)
U(1B)-N(3B)	2.633(5)
U(1B)-N(1B)	2.650(5)
U(1B)-C(7B)	2.686(5)
U(1B)-C(2B)	2.691(6)
U(1B)-C(6B)	2.694(5)
U(1B)-C(8B)	2.704(5)
U(1B)-C(3B)	2.706(5)
U(1B)-C(5B)	2.723(5)
U(1B)-C(1B)	2.742(6)
U(1B)-C(4B)	2.804(5)
Si(1B)-C(12B)	1.883(7)
Si(1B)-C(1B)	1.887(6)
Si(1B)-C(9B)	1.911(6)
Si(1B)-C(15B)	1.913(10)
Si(1B)-C(15C)	1.921(15)
Si(2B)-C(21B)	1.887(6)
Si(2B)-C(18B)	1.890(6)
Si(2B)-C(24B)	1.898(6)
Si(2B)-C(4B)	1.899(5)
N(1B)-C(27B)	1.354(7)
N(1B)-N(2B)	1.385(6)
N(2B)-C(29B)	1.360(8)
N(2B)-B(1B)	1.540(8)
N(3B)-C(32B)	1.354(7)
N(3B)-N(4B)	1.391(7)
N(4B)-C(34B)	1.360(7)
N(4B)-B(1B)	1.543(8)
N(5B)-C(37B)	1.339(7)
N(5B)-N(6B)	1.396(6)

N(6B)-C(39B)	1.360(7)
N(6B)-B(1B)	1.526(8)
C(1B)-C(2B)	1.417(8)
C(1B)-C(8B)	1.426(8)
C(2B)-C(3B)	1.413(7)
C(3B)-C(4B)	1.430(7)
C(4B)-C(5B)	1.416(7)
C(5B)-C(6B)	1.405(7)
C(6B)-C(7B)	1.402(7)
C(7B)-C(8B)	1.413(8)
C(9B)-C(11B)	1.531(8)
C(9B)-C(10B)	1.533(8)
C(12B)-C(14B)	1.534(9)
C(12B)-C(13B)	1.536(9)
C(18B)-C(19B)	1.529(9)
C(18B)-C(20B)	1.559(9)
C(21B)-C(23B)	1.537(9)
C(21B)-C(22B)	1.552(8)
C(24B)-C(25B)	1.545(8)
C(24B)-C(26B)	1.548(8)
C(27B)-C(28B)	1.381(8)
C(27B)-C(30B)	1.489(9)
C(28B)-C(29B)	1.375(9)
C(29B)-C(31B)	1.503(9)
C(32B)-C(33B)	1.383(9)
C(32B)-C(35B)	1.487(9)
C(33B)-C(34B)	1.371(9)
C(34B)-C(36B)	1.496(9)
C(37B)-C(38B)	1.384(8)
C(37B)-C(40B)	1.486(8)
C(38B)-C(39B)	1.366(8)
C(39B)-C(41B)	1.501(8)

C(15B)-C(16B)	1.524(12)
C(15B)-C(17B)	1.530(11)
C(15C)-C(17C)	1.529(17)
C(15C)-C(16C)	1.534(17)

N(1)-U-N(3)	76.16(14)
N(1)-U-N(5)	70.91(15)
N(3)-U-N(5)	81.27(15)
C(12)-Si(1)-C(1)	109.3(2)
C(12)-Si(1)-C(15)	107.6(3)
C(1)-Si(1)-C(15)	112.6(3)
C(12)-Si(1)-C(9)	111.5(3)
C(1)-Si(1)-C(9)	108.0(2)
C(15)-Si(1)-C(9)	107.9(3)
C(18)-Si(2)-C(4)	114.4(3)
C(18)-Si(2)-C(24)	105.5(3)
C(4)-Si(2)-C(24)	108.0(3)
C(18)-Si(2)-C(21)	106.6(3)
C(4)-Si(2)-C(21)	108.5(3)
C(24)-Si(2)-C(21)	114.0(3)
C(27)-N(1)-N(2)	106.6(4)
C(27)-N(1)-U	135.4(4)
N(2)-N(1)-U	117.7(3)
C(29)-N(2)-N(1)	108.1(4)
C(29)-N(2)-B(1)	127.8(5)
N(1)-N(2)-B(1)	122.7(5)
C(32)-N(3)-N(4)	106.8(4)
C(32)-N(3)-U	135.6(4)
N(4)-N(3)-U	114.0(3)
C(34)-N(4)-N(3)	109.2(5)
C(34)-N(4)-B(1)	126.5(5)
N(3)-N(4)-B(1)	124.0(4)

C(37)-N(5)-N(6)	106.0(5)
C(37)-N(5)-U	136.7(4)
N(6)-N(5)-U	117.3(3)
C(39)-N(6)-N(5)	109.6(5)
C(39)-N(6)-B(1)	127.4(5)
N(5)-N(6)-B(1)	122.9(5)
C(8)-C(1)-C(2)	131.1(5)
C(8)-C(1)-Si(1)	115.5(4)
C(2)-C(1)-Si(1)	113.1(4)
C(3)-C(2)-C(1)	137.1(5)
C(2)-C(3)-C(4)	137.9(5)
C(5)-C(4)-C(3)	128.8(5)
C(5)-C(4)-Si(2)	117.3(4)
C(3)-C(4)-Si(2)	113.7(4)
C(4)-C(5)-C(6)	138.1(5)
C(7)-C(6)-C(5)	135.6(5)
C(6)-C(7)-C(8)	134.8(5)
C(7)-C(8)-C(1)	136.5(5)
C(11)-C(9)-C(10)	109.7(5)
C(11)-C(9)-Si(1)	113.5(4)
C(10)-C(9)-Si(1)	113.9(4)
C(13)-C(12)-C(14)	109.1(5)
C(13)-C(12)-Si(1)	114.2(4)
C(14)-C(12)-Si(1)	115.5(4)
C(16)-C(15)-C(17)	109.2(5)
C(16)-C(15)-Si(1)	112.6(4)
C(17)-C(15)-Si(1)	112.3(4)
C(20)-C(18)-C(19)	108.5(8)
C(20)-C(18)-Si(2)	116.2(6)
C(19)-C(18)-Si(2)	113.3(5)
C(23)-C(21)-C(22)	109.8(6)
C(23)-C(21)-Si(2)	118.1(5)

C(22)-C(21)-Si(2)	112.4(5)
C(25)-C(24)-C(26)	110.6(7)
C(25)-C(24)-Si(2)	116.2(6)
C(26)-C(24)-Si(2)	113.1(5)
N(1)-C(27)-C(28)	109.7(5)
N(1)-C(27)-C(30)	121.9(5)
C(28)-C(27)-C(30)	128.3(5)
C(29)-C(28)-C(27)	106.9(5)
C(28)-C(29)-N(2)	108.6(5)
C(28)-C(29)-C(31)	129.2(5)
N(2)-C(29)-C(31)	122.2(5)
N(3)-C(32)-C(33)	109.1(6)
N(3)-C(32)-C(35)	124.6(5)
C(33)-C(32)-C(35)	126.3(6)
C(34)-C(33)-C(32)	107.0(5)
N(4)-C(34)-C(33)	107.9(6)
N(4)-C(34)-C(36)	123.5(6)
C(33)-C(34)-C(36)	128.6(6)
N(5)-C(37)-C(38)	109.7(6)
N(5)-C(37)-C(40)	123.1(6)
C(38)-C(37)-C(40)	127.2(6)
C(39)-C(38)-C(37)	106.9(6)
N(6)-C(39)-C(38)	107.8(6)
N(6)-C(39)-C(41)	123.9(6)
C(38)-C(39)-C(41)	128.3(6)
N(4)-B(1)-N(6)	112.4(5)
N(4)-B(1)-N(2)	112.8(5)
N(6)-B(1)-N(2)	110.0(5)
N(5B)-U(1B)-N(3B)	77.46(15)
N(5B)-U(1B)-N(1B)	71.72(14)
N(3B)-U(1B)-N(1B)	80.32(15)
C(12B)-Si(1B)-C(1B)	109.3(3)

C(12B)-Si(1B)-C(9B)	112.5(3)
C(1B)-Si(1B)-C(9B)	107.7(3)
C(12B)-Si(1B)-C(15B)	116.9(4)
C(1B)-Si(1B)-C(15B)	104.8(4)
C(9B)-Si(1B)-C(15B)	105.1(4)
C(12B)-Si(1B)-C(15C)	90.8(9)
C(1B)-Si(1B)-C(15C)	118.1(9)
C(9B)-Si(1B)-C(15C)	117.3(8)
C(15B)-Si(1B)-C(15C)	26.1(7)
C(21B)-Si(2B)-C(18B)	108.7(3)
C(21B)-Si(2B)-C(24B)	111.8(3)
C(18B)-Si(2B)-C(24B)	106.4(3)
C(21B)-Si(2B)-C(4B)	108.8(3)
C(18B)-Si(2B)-C(4B)	113.0(3)
C(24B)-Si(2B)-C(4B)	108.0(3)
C(27B)-N(1B)-N(2B)	105.9(5)
C(27B)-N(1B)-U(1B)	136.8(4)
N(2B)-N(1B)-U(1B)	116.9(3)
C(29B)-N(2B)-N(1B)	109.6(5)
C(29B)-N(2B)-B(1B)	127.3(5)
N(1B)-N(2B)-B(1B)	123.1(5)
C(32B)-N(3B)-N(4B)	106.2(5)
C(32B)-N(3B)-U(1B)	136.4(4)
N(4B)-N(3B)-U(1B)	114.2(3)
C(34B)-N(4B)-N(3B)	109.5(5)
C(34B)-N(4B)-B(1B)	126.1(5)
N(3B)-N(4B)-B(1B)	124.1(4)
C(37B)-N(5B)-N(6B)	105.7(4)
C(37B)-N(5B)-U(1B)	135.9(4)
N(6B)-N(5B)-U(1B)	117.9(3)
C(39B)-N(6B)-N(5B)	109.0(5)
C(39B)-N(6B)-B(1B)	127.4(5)

N(5B)-N(6B)-B(1B)	122.0(5)
C(2B)-C(1B)-C(8B)	130.6(5)
C(2B)-C(1B)-Si(1B)	111.7(4)
C(8B)-C(1B)-Si(1B)	117.6(4)
C(3B)-C(2B)-C(1B)	136.9(5)
C(2B)-C(3B)-C(4B)	138.4(5)
C(5B)-C(4B)-C(3B)	129.4(5)
C(5B)-C(4B)-Si(2B)	116.9(4)
C(3B)-C(4B)-Si(2B)	113.3(4)
C(6B)-C(5B)-C(4B)	137.6(5)
C(7B)-C(6B)-C(5B)	134.5(5)
C(6B)-C(7B)-C(8B)	136.0(5)
C(7B)-C(8B)-C(1B)	136.3(5)
C(11B)-C(9B)-C(10B)	108.0(5)
C(11B)-C(9B)-Si(1B)	114.5(4)
C(10B)-C(9B)-Si(1B)	115.5(4)
C(14B)-C(12B)-C(13B)	109.3(6)
C(14B)-C(12B)-Si(1B)	115.2(5)
C(13B)-C(12B)-Si(1B)	113.4(4)
C(19B)-C(18B)-C(20B)	107.9(6)
C(19B)-C(18B)-Si(2B)	113.4(5)
C(20B)-C(18B)-Si(2B)	114.0(4)
C(23B)-C(21B)-C(22B)	109.0(5)
C(23B)-C(21B)-Si(2B)	114.7(4)
C(22B)-C(21B)-Si(2B)	115.0(5)
C(25B)-C(24B)-C(26B)	109.5(5)
C(25B)-C(24B)-Si(2B)	113.6(4)
C(26B)-C(24B)-Si(2B)	115.1(4)
N(1B)-C(27B)-C(28B)	110.1(6)
N(1B)-C(27B)-C(30B)	122.8(5)
C(28B)-C(27B)-C(30B)	127.1(6)
C(29B)-C(28B)-C(27B)	106.7(6)

N(2B)-C(29B)-C(28B)	107.7(5)
N(2B)-C(29B)-C(31B)	123.7(6)
C(28B)-C(29B)-C(31B)	128.5(6)
N(3B)-C(32B)-C(33B)	109.2(6)
N(3B)-C(32B)-C(35B)	123.9(5)
C(33B)-C(32B)-C(35B)	126.9(6)
C(34B)-C(33B)-C(32B)	107.7(6)
N(4B)-C(34B)-C(33B)	107.2(5)
N(4B)-C(34B)-C(36B)	123.4(6)
C(33B)-C(34B)-C(36B)	129.4(6)
N(5B)-C(37B)-C(38B)	110.7(5)
N(5B)-C(37B)-C(40B)	121.9(5)
C(38B)-C(37B)-C(40B)	127.3(5)
C(39B)-C(38B)-C(37B)	106.4(5)
N(6B)-C(39B)-C(38B)	108.2(5)
N(6B)-C(39B)-C(41B)	122.5(5)
C(38B)-C(39B)-C(41B)	129.3(6)
N(6B)-B(1B)-N(2B)	109.9(5)
N(6B)-B(1B)-N(4B)	113.4(5)
N(2B)-B(1B)-N(4B)	111.5(5)
C(16B)-C(15B)-C(17B)	109.1(9)
C(16B)-C(15B)-Si(1B)	110.1(8)
C(17B)-C(15B)-Si(1B)	117.3(7)

Least-squares planes (x,y,z in crystal coordinates) and deviations from them

(* indicates atom used to define plane)

11.5836 (0.0130) x + 10.8309 (0.0177) y - 2.6852 (0.0269) z = 10.6548 (0.0152)

* 0.0373 (0.0041) C1

* -0.0016 (0.0044) C2

* -0.0288 (0.0044) C3

* 0.0032 (0.0043) C4

* 0.0196 (0.0044) C5

* 0.0071 (0.0045) C6

* -0.0220 (0.0044) C7

* -0.0147 (0.0042) C8

-1.9993 (0.0019) U

0.3771 (0.0058) Si1

0.1778 (0.0060) Si2

Rms deviation of fitted atoms = 0.0205

11.7228 (0.0126) x - 5.5842 (0.0213) y + 7.1567 (0.0237) z = 0.9189 (0.0357)

Angle to previous plane (with approximate esd) = 75.64 (0.09)

* -0.0071 (0.0043) C1B

* 0.0226 (0.0042) C2B

* 0.0097 (0.0042) C3B

* -0.0339 (0.0041) C4B

* 0.0067 (0.0042) C5B

* 0.0211 (0.0042) C6B

* -0.0022 (0.0041) C7B

* -0.0169 (0.0042) C8B

1.9939 (0.0018) U1B

-0.1063 (0.0057) Si1B

-0.3696 (0.0055) Si2B

Rms deviation of fitted atoms = 0.0180

Table 13.

Crystal data and structure refinement for **3.2**

[U(κ^3-Tp^{Me2})(η^8-C_8H_4{Si^{i}Pr$_3$-1,4}$_2$)]

Identification code	apr709	
Empirical formula	C41 H68 B N6 Si2 U	
Formula weight	950.03	
Temperature	173(2) K	
Wavelength	0.71073 Å	
Crystal system	Monoclinic	
Space group	*P* $2_1/c$ (No.14)	
Unit cell dimensions	a = 11.1026(2) Å	α= 90°.
	b = 26.7178(6) Å	β= 117.665(1)°.
	c = 16.7781(3) Å	γ = 90°.
Volume	4408.02(15) Å^3	
Z	4	
Density (calculated)	1.43 Mg/m^3	
Absorption coefficient	3.77 mm^{-1}	
F(000)	1924	
Crystal size	0.30 x 0.28 x 0.02 mm^3	
Theta range for data collection	3.43 to 27.48°.	
Index ranges	-14<=h<=13, -33<=k<=33, -21<=l<=21	
Reflections collected	53016	
Independent reflections	9985 [R(int) = 0.095]	
Reflections with I>2sigma(I)	8271	
Completeness to theta = 27.48°	98.7 %	
Absorption correction	Semi-empirical from equivalents	
Tmax. and Tmin.	0.6307and 0.4552	
Refinement method	Full-matrix least-squares on F^2	
Data / restraints / parameters	9985 / 7 / 488	
Goodness-of-fit on F^2	1.239	

Final R indices [I>2sigma(I)]	R1 = 0.064, wR2 = 0.142
R indices (all data)	R1 = 0.081, wR2 = 0.148
Largest diff. peak and hole	4.139 and -2.775 e.Å^{-3} (near to uranium)

One of the *i*-propyl groups on the pentalene ligand is disordered

Data collection KappaCCD , Program package WinGX , Abs correction MULTISCAN

Refinement using SHELXL-97 , Drawing using ORTEP-3 for Windows

Table 14.

Atomic coordinates (x 10^4) and equivalent isotropic displacement parameters (Å^{2}x 10^3)

for apr709. U(eq) is defined as one third of the trace of the orthogonalized U^{ij} tensor.

	x	y	z	U(eq)
U	371(1)	9497(1)	7777(1)	22(1)
Si(1)	-1391(2)	8349(1)	5795(2)	30(1)
Si(2)	-2135(2)	10825(1)	6966(2)	29(1)
N(1)	2236(7)	9706(3)	9401(5)	35(2)
N(2)	3355(7)	9395(3)	9744(4)	35(2)
N(3)	889(7)	8718(3)	8827(5)	30(2)
N(4)	2220(7)	8556(3)	9170(5)	31(2)
N(5)	2718(7)	9412(3)	7835(4)	28(2)
N(6)	3430(6)	9020(3)	8378(4)	27(1)
C(1)	-1170(8)	9014(3)	6151(5)	26(2)
C(2)	-441(8)	9373(3)	5894(5)	30(2)
C(3)	-673(8)	9869(3)	6066(5)	25(2)
C(4)	-1640(7)	9851(3)	6418(5)	25(2)
C(5)	-1933(7)	9328(3)	6463(5)	25(2)
C(6)	-2389(7)	9295(3)	7148(5)	29(2)
C(7)	-2349(7)	9774(3)	7475(5)	26(2)
C(8)	-1827(7)	10137(3)	7086(5)	24(2)

C(9)	-2540(9)	8325(3)	4532(6)	39(2)
C(10)	-2269(11)	8720(4)	3989(7)	50(3)
C(11)	-2581(14)	7811(5)	4117(8)	69(4)
C(12)	-2254(9)	8002(4)	6377(7)	42(2)
C(13)	-3756(10)	8156(4)	6034(8)	51(3)
C(14)	-2169(12)	7429(4)	6360(9)	60(3)
C(15)	302(9)	8027(3)	6111(6)	35(2)
C(16)	1180(11)	7993(4)	7132(7)	50(3)
C(17)	1150(10)	8253(4)	5685(8)	49(3)
C(18)	-3742(8)	10924(3)	5871(5)	29(2)
C(19)	-4907(9)	10606(4)	5867(7)	47(3)
C(20)	-3587(10)	10806(4)	5036(5)	42(2)
C(21)	-707(10)	11138(4)	6845(7)	46(2)
C(22)	-868(12)	11697(4)	6736(7)	54(3)
C(23)	751(10)	10991(5)	7605(8)	62(3)
C(24)	-2050(20)	11186(5)	7969(10)	35(5) [a]
C(25)	-2960(30)	11647(9)	7670(30)	46(8) [a]
C(26)	-2472(14)	10849(5)	8527(7)	45(5) [a]
C(24A)	-2677(14)	11032(5)	7864(7)	32(4) [b]
C(25A)	-3390(40)	11538(9)	7720(30)	59(10) [b]
C(26A)	-1638(8)	10986(4)	8850(5)	53(6) [b]
C(27)	2494(10)	10077(4)	9985(6)	42(2)
C(28)	3771(12)	10018(5)	10694(7)	58(3)
C(29)	4299(10)	9593(5)	10541(6)	49(3)
C(30)	1468(14)	10464(5)	9836(8)	65(3)
C(31)	5648(10)	9346(6)	11089(7)	68(4)
C(32)	233(9)	8368(3)	9038(5)	30(2)
C(33)	1082(9)	7982(4)	9505(7)	42(2)
C(34)	2361(10)	8114(4)	9596(7)	45(2)
C(35)	-1211(8)	8422(4)	8848(6)	36(2)
C(36)	3674(12)	7832(5)	10078(10)	76(4)
C(37)	3194(8)	9470(3)	7232(5)	31(2)

C(38)	4164(8)	9108(4)	7377(6)	35(2)
C(39)	4305(8)	8831(4)	8100(6)	34(2)
C(40)	2721(10)	9891(4)	6566(6)	39(2)
C(41)	5200(11)	8392(4)	8528(8)	54(3)
B	3416(8)	8907(4)	9281(5)	30(2)
M(1)	-1786	9589	6440	10
M(2)	1948	9279	8688	10

a = 50.2 %, *b* = 49.8 %

M(1) = midpoint of C(4)-C(5) bond, M(2) = centroid defined from N(1), N(3) and N(5)

Table 15.

Bond lengths [Å] and angles [°] for apr709.

U-M(2)	1.8041(3)
U-M(1)	2.4165(3)
U-C(4)	2.520(7)
U-C(5)	2.524(7)
U-N(5)	2.572(7)
U-N(1)	2.604(7)
U-N(3)	2.611(7)
U-C(3)	2.736(7)
U-C(8)	2.755(7)
U-C(1)	2.775(7)
U-C(6)	2.791(8)
U-C(2)	2.873(8)
U-C(7)	2.916(7)
Si(1)-C(1)	1.854(8)
Si(1)-C(12)	1.896(10)
Si(1)-C(9)	1.901(9)
Si(1)-C(15)	1.904(9)
Si(2)-C(8)	1.865(8)

Si(2)-C(21)	1.884(10)
Si(2)-C(18)	1.893(8)
Si(2)-C(24)	1.902(14)
N(1)-C(27)	1.327(11)
N(1)-N(2)	1.378(11)
N(2)-C(29)	1.365(11)
N(2)-B	1.536(12)
N(3)-C(32)	1.330(10)
N(3)-N(4)	1.384(9)
N(4)-C(34)	1.350(12)
N(4)-B	1.565(11)
N(5)-C(37)	1.351(10)
N(5)-N(6)	1.372(9)
N(6)-C(39)	1.356(10)
N(6)-B	1.552(10)
C(1)-C(2)	1.445(12)
C(1)-C(5)	1.451(11)
C(2)-C(3)	1.403(11)
C(3)-C(4)	1.447(11)
C(4)-C(5)	1.444(12)
C(4)-C(8)	1.447(11)
C(5)-C(6)	1.458(11)
C(6)-C(7)	1.387(12)
C(7)-C(8)	1.432(11)
C(9)-C(10)	1.514(14)
C(9)-C(11)	1.531(14)
C(12)-C(14)	1.536(15)
C(12)-C(13)	1.546(13)
C(15)-C(16)	1.531(13)
C(15)-C(17)	1.544(14)
C(18)-C(20)	1.522(11)
C(18)-C(19)	1.545(13)

C(21)-C(22)	1.507(14)
C(21)-C(23)	1.576(14)
C(27)-C(28)	1.373(15)
C(27)-C(30)	1.473(16)
C(28)-C(29)	1.354(17)
C(29)-C(31)	1.499(15)
C(32)-C(33)	1.371(12)
C(32)-C(35)	1.490(11)
C(33)-C(34)	1.401(13)
C(34)-C(36)	1.501(13)
C(37)-C(38)	1.382(12)
C(37)-C(40)	1.496(12)
C(38)-C(39)	1.367(13)
C(39)-C(41)	1.489(13)
C(24)-C(26)	1.523(13)
C(24)-C(25)	1.524(15)

M(2)-U-M(1)	166.597(16)
C(1)-Si(1)-C(12)	109.0(4)
C(1)-Si(1)-C(9)	108.2(4)
C(12)-Si(1)-C(9)	108.6(4)
C(1)-Si(1)-C(15)	112.1(4)
C(12)-Si(1)-C(15)	107.8(4)
C(9)-Si(1)-C(15)	111.1(4)
C(8)-Si(2)-C(21)	109.1(4)
C(8)-Si(2)-C(18)	106.6(4)
C(21)-Si(2)-C(18)	107.2(4)
C(8)-Si(2)-C(24)	118.2(5)
C(21)-Si(2)-C(24)	99.8(7)
C(18)-Si(2)-C(24)	115.2(6)
C(27)-N(1)-N(2)	107.3(8)
C(27)-N(1)-M(2)	177.9(7)

N(2)-N(1)-M(2)	73.0(5)
C(27)-N(1)-U	136.6(7)
N(2)-N(1)-U	115.6(5)
M(2)-N(1)-U	42.91(18)
C(29)-N(2)-N(1)	108.0(8)
C(29)-N(2)-B	129.0(8)
N(1)-N(2)-B	122.9(6)
C(32)-N(3)-N(4)	106.2(7)
C(32)-N(3)-U	139.8(6)
N(4)-N(3)-U	112.9(5)
C(34)-N(4)-N(3)	109.5(7)
C(34)-N(4)-B	125.3(7)
N(3)-N(4)-B	123.0(7)
C(37)-N(5)-N(6)	106.3(7)
C(37)-N(5)-U	134.7(5)
N(6)-N(5)-U	110.8(4)
C(39)-N(6)-N(5)	109.9(6)
C(39)-N(6)-B	126.7(7)
N(5)-N(6)-B	122.1(6)
C(2)-C(1)-C(5)	102.9(7)
C(2)-C(1)-Si(1)	123.3(6)
C(5)-C(1)-Si(1)	131.2(6)
C(3)-C(2)-C(1)	112.7(7)
C(2)-C(3)-C(4)	107.1(7)
C(5)-C(4)-C(3)	106.3(7)
C(5)-C(4)-C(8)	110.7(7)
C(3)-C(4)-C(8)	134.3(7)
C(4)-C(5)-C(1)	111.0(7)
C(4)-C(5)-C(6)	105.6(7)
C(1)-C(5)-C(6)	136.3(8)
C(7)-C(6)-C(5)	107.3(7)
C(6)-C(7)-C(8)	112.9(7)

C(7)-C(8)-C(4)	103.3(7)
C(7)-C(8)-Si(2)	128.5(6)
C(4)-C(8)-Si(2)	121.4(6)
C(10)-C(9)-C(11)	108.9(9)
C(10)-C(9)-Si(1)	115.4(7)
C(11)-C(9)-Si(1)	113.6(7)
C(14)-C(12)-C(13)	108.9(8)
C(14)-C(12)-Si(1)	115.3(8)
C(13)-C(12)-Si(1)	113.2(7)
C(16)-C(15)-C(17)	109.4(8)
C(16)-C(15)-Si(1)	111.8(7)
C(17)-C(15)-Si(1)	115.5(6)
C(20)-C(18)-C(19)	109.6(8)
C(20)-C(18)-Si(2)	113.9(6)
C(19)-C(18)-Si(2)	109.7(6)
C(22)-C(21)-C(23)	111.3(9)
C(22)-C(21)-Si(2)	113.2(8)
C(23)-C(21)-Si(2)	113.8(7)
N(1)-C(27)-C(28)	109.6(10)
N(1)-C(27)-C(30)	121.0(9)
C(28)-C(27)-C(30)	129.4(10)
C(29)-C(28)-C(27)	107.2(9)
C(28)-C(29)-N(2)	107.8(9)
C(28)-C(29)-C(31)	130.5(10)
N(2)-C(29)-C(31)	121.6(11)
N(3)-C(32)-C(33)	111.5(8)
N(3)-C(32)-C(35)	122.9(8)
C(33)-C(32)-C(35)	125.5(8)
C(32)-C(33)-C(34)	105.3(8)
N(4)-C(34)-C(33)	107.5(8)
N(4)-C(34)-C(36)	124.7(9)
C(33)-C(34)-C(36)	127.8(9)

N(5)-C(37)-C(38)	109.3(8)
N(5)-C(37)-C(40)	121.5(8)
C(38)-C(37)-C(40)	129.1(8)
C(39)-C(38)-C(37)	107.2(7)
N(6)-C(39)-C(38)	107.3(8)
N(6)-C(39)-C(41)	123.5(8)
C(38)-C(39)-C(41)	129.2(8)
C(26)-C(24)-C(25)	109.7(17)
C(26)-C(24)-Si(2)	110.0(8)
C(25)-C(24)-Si(2)	111.1(15)
N(2)-B-N(6)	110.6(7)
N(2)-B-N(4)	109.6(6)
N(6)-B-N(4)	113.2(6)

Least-squares planes (x,y,z in crystal coordinates) and deviations from them

(* indicates atom used to define plane)

4.1278 (0.0401) x - 1.3255 (0.0971) y + 10.8788 (0.0496) z = 5.0022 (0.0992)

* 0.0121 (0.0046) C1

* -0.0144 (0.0049) C2

* 0.0107 (0.0046) C3

* -0.0026 (0.0044) C4

* -0.0058 (0.0046) C5

2.3528 (0.0035) U

-0.3784 (0.0120) Si1

Rms deviation of fitted atoms = 0.0101

- 7.7525 (0.0300) x + 4.5786 (0.0972) y - 4.8886 (0.0604) z = 2.6207 (0.1060)

Angle to previous plane (with approximate esd) = 24.16 (0.55)

* 0.0234 (0.0044) C4

* -0.0108 (0.0044) C5

* -0.0070 (0.0046) C6

* 0.0216 (0.0047) C7

* -0.0272 (0.0044) C8

-2.3619 (0.0035) U

0.5858 (0.0117) Si2

Rms deviation of fitted atoms = 0.0196

Table 16.

Crystal data and structure refinement for **3.3**

[U(η^8-C_8H_6{Si^{i}Pr$_3$-1,4}$_2$)(κ^2-dmpz)$_2$(η^1-CNMe)]

Identification code	aug109	
Empirical formula	C38 H65 N5 Si2 U	
Formula weight	886.16	
Temperature	173(2) K	
Wavelength	0.71073 Å	
Crystal system	Monoclinic	
Space group	P 2_1/c (No.14)	
Unit cell dimensions	a = 11.1426(1) Å	α= 90°.
	b = 15.3770(2) Å	β= 109.926(1)°.
	c = 25.9618(3) Å	γ = 90°.
Volume	4181.98(8) Å^3	
Z	4	
Density (calculated)	1.41 Mg/m^3	
Absorption coefficient	3.97 mm^{-1}	
F(000)	1792	
Crystal size	0.28 x 0.14 x 0.08 mm^3	
Theta range for data collection	3.50 to 27.86°.	
Index ranges	-14<=h<=14, -20<=k<=19, -34<=l<=33	
Reflections collected	68954	
Independent reflections	9892 [R(int) = 0.058]	
Reflections with I>2sigma(I)	8796	
Completeness to theta = 27.86°	99.3 %	
Absorption correction	Semi-empirical from equivalents	
Tmax. and Tmin.	0.6240 and 0.3960	
Refinement method	Full-matrix least-squares on F^2	
Data / restraints / parameters	9892 / 0 / 420	
Goodness-of-fit on F^2	1.097	

Final R indices [I>2sigma(I)]	R1 = 0.025, wR2 = 0.050
R indices (all data)	R1 = 0.032, wR2 = 0.052
Largest diff. peak and hole	0.97 and -1.18 e.Å^{-3}

Data collection KappaCCD , Program package WinGX , Abs correction MULTISCAN

Refinement using SHELXL-97 , Drawing using ORTEP-3 for Windows

Table 17.

Atomic coordinates (x 10^4) and equivalent isotropic displacement parameters (Å^{2}x 10^3)

for aug109. U(eq) is defined as one third of the trace of the orthogonalized U^{ij} tensor.

	x	y	z	U(eq)
U	8461(1)	1205(1)	7614(1)	17(1)
Si(1)	12414(1)	857(1)	8721(1)	21(1)
Si(2)	8515(1)	738(1)	5960(1)	20(1)
N(1)	6404(2)	1780(1)	7184(1)	26(1)
N(2)	6248(2)	887(1)	7151(1)	25(1)
N(3)	8127(2)	1734(2)	8408(1)	27(1)
N(4)	8072(2)	842(2)	8438(1)	29(1)
N(5)	8083(2)	-1236(2)	7737(1)	29(1)
C(1)	11084(2)	1238(2)	8078(1)	19(1)
C(2)	10765(2)	633(2)	7635(1)	20(1)
C(3)	9979(2)	609(2)	7079(1)	20(1)
C(4)	9135(2)	1174(2)	6689(1)	19(1)
C(5)	8773(2)	2045(2)	6751(1)	22(1)
C(6)	9057(2)	2663(2)	7175(1)	22(1)
C(7)	9814(2)	2686(2)	7730(1)	22(1)
C(8)	10651(2)	2099(2)	8101(1)	20(1)
C(9)	13994(3)	1061(2)	8611(1)	30(1)
C(10)	14271(3)	2036(2)	8584(2)	43(1)
C(11)	14086(3)	603(2)	8099(1)	43(1)

C(12)	12429(3)	1532(2)	9334(1)	27(1)
C(13)	13626(3)	1392(2)	9840(1)	45(1)
C(14)	11230(3)	1453(2)	9494(1)	38(1)
C(15)	12274(3)	-358(2)	8820(1)	30(1)
C(16)	13439(3)	-761(2)	9257(2)	50(1)
C(17)	11054(3)	-636(2)	8919(2)	44(1)
C(18)	9797(3)	965(2)	5646(1)	28(1)
C(19)	10033(3)	1938(2)	5599(1)	44(1)
C(20)	11053(3)	507(2)	5959(1)	40(1)
C(21)	7022(3)	1337(2)	5524(1)	29(1)
C(22)	6530(3)	1009(3)	4927(1)	47(1)
C(23)	5905(3)	1357(2)	5741(1)	40(1)
C(24)	8298(3)	-484(2)	5963(1)	26(1)
C(25)	8174(4)	-937(2)	5419(1)	44(1)
C(26)	7203(3)	-755(2)	6158(1)	40(1)
C(27)	5272(2)	2153(2)	6927(1)	31(1)
C(28)	4363(3)	1504(2)	6727(1)	34(1)
C(29)	5011(2)	720(2)	6879(1)	29(1)
C(30)	5168(3)	3117(2)	6872(2)	55(1)
C(31)	4533(3)	-197(2)	6773(2)	44(1)
C(32)	7927(3)	2077(2)	8845(1)	37(1)
C(33)	7731(3)	1404(2)	9164(1)	44(1)
C(34)	7819(3)	641(2)	8895(1)	39(1)
C(35)	7962(4)	3033(3)	8924(2)	62(1)
C(36)	7690(4)	-288(3)	9042(2)	63(1)
C(37)	8240(3)	-524(2)	7657(1)	29(1)
C(38)	7910(3)	-2127(2)	7864(2)	44(1)
M(1)	9907(5)	1643(4)	7405(9)	10

M(1) = centroid of COT-ring

Table 18.

Bond lengths [Å] and angles [°] for aug109.

U-M(1)	1.987(7)
U-N(1)	2.353(2)
U-N(3)	2.360(2)
U-N(4)	2.387(2)
U-N(2)	2.397(2)
U-C(37)	2.675(3)
U-C(3)	2.691(2)
U-C(7)	2.692(2)
U-C(2)	2.698(2)
U-C(6)	2.700(2)
U-C(8)	2.710(2)
U-C(5)	2.711(2)
U-C(4)	2.752(2)
U-C(1)	2.757(2)
Si(1)-C(12)	1.897(3)
Si(1)-C(15)	1.900(3)
Si(1)-C(9)	1.904(3)
Si(1)-C(1)	1.907(3)
Si(2)-C(24)	1.896(3)
Si(2)-C(4)	1.901(3)
Si(2)-C(21)	1.901(3)
Si(2)-C(18)	1.903(3)
N(1)-C(27)	1.338(3)
N(1)-N(2)	1.384(3)
N(2)-C(29)	1.342(3)
N(3)-C(32)	1.336(3)
N(3)-N(4)	1.377(3)
N(4)-C(34)	1.346(3)
N(5)-C(37)	1.140(3)

N(5)-C(38)	1.438(3)
C(1)-C(8)	1.418(3)
C(1)-C(2)	1.427(3)
C(2)-C(3)	1.412(3)
C(3)-C(4)	1.420(3)
C(4)-C(5)	1.423(3)
C(5)-C(6)	1.407(4)
C(6)-C(7)	1.401(4)
C(7)-C(8)	1.414(3)
C(9)-C(10)	1.537(4)
C(9)-C(11)	1.538(4)
C(12)-C(14)	1.532(4)
C(12)-C(13)	1.534(4)
C(15)-C(17)	1.527(4)
C(15)-C(16)	1.533(4)
C(18)-C(20)	1.529(4)
C(18)-C(19)	1.532(4)
C(21)-C(23)	1.532(4)
C(21)-C(22)	1.541(4)
C(24)-C(26)	1.529(4)
C(24)-C(25)	1.540(4)
C(27)-C(28)	1.390(4)
C(27)-C(30)	1.490(4)
C(28)-C(29)	1.392(4)
C(29)-C(31)	1.498(4)
C(32)-C(33)	1.389(5)
C(32)-C(35)	1.482(5)
C(33)-C(34)	1.385(5)
C(34)-C(36)	1.499(5)

N(1)-U-N(3)	82.39(8)
N(1)-U-N(4)	93.95(8)

N(3)-U-N(4)	33.71(8)
N(1)-U-N(2)	33.86(8)
N(3)-U-N(2)	93.89(8)
N(4)-U-N(2)	86.14(8)
N(1)-U-C(37)	107.76(8)
N(3)-U-C(37)	105.24(8)
N(4)-U-C(37)	71.56(8)
N(2)-U-C(37)	74.03(8)
C(12)-Si(1)-C(15)	113.77(13)
C(12)-Si(1)-C(9)	106.95(13)
C(15)-Si(1)-C(9)	107.76(13)
C(12)-Si(1)-C(1)	110.40(11)
C(15)-Si(1)-C(1)	110.21(12)
C(9)-Si(1)-C(1)	107.46(12)
C(24)-Si(2)-C(4)	110.45(11)
C(24)-Si(2)-C(21)	113.34(13)
C(4)-Si(2)-C(21)	111.69(12)
C(24)-Si(2)-C(18)	107.38(12)
C(4)-Si(2)-C(18)	106.88(12)
C(21)-Si(2)-C(18)	106.73(12)
C(27)-N(1)-N(2)	108.5(2)
C(27)-N(1)-U	176.05(19)
N(2)-N(1)-U	74.78(13)
C(29)-N(2)-N(1)	107.9(2)
C(29)-N(2)-U	178.4(2)
N(1)-N(2)-U	71.36(13)
C(32)-N(3)-N(4)	108.8(2)
C(32)-N(3)-U	176.9(2)
N(4)-N(3)-U	74.24(13)
C(34)-N(4)-N(3)	107.8(2)
C(34)-N(4)-U	178.5(2)
N(3)-N(4)-U	72.05(13)

C(37)-N(5)-C(38)	177.3(3)
C(8)-C(1)-C(2)	130.4(2)
C(8)-C(1)-Si(1)	115.05(18)
C(2)-C(1)-Si(1)	114.26(17)
C(8)-C(1)-U	73.15(13)
C(2)-C(1)-U	72.57(13)
Si(1)-C(1)-U	140.18(11)
C(3)-C(2)-C(1)	137.6(2)
C(3)-C(2)-U	74.54(14)
C(1)-C(2)-U	77.13(13)
C(2)-C(3)-C(4)	138.0(2)
C(2)-C(3)-U	75.08(14)
C(4)-C(3)-U	77.28(14)
C(3)-C(4)-C(5)	129.7(2)
C(3)-C(4)-Si(2)	114.91(18)
C(5)-C(4)-Si(2)	115.08(18)
C(3)-C(4)-U	72.50(13)
C(5)-C(4)-U	73.31(14)
Si(2)-C(4)-U	139.48(11)
C(6)-C(5)-C(4)	136.7(2)
C(6)-C(5)-U	74.52(14)
C(4)-C(5)-U	76.50(14)
C(7)-C(6)-C(5)	135.9(2)
C(7)-C(6)-U	74.60(14)
C(5)-C(6)-U	75.35(14)
C(6)-C(7)-C(8)	135.3(2)
C(6)-C(7)-U	75.28(14)
C(8)-C(7)-U	75.54(14)
C(7)-C(8)-C(1)	136.2(2)
C(7)-C(8)-U	74.11(14)
C(1)-C(8)-U	76.80(14)
C(10)-C(9)-C(11)	109.5(3)

C(10)-C(9)-Si(1)	112.21(19)
C(11)-C(9)-Si(1)	113.1(2)
C(14)-C(12)-C(13)	110.0(2)
C(14)-C(12)-Si(1)	115.1(2)
C(13)-C(12)-Si(1)	113.4(2)
C(17)-C(15)-C(16)	109.9(3)
C(17)-C(15)-Si(1)	114.6(2)
C(16)-C(15)-Si(1)	114.2(2)
C(20)-C(18)-C(19)	110.0(3)
C(20)-C(18)-Si(2)	111.85(19)
C(19)-C(18)-Si(2)	112.8(2)
C(23)-C(21)-C(22)	108.7(2)
C(23)-C(21)-Si(2)	116.45(19)
C(22)-C(21)-Si(2)	112.3(2)
C(26)-C(24)-C(25)	110.4(2)
C(26)-C(24)-Si(2)	112.8(2)
C(25)-C(24)-Si(2)	114.60(19)
N(1)-C(27)-C(28)	108.8(2)
N(1)-C(27)-C(30)	120.2(3)
C(28)-C(27)-C(30)	130.9(3)
C(27)-C(28)-C(29)	105.9(2)
N(2)-C(29)-C(28)	108.9(2)
N(2)-C(29)-C(31)	120.9(3)
C(28)-C(29)-C(31)	130.2(3)
N(3)-C(32)-C(33)	108.5(3)
N(3)-C(32)-C(35)	120.3(3)
C(33)-C(32)-C(35)	131.1(3)
C(34)-C(33)-C(32)	106.1(3)
N(4)-C(34)-C(33)	108.8(3)
N(4)-C(34)-C(36)	120.7(3)
C(33)-C(34)-C(36)	130.5(3)
N(5)-C(37)-U	170.0(2)

Least-squares planes (x,y,z in crystal coordinates) and deviations from them

(* indicates atom used to define plane)

10.0680 (0.0030) x + 5.2660 (0.0092) y - 14.2795 (0.0135) z = 0.2666 (0.0117)

* 0.0100 (0.0018) C1_a

* 0.0027 (0.0019) C2_a

* -0.0073 (0.0019) C3_a

* -0.0025 (0.0018) C4_a

* 0.0033 (0.0019) C5_a

* 0.0093 (0.0019) C6_a

* -0.0095 (0.0019) C7_a

* -0.0060 (0.0019) C8_a

0.2295 (0.0026) Si1_a

0.1839 (0.0026) Si2_a

-1.9870 (0.0008) U

Rms deviation of fitted atoms = 0.0070

Table 19.

Crystal data and structure refinement for **4.1**

[U(η^5-Ind^{Me6})(η^8-C_8H_6{Si^{i}Pr$_3$-1,4}$_2$)]

Identification code	apr508	
Empirical formula	C41 H67 Si2 U	
Formula weight	854.16	
Temperature	173(2) K	
Wavelength	0.71073 Å	
Crystal system	Monoclinic	
Space group	$P2_1/n$ (No.14)	
Unit cell dimensions	a = 15.2508(2) Å	α= 90°.
	b = 26.5518(5) Å	β= 96.332(1)°.
	c = 19.8423(4) Å	γ = 90°.
Volume	7985.8(2) Å^3	
Z	8	
Density (calculated)	1.42 Mg/m^3	
Absorption coefficient	4.15 mm^{-1}	
F(000)	3464	
Crystal size	0.20 x 0.03 x 0.01 mm^3	
Theta range for data collection	3.46 to 26.01°.	
Index ranges	-18<=h<=16, -32<=k<=32, -24<=l<=24	
Reflections collected	112708	
Independent reflections	15662 [R(int) = 0.184]	
Reflections with I>2sigma(I)	9603	
Completeness to theta = 26.01°	99.6 %	
Tmax. and Tmin.	0.8116 and 0.7427	
Refinement method	Full-matrix least-squares on F^2	
Data / restraints / parameters	15662 / 0 / 829	
Goodness-of-fit on F^2	1.036	
Final R indices [I>2sigma(I)]	R1 = 0.062, wR2 = 0.076	

R indices (all data) R1 = 0.132, wR2 = 0.090

Largest diff. peak and hole 0.71 and -0.80 e.Å^{-3}

Very weak diffraction .

Two independent molecules of essentially the same geometry.

Data collection KappaCCD , Program package WinGX , Abs correction MULTISCAN

Refinement using SHELXL-97 , Drawing using ORTEP-3 for Windows

Table 20.

Atomic coordinates (x 10^4) and equivalent isotropic displacement parameters (Å^{2}x 10^3)

for apr508. U(eq) is defined as one third of the trace of the orthogonalized U^{ij} tensor.

	x	y	z	U(eq)
U	930(1)	1074(1)	1754(1)	27(1)
Si(1)	1705(1)	287(1)	3683(1)	24(1)
Si(2)	1563(1)	2638(1)	2128(1)	26(1)
C(1)	1214(4)	791(3)	3080(4)	24(2)
C(2)	1796(4)	1199(3)	2975(4)	23(2)
C(3)	1771(5)	1679(3)	2673(4)	28(2)
C(4)	1121(5)	1993(3)	2317(4)	26(2)
C(5)	202(5)	1908(3)	2137(4)	31(2)
C(6)	-417(4)	1526(3)	2219(4)	28(2)
C(7)	-370(5)	1047(3)	2523(4)	31(2)
C(8)	293(4)	744(3)	2865(4)	28(2)
C(9)	1006(5)	-306(3)	3617(4)	28(2)
C(10)	1254(5)	-688(3)	4192(4)	42(2)
C(11)	919(5)	-566(3)	2932(4)	43(2)
C(12)	1687(5)	535(3)	4573(4)	29(2)
C(13)	2243(5)	1014(3)	4713(4)	33(2)
C(14)	736(5)	640(3)	4731(4)	38(2)
C(15)	2905(4)	163(3)	3548(4)	26(2)

C(16)	3410(5)	-154(3)	4110(4)	39(2)
C(17)	3012(5)	-59(4)	2852(4)	46(2)
C(18)	1637(5)	3009(3)	2936(4)	36(2)
C(19)	2296(5)	2810(3)	3505(4)	48(3)
C(20)	719(6)	3073(4)	3193(5)	56(3)
C(21)	772(5)	2986(3)	1482(4)	31(2)
C(22)	675(6)	2752(3)	770(4)	48(3)
C(23)	982(5)	3548(3)	1433(5)	49(2)
C(24)	2703(5)	2569(3)	1845(4)	31(2)
C(25)	3152(6)	3067(4)	1714(6)	65(3)
C(26)	2759(6)	2216(4)	1246(5)	54(3)
C(27)	1331(5)	729(3)	568(4)	36(2)
C(28)	2227(5)	567(4)	681(4)	43(2)
C(29)	2397(6)	85(4)	935(5)	50(3)
C(30)	1694(6)	-245(4)	1069(4)	45(2)
C(31)	823(6)	-92(3)	987(4)	40(2)
C(32)	626(5)	403(3)	741(4)	35(2)
C(33)	-166(5)	696(3)	670(4)	38(2)
C(34)	33(5)	1176(3)	428(4)	33(2)
C(35)	958(5)	1203(3)	380(4)	35(2)
C(36)	2944(5)	929(4)	508(5)	57(3)
C(37)	3354(6)	-91(4)	1043(5)	74(4)
C(38)	1950(6)	-776(4)	1305(5)	61(3)
C(39)	64(6)	-438(3)	1116(5)	50(3)
C(40)	-1109(5)	536(4)	747(5)	54(3)
C(41)	-614(6)	1592(4)	240(5)	54(3)
U(1B)	6068(1)	1431(1)	3023(1)	25(1)
Si(1B)	6291(1)	2166(1)	1053(1)	24(1)
Si(2B)	6701(1)	-129(1)	2671(1)	26(1)
C(1B)	5992(4)	1693(3)	1703(4)	20(2)
C(2B)	6637(5)	1309(3)	1815(4)	24(2)
C(3B)	6704(5)	827(3)	2130(4)	25(2)

C(4B)	6171(4)	507(3)	2487(4)	22(2)
C(5B)	5289(5)	573(3)	2646(4)	28(2)
C(6B)	4628(4)	954(3)	2533(4)	26(2)
C(7B)	4568(4)	1422(3)	2247(3)	25(2)
C(8B)	5129(5)	1730(3)	1905(4)	28(2)
C(9B)	5563(5)	2744(3)	1042(4)	34(2)
C(10B)	5554(5)	3054(3)	393(5)	56(3)
C(11B)	5735(5)	3083(3)	1660(5)	50(3)
C(12B)	6040(5)	1837(3)	211(4)	30(2)
C(13B)	6642(6)	1392(3)	105(4)	49(2)
C(14B)	5066(5)	1668(4)	102(5)	56(3)
C(15B)	7510(5)	2318(3)	1194(4)	32(2)
C(16B)	7822(5)	2672(3)	657(5)	50(3)
C(17B)	7827(5)	2515(3)	1909(4)	48(3)
C(18B)	6650(5)	-488(3)	1846(4)	39(2)
C(19B)	7225(7)	-280(4)	1331(5)	59(3)
C(20B)	5689(6)	-538(4)	1515(5)	67(3)
C(21B)	6062(5)	-506(3)	3263(4)	36(2)
C(22B)	6159(5)	-304(4)	3973(4)	48(3)
C(23B)	6289(5)	-1078(3)	3278(5)	56(3)
C(24B)	7906(5)	-44(3)	3010(4)	34(2)
C(25B)	8371(5)	-536(3)	3218(5)	49(3)
C(26B)	8064(5)	351(3)	3587(4)	42(2)
C(27B)	6663(5)	1901(3)	4165(4)	38(2)
C(28B)	7487(6)	2135(5)	4088(5)	58(3)
C(29B)	7482(7)	2621(5)	3813(5)	68(4)
C(30B)	6675(8)	2874(4)	3636(5)	63(3)
C(31B)	5861(6)	2661(4)	3692(4)	47(3)
C(32B)	5847(5)	2157(3)	3955(4)	34(2)
C(33B)	5153(5)	1813(3)	4044(4)	28(2)
C(34B)	5534(5)	1370(3)	4334(4)	29(2)
C(35B)	6447(5)	1411(3)	4396(4)	36(2)

C(36B)	8314(6)	1831(5)	4303(5)	84(4)
C(37B)	8348(7)	2881(6)	3733(6)	126(6)
C(38B)	6730(8)	3421(4)	3397(6)	100(5)
C(39B)	4998(7)	2936(4)	3491(6)	70(3)
C(40B)	4169(5)	1891(3)	3954(5)	50(3)
C(41B)	5015(5)	923(3)	4552(4)	41(2)

Table 21.

Bond lengths [Å] and angles [°] for apr508.

U-M(1)	1.907(8)
U-M(2)	2.459(8)
U-C(5)	2.626(8)
U-C(7)	2.631(7)
U-C(6)	2.632(7)
U-C(2)	2.649(7)
U-C(8)	2.652(8)
U-C(3)	2.652(8)
U-C(27)	2.659(8)
U-C(4)	2.686(8)
U-C(32)	2.688(8)
U-C(1)	2.724(7)
U-C(35)	2.753(8)
U-C(33)	2.764(8)
U-C(34)	2.842(8)
Si(1)-C(12)	1.888(8)
Si(1)-C(1)	1.892(8)
Si(1)-C(9)	1.898(7)
Si(1)-C(15)	1.908(7)
Si(2)-C(18)	1.875(8)
Si(2)-C(4)	1.893(8)
Si(2)-C(24)	1.894(7)

Si(2)-C(21)	1.899(7)
C(1)-C(8)	1.427(9)
C(1)-C(2)	1.432(10)
C(2)-C(3)	1.408(10)
C(3)-C(4)	1.421(10)
C(4)-C(5)	1.427(9)
C(5)-C(6)	1.407(10)
C(6)-C(7)	1.406(10)
C(7)-C(8)	1.408(10)
C(9)-C(11)	1.517(10)
C(9)-C(10)	1.542(10)
C(12)-C(13)	1.537(10)
C(12)-C(14)	1.542(10)
C(15)-C(17)	1.526(10)
C(15)-C(16)	1.534(10)
C(18)-C(19)	1.522(10)
C(18)-C(20)	1.553(11)
C(21)-C(23)	1.534(11)
C(21)-C(22)	1.536(11)
C(24)-C(26)	1.522(11)
C(24)-C(25)	1.525(11)
C(27)-C(35)	1.412(11)
C(27)-C(28)	1.427(11)
C(27)-C(32)	1.451(11)
C(28)-C(29)	1.390(13)
C(28)-C(36)	1.524(12)
C(29)-C(30)	1.432(13)
C(29)-C(37)	1.524(11)
C(30)-C(31)	1.381(11)
C(30)-C(38)	1.521(12)
C(31)-C(32)	1.422(12)
C(31)-C(39)	1.523(11)

C(32)-C(33)	1.431(11)
C(33)-C(34)	1.408(11)
C(33)-C(40)	1.523(11)
C(34)-C(35)	1.426(10)
C(34)-C(41)	1.500(11)
U(1B)-M(3)	1.901(8)
U(1B)-M(4)	2.459(8)
U(1B)-C(7B)	2.614(7)
U(1B)-C(6B)	2.627(7)
U(1B)-C(8B)	2.627(7)
U(1B)-C(5B)	2.638(7)
U(1B)-C(3B)	2.651(7)
U(1B)-C(2B)	2.657(7)
U(1B)-C(27B)	2.658(8)
U(1B)-C(4B)	2.685(7)
U(1B)-C(1B)	2.700(7)
U(1B)-C(32B)	2.718(8)
U(1B)-C(35B)	2.722(7)
U(1B)-C(33B)	2.776(7)
U(1B)-C(34B)	2.815(7)
Si(1B)-C(12B)	1.886(8)
Si(1B)-C(1B)	1.893(7)
Si(1B)-C(15B)	1.893(7)
Si(1B)-C(9B)	1.894(8)
Si(2B)-C(18B)	1.887(9)
Si(2B)-C(4B)	1.890(7)
Si(2B)-C(21B)	1.892(8)
Si(2B)-C(24B)	1.900(8)
C(1B)-C(2B)	1.415(9)
C(1B)-C(8B)	1.421(9)
C(2B)-C(3B)	1.424(9)
C(3B)-C(4B)	1.418(10)

C(4B)-C(5B)	1.427(10)
C(5B)-C(6B)	1.428(10)
C(6B)-C(7B)	1.365(10)
C(7B)-C(8B)	1.409(10)
C(9B)-C(11B)	1.520(11)
C(9B)-C(10B)	1.529(11)
C(12B)-C(13B)	1.526(11)
C(12B)-C(14B)	1.544(10)
C(15B)-C(16B)	1.535(10)
C(15B)-C(17B)	1.539(11)
C(18B)-C(19B)	1.523(12)
C(18B)-C(20B)	1.544(11)
C(21B)-C(22B)	1.500(11)
C(21B)-C(23B)	1.559(11)
C(24B)-C(25B)	1.520(10)
C(24B)-C(26B)	1.552(11)
C(27B)-C(28B)	1.426(11)
C(27B)-C(35B)	1.430(11)
C(27B)-C(32B)	1.439(11)
C(28B)-C(29B)	1.400(15)
C(28B)-C(36B)	1.519(13)
C(29B)-C(30B)	1.412(15)
C(29B)-C(37B)	1.514(12)
C(30B)-C(31B)	1.381(13)
C(30B)-C(38B)	1.532(14)
C(31B)-C(32B)	1.436(12)
C(31B)-C(39B)	1.520(12)
C(32B)-C(33B)	1.423(10)
C(33B)-C(34B)	1.407(11)
C(33B)-C(40B)	1.507(10)
C(34B)-C(35B)	1.389(10)
C(34B)-C(41B)	1.514(10)

M(1)-U-M(2)	154.6(3)
M(3)-U(1B)-M(4)	153.9(3)
C(12)-Si(1)-C(1)	107.4(3)
C(12)-Si(1)-C(9)	106.7(3)
C(1)-Si(1)-C(9)	111.3(3)
C(12)-Si(1)-C(15)	107.7(3)
C(1)-Si(1)-C(15)	110.6(3)
C(9)-Si(1)-C(15)	112.7(3)
C(18)-Si(2)-C(4)	107.2(4)
C(18)-Si(2)-C(24)	109.5(4)
C(4)-Si(2)-C(24)	109.2(3)
C(18)-Si(2)-C(21)	107.2(4)
C(4)-Si(2)-C(21)	111.1(3)
C(24)-Si(2)-C(21)	112.5(4)
C(8)-C(1)-C(2)	128.9(7)
C(8)-C(1)-Si(1)	115.8(5)
C(2)-C(1)-Si(1)	114.8(5)
C(8)-C(1)-U	71.8(4)
C(2)-C(1)-U	71.7(4)
Si(1)-C(1)-U	144.6(4)
C(3)-C(2)-C(1)	139.5(7)
C(3)-C(2)-U	74.7(4)
C(1)-C(2)-U	77.5(4)
C(2)-C(3)-C(4)	136.7(7)
C(2)-C(3)-U	74.5(4)
C(4)-C(3)-U	75.9(4)
C(3)-C(4)-C(5)	130.1(7)
C(3)-C(4)-Si(2)	112.7(5)
C(5)-C(4)-Si(2)	117.0(5)
C(3)-C(4)-U	73.3(4)
C(5)-C(4)-U	72.1(4)

Si(2)-C(4)-U	139.9(4)
C(6)-C(5)-C(4)	137.6(7)
C(6)-C(5)-U	74.7(4)
C(4)-C(5)-U	76.7(4)
C(7)-C(6)-C(5)	134.3(7)
C(7)-C(6)-U	74.5(4)
C(5)-C(6)-U	74.2(4)
C(6)-C(7)-C(8)	136.4(7)
C(6)-C(7)-U	74.5(4)
C(8)-C(7)-U	75.4(4)
C(7)-C(8)-C(1)	136.5(7)
C(7)-C(8)-U	73.7(4)
C(1)-C(8)-U	77.4(4)
C(11)-C(9)-C(10)	110.8(7)
C(11)-C(9)-Si(1)	115.6(5)
C(10)-C(9)-Si(1)	113.9(5)
C(13)-C(12)-C(14)	109.1(6)
C(13)-C(12)-Si(1)	113.1(5)
C(14)-C(12)-Si(1)	111.4(5)
C(17)-C(15)-C(16)	110.6(7)
C(17)-C(15)-Si(1)	113.2(5)
C(16)-C(15)-Si(1)	113.9(5)
C(19)-C(18)-C(20)	109.8(7)
C(19)-C(18)-Si(2)	115.1(6)
C(20)-C(18)-Si(2)	111.5(6)
C(23)-C(21)-C(22)	109.6(7)
C(23)-C(21)-Si(2)	113.2(5)
C(22)-C(21)-Si(2)	114.4(6)
C(26)-C(24)-C(25)	109.5(7)
C(26)-C(24)-Si(2)	115.0(6)
C(25)-C(24)-Si(2)	114.3(6)
C(35)-C(27)-C(28)	131.3(8)

C(35)-C(27)-C(32)	107.9(7)
C(28)-C(27)-C(32)	120.3(8)
C(35)-C(27)-U	78.6(5)
C(28)-C(27)-U	106.0(5)
C(32)-C(27)-U	75.4(4)
C(29)-C(28)-C(27)	118.2(8)
C(29)-C(28)-C(36)	123.6(8)
C(27)-C(28)-C(36)	118.2(9)
C(28)-C(29)-C(30)	121.2(8)
C(28)-C(29)-C(37)	118.0(9)
C(30)-C(29)-C(37)	120.7(10)
C(31)-C(30)-C(29)	121.8(9)
C(31)-C(30)-C(38)	121.3(9)
C(29)-C(30)-C(38)	116.9(8)
C(30)-C(31)-C(32)	118.5(8)
C(30)-C(31)-C(39)	122.8(9)
C(32)-C(31)-C(39)	118.7(8)
C(31)-C(32)-C(33)	132.9(8)
C(31)-C(32)-C(27)	120.0(7)
C(33)-C(32)-C(27)	106.9(8)
C(31)-C(32)-U	110.1(5)
C(33)-C(32)-U	77.7(5)
C(27)-C(32)-U	73.1(4)
C(34)-C(33)-C(32)	108.4(7)
C(34)-C(33)-C(40)	121.9(8)
C(32)-C(33)-C(40)	129.4(8)
C(34)-C(33)-U	78.5(5)
C(32)-C(33)-U	71.9(4)
C(40)-C(33)-U	121.3(6)
C(33)-C(34)-C(35)	108.6(7)
C(33)-C(34)-C(41)	126.2(8)
C(35)-C(34)-C(41)	125.2(8)

C(33)-C(34)-U	72.4(5)
C(35)-C(34)-U	71.8(4)
C(41)-C(34)-U	122.5(5)
C(27)-C(35)-C(34)	108.1(8)
C(27)-C(35)-U	71.2(5)
C(34)-C(35)-U	78.7(4)
C(12B)-Si(1B)-C(1B)	104.8(3)
C(12B)-Si(1B)-C(15B)	109.3(4)
C(1B)-Si(1B)-C(15B)	110.3(3)
C(12B)-Si(1B)-C(9B)	107.7(4)
C(1B)-Si(1B)-C(9B)	111.1(3)
C(15B)-Si(1B)-C(9B)	113.2(4)
C(18B)-Si(2B)-C(4B)	107.9(4)
C(18B)-Si(2B)-C(21B)	107.2(4)
C(4B)-Si(2B)-C(21B)	110.7(3)
C(18B)-Si(2B)-C(24B)	108.3(4)
C(4B)-Si(2B)-C(24B)	109.8(3)
C(21B)-Si(2B)-C(24B)	112.8(4)
C(2B)-C(1B)-C(8B)	130.9(7)
C(2B)-C(1B)-Si(1B)	111.7(5)
C(8B)-C(1B)-Si(1B)	116.5(5)
C(2B)-C(1B)-U(1B)	73.0(4)
C(8B)-C(1B)-U(1B)	71.7(4)
Si(1B)-C(1B)-U(1B)	147.6(4)
C(1B)-C(2B)-C(3B)	136.9(7)
C(1B)-C(2B)-U(1B)	76.4(4)
C(3B)-C(2B)-U(1B)	74.2(4)
C(4B)-C(3B)-C(2B)	137.8(7)
C(4B)-C(3B)-U(1B)	75.9(4)
C(2B)-C(3B)-U(1B)	74.7(4)
C(3B)-C(4B)-C(5B)	130.0(7)
C(3B)-C(4B)-Si(2B)	112.1(5)

C(5B)-C(4B)-Si(2B)	117.4(5)
C(3B)-C(4B)-U(1B)	73.3(4)
C(5B)-C(4B)-U(1B)	72.6(4)
Si(2B)-C(4B)-U(1B)	141.4(3)
C(4B)-C(5B)-C(6B)	136.0(7)
C(4B)-C(5B)-U(1B)	76.3(4)
C(6B)-C(5B)-U(1B)	73.8(4)
C(7B)-C(6B)-C(5B)	136.4(7)
C(7B)-C(6B)-U(1B)	74.4(4)
C(5B)-C(6B)-U(1B)	74.7(4)
C(6B)-C(7B)-C(8B)	135.3(7)
C(6B)-C(7B)-U(1B)	75.4(4)
C(8B)-C(7B)-U(1B)	74.9(4)
C(7B)-C(8B)-C(1B)	136.5(7)
C(7B)-C(8B)-U(1B)	73.9(4)
C(1B)-C(8B)-U(1B)	77.4(4)
C(11B)-C(9B)-C(10B)	110.2(7)
C(11B)-C(9B)-Si(1B)	115.0(6)
C(10B)-C(9B)-Si(1B)	113.3(6)
C(13B)-C(12B)-C(14B)	109.9(7)
C(13B)-C(12B)-Si(1B)	114.5(5)
C(14B)-C(12B)-Si(1B)	111.0(5)
C(16B)-C(15B)-C(17B)	110.0(7)
C(16B)-C(15B)-Si(1B)	113.7(6)
C(17B)-C(15B)-Si(1B)	114.4(5)
C(19B)-C(18B)-C(20B)	109.6(8)
C(19B)-C(18B)-Si(2B)	115.4(6)
C(20B)-C(18B)-Si(2B)	111.1(6)
C(22B)-C(21B)-C(23B)	109.3(7)
C(22B)-C(21B)-Si(2B)	113.0(6)
C(23B)-C(21B)-Si(2B)	113.5(6)
C(25B)-C(24B)-C(26B)	110.6(7)

C(25B)-C(24B)-Si(2B)	113.5(6)
C(26B)-C(24B)-Si(2B)	114.0(5)
C(28B)-C(27B)-C(35B)	131.9(9)
C(28B)-C(27B)-C(32B)	120.5(9)
C(35B)-C(27B)-C(32B)	107.5(7)
C(28B)-C(27B)-U(1B)	109.6(6)
C(35B)-C(27B)-U(1B)	77.1(5)
C(32B)-C(27B)-U(1B)	76.8(4)
C(29B)-C(28B)-C(27B)	118.5(9)
C(29B)-C(28B)-C(36B)	124.7(9)
C(27B)-C(28B)-C(36B)	116.9(10)
C(28B)-C(29B)-C(30B)	120.2(9)
C(28B)-C(29B)-C(37B)	119.6(12)
C(30B)-C(29B)-C(37B)	120.2(12)
C(31B)-C(30B)-C(29B)	123.4(10)
C(31B)-C(30B)-C(38B)	119.6(11)
C(29B)-C(30B)-C(38B)	116.9(10)
C(30B)-C(31B)-C(32B)	117.5(9)
C(30B)-C(31B)-C(39B)	122.8(10)
C(32B)-C(31B)-C(39B)	119.7(8)
C(33B)-C(32B)-C(31B)	133.2(8)
C(33B)-C(32B)-C(27B)	106.9(7)
C(31B)-C(32B)-C(27B)	119.9(8)
C(33B)-C(32B)-U(1B)	77.2(4)
C(31B)-C(32B)-U(1B)	114.0(5)
C(27B)-C(32B)-U(1B)	72.2(5)
C(34B)-C(33B)-C(32B)	108.0(7)
C(34B)-C(33B)-C(40B)	121.7(7)
C(32B)-C(33B)-C(40B)	129.9(8)
C(34B)-C(33B)-U(1B)	77.0(4)
C(32B)-C(33B)-U(1B)	72.8(4)
C(40B)-C(33B)-U(1B)	122.6(5)

C(35B)-C(34B)-C(33B)	109.6(7)
C(35B)-C(34B)-C(41B)	126.0(8)
C(33B)-C(34B)-C(41B)	124.4(7)
C(35B)-C(34B)-U(1B)	71.8(4)
C(33B)-C(34B)-U(1B)	73.9(4)
C(41B)-C(34B)-U(1B)	121.5(5)
C(34B)-C(35B)-C(27B)	107.9(7)
C(34B)-C(35B)-U(1B)	79.2(4)
C(27B)-C(35B)-U(1B)	72.1(4)

M(1) is the centroid of the C(1) to C(8) ring M(3) is the value for the B molecule

M(2) is the centroid of the C(27),C(32),C(33),C(34),C(35) ring M(4) is the values for the B molecule

Least-squares planes (x,y,z in crystal coordinates) and deviations from them

(* indicates atom used to define plane)

- 4.4628 (0.0294) x + 10.8152 (0.0485) y + 17.7019 (0.0176) z = 5.7588 (0.0058)

*	0.0071 (0.0058)	C1_a
*	0.0033 (0.0058)	C2_a
*	-0.0016 (0.0061)	C3_a
*	-0.0024 (0.0060)	C4_a
*	-0.0031 (0.0060)	C5_a
*	0.0062 (0.0061)	C6_a
*	0.0047 (0.0062)	C7_a
*	-0.0142 (0.0061)	C8_a
	-1.9065 (0.0026)	U
	0.3104 (0.0081)	Si1_a
	0.1631 (0.0084)	Si2_a

Rms deviation of fitted atoms = 0.0065

0.9784 (0.0600) x + 8.2255 (0.0977) y + 18.5679 (0.0271) z = 1.7819 (0.0082)

Angle to previous plane (with approximate esd) = 21.86 (0.27)

* 0.0033 (0.0049) C27_a

* -0.0129 (0.0049) C32_a

* 0.0179 (0.0050) C33_a

* -0.0158 (0.0049) C34_a

* 0.0075 (0.0049) C35_a

2.4501 (0.0034) U

-0.0624 (0.0148) C40_a

-0.0869 (0.0143) C41_a

Rms deviation of fitted atoms = 0.0127

- 0.3475 (0.0468) x + 9.3573 (0.0804) y + 18.5004 (0.0230) z = 1.7085 (0.0073)

Angle to previous plane (with approximate esd) = 5.60 (0.32)

* -0.0211 (0.0055) C27_a

* 0.0038 (0.0058) C28_a

* 0.0168 (0.0061) C29_a

* -0.0202 (0.0060) C30_a

* 0.0026 (0.0058) C31_a

* 0.0180 (0.0056) C32_a

-0.0022 (0.0133) C36_a

0.0202 (0.0140) C37_a

-0.0571 (0.0133) C39_a

-0.0571 (0.0133) C39_a

Rms deviation of fitted atoms = 0.0157

3.9960 (0.0276) x + 11.2840 (0.0456) y + 16.5141 (0.0210) z = 7.1306 (0.0125)

Angle to previous plane (with approximate esd) = 17.36 (0.25)

* -0.0134 (0.0057) C1B_a

* -0.0042 (0.0057) C2B_a

* -0.0013 (0.0057) C3B_a

* 0.0142 (0.0056) C4B_a

* -0.0003 (0.0057) C5B_a

* -0.0217 (0.0058) C6B_a

* 0.0096 (0.0057) C7B_a

* 0.0170 (0.0059) C8B_a

1.9008 (0.0024) U1B

-0.4339 (0.0078) Si1B_a

-0.1878 (0.0078) Si2B_a

Rms deviation of fitted atoms = 0.0125

- 1.9523 (0.0594) x + 9.6400 (0.0980) y + 18.4815 (0.0286) z = 8.2333 (0.0368)

Angle to previous plane (with approximate esd) = 23.01 (0.27)

* -0.0036 (0.0050) C27B_a

* 0.0132 (0.0050) C32B_a

* -0.0182 (0.0049) C33B_a

* 0.0162 (0.0049) C34B_a

* -0.0077 (0.0049) C35B_a

```
    -2.4521 (0.0034)  U1B

     0.0825 (0.0143)  C40B_a

     0.0898 (0.0139)  C41B_a


 Rms deviation of fitted atoms =   0.0130



 - 1.2465 (0.0524) x + 10.0079 (0.0868) y + 18.3743 (0.0264) z =
8.7125 (0.0361)


 Angle to previous plane (with approximate esd) =  2.77 ( 0.37 )


 *    0.0128 (0.0060)  C27B_a

 *    0.0034 (0.0068)  C28B_a

 *   -0.0163 (0.0072)  C29B_a

 *    0.0128 (0.0068)  C30B_a

 *    0.0037 (0.0061)  C31B_a

 *   -0.0164 (0.0058)  C32B_a

    -0.0107 (0.0157)  C36B_a

    -0.0103 (0.0177)  C37B_a

     0.1131 (0.0168)  C38B_a

     0.0179 (0.0152)  C39B_a


 Rms deviation of fitted atoms =   0.0122
```

Table 22.

Crystal data and structure refinement for **4.2**

[U(η^5-Ind^{Me7})(η-C_8H_4{Si^{i}Pr$_3$-1,4}$_2$)]

Identification code	jul509	
Empirical formula	C42 H69 Si2 U	
Formula weight	868.18	
Temperature	173(2) K	
Wavelength	0.71073 Å	
Crystal system	Monoclinic	
Space group	$P2_1/n$ (No.14)	
Unit cell dimensions	a = 15.2615(1) Å	α= 90°.
	b = 26.6255(3) Å	β= 96.016(1)°.
	c = 20.1330(2) Å	γ = 90°.
Volume	8135.89(13) Å^3	
Z	8	
Density (calculated)	1.42 Mg/m^3	
Absorption coefficient	4.08 mm^{-1}	
F(000)	3528	
Crystal size	0.22 x 0.15 x 0.06 mm^3	
Theta range for data collection	3.41 to 27.48°.	
Index ranges	-19<=h<=19, -34<=k<=34, -26<=l<=26	
Reflections collected	113101	
Independent reflections	18524 [R(int) = 0.087]	
Reflections with I>2sigma(I)	13965	
Completeness to theta = 27.48°	99.3 %	
Absorption correction	Semi-empirical from equivalents	
Tmax. and Tmin.	0.6328 and 0.4845	
Refinement method	Full-matrix least-squares on F^2	
Data / restraints / parameters	18524 / 0 / 825	
Goodness-of-fit on F^2	1.041	

Final R indices [I>2sigma(I)]	R1 = 0.046, wR2 = 0.077
R indices (all data)	R1 = 0.076, wR2 = 0.085
Largest diff. peak and hole	2.318 and -1.007 e.Å^{-3} (near uranium)

Crystal structure isomorphous with the Ind-Me_6 analogue (two independent molecules with essentially the same geometry)

Data collection KappaCCD , Program package WinGX , Abs correction MULTISCAN

Refinement using SHELXL-97 , Drawing using ORTEP-3 for Windows

Table 23.

Atomic coordinates (x 10^4) and equivalent isotropic displacement parameters (Å^{2}x 10^3)

for jul509. U(eq) is defined as one third of the trace of the orthogonalized U^{ij} tensor.

	x	y	z	U(eq)
U	915(1)	1095(1)	1727(1)	27(1)
U(1B)	6051(1)	1475(1)	2986(1)	23(1)
Si(1)	1660(1)	322(1)	3629(1)	20(1)
Si(2)	1482(1)	2672(1)	2133(1)	25(1)
C(1)	1164(3)	819(2)	3035(2)	21(1)
C(2)	1741(3)	1227(2)	2949(2)	24(1)
C(3)	1703(3)	1710(2)	2648(2)	27(1)
C(4)	1067(3)	2018(2)	2287(3)	28(1)
C(5)	148(3)	1928(2)	2086(3)	29(1)
C(6)	-450(3)	1537(2)	2166(3)	31(1)
C(7)	-413(3)	1062(2)	2458(3)	30(1)
C(8)	244(3)	766(2)	2816(2)	26(1)
C(9)	955(3)	-269(2)	3568(2)	26(1)
C(10)	1194(4)	-645(2)	4131(3)	40(1)
C(11)	883(4)	-532(2)	2896(3)	39(1)
C(12)	1645(3)	568(2)	4504(2)	27(1)

C(13)	709(3)	669(2)	4677(3)	42(1)
C(14)	2222(3)	1034(2)	4658(3)	34(1)
C(15)	2852(3)	203(2)	3480(2)	26(1)
C(16)	2967(4)	-4(2)	2787(3)	48(2)
C(17)	3368(3)	-121(2)	4018(3)	42(1)
C(18)	1476(4)	3030(2)	2943(3)	37(1)
C(19)	2150(4)	2837(2)	3505(3)	49(2)
C(20)	556(4)	3049(3)	3178(3)	61(2)
C(21)	2656(3)	2635(2)	1899(3)	32(1)
C(22)	3083(4)	3146(2)	1814(4)	56(2)
C(23)	2764(4)	2303(3)	1301(3)	51(2)
C(24)	711(3)	3021(2)	1490(3)	33(1)
C(25)	919(4)	3591(2)	1460(3)	52(2)
C(26)	629(4)	2796(2)	789(3)	51(2)
C(27)	607(4)	381(2)	776(3)	38(1)
C(28)	767(4)	-124(2)	1015(3)	45(2)
C(29)	1626(4)	-298(2)	1099(3)	44(2)
C(30)	2340(4)	28(3)	962(3)	52(2)
C(31)	2213(4)	503(2)	713(3)	45(2)
C(32)	1312(4)	687(2)	590(3)	40(1)
C(33)	971(4)	1163(2)	367(3)	46(2)
C(34)	57(4)	1143(2)	421(3)	44(2)
C(35)	-189(4)	683(2)	685(3)	42(1)
C(36)	-35(5)	-436(3)	1138(3)	63(2)
C(37)	1828(5)	-831(3)	1321(4)	71(2)
C(38)	3287(5)	-169(3)	1089(4)	78(2)
C(39)	2975(5)	831(3)	572(4)	71(2)
C(40)	1427(5)	1568(3)	4(3)	63(2)
C(41)	-576(5)	1564(3)	198(3)	62(2)
C(42)	-1138(4)	550(3)	765(3)	64(2)
Si(1B)	6231(1)	2136(1)	992(1)	24(1)
Si(2B)	6687(1)	-100(1)	2730(1)	26(1)

C(1B)	5949(3)	1682(2)	1663(2)	24(1)
C(2B)	6593(3)	1299(2)	1792(2)	27(1)
C(3B)	6673(3)	837(2)	2140(2)	28(1)
C(4B)	6155(3)	532(2)	2523(2)	26(1)
C(5B)	5277(3)	601(2)	2695(2)	27(1)
C(6B)	4620(3)	972(2)	2570(3)	29(1)
C(7B)	4544(3)	1434(2)	2236(2)	28(1)
C(8B)	5091(3)	1732(2)	1870(2)	25(1)
C(9B)	5484(3)	2710(2)	947(3)	31(1)
C(10B)	5460(4)	2997(2)	282(3)	51(2)
C(11B)	5678(4)	3069(2)	1527(3)	48(2)
C(12B)	5973(4)	1790(2)	178(3)	42(1)
C(13B)	5002(5)	1623(3)	85(3)	62(2)
C(14B)	6587(5)	1343(2)	85(3)	60(2)
C(15B)	7451(3)	2302(2)	1117(3)	31(1)
C(16B)	7756(4)	2511(2)	1810(3)	49(2)
C(17B)	7742(4)	2646(2)	570(4)	56(2)
C(18B)	6579(4)	-483(2)	1932(3)	39(1)
C(19B)	7119(5)	-294(2)	1389(3)	61(2)
C(20B)	5609(5)	-544(3)	1658(4)	71(2)
C(21B)	7906(3)	-9(2)	3023(3)	31(1)
C(22B)	8373(4)	-504(2)	3240(3)	47(2)
C(23B)	8099(4)	387(2)	3568(3)	43(1)
C(24B)	6087(3)	-458(2)	3365(3)	33(1)
C(25B)	6316(4)	-1022(2)	3398(4)	51(2)
C(26B)	6182(4)	-230(2)	4053(3)	46(2)
C(27B)	5762(3)	2241(2)	3821(2)	27(1)
C(28B)	5728(4)	2722(2)	3499(3)	33(1)
C(29B)	6508(4)	2962(2)	3418(3)	36(1)
C(30B)	7335(4)	2742(2)	3648(3)	42(1)
C(31B)	7401(4)	2280(2)	3955(3)	41(1)
C(32B)	6593(3)	2023(2)	4071(2)	28(1)

C(33B)	6429(4)	1537(2)	4346(2)	33(1)
C(34B)	5502(4)	1472(2)	4276(2)	32(1)
C(35B)	5080(3)	1887(2)	3942(2)	29(1)
C(36B)	4842(4)	2945(2)	3270(3)	46(2)
C(37B)	6517(5)	3484(2)	3119(3)	53(2)
C(38B)	8174(4)	3031(3)	3540(4)	72(2)
C(39B)	8270(4)	2036(3)	4188(5)	83(3)
C(40B)	7079(4)	1198(2)	4748(3)	47(2)
C(41B)	5028(4)	1037(2)	4545(3)	45(2)
C(42B)	4091(3)	1943(2)	3845(3)	44(1)

Table 24.

Bond lengths [Å] and angles [°] for jul509.

U-M(1)	1.917(16)
U-M(2)	2.460(9)
U-C(6)	2.625(5)
U-C(7)	2.628(5)
U-C(5)	2.644(5)
U-C(32)	2.661(5)
U-C(3)	2.663(5)
U-C(8)	2.665(5)
U-C(2)	2.667(5)
U-C(4)	2.703(5)
U-C(27)	2.705(5)
U-C(1)	2.722(4)
U-C(33)	2.753(5)
U-C(35)	2.775(5)
U-C(34)	2.814(5)
U(1B)-M(3)	1.906(7)
U(1B)-M(4)	2.46(2)
U(1B)-C(7B)	2.619(5)

U(1B)-C(6B)	2.622(5)
U(1B)-C(8B)	2.642(5)
U(1B)-C(5B)	2.648(5)
U(1B)-C(3B)	2.652(5)
U(1B)-C(2B)	2.665(5)
U(1B)-C(32B)	2.684(5)
U(1B)-C(4B)	2.689(5)
U(1B)-C(27B)	2.708(5)
U(1B)-C(1B)	2.710(5)
U(1B)-C(33B)	2.743(5)
U(1B)-C(35B)	2.775(5)
U(1B)-C(34B)	2.810(5)
Si(1)-C(12)	1.882(5)
Si(1)-C(1)	1.889(4)
Si(1)-C(15)	1.900(5)
Si(1)-C(9)	1.901(5)
Si(2)-C(18)	1.889(6)
Si(2)-C(4)	1.890(5)
Si(2)-C(24)	1.897(5)
Si(2)-C(21)	1.903(5)
C(1)-C(2)	1.421(6)
C(1)-C(8)	1.434(6)
C(2)-C(3)	1.418(6)
C(3)-C(4)	1.413(6)
C(4)-C(5)	1.439(7)
C(5)-C(6)	1.405(7)
C(6)-C(7)	1.395(7)
C(7)-C(8)	1.412(7)
C(9)-C(11)	1.517(7)
C(9)-C(10)	1.528(7)
C(12)-C(13)	1.530(7)
C(12)-C(14)	1.535(7)

C(15)-C(16)	1.528(7)
C(15)-C(17)	1.537(7)
C(18)-C(20)	1.529(8)
C(18)-C(19)	1.537(8)
C(21)-C(23)	1.517(8)
C(21)-C(22)	1.525(7)
C(24)-C(26)	1.525(8)
C(24)-C(25)	1.555(7)
C(27)-C(32)	1.429(8)
C(27)-C(28)	1.440(8)
C(27)-C(35)	1.453(8)
C(28)-C(29)	1.383(8)
C(28)-C(36)	1.521(8)
C(29)-C(30)	1.443(9)
C(29)-C(37)	1.510(9)
C(30)-C(31)	1.368(9)
C(30)-C(38)	1.534(9)
C(31)-C(32)	1.456(8)
C(31)-C(39)	1.506(9)
C(32)-C(33)	1.424(8)
C(33)-C(34)	1.410(8)
C(33)-C(40)	1.513(8)
C(34)-C(35)	1.402(8)
C(34)-C(41)	1.516(8)
C(35)-C(42)	1.517(8)
Si(1B)-C(12B)	1.886(6)
Si(1B)-C(1B)	1.895(5)
Si(1B)-C(9B)	1.903(5)
Si(1B)-C(15B)	1.903(5)
Si(2B)-C(18B)	1.895(5)
Si(2B)-C(4B)	1.897(5)
Si(2B)-C(24B)	1.904(5)

Si(2B)-C(21B)	1.907(5)
C(1B)-C(8B)	1.421(6)
C(1B)-C(2B)	1.423(7)
C(2B)-C(3B)	1.413(7)
C(3B)-C(4B)	1.417(7)
C(4B)-C(5B)	1.430(7)
C(5B)-C(6B)	1.412(7)
C(6B)-C(7B)	1.400(7)
C(7B)-C(8B)	1.415(7)
C(9B)-C(11B)	1.515(8)
C(9B)-C(10B)	1.538(7)
C(12B)-C(14B)	1.538(8)
C(12B)-C(13B)	1.541(8)
C(15B)-C(16B)	1.529(8)
C(15B)-C(17B)	1.536(7)
C(18B)-C(19B)	1.522(8)
C(18B)-C(20B)	1.533(8)
C(21B)-C(23B)	1.528(7)
C(21B)-C(22B)	1.541(7)
C(24B)-C(26B)	1.505(8)
C(24B)-C(25B)	1.541(7)
C(27B)-C(28B)	1.434(7)
C(27B)-C(32B)	1.437(7)
C(27B)-C(35B)	1.442(7)
C(28B)-C(29B)	1.376(7)
C(28B)-C(36B)	1.504(7)
C(29B)-C(30B)	1.423(8)
C(29B)-C(37B)	1.517(8)
C(30B)-C(31B)	1.376(8)
C(30B)-C(38B)	1.529(8)
C(31B)-C(32B)	1.450(7)
C(31B)-C(39B)	1.506(8)

C(32B)-C(33B)	1.439(7)
C(33B)-C(34B)	1.418(7)
C(33B)-C(40B)	1.512(7)
C(34B)-C(35B)	1.414(7)
C(34B)-C(41B)	1.495(7)
C(35B)-C(42B)	1.510(7)

M(1)-U-M(2)	154.3(4)
M(3)-U(1B)-M(4)	152.3(3)
C(12)-Si(1)-C(1)	107.8(2)
C(12)-Si(1)-C(15)	108.1(2)
C(1)-Si(1)-C(15)	110.1(2)
C(12)-Si(1)-C(9)	106.6(2)
C(1)-Si(1)-C(9)	110.6(2)
C(15)-Si(1)-C(9)	113.4(2)
C(18)-Si(2)-C(4)	107.0(2)
C(18)-Si(2)-C(24)	106.5(2)
C(4)-Si(2)-C(24)	111.6(2)
C(18)-Si(2)-C(21)	109.2(2)
C(4)-Si(2)-C(21)	109.5(2)
C(24)-Si(2)-C(21)	112.9(2)
C(2)-C(1)-C(8)	129.7(4)
C(2)-C(1)-Si(1)	113.7(3)
C(8)-C(1)-Si(1)	116.0(3)
C(3)-C(2)-C(1)	138.3(4)
C(3)-C(2)-U	74.4(3)
C(1)-C(2)-U	76.9(3)
C(4)-C(3)-C(2)	137.8(4)
C(3)-C(4)-C(5)	130.2(4)
C(3)-C(4)-Si(2)	113.3(3)
C(5)-C(4)-Si(2)	116.1(3)
C(6)-C(5)-C(4)	135.8(4)

C(7)-C(6)-C(5)	136.3(5)
C(6)-C(7)-C(8)	135.8(5)
C(7)-C(8)-C(1)	136.2(4)
C(11)-C(9)-C(10)	110.4(4)
C(11)-C(9)-Si(1)	115.3(3)
C(10)-C(9)-Si(1)	113.8(3)
C(13)-C(12)-C(14)	109.9(4)
C(13)-C(12)-Si(1)	112.1(4)
C(14)-C(12)-Si(1)	114.1(3)
C(16)-C(15)-C(17)	109.9(4)
C(16)-C(15)-Si(1)	114.0(3)
C(17)-C(15)-Si(1)	114.3(3)
C(20)-C(18)-C(19)	110.3(5)
C(20)-C(18)-Si(2)	111.8(4)
C(19)-C(18)-Si(2)	113.8(4)
C(23)-C(21)-C(22)	110.4(5)
C(23)-C(21)-Si(2)	114.2(4)
C(22)-C(21)-Si(2)	113.9(4)
C(26)-C(24)-C(25)	110.1(5)
C(26)-C(24)-Si(2)	115.1(4)
C(25)-C(24)-Si(2)	113.0(4)
C(32)-C(27)-C(28)	120.9(6)
C(32)-C(27)-C(35)	107.0(5)
C(28)-C(27)-C(35)	132.0(5)
C(29)-C(28)-C(27)	118.6(5)
C(29)-C(28)-C(36)	124.4(6)
C(27)-C(28)-C(36)	116.9(6)
C(28)-C(29)-C(30)	120.0(6)
C(28)-C(29)-C(37)	120.9(6)
C(30)-C(29)-C(37)	119.1(6)
C(31)-C(30)-C(29)	123.0(6)
C(31)-C(30)-C(38)	118.2(7)

C(29)-C(30)-C(38)	118.8(6)
C(30)-C(31)-C(32)	117.9(6)
C(30)-C(31)-C(39)	121.5(6)
C(32)-C(31)-C(39)	120.5(6)
C(33)-C(32)-C(27)	109.2(5)
C(33)-C(32)-C(31)	131.3(6)
C(27)-C(32)-C(31)	119.1(5)
C(34)-C(33)-C(32)	105.9(5)
C(34)-C(33)-C(40)	124.9(6)
C(32)-C(33)-C(40)	127.9(6)
C(35)-C(34)-C(33)	111.6(5)
C(35)-C(34)-C(41)	124.7(6)
C(33)-C(34)-C(41)	123.7(6)
C(34)-C(35)-C(27)	106.1(5)
C(34)-C(35)-C(42)	122.8(6)
C(27)-C(35)-C(42)	130.8(6)
C(12B)-Si(1B)-C(1B)	105.3(2)
C(12B)-Si(1B)-C(9B)	106.3(2)
C(1B)-Si(1B)-C(9B)	111.5(2)
C(12B)-Si(1B)-C(15B)	109.9(3)
C(1B)-Si(1B)-C(15B)	110.2(2)
C(9B)-Si(1B)-C(15B)	113.2(2)
C(18B)-Si(2B)-C(4B)	107.1(2)
C(18B)-Si(2B)-C(24B)	107.2(2)
C(4B)-Si(2B)-C(24B)	111.5(2)
C(18B)-Si(2B)-C(21B)	109.0(2)
C(4B)-Si(2B)-C(21B)	109.7(2)
C(24B)-Si(2B)-C(21B)	112.2(2)
C(8B)-C(1B)-C(2B)	130.8(4)
C(8B)-C(1B)-Si(1B)	115.8(3)
C(2B)-C(1B)-Si(1B)	112.6(3)
C(3B)-C(2B)-C(1B)	137.5(5)

C(2B)-C(3B)-C(4B)	138.1(5)
C(3B)-C(4B)-C(5B)	130.5(4)
C(3B)-C(4B)-Si(2B)	112.2(3)
C(5B)-C(4B)-Si(2B)	116.8(3)
C(6B)-C(5B)-C(4B)	135.4(4)
C(7B)-C(6B)-C(5B)	136.2(5)
C(6B)-C(7B)-C(8B)	136.0(5)
C(7B)-C(8B)-C(1B)	135.5(4)
C(11B)-C(9B)-C(10B)	110.1(5)
C(11B)-C(9B)-Si(1B)	113.7(4)
C(10B)-C(9B)-Si(1B)	113.6(4)
C(14B)-C(12B)-C(13B)	110.6(5)
C(14B)-C(12B)-Si(1B)	114.3(4)
C(13B)-C(12B)-Si(1B)	111.0(4)
C(16B)-C(15B)-C(17B)	110.7(5)
C(16B)-C(15B)-Si(1B)	113.9(4)
C(17B)-C(15B)-Si(1B)	113.3(4)
C(19B)-C(18B)-C(20B)	110.7(6)
C(19B)-C(18B)-Si(2B)	115.2(4)
C(20B)-C(18B)-Si(2B)	110.9(4)
C(23B)-C(21B)-C(22B)	109.7(5)
C(23B)-C(21B)-Si(2B)	114.7(4)
C(22B)-C(21B)-Si(2B)	112.7(3)
C(26B)-C(24B)-C(25B)	110.7(5)
C(26B)-C(24B)-Si(2B)	114.2(4)
C(25B)-C(24B)-Si(2B)	113.2(4)
C(28B)-C(27B)-C(32B)	120.5(5)
C(28B)-C(27B)-C(35B)	131.9(5)
C(32B)-C(27B)-C(35B)	107.6(4)
C(28B)-C(27B)-U(1B)	113.1(3)
C(32B)-C(27B)-U(1B)	73.6(3)
C(35B)-C(27B)-U(1B)	77.3(3)

C(29B)-C(28B)-C(27B)	118.5(5)
C(29B)-C(28B)-C(36B)	122.8(5)
C(27B)-C(28B)-C(36B)	118.7(5)
C(28B)-C(29B)-C(30B)	121.3(5)
C(28B)-C(29B)-C(37B)	121.1(5)
C(30B)-C(29B)-C(37B)	117.4(5)
C(31B)-C(30B)-C(29B)	122.3(5)
C(31B)-C(30B)-C(38B)	119.4(6)
C(29B)-C(30B)-C(38B)	118.3(6)
C(30B)-C(31B)-C(32B)	118.1(5)
C(30B)-C(31B)-C(39B)	123.1(6)
C(32B)-C(31B)-C(39B)	118.9(6)
C(27B)-C(32B)-C(33B)	108.4(4)
C(27B)-C(32B)-C(31B)	119.2(5)
C(33B)-C(32B)-C(31B)	132.1(5)
C(34B)-C(33B)-C(32B)	106.5(4)
C(34B)-C(33B)-C(40B)	124.8(5)
C(32B)-C(33B)-C(40B)	127.8(5)
C(35B)-C(34B)-C(33B)	110.5(4)
C(35B)-C(34B)-C(41B)	124.3(5)
C(33B)-C(34B)-C(41B)	125.1(5)
C(34B)-C(35B)-C(27B)	106.9(4)
C(34B)-C(35B)-C(42B)	122.6(5)
C(27B)-C(35B)-C(42B)	130.0(5)

M(1) is the centroid of the C(1) to C(8) ring M(3) is the value for the B molecule

M(2) is the centroid of the C(27),C(32),C(33),C(34),C(35) ring M(4) is the values for the B molecule

Least-squares planes (x,y,z in crystal coordinates) and deviations from them

(* indicates atom used to define plane)

- 4.8787 (0.0196) x + 10.7533 (0.0325) y + 17.8364 (0.0124) z = 5.7282 (0.0041)

* -0.0020 (0.0037) C1_a

* 0.0016 (0.0038) C2_a

* 0.0018 (0.0039) C3_a

* 0.0002 (0.0040) C4_a

* -0.0067 (0.0041) C5_a

* 0.0073 (0.0041) C6_a

* -0.0016 (0.0041) C7_a

* -0.0007 (0.0039) C8_a

-1.9170 (0.0018) U

0.2806 (0.0054) Si1_a

0.2271 (0.0056) Si2_a

Rms deviation of fitted atoms = 0.0037

1.0833 (0.0418) x + 9.4019 (0.0683) y + 18.5285 (0.0216) z = 1.8748 (0.0051)

Angle to previous plane (with approximate esd) = 23.14 (0.19)

* -0.0132 (0.0033) C27_a

* 0.0058 (0.0033) C32_a

* 0.0044 (0.0034) C33_a

* -0.0132 (0.0035) C34_a

* 0.0162 (0.0034) C35_a

2.4536 (0.0024) U

-0.2378 (0.0104) C40_a

-0.0994 (0.0104) C41_a

-0.0630 (0.0103) C42_a

Rms deviation of fitted atoms = 0.0115

- 0.1327 (0.0328) x + 9.5125 (0.0536) y + 18.7182 (0.0158) z = 1.7748 (0.0049)

Angle to previous plane (with approximate esd) = 4.57 (0.24)

* 0.0318 (0.0037) C27_a

* -0.0024 (0.0038) C28_a

* -0.0236 (0.0039) C29_a

* 0.0204 (0.0040) C30_a

* 0.0087 (0.0039) C31_a

* -0.0349 (0.0037) C32_a

-0.0592 (0.0094) C36_a

-0.1166 (0.0101) C37_a

0.0595 (0.0102) C38_a

0.0473 (0.0099) C39_a

Rms deviation of fitted atoms = 0.0234

4.2845 (0.0197) x + 12.6333 (0.0298) y + 16.1120 (0.0157) z = 7.3622 (0.0086)

Angle to previous plane (with approximate esd) = 18.87 (0.18)

* -0.0090 (0.0037) C1B_a

* -0.0091 (0.0039) C2B_a

* 0.0015 (0.0039) C3B_a

* 0.0114 (0.0038) C4B_a

* -0.0004 (0.0038) C5B_a

* -0.0130 (0.0039) C6B_a

* -0.0019 (0.0039) C7B_a

* 0.0204 (0.0038) C8B_a

1.9056 (0.0017) U1B

-0.3945 (0.0053) Si1B_a

-0.2253 (0.0054) Si2B_a

Rms deviation of fitted atoms = 0.0105

- 2.4675 (0.0370) x + 11.4249 (0.0601) y + 18.1342 (0.0218) z = 8.0631 (0.0236)

Angle to previous plane (with approximate esd) = 25.89 (0.18)

* 0.0044 (0.0030) C27B_a

* 0.0039 (0.0030) C32B_a

* -0.0111 (0.0031) C33B_a

* 0.0142 (0.0031) C34B_a

* -0.0114 (0.0030) C35B_a

-2.4554 (0.0022) U1B

0.1695 (0.0092) C40B_a

0.1229 (0.0092) C41B_a

0.1212 (0.0092) C42B_a

Rms deviation of fitted atoms = 0.0099

- 1.7860 (0.0319) x + 12.1250 (0.0491) y + 17.9178 (0.0190) z = 8.5474 (0.0221)

Angle to previous plane (with approximate esd) = 2.99 (0.26)

* -0.0131 (0.0034) C27B_a

* -0.0013 (0.0035) C28B_a

* 0.0058 (0.0037) C29B_a

* 0.0043 (0.0039) C30B_a

* -0.0182 (0.0039) C31B_a

* 0.0224 (0.0035) C32B_a

0.0188 (0.0090) C36B_a

0.1007 (0.0092) C37B_a

0.0116 (0.0105) C38B_a

-0.0504 (0.0116) C39B_a

Rms deviation of fitted atoms = 0.0133

Table 25.

Crystal data and structure refinement for (**4.3**)

$[(U(\eta^5\text{-}Ind^{Me6})(\eta^8\text{-}C_8H_6\{Si^iPr_3\text{-}1,4\}_2))_2(\mu\text{-}\eta^2\text{:}\eta^2\text{-}C_4O_4)] \cdot 4(pentane)$

Identification code	mar1308	
Empirical formula	C86 H134 O4 Si4 U2 . 4(C5 H12)	
Formula weight	2108.94	
Temperature	173(2) K	
Wavelength	0.71073 Å	
Crystal system	Monoclinic	
Space group	C2/m (No.12)	
Unit cell dimensions	a = 25.7129(11) Å	α= 90°.
	b = 20.1749(9) Å	β= 116.292(2)°.
	c = 12.0421(4) Å	γ = 90°.
Volume	5600.6(4) $Å^3$	
Z	2	
Density (calculated)	1.25 Mg/m^3	
Absorption coefficient	2.98 mm^{-1}	
F(000)	2180	
Crystal size	0.25 x 0.1 x 0.05 mm^3	
Theta range for data collection	3.47 to 26.04°.	
Index ranges	-31<=h<=31, -24<=k<=24, -14<=l<=13	
Reflections collected	33000	
Independent reflections	5653 [R(int) = 0.075]	
Reflections with I>2sigma(I)	4855	
Completeness to theta = 26.04°	99.3 %	
Tmax. and Tmin.	0.7294 and 0.6053	
Refinement method	Full-matrix least-squares on F^2	
Data / restraints / parameters	5653 / 12 / 256	
Goodness-of-fit on F^2	1.133	
Final R indices [I>2sigma(I)]	R1 = 0.040, wR2 = 0.090	

R indices (all data) R1 = 0.054, wR2 = 0.095

Largest diff. peak and hole 0.90 and -0.98 e.Å^{-3}

The molecular site symmetry is 2/m

There is Me/H disorder at C(21) positions related by the crystallographic mirror plane. The two very poorly defined pentane solvate molecules were included with a single isotropic displacement parameter and with 1,2and 1,3 C..C distance restraints.

Data collection KappaCCD , Program package WinGX , Abs correction MULTISCAN

Refinement using SHELXL-97 , Drawing using ORTEP-3 for Windows

Table 26.

Atomic coordinates (x 10^4) and equivalent isotropic displacement parameters (Å^{2}x 10^3)

for mar1308. U(eq) is defined as one third of the trace of the orthogonalized U^{ij} tensor.

	x	y	z	U(eq)
U	1165(1)	5000	3194(1)	27(1)
Si	1878(1)	3265(1)	2090(1)	35(1)
O(1)	474(1)	4264(2)	1569(3)	31(1)
C(1)	200(2)	4643(2)	666(4)	28(1)
C(2)	1846(2)	4126(2)	2698(4)	30(1)
C(3)	2056(2)	4155(3)	4012(4)	34(1)
C(4)	2214(2)	4654(3)	4919(4)	34(1)
C(5)	1701(2)	4649(2)	1829(4)	30(1)
C(6)	1435(3)	3191(3)	340(5)	45(1)
C(7)	1644(3)	2632(3)	-233(6)	59(2)
C(8)	777(3)	3115(4)	-112(6)	70(2)
C(9)	1688(3)	2615(3)	2980(5)	46(1)
C(10)	1783(4)	1897(3)	2666(7)	73(2)
C(11)	1086(3)	2686(4)	2931(7)	64(2)
C(12)	2668(2)	3148(3)	2443(5)	43(1)
C(13)	2869(3)	3680(3)	1800(6)	55(2)
C(14)	3083(3)	3143(3)	3838(6)	57(2)
C(15)	167(3)	5000	3513(7)	54(3)

C(16)	475(3)	4437(3)	4126(5)	50(2)
C(17)	963(2)	4649(3)	5237(4)	34(1)
C(18)	1375(3)	4284(3)	6262(5)	44(1)
C(19)	1759(2)	4644(3)	7260(5)	47(1)
C(20)	-414(4)	5000	2392(9)	107(5)
C(21)	128(6)	3851(6)	3697(12)	51(3)
C(22)	1370(3)	3542(3)	6220(7)	67(2)
C(23)	2196(3)	4285(5)	8424(6)	83(3)
C(1S)	114(9)	1839(14)	4543(14)	370(8)
C(2S)	-290(12)	1882(15)	3303(14)	370(8)
C(3S)	-210(20)	1370(20)	2480(30)	370(8)
C(4S)	941(18)	0	5530(30)	370(8)
C(5S)	1337(14)	0	4940(30)	370(8)*
C(6S)	923(12)	0	3570(30)	370(8)
C(7S)	1339(13)	0	3020(30)	370(8)
C(8S)	995(17)	0	1650(30)	370(8)

*** occupancy 0.5**

Table 27.

Bond lengths [Å] and angles [°] for mar1308.

U-M(1)	1.9475(5)
U-O(1)	2.472(3)
U-M(2)	2.496(5)
Si-C(9)	1.890(5)
Si-C(12)	1.899(6)
Si-C(2)	1.900(5)
Si-C(6)	1.905(6)
O(1)-C(1)	1.259(5)
C(1)-C(1)”	1.442(9)
C(1)-C(1)’	1.472(9)
C(2)-C(5)	1.416(7)

C(2)-C(3)	1.429(7)
C(3)-C(4)	1.407(7)
C(4)-C(4)”	1.396(10)
C(5)-C(5)”	1.416(9)
C(6)-C(7)	1.537(8)
C(6)-C(8)	1.540(9)
C(9)-C(11)	1.531(8)
C(9)-C(10)	1.543(8)
C(12)-C(13)	1.540(8)
C(12)-C(14)	1.541(8)
C(15)-C(16)	1.394(8)
C(15)-C(20)	1.506(12)
C(16)-C(21)	1.433(12)
C(16)-C(17)	1.436(7)
C(17)-C(17)”	1.415(10)
C(17)-C(18)	1.425(7)
C(18)-C(19)	1.376(8)
C(18)-C(22)	1.498(9)
C(19)-C(19)”	1.438(12)
C(19)-C(23)	1.535(8)

M(1)-U-O(1)	115.6(1)
O(1)-U-O(1)”	73.87(14)
M(1)-U-M(2)	141.8(1)
O(1)-U-M(2)	94.4(1)
C(9)-Si-C(12)	107.8(3)
C(9)-Si-C(2)	110.5(2)
C(12)-Si-C(2)	104.6(2)
C(9)-Si-C(6)	113.3(3)
C(12)-Si-C(6)	107.1(3)
C(2)-Si-C(6)	113.0(2)
C(1)-O(1)-U	104.5(3)

O(1)-C(1)-C(1)”	127.4(3)
O(1)-C(1)-C(1)’	142.6(3)
C(1)”-C(1)-C(1)’	90.0
C(5)-C(2)-C(3)	129.4(5)
C(5)-C(2)-Si	116.0(3)
C(3)-C(2)-Si	113.9(3)
C(4)-C(3)-C(2)	136.7(5)
C(4)”-C(4)-C(3)	135.7(3)
C(2)-C(5)-C(5)”	138.2(3)
C(7)-C(6)-C(8)	108.4(5)
C(7)-C(6)-Si	113.5(4)
C(8)-C(6)-Si	115.0(4)
C(11)-C(9)-C(10)	110.3(6)
C(11)-C(9)-Si	115.1(4)
C(10)-C(9)-Si	113.8(4)
C(13)-C(12)-C(14)	109.2(5)
C(13)-C(12)-Si	111.3(4)
C(14)-C(12)-Si	113.6(4)
C(16)”-C(15)-C(16)	109.0(7)
C(16)”-C(15)-C(20)	125.5(4)
C(16)-C(15)-C(20)	125.5(4)
C(15)-C(16)-C(21)	111.3(7)
C(15)-C(16)-C(17)	108.0(5)
C(21)-C(16)-C(17)	136.8(7)
C(17)”-C(17)-C(18)	121.1(3)
C(17)”-C(17)-C(16)	107.3(3)
C(18)-C(17)-C(16)	131.4(5)
C(19)-C(18)-C(17)	117.1(5)
C(19)-C(18)-C(22)	123.2(5)
C(17)-C(18)-C(22)	119.7(6)
C(18)-C(19)-C(19)”	121.8(3)
C(18)-C(19)-C(23)	120.1(6)

C(19)"-C(19)-C(23) 118.1(4)

M(1) is the centroid of the cot ring

M(2) is the centroid of the "Cp" fragment of the fulvalene ring

Symmetry transformations used to generate equivalent atoms: " x,-y+1,z ' -x,y,-z #3 -x,y,-z+1

```
Least-squares planes (x,y,z in crystal coordinates) and deviations
from them

 (* indicates atom used to define plane)


  25.5827 (0.0049) x - 0.0000 (0.0004) y - 4.2220 (0.0206) z = 3.5787
(0.0064)


 *    0.0005 (0.0028)  C5_a

 *    0.0042 (0.0039)  C2_a

 *   -0.0122 (0.0040)  C3_a

 *    0.0074 (0.0028)  C4_a

 *    0.0005 (0.0028)  C5_$2a

 *    0.0042 (0.0039)  C2_$2a

 *   -0.0122 (0.0040)  C3_$2a

 *    0.0074 (0.0028)  C4_$2a

     -1.9472 (0.0024)  U

      0.3425 (0.0038)  Si_a


 Rms deviation of fitted atoms =   0.0075



 - 22.1432 (0.0446) x + 0.0000 (0.0004) y + 10.0814 (0.0225) z =
3.1360 (0.0133)


 Angle to previous plane (with approximate esd) = 36.32 ( 0.17 )


 *    0.0362 (0.0048)  C15_a

 *   -0.0287 (0.0038)  C16_a
```

```
*    0.0106 (0.0014)  C17_a
*   -0.0287 (0.0038)  C16_$2a
*    0.0106 (0.0014)  C17_$2a
    -2.4953 (0.0031)  U
     0.1925 (0.0135)  C20_a
     0.3090 (0.0124)  C21_a
     0.1322 (0.0094)  C18_a

Rms deviation of fitted atoms =   0.0252


- 23.5121 (0.0296) x - 0.0000 (0.0006) y + 9.2477 (0.0219) z = 2.5715
(0.0177)

Angle to previous plane (with approximate esd) =  6.67 ( 0.31 )

*    0.0067 (0.0020)  C17_a
*   -0.0137 (0.0042)  C18_a
*    0.0070 (0.0021)  C19_a
*    0.0067 (0.0020)  C17_$2a
*   -0.0137 (0.0042)  C18_$2a
*    0.0070 (0.0021)  C19_$2a
    -0.0419 (0.0077)  C22_a
     0.0550 (0.0111)  C23_a

Rms deviation of fitted atoms =   0.0097
```